Tunnelling in soils: movements and structures

Mitsuo Tsutsumi

TUNNELLING IN SOILS - MOVEMENTS AND STRUCTURES

Mitsuo Tsutsumi

Department of Geological Sciences

University of Durham

Submitted in partial fulfillment of the requirements

for the degree of Doctor of Philosophy

December 1983.

To my wife Helena Maria

with many thanks.

AKNOWLEDGEMENTS

I would like to express my gratitude to the following people and organizations, without whose direct or indirect help this research would not have been possible.

My supervisor, Prof. P.B. Attewell, for giving me the opportunity, advice and his encouragement to carry out the research presented in this dissertation.

The CAPES and the Universidade Federal de Vicosa for the opportunity and financial support.

Prof. J. A. Comastri, now Head of Centro de Ciências Exatas e Tecnológicas of Universidade Federal de Viçosa for the opportunity and his support.

Dr. G. Sediyama for giving me his assistance and support from Brazil during the course of this work.

Dr. M. J. Reeves (now of the University of Saskatchewan) for supervision during the early computational stages of the work.

The staff of the Durham University Computer Unit for providing me with facilities to carry out the numerical analysis described in the thesis.

ABSTRACT

The present dissertation describes some of the ground movement problems associated with tunnelling in soft ground. A possible response of pipelines to such ground movements is also studied in the context of a case history of pipes lying parallel to a tunnel centre line.

Analyses of tunnel excavation with and without lining installation, and of the pipe behaviour, have been performed by means of the finite element method. Four examples of analysis and their results are presented, with the main characteristics related the each being highlighted.

Field observations of ground movements caused by tunnelling in soil have been gathered together and added to those presented by Peck (1969) and Attewell (1977) in order to attempt to define empirical relations that could describe a geometric form of settlement profile and to predict its magnitude.

A three-dimensional finite element program has been written in order to carry out the style of analysis that two-dimensional models cannot accommodate. The isoparametric hexahedral rectangular element has been used in view of its facility in programming and discretising the medium of interest. The computer program has been developed to allow for different loading conditions and calculations to be carried out using linear material behaviour only. Features which have been considered in the tunnel-ground-pipes analyses include simulation of incremental construction.

Because it was clearly impractical to model the entire system of interest by means of a single finite element mesh, an alternative analytical-numerical hybrid technique is described.

TABLE OF CONTENTS

CHAPTER 4

THE FINITE ELEMENT TECHNIQUE TO SIMULATE TUNNELLING.

CHAPTER 5

THE THREE-DIMENSIONAL FINITE ELEMENT PROGRAM.

CHAPTER 6

SITE AND MODEL USED IN THE ANALYSES.

CHAPTER 7

FINITE ELEMENT CALCULATIONS AND DISCUSSION.

LIST OF TABLES

LIST OF FIGURES

NOTATIONS

A' - 24" pipe (parallel to and above the tunnel centre line.

B' - 12" pipe (parallel to and 1.7 m from the tunnel centre line).

C' - 18" pipe (parallel to and 6.5 m from the tunnel centre line).

{B} - element stress/strain matrix.

c_u - undrained shear strength.

{D} - element elasticity matrix.

De - external diameter of the pipe.

Di - internal diameter of the pipe.

{d} - nodal displacement vector.

{dF} - vector of nodal releasing forces variations.

E - modulus of elasticity of materials.

E* - 'equivalent' modulus of elasticity of pipes.

EI - pipe stiffness.

E*I* - 'equivalent' pipe stiffness.

{F} - vector of nodal releasing forces.

I - moment of inertia for pipes.

I* - 'equivalent' moment of inertia for pipes.

i - inflexion distance ($i=z_o/2$).

K - coefficient of earth pressure.

{K} - element stiffness matrix.

K_a - 'material' constant.

n - empirical constant.

OFS - Simple Overload Factor.

R - tunnel radius.

S - excavated surface.

x , y , z - are the cartesian coordinates.
z is vertical and perpendicular to xy plane.
y is horizontal and perpendicular to zx plane.
x is perpendiculat to yz plane.
Tunnel and/or pipe axis is always positioned parallel to the x direction.
Sign convention as indicated in the Figure below :

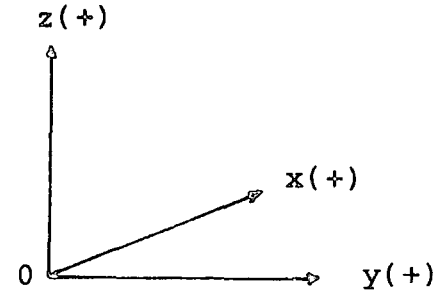

u , v , w - are displacements in the x , y and z directions , respectively. Sign convention is similar to that for cartesian coordinates.

V - ground loss.

V_s - volume of settlement trough.

w_{max} - maximum settlement.

z - depth to the point of ground displacement interest.

z_o - depth of the tunnel axis.

ε_x, ε_y, ε_z - are the normal strains in the x, y and z directions, respectively.
Tensile is positive and compressive is negative.

$\{\varepsilon\}$ - nodal strain vector.

σ_o - applied stress.

σ_c - confining pressure.

σ_{ef} - stress at failure.

$\{\sigma\}$ - nodal stress vector.

σ_x, σ_y, σ_z - are the normal stresses the in x , y and z directions, respectively. Sign convention is similar to that for strains.

Φ' - effective friction angle of the soil.

ν - Poisson's ratio of materials.

γ - soil unit weight.

lateral - means y direction (horizontal and perpendicular to the tunnel and/or pipe axis).

vertical - means z direction (vertical and perpendicular to the tunnel and/or pipe axis).

longitudinal - means x direction (horizontal and parallel to the tunnel and/or pipe axis).

transverse - means in the y direction and usually defines a vertical (yz) plane.

horizontal - means in the y and/or x directions and usually defines a horizontal (xy) plane.

settlement - is related to vertical movements on ground surface (negative w).

Distances preceded by a negative sign means behind the tunnel face (opposite to the direction of tunnel face advance).

CHAPTER 1

INTRODUCTION.

1.1 THE NEED FOR TUNNELLING IN SOIL.

It is generally believed that tunnelling was one of man's first construction activities in engineering. At an early period, he found necessary to enlarge his cave in order to improve his living conditions and to protect his own environment. Later, the collection of water and minerals provided a major reason for men to bore through the ground. Today, tunnelling has been used for many purposes, such as drainage, sewerage, storage, transportation and so on.

Social development and mobility has contributed to increasing demands on passenger and goods transportation. These demands are particularly serious in urban environments and the need for tunnels in these areas

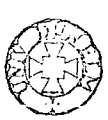

is progressively increasing with the growth of populations.

1.2 THE NEED FOR UNDERSTANDING TUNNELLING IN SOIL.

Increasing use of tunnels has created a requirement for improved design methods because they are regarded as one of the most expensive civil engineering constructions.

In recent years many tunnels have been constructed in densely populated areas. The construction of tunnels in these areas is particularly critical because ground movements must be kept below some allowable limits in order to avoid damage to overlying or adjacent structures.

Considerable research effort has been devoted over the past few years to understanding movements caused by tunnelling in soft ground and its effects on structures.

Although many advances in design and construction have been so made, the prediction of ground movements is still regarded with major concern. The prediction of the magnitude and distribution of ground movements still depends largely on the skill and previous experience of the engineer to apply an appropriate method of calculation

based on a simplified view of the ground medium. At the present time, predictions of settlement are somewhat speculative because of the complexity of the problem. Because of the many simplifications necessarily made to predict these movements, the results obtained by theoretical means serve only as a guide to control the process of tunnel contruction, to define the extent of pre-tunnelling structural surveys, and sometimes to apportion responsibilities for damage.

The reliability of the forecast of ground movements bears on the overall cost of the project because it may affect construction methods, additional calculations and the investigations required. There are basically three methods for predicting the ground behaviour caused by tunnelling in soil : theoretical (including numerical) analyses, laboratory models, and surveys on case history data leading to the formulation of empirical relations. The choice of the method depends on the accuracy desired, and mainly on parameters available for the analysis.

A tunnel design cannot be considered successful until the magnitudes of the expected ground movements are adequately known.

As a starting point three requirements must be taken into account by the tunnel designer. The first one

is that the local geological and groundwater conditions must allow the excavation face to advance safely and be able to preserve the integrity of the opening at least temporarily until primary support can be installed. The second requirement is that the tunnel should be able to resist all predicted adverse ground conditions to which it may be subjected during its lifetime. The last requirement is that the ground movements caused by tunnelling should not excessively damage any above-ground and/or in-ground structure in the tunnel vicinity.

1.3 EXCAVATION AND SUPPORT PROBLEMS.

It is a normal procedure in soft ground tunnelling to excavate the tunnel to a certain distance in advance of the shield body first, and then erect the lining in two stages to complete the sequence. The creation of the cavity in a stressed medium at first, and then the primary stage of support installation, allows the ground to move until the whole system acquires a new equilibrium condition. The magnitude of these movements depends on the time that the ground is left unsupported, the rate of shield advance related to the deformation rate of the soil, and the flexibility of the lining. The objectives of the most modern open-shield tunnelling techniques are to reduce to a minimum the time between excavation and

placing of the lining. In doing so, the entry of water into the tunnel is inhibited, and the loss of ground is reduced. The loss of ground is a parameter which is defined as the difference between the volume of material actually excavated and the design volume as represented by the cut surface of the soil.

The purpose of the second stage of lining placement is to provide a permanent finishing for the inside of the tunnel if the function of the tunnel so requires it. This secondary lining should have no real effect on ground settlement in particular, and on ground movements in general.

Precast concrete or cast iron bolted segments are usually employed for the primary lining of most circular soft ground tunnels. They are bolted together, caulked, and erected within the tailskin of the shield. An annular void around the outside of the assembled lining is inevitable in this procedure. Later, this void is filled, usually with grout but sometimes with grouted pea gravel or its equivalent (for example, Lytag), but any areas left ungrouted will contribute to the ground settlement. In the case of using a conventional bolted lining for tunnels constructed with a shield it is usually decided to over-cut the tunnel slightly in size in order to assist

steering of the shield. This procedure can also increase the amount of contact grouting required behind the erected lining.

An alternative method of tunnelling is pipe-jacking. This process is more suitable for extremely soft ground because of its cutting method. This method has the advantage of avoiding the degrees of settlement caused by more widespread excavation and lining placement techniques. The only significant source of ground loss with this method is the intrusion of the soil through the face, and it is noted that there might be some associated ground heave ahead of the tunnel. The first applications of this procedure have been restricted to short drives because of high skin friction between lining and surrounding soil. Nowadays, this friction can be reduced dramatically by the use of bentonite as a lubricant, and the drive lengths have been increased considerably.

1.4 STYLE OF GROUND MOVEMENTS WITH THE TUNNELLING PROCESS AND METHODS OF LIMITING GROUND MOVEMENTS.

1.4.1 SOURCES OF GROUND MOVEMENTS.

Several phenomena take place during the tunnelling

process in soft ground. The following may be related to the process : soil disturbance during construction, drainage of ground through water seepage into the tunnel, loss of ground, squatting of the primary lining, limitations of grouting, and so on. Each of the settlement sources depends directly on the ground conditions. In the following Sections some of the most important causes of settlement will be emphasized and an alternative solution for displacement prediction will be given.

1.4.2 GROUND LOSS.

A very important variable for any settlement prediction is the ground loss (V), if the initial ground loss is assumed to occur under undrained conditions. In this case the volume of the settlement trough (V_s) can be taken as equal to the volume of ground loss in the tunnel because there is assumed to be no volume change in the ground.

The value of V_s depends upon both ground conditions and construction method. Ground instability, construction procedure, shield design, and lining design are the main factors contributing to the volume loss.

a) Ground instability.

Soil instability can be distinguished in soft ground tunnelling according to different types of soils. In cohesive granular soils ravelling may occur in the face or more usually in the roof of the tunnel. The effects of ravelling can be mitigated to some extent by the provision of support to the ground, notably by the use of forward poling plates on the shield.

Running ground is a typical occurrence in dry sand or loose gravel. Peck (1969) pointed out that, if unconstrained, these materials run into the face until they reach their angle of repose. Even using special techniques to excavate this type of soil, large settlements may occur. There is also the problem of collapse of such material on to the tail of a shield.

In the above types of ground, the problem is aggravated if seepage pressures are permitted to built up, because the soil particles will run into the face in the manner of a liquid, filling the entire heading (Peck, 1969). This type of failure can be avoided by the use of compressed air, by stabilising the ground by drainage (usually well-point de-watering in advance of the face) or chemical grouting, by temporarily freezing the ground, or

by the use of an enclosed-face type of slurry shield.

If a tunnel is excavated in cohesive soil, plastic shear failure may occur at the face when the shear strength of the soil is exceeded. This type of failure could result in very large settlements, consisting of rapid movements of ground axially into the face. The most general practice is to stabilise the soil by the use of compressed air, a technique which is technologically most simple but which has well-known physiological drawbacks.

Broms and Bennermark (1967) developed a type of stability criterion to analyse the behaviour of cohesive soil relating to openings in vertical retaining walls. Attewell and Boden (1971) developed this criterion further, extending it to tunnels and taking major account of the soil deformation rate, a feature not considered by Broms and Bennermark.

The two types of soil discussed briefly above are those having well-known properties. However, most cases of tunnelling (for example, in glacial clays) concern mixed faces of cohesive and granular soils and the judgement as to choise and feasibility of different (temporary) ground improvement and construction options becomes much more difficult than for faces consisting of a single soil material type.

b) Shield design.

Ground loss occurs around a shield in several ways. The most evident one is the soil movement into the excavation face proper.

At the tail of the shield, ground losses are caused by the soil intrusion into the tunnel through the surface left unsupported until a primary lining offers full resistance.

Ground loss also occurs due to the cutting of the excavation area slightly greater then the tunnel circular section in order to counteract among other things the natural tendency of the shield to dive off level into the ground under its own weight. The use of a bead, either round the whole of the leading edge of the hood of the shield, or around the upper 180° of the hood, also facilitates steering the shield on line and around curves.

Another source of ground loss is the disturbance of the soil around the tunnel when shield moves forward. The remoulded soil is then compressed under the existing ground stresses and so contributes to additional settlement through its reduced shear strength and its ability to deform inwards more easily.

Cording and Hanmire (1975) and Attewell (1977) have analysed the effects of shield tunnelling on ground settlement and have presented detailed discussions on the subject. They have derived several expressions to calculate the total ground loss around a shield.

c) Construction procedure.

For bolted lining construction, the void formed around lining rings and behind a tailskin is an inevitable consequence of this method of tunnelling. This void is generally grouted after the shield has passed, although further inward ground movements can occur as the grout 'bleeds' during setting. The effect of this occurrence during the excavation can be reduced by increasing the mean rate of shield advance, reducing the time during which a particular element of ground remains unsupported, designing a quick-set, low-bleed grout, grouting as soon as possible, and using a shorter shield.

d) Lining design.

Real linings are neither perfectly flexible nor perfectly rigid. Because of this property the lining deforms when it interacts with the surrounding soil. Typically, the vertical diameter tends to decrease (squat)

while the horizontal diameter tends to increase. The magnitude of these deformations depends directly on the stresses in the ground, the strength of the soil, and the flexibility of the lining. It is noted that tunnel linings in the London Clay still squat even though K_o at typical tunnel depths tends to 2.65.

1.4.3 GROUND DEWATERING.

Several problems arise when tunnels are driven below the water table. The principal problem concerns the face instability which becomes particularly serious when the tunnel is constructed in granular soils. Another consequence of excavation in such a condition is the inevitable seepage into the tunnel through both the face and the tunnel walls. Two distinct phenomena can be identified : the first is the generation of seepage forces within the soil, the force acting in the direction of flow, and towards the excavation. The second effect is the dilation of the soil adjacent to the excavation, the creation of a zone around the tunnel having reduced or negative porewater pressures, and nearby the entrainment of groundwater from above and from the sides towards the tunnel, so leading to a situation of enhanced effective ground pressures caused by drawdrown at and in the

vicinity of ground surface if re-charge facilities are absent.

Seepage into the tunnel can be reduced by the use of ground treatment and/or compressed air. However, if compressed air is used it is usual to remove internal pressurisation after re-caulking and before the installation of a secondary lining. From this stage, and with inadequate caulking until completion of the secondary lining, the water may continue to seep into the tunnel. It is also possible that the tunnel continues to act as a drain through the zone of disturbed soil around the tunnel that has dilated and been only partially re-compressed by lining resistance to inward soil deformation.

1.5 EFFECT OF GROUND MOVEMENTS ON STRUCTURES.

The response of structures to the ground deformation is complex. It depends mainly on the shape and stiffness of the structure, and the magnitude and distribution of displacements. Many researchers have considered this problem based on an observational approach and they have proposed tolerable values of deformation parameters for particular types of structures. For buildings, they divided settlement damage into categories:

architectural, functional and structural. The first category involves only the panel walls, floors, or finishes, and the structure itself is quite safe. An intermediate, functional,level of damage involves only the frame, and it can be regarded as unacceptable by its occupiers, or intolerable in some places such as hospitals, public buildings, and so on. The last category, structural, must be avoided because weakening of the building or part of the building can render it unsafe. If this third possibility is predicted, decisions will have to be taken with respect to the tunnel design or strengthening of the structure under consideration.

Ground deformation may also damage services such as sewers, gas mains, and so on. Usually, pipes are provided for these services, and damage will also depend upon the nature of the movements and material used. If the pipe is made of brittle material, such as cast iron or concrete and is old, it may then become more vulnerable to failure, and may have to be replaced before tunnelling proceeds by a more ductile and durable pipe material such as polyethylene. Table 1.1, after Attewell and Yeates (1984), shows different materials and their respective typical properties as used in Britain.

For the point of view of the structural engineer,

failure can be caused by joint leakage, excessive pipe yielding or pipe fracture. A joint leakage type of failure, which is the most common failure in old iron pipelines, is accepted as an almost routine maintenance problem. Pipe yielding failure sometimes occurs without immediate fracture and only becomes apparent later when the fracture has developed due to the increase of static load and/or reduced fatigue strength.

It has been established that for pipelines made of brittle material, the primary sources of fracture are related to differential displacements and/or corrosion. The former source arises from traffic loading, ground temperature and moisture change, and ground movements associated with any adjacent construction. The latter source is related to the age and type of the material, to the (variable) ground moisture content and the ground chemistry.

Surveys on gas and water distribution systems made in the United Kingdom and 100 largest cities in the United States revealed that over 90% of the distribution system consists of grey iron pipework.

Before analysing the damage that may occur in the structure, it is necessary to predict with some degree of

reliability the ground displacements that may induce the damage. So far, there has been little research performed on structural (building) or pipe response to the soft ground movements caused by tunnelling. In this thesis, Chapter 2 is concerned with both the character of ground deformation and its possible consequences with respect to structures and services. The detail of building deformation is not considered in this thesis.

TABLE 1.1 Typical pipe material properties (Attewell and Yeates, 1984)
For short-term static loading in direct tension (gradually applied, non-repeated loading without creep and at 20°C) (1) (3).

MATERIAL	ULTIMATE TENSILE STRESS N/mm²	LOWER YIELD STRESS OR PROOF STRESS N/mm²	TYPICAL MAX. DESIGN STRESS FOR WORKING LOADS N/mm²	DESIGN STRESS/ ULTIMATE STRESS	DESIGN STRESS/ YIELD OR PROOF STRESS	SECANT ELASTIC MODULUS TO MAX. DESIGN STRESS GN/m²	ELASTIC STRAIN EQUIVALENT TO DESIGN STRESS microstrain
GREY IRON							
Pit cast before year 1914	110 to 140	70 to 90	27 to 35			67 to 87	400 to 400
Vertically cast to BS78:1917	145	95	36	0.25	0.38	90	400
Vertically cast to BS78:1965	155	100	38			93	400
Spun cast to BS1211:1958							
over 16 in.dia. grade 12;	185	120	46			103	450
3 in. to 16 in.dia.grade 14	215	140	54			108	500
	20N/mm²	0.1% proof stress					
DUCTILE IRON							
Spun cast to BS 4772		0.2% proof stress					
grade 420/12 material	420 min.	300 min.	155	0.37	0.52	165	940
MILD STEEL		yield or 0.2% proof stress		depending on duty			
to BS 534:1966			generally				
grade 320 material	320 min.	195 min.	80-115 (occasionally up to 140)	0.25 - 0.36 (occasionally up to 0.44)	0.4 - 0.6 (occasionally up to 0.77)	210	380-550
grade 410	410 min.	235 min.	95-140				450-660
(2) PLASTIC							
UPVC to BS 3505	45 min.	-	20	0.5	-	2.8	7000
MDPE	30 at 50 mm/min.	19 upper yield	7	0.4	-	0.7	10000
HDPE type 1	19 at strain rate 125 mm/min.	-	8	0.4	-	-	-
HDPE type 2	32 at strain rate 125 mm/min.	14 lower yield 22 upper yield	8	0.25	0.57	0.9	9000

(1) For iron and steel pipes, creep is not significant at 20°C at the maximum design stress indicated. These stresses are therefore also used for long-term loading.

(2) After 50 years, plastic properties are UPVC at 10°C - UTS = 25 N/mm², max. design stress = 12 N/mm², creep modulus = 1.4 GN/m².
MDPE at 20°C - U.T.S. = 8.0 N/mm², max. design stress = 5 N/mm², creep modulus at 3 N/mm² = 0.13 GN/m².
MDPE type 1 at 20°C - U.T.S. = 6.5 N/mm², max. design stress = 5 N/mm², creep modulus at 3 N/mm² = 0.13 GN/m².
MDPE type 2 at 20°C - U.T.S. = 9.5 N/mm², max. design stress = 5 N/mm², creep modulus at 3 N/mm² = 0.13 GN/m².
MDPE type 1 at 10°C - U.T.S. = 9.5 N/mm².
MDPE type 2 at 10°C - U.T.S. = 2.5 N/mm².

(3) For all the above materials the maximum design tensile bending stress is not less than the maximum design direct tensile stress.

CHAPTER 2

METHODS OF ANALYSING GROUND DISPLACEMENTS.

2.1 INTRODUCTION.

Several problems arise when a tunnel is excavated in soil. The most important of these concern the stability of the excavated surface, displacements and settlements at and close to ground surface, lining loads and the effects of ground movements on in-ground and/or above-ground structures. Each problem is interactive with another or others, and is affected by parameters such as loss sources and the magnitude, distribution and rate of displacements which occur when the face advances. Many theoretical relationships have been developed to deal with these problems, but at present they are only approximations of actual problems. Hence, every result obtained by theoretical means must be verified by tests

and field observations, and appropriate adjustments must be made by using empirical factors.

There are basically three approaches to analysing soft ground behaviour caused by tunnelling : theoretical methods, laboratory models, and surveys on actual ground movements. None of these approaches can take into account the quality of workmanship which can have a major effect on the final state of the disturbed medium, particularly in the case of tunnelling in granular soil. It thus follows that any calculated displacements must be treated with caution, the actual factors likely to contribute on site to the ground movements being given very careful weighting at the site investigation stage.

2.2 THEORY.

All theories dealing with surface movements begin with the size of the depression left in the wake of excavation.

Several empirical mining formulae have been developed over the past years, relating the amount of surface subsidence to the size of the excavation and to the depth of the cover. Martos (1969) investigated the

problem of surface subsidence based on statistical evaluation of actual observations. Later, he developed further the assumed mathematical model in order to consider not only vertical but also horizontal displacements of the subsidence trough.

An interesting estimate of surface settlement was worked out by Litviniszyn (1955), and by Sweet and Bogdanoff (1965), based on stochastic theories of ground movements. The model developed by the latter authors has enjoyed some large measure of acceptance, and it is also used in this work.

The stochastic approach assumes that the ground material is represented by discs or spheres, if the analysis is carried out in two- or three-dimensions, respectively. All the model particles have the same size. The removal of any particle within the media is regarded as analogous to the tunnel excavation process. This removal creates a empty space that could be filled by either of the two particles above and adjacent to it. These particles, however, would have to be replaced in turn by the particles immediately above them. The downward movements of particles (each particle movement downwards having an obvious and simply-specifiable probability) will take place until the void reaches the

ground surface. As a result of this mechanism, a settlement trough will develop in the surface. Case history evidence has shown that the settlement trough formed by this process can conveniently be described by an error function, or normal probability curve. The variation of surface settlement (w) at a transverse distance (y) from the tunnel centre line (y=0) is expressed as

$$w = w_{max} \cdot \exp(-y^2/2i^2) \qquad (2.1)$$

where w_{max} is the maximum settlement which is assumed to occur above the tunnel centre line, and i is the standard deviation of the error function.

Equation 2.1 is completely defined if both w_{max} and i are known. Sweet and Bogdanof (1965) have suggested the following general expression to calculate the standard deviation i,

$$i/R = K_a \cdot (z/R)^n \qquad (2.2)$$

where R = half-width of the opening,

z = depth of the opening,

K_a = 'material constant',

and n = empirical value.

By integration of equation 2.1, a general expression of settlement volume, V_s , per unit advance is obtained :

$$V_s = 2.5 \cdot i \cdot w_{max} \qquad (2.3)$$

Given a value of V_s and adopting appropriate values of K_a and n , the settlement profile can be evaluated.

Equations 2.1 to 2.3 give no indication of lateral ground movements or displacements parallel to the tunnel.

Attewell and Woodman (1982) developed a method of analysis for a full three-dimensional ground movement profile, based on a cumulative probability function for the longitudinal settlement distribution on the tunnel centre line. They have shown reasonable agreement with case history data for a range of ground conditions.

The stress path method (Atkinson and Branby,1978) is another analytical approach well suited for examining the actual ground conditions around a tunnel in clay. This method is a procedure that may be used to estimate either the strength or the deformation of representative elements of soils in the deformation field. The basic

idea involves determining in the laboratory how a soil element behaves when it is subjected to specified in situ loading conditions. Thus, the procedure followed in this method of analysis is to remove several undisturbed samples of soil from the ground, and subject them to the estimated changes in total or effective stresses that occur in the soil element in the ground during the various stages of the construction process. Both the deformations and the failure strength are observed and they may be used to estimate overall deformation of the ground.

It is important to notice that the effect of drainage in the field can be modelled by allowing the soil sample to drain between each stage of loading if construction is slow, or only at the end of loading if construction is rapid.

Although the stress path method presents several advantages, there are certain difficulties with the method which must be faced. The major difficulty, if not an impossibility, is to simulate the actual field loading/unloading conditions in the laboratory. Nevertheless, despite many difficulties, and accepting that the method provides only qualitative and generalized solutions, certain results and conclusions can usefully be noted for practical purposes.

The finite element method is a powerful instrument for solving engineering problems and it has been successfully applied to tunnelling analyses over the past few years. This method of analysis is considered in Section 2.7.

2.3 ON SITE MEASUREMENTS.

Results from field measurements, their compilation and their empirical use provide a powerful means of analysing ground movements caused by tunnelling in soil. They may also be used to control the tunnel construction process and they serve as a primary source of information required for estimating ground movements with advance of the tunnel face. The acquisition of reliable field data is an essential prerequisite for any successful study.

The first major review of field data records of tunnelling in soft ground was presented in Peck's State-of-the-Art Report at the International Congress on Soil Mechanics and Foundation Engineering held in Mexico City in 1969. In his work, he grouped observed surface movements for four distinctive types of soils and he indicated several factors that govern the surface settlement. As a rule, he pointed out, the settlements above a single tunnel are more or less symmetrical about

the vertical axis of the tunnel and they form a depression with a shape roughly resembling an error function or normal probability curve.

Several other workers (Attewell, 1977; Glossop, 1978; O'Reilly and New, 1982) have carried out surveys of case history data and they have suggested different empirical values for parameters K_a and n in equation 2.2.

In the present work, it was decided to develop a little further the bank of case history data reported in previous works, from which specification of new values of empirical parameters in equation 2.2 could be attempted. This matter will be discussed later in Section 2.5.

2.4 MODELLING.

Physical models are used in an attempt to replicate, observe and record the actual deformations that take place in the soil around an opening. This method involves construction of a scaled model of a real tunnel and then observing the nature of the soil deformation when the tunnel experiences a range of internal and/or external stress variations. The major difficulty in this procedure is to reproduce all details of the tunnelling process in a model. However, several tunnel model tests have been

carried out in clays and sands and from which the observed data were used for comparison with existing methods of calculation.

From model tunnels, Atkinson and Potts (1976) derived two expressions for the point of inflexion i.

$i = 0.25 (z_o + R)$ for sand without surface loading

and,

$i = 0.125 (3z_o + R)$ for dense sand and overconsolidated kaolin, both with surface loading.

Where z_o is the depth of soil cover , and R is the excavation radius.

Cording et al.(1976) have also used physical models to study the relationship between the volume of ground loss into the tunnel, the shape of settlement trough, and volume changes developed in the soil.

The laboratory experiments have been performed on models under normal gravitational acceleration or accelerated in a large diameter centrifuge in order to increase the stresses due to body-weight forces. The latter type of model has been tested in granular soils and a constant acceleration applied to induce stresses in the model equal to those in an equivalent prototype structure larger than the model.

It should be emphasized here that laboratory experiments are basically plane strain models.

Another type of model is also used to analyse the ground behaviour during tunnelling operations through soils. When a tunnel is excavated the major problem is the uncontrolled intrusive movement of soil from the working face. This movement is transmitted to the surface and consequently a settlement trough is formed.

The intrusion of the soil into the tunnel is directly related to the ground loss. Consequently, the rate process is an important factor, since when taken into account with the rate of tunnel face advance they determine the volume of ground loss at the tunnel.

Broms and Bennermark (1967) studied the extrusion of clay from a small vertical opening in the side of a cylinder. This was deemed to be analogous to the soil extrusion from a hole in a retaining wall. They found a stability relationship to define the failure that could occur :

$$\frac{(\sigma_o - \sigma_c)}{c_u} = 6 \text{ to } 8$$

where σ_o = applied stress,

σ_c = confining pressure,

and c_u = undrained shear strength.

In the context of the clay soil intrusion at a tunnel face, Deere et al.(1969) termed the relationship 'Simple Overload Factor' (OFS). Broms and Bennermark found an OFS value of 6.28 (Glossop, 1978) from a theoretical analysis of semi-circular shear failure at the tunnel face, and this value showed good agreeement with the experimental results. However, Moretto (1969), Peck (1969), Ward (1969), and Kuesel (1972) have noted unstable conditions at lower stability ratios.

Attewell and Boden (1971) have proposed another stability ratio based on extrusion tests. By examining the failure concepts upon which previous similar works were based they suggested that a ratio derived from the maximum acceleration of intrusive movement more appropriately defines the critical depth of interest in a practical tunnelling situation. It was found that acceleration of intrusive movement starts when σ_{ef}/c_u exceeds 4.5, where σ_{ef} is the stress at failure. These authors, and Attewell and Boden (1972) have attempted to relate σ_{ef}/c_u to the liquidity index.

The advantage of the extrusion test is that it

facilitates prediction of the rate of soil intrusion at a tunnel face for any depth of tunnel axis, and, by measuring the actual extrusion movement, prediction of levels of criticality. This prediction is an invaluable parameter in any attempt to relate ground loss to the tunnel construction process.

2.5 SURVEY OF ACTUAL GROUND MOVEMENTS : EMPIRICAL RELATIONS BETWEEN VARIABLES.

The main purpose of this Section is to attempt to define empirical relationships from case history data in order to describe a geometrical form of settlement profile and to predict its magnitude.

Several researchers (Peck, 1969; Attewell, 1977; Glossop, 1978; and O'Reilly and New, 1982) have presented several conclusions from the analyses of case history data and given general guidance for predicting the surface settlement when a tunnel is excavated. All of them have demonstrated the reasonable validity of the normal probability curve for describing the transverse profile of the settlement trough.

In the present work, field data were gathered

together and added to those presented previously by Peck (1969) and Attewell (1977). This work is summarized in Table 2.1.

One of the methods for estimating the parameters of the normal probability curve is based on earlier stochastic arguments (equation 2.2). Peck (1969) has suggested a K_a value of unity and an exponent n equal to 0.8 for clay soils, both estimated from tunnel diameter 2R, and axis depth z_o. Attewell (1977) in his State-of-the-Art Review suggests that the exponent n may itself be closer to unity. This means that i is equivalent to half of the tunnel axis depth for clay soils.

O'Reilly and New (1982) grouped field data on U.K. tunnels for both cohesive and granular soils. Multiple linear regression analyses were performed and they presented the following relations :

$$i = 0.43z_o + 1.1 \text{ for cohesive soils,}$$

and,

$$i = 0.28z_o + 0.1 \text{ for granular soils}$$

where, i and z_o are in metres. Although these equations were related to a particular range of tunnelling

conditions, it has been suggested that for most practical purposes they be simplified to a single expression of the form

$$i = K^* \cdot z_o$$

with $K^* = 0.5$ for cohesive and $K^* = 0.25$ for granular soils. Reviewing the same field data, O'Reilly and New (1982) suggest that K^* varies between 0.4 for stiff clays and 0.7 for soft silty clays. For dry granular materials, K^* varies between 0.2 and 0.3.

Schmidt and Peck (1972) have proposed a more general relation :

$$i/R = (z_o/2R)^n$$

where n is an empirical constant. They have suggested the value of 0.8 for this constant based on empirical studies of several case histories.

In order to estimate the value of the standard deviation parameter i, ninety field data have been searched and assembled in Table 2.1. The study was carried out separating these data in two groups according to the type of the soil. Dimensionless values of i/R were

plotted against another dimensionless value z/2R, for both cohesive and granular soils. A linear regression analysis was performed for both plots and the results shown in Figures 2.1 and 2.2. The linear regression lines obtained by O'Reilly and New (1982) were also drawn in these Figures. Nineteen data cases from Table 2.1 were not considered because some of the information necessary for this study was not found.

Analysis of data from 41 case histories for cohesive soils showed that the linear relationship is not unreasonable. Figure 2.1 shows that the regression line intercept with the i/R axis is close to 0.5 and its slope is steeper than that suggested by O'Reilly and New (1982) from U.K. tunnels.

Although 30 data cases for granular soils were used, the relationship between variables is not confirmed. As seen in Figure 2.2, 23 data points from the total of 30 are located within an area limited vertically between 0.5 and 2.0 (z_o/2R), and horizontally between 1.5 and 2.5 (i/R). However, a linear regression analysis was also carried out and it was found that the regression line intercepts the i/R axis close to unity.

As can be seen in Figure 2.2 for granular soil,

the two regression lines are approximately parallel and the separation of intercept points with the i/R axis is approximately equal to unity.

Based on data shown in both Figures, it seems to be more appropriate to generalise and suggest an n value equal to unity for both cohesive and non-cohesive soil. This evidence confirms the suggestion made by Attewell (1977). By adopting both K_a and n equal to unity, $i=z_o/2$ which is also compatible with the expression suggested by O'Reilly and New (1982) for cohesive soils.

Once knowing the value of i (and the maximum value of the settlement, assumed to lie on the tunnel centre line), the geometrical form of the settlement profile is established. As was discussed in Section 2.2, the maximum settlement w_{max} can be evaluated (equation 2.2) once the value of ground lost (V) is estimated.

An alternative approach to ground loss is to attempt to find an empirical relationship between the observed volumes, V_s, and some obtainable parameter.

Glossop (1978) made an attempt to relate percentage volume loss (V %) to the Stability Ratio (OFS). Both values were plotted graphically using log-linear axes

and the regression analysis has given the following equation :

$$V\ (\%) = -\ 1.14 + 1.33\ OFS.$$

Obviously, this equation gives the first member negative if OFS is too small, but, as an approximate guide, he suggested that OFS values should be greater than 1.3. Glossop attempted also to develop a model that takes into account the tunnel advance rate, tunnel diameter, rate of soil intrusion and time elapsed between excavation and contact grout injection. However, the model seems to be tenuous because it has been tested on only few data.

Attewell (1977) has reviewed with detail the sources of ground loss and the contribution of each of the factors to it. For dense granular soil, with good ground control at the tunnel, V_s was estimated to be 1% to 2% of the tunnel face area. In clay soil, V_s may be estimated at 1% of the tunnel face area if $OFS<4$ and 1% to 5% if $4<OFS<6$.

O'Reilly and New (1982) examined case history data and they have suggested a range of values for V_s according to soil type and tunnel construction method. For stiff fissured clay, driven with or without a shield, V_s varies

between 0.5% and 3%, and for glacial deposits excavated in free air with the use of a shield, $2\% < V_s < 2.5\%$ and $1\% < V_s < 1.25\%$ if compressed air is used. For recent silty clay deposits, with shield excavation in free air, $30\% < V_s < 45\%$, and if excavated with compressed air, $5\% < V_s < 20\%$.

In order to estimate the value of ground loss, V, an attempt was made using data from Table 2.1 assuming that no volume change occurs in the ground during tunnel excavation. Again, the field data were separated into two groups, 41 for cohesive soils and 30 for granular soils. For each of these groups, the values of V_s were separated and have given the following figures :

	Number of cases	
	cohesive	non-cohesive
$V_s \leq 2\%$	23	17
$2\% < V_s \leq 4\%$	8	6
$4\% < V_s \leq 6\%$	2	2
$V_s > 6\%$	5	2
Total	38	27

As can be seen above, the percentage of the total number of tunnels having a ground loss below 2% is high for both groups. If the upper limit of ground loss is

increased to 4%, this percentage goes up to 81.5% and 85% for cohesive and granular soils, respectively. This difference may be attributed to the basic mechanisms of ground movements in both types of materials.

Values of ground loss volume (log axis) and Overload Factor (linear axis) for cohesive soil have been plotted and shown in Figure 2.3, in order to examine in some detail the potential ground losses. Logarithmic regression analysis has been performed using these data and the resulting curve is presented. When the Overload Factor is smaller than about 1, the theoretical potential ground loss is less than about 1%. For Overload Factors between about 1 and 3, the potential ground loss might be up to 2%. For a value close to 8, the V_s is approximately 5%. Clough and Schmidt (1981) have reported higher values of V_s for the same range of Overload Factor values.

2.6 INTERACTION BETWEEN GROUND MOVEMENTS AND STRUCTURES.

Buildings and buried services respond to ground movements by different degrees of deformation according to their rigidity and the position of their constitutive elements.

Several workers have studied the effect of movements on buildings and presented recommendations on allowable settlements of structures. Among these, perhaps the best-known studies are those of Skempton and McDonald (1956), Polskin and Tokar (1957) and Burland and Wroth (1975). More recently, Wahls (1981) has also studied this matter in some detail. There is, however, a basic feature in the tunnelling process that is not entirely compatible with these recommendations : buildings impose long-term self-weight settlement and deformations, and much of any potential damage can be prevented by taking up deformation during the construction stage, while tunnel construction induces most of the movements in a structure very quickly and prevention against damage cannot thus be achieved.

Once the ground deformations due to tunnelling have been estimated, their effects on nearby structures and services may be predicted. The analysis of interactions between structures and ground are invariably quite complex because of the uniqueness of conditions at each site. The problem is inherently less difficult for services because of the relative geometrical simplicity of the system. Buildings vary so much one from another and seldom perform as designed because the actual material properties are different from those assumed in the design. It is well-known that ground movements may be modified by

soil-structure interaction, but the behaviour of structures or buried services subsequent to initial damage is not usually considered in analyses. Such complexities cannot be taken into account in any analytical solutions, and these methods can be used only for certain simplified situations.

In order to tackle the problem of soil-structure interaction it is necessary to have a clear and consistent set of definitions describing the types of movements and deformations experienced by structures or services.

Since the response of above-ground structures to ground movements is out of the scope of this study, only the case of in-ground structures will be considered. It is noted that Attewell and Yeates (1984) have recently studied the two dimensional ground-structure interaction problem of an open frame structure affected by tunnelling-induced settlement.

The stresses and displacements developed in a buried pipe during nearby tunnel excavation are very difficult to predict theoretically because they are strongly influenced by the nature of the soil-pipe interaction. The problem is further complicated by other factors such as the age of the pipe, its in-trench

construction, traffic loading, other long-term quasi-static stresses , and so on.

When a pipe is laid in the ground it will obviously be affected to some extent by the movement of that ground. In the context of soft ground tunnelling the area where the ground is under tension is of the greatest concern as regards the possible failure of pipelines. The level of risk to a main is, in practice, very wide because of a large variations of material properties. In many cases, old pipes might be highly stressed because of deterioration in material quality and changes in past loading conditions.

Although during recent years the effect of ground movements caused by tunnelling in soft ground have been reported in the literature, the truly three-dimensional situation of the problem has been ignored in these studies. It is known that when the tunnel face progresses, buried pipelines within the ground settlement trough may respond by compressing, stretching, bending, shearing, warping and twisting. Such a complex response will depend largely on the relative stiffness between pipe and surrounding soil, and the relative position of the portion of the pipeline to the tunnel drive.

In an initial study it may be assumed that the

pipe deforms conformably with the predicted ground deformations which develop without the presence of the pipe. A pipe on or close to and roughly parallel to the tunnel centre line could thus fail in bending, particularly if above a shallow tunnel where the induced radii of ground curvature could be small. This same mode of failure could apply to a jointless pipeline at right angles to a centre line. Additionally, direct horizontal tensions towards the limbs of a settlement trough could suplement the induced bending tensions to facilitate failure. The ground-structure interaction associated with horizontal movements is somewhat analogous to the skin friction problem in piles (Poulos and Davis, 1980). Major difficulties in such kind of analyses relate to the definition of fixidity (zero movement) points on the pipeline and to the definition of appropriate soil physical properties.

Once the result is obtained using a selected method of calculation, comparison is then made with appropriate allowable pipe deformations in order to verify if damage may occur. Generally, axial tensile stress (compounded from components of direct tension and bending tension) may be chosen as the most appropriate limiting criterion for failure of brittle pipe material. Occasionally, limitation of extension on a pipeline joint may be important.

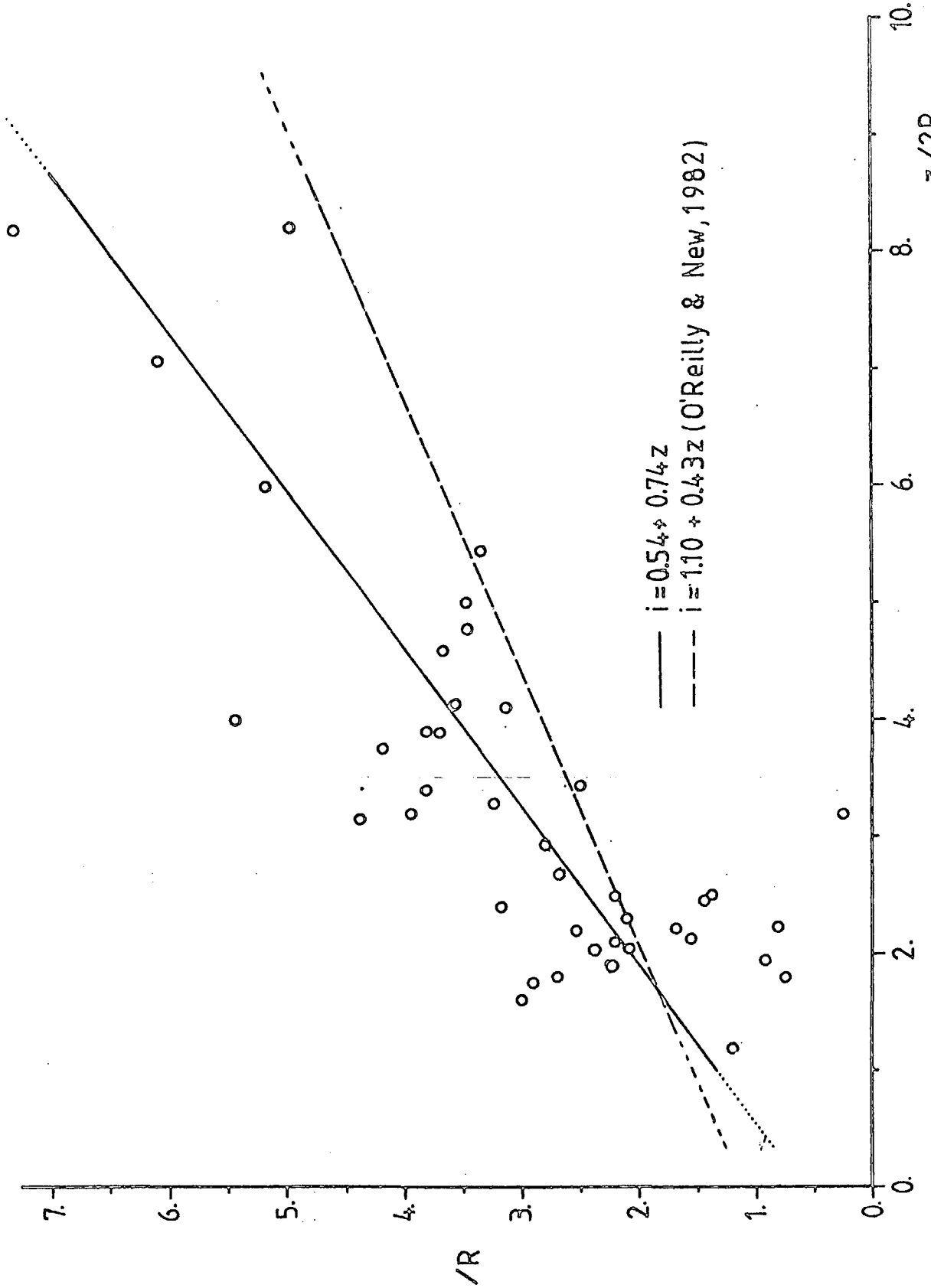

FIG. 2.1) Cohesive soils - i/R vs z/2R.

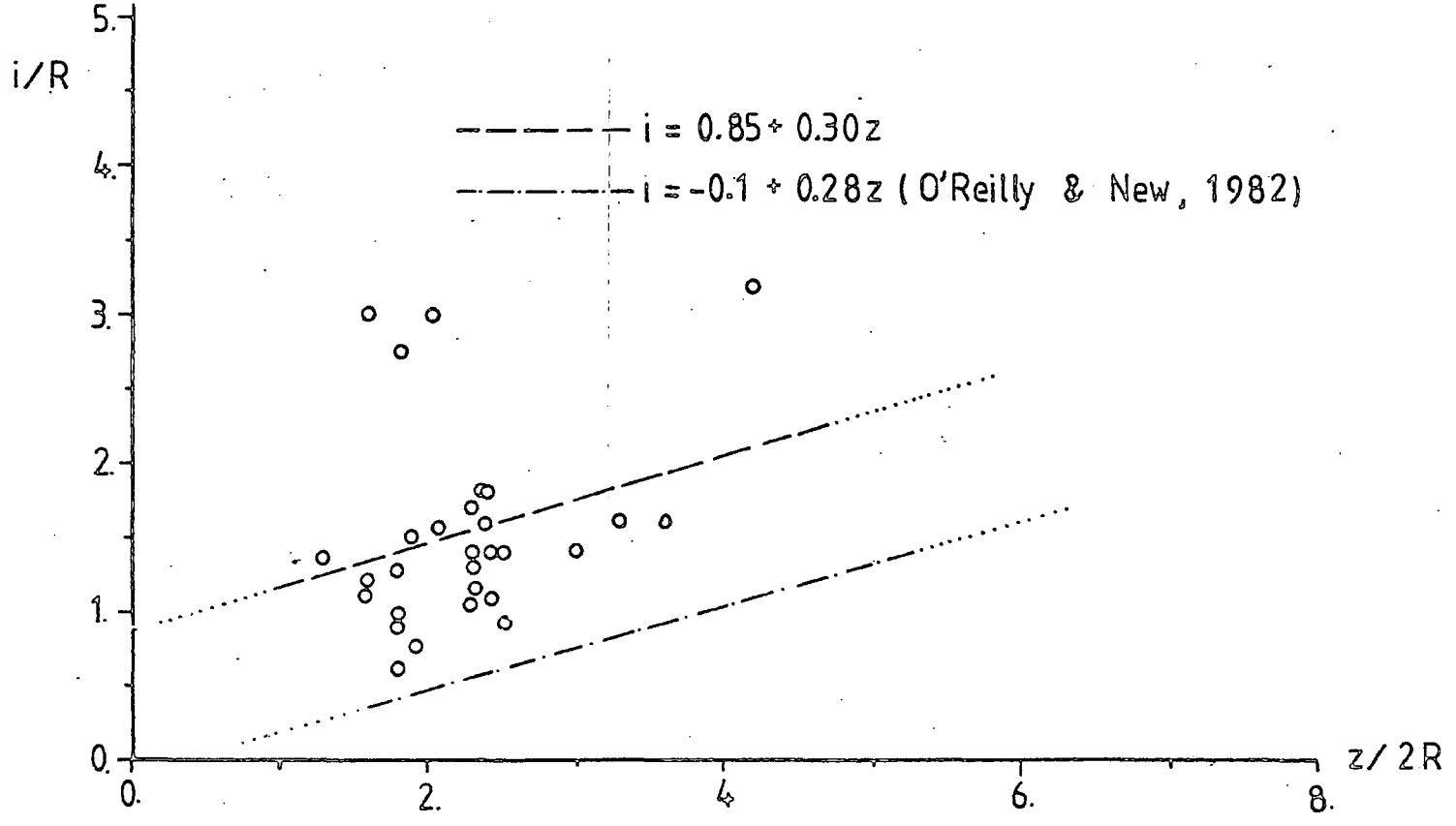

FIG. 2.2) Granular soils - i/R vs z/2R.

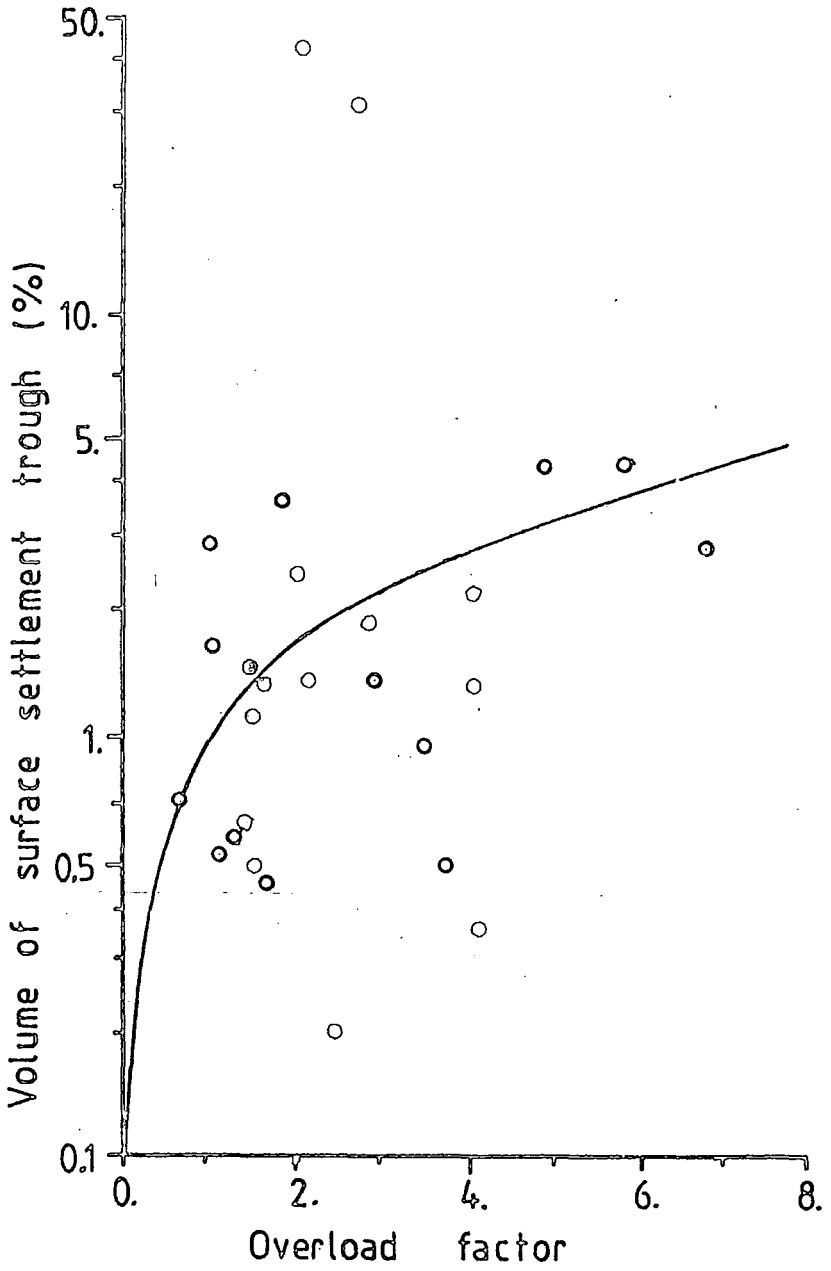

FIG. 2.3) Volume of surface settlement trough vs Overload factor for tunnel in cohesive soils.

TABLE 2.1 - DATA ON TUNNELS AND TUNNELLING CONDITIONS (generally after Peck, 1969; Attewell, 1977, but with additions).

TUNNEL	TUNNEL DATA			SETTL.	GEOTECHN. PROPERT.		VOLUMES			TROUGH				TUNNELLING METHOD AND SOIL CONDITIONS.
	Depth z (m)	Diam. 2R (m)	z/2R	(mm)	c_u (kN/m^2)	$\gamma z/c_u$	V_{exc} (m^3/m)	V_s (m^3/m)	V_s (%)	i (m)	i/R	3i (m)	w =2.5i (m)	
1. LONDON TRANSPORT FLEET LINE, GREEN PK. (Attewell & Farmer, 1974, a,b)	29.3	4.15	7.06	6.17	270	2.1	13.52	0.199	1.4	12.6	6.1	37.8	32. (β=46°)	Shield construction. Cast iron lining, 7 segments per ring, erected in shield tail. Annulus behind rings contact grouted every shove. Stiff, fissured, over-consolidated London Clay. Tunnel horizon blue clay overlain by weathered brown clay.
2. N.W.A SEWERAGE SCHEME, TYNESIDE, HEBBURN. (Attewell et al, 1975)	7.5	2.01	3.9	7.86	75	2.02	3.17	0.077	2.42	3.9	3.71	11.7	9.75	Shield construction. 5 segment precast concrete lining per ring erected in shield tail. Annulus behind rings contact grouted every three rings. Laminated clay overlain by stony clay.
3. N.W.A SEWERAGE SCHEME, WILLINGTON QUAY SYPHON, CONTRACT 32. (Attewell & Farmer, 1976)	13.375	4.25	3.15	81.5	33	9.4	24.37	1.86	13.1	9.1	4.28	27.3	22.7 (β=57°)	Shield construction. Compressed air pressure 90 kN/m^2. 7 segment precast concrete lining per ring erected in shield tail. Annulus behind rings contact grouted every three rings. Silty alluvium/alluvial with sand and gravel lenses containing water at artesian pressure.
4. N.W.A. SEWERAGE SCHEME, TYNE-SIDE, HOWDON. (Glossop, 1978)	14.18	3.625	3.91	11.2	100	2.98	0.37	0.194	1.9	6.9	3.81	20.7	17.25 (β=47°)	Shieldless construction. 5 segment pre-cast concrete lining per ring erected up to the face. Annulus behind rings contact grouted every three rings. Boulder/Stony clay.

* Estimated value.

(Continued overleaf)

Table 2.1 Continued.

TUNNEL	TUNNEL DATA			SETTL.	GEOTECH. PROPERT.		VOLUMES			TROUGH				TUNNELLING METHOD AND SOIL CONDITIONS.
	Depth z (m)	Diam. 2R (m)	z/2R	(mm)	c_u (kN/m^2)	$\gamma z/c_u$	V_{exc} (m^3/m)	V_s (m^3/m)	V_s (%)	i (m)	i/R	3i (m)	w=2.5i (m)	
5. LONDON TRANSPORT FLEET LINE REGENTS PARK, NORTHBOUND TUNNEL (Barratt & Tyler, 1975)	20	4.15	8.2	7	230	1.70	13.52	0.18	1.3	10.3	4.96	30.9	25.75 (β=50°)	Shield construction. Expanded concrete segmental lining. Stiff fissured, over-consolidated London Clay.
6. LONDON TRANSPORT FLEET LINE, REGENTS PARK, SOUTHBOUND TUNNEL (Barratt & Tyler, 1976)	34	4.15	8.2	5	230	1.7	13.52	0.19	1.4	15.2	7.32	45.6	38 (β=47°)	Shield construction. Expanded concrete segmental lining. Stiff fissured, over-consolidated London Clay.
7. LONDON TRANSPORT EXPERIMENTAL TUNNEL. NEW CROSS. (Boden & McCaul, 1976)	10	4.15	2.4	21.5	-	-	13.52			5	1.82	15	12.5 (β=46°)	Slurry (bentonite) shield. Sandy gravel.
8. TRRL TUNNELLING TRIALS. CHINNOR (Higgett & Boden, 1974; McCaul et al, 1976)	8	5	1.6	8	-	-				7	3	21	17.5 (β=7°)	Full face tunnelling machine, cruciform head with drag picks jacking against a two-section reaction ring. Lining comprised mining arches at 1m spacing. Highly discontinuous Lower Chalk formation.
9. WASHINGTON D.C. METRO, LAFAYETTE SQUARE. (Butler & Hampton, 1975)	11.6	6.4	2.25	112.8	-	-	4.60	1.21	3.8	4.5	1.4	13.5	11.25 (β=35°)	Shield construction with bucket digger. Primary liner of steel ribs and hardwood lagging boards expanding during and after the shove. Sand-cement - bentonite grout injected originally through liner but later through of shield at the front. Sand and gravel interbeded silty sand, sand and clay.

* Estimated value.

(Continued overleaf)

Table 2.1 Continued.

TUNNEL	TUNNEL DATA			SETTL.	GEOTECH. PROPERT.		VOLUMES			TROUGH				TUNNELLING METHOD AND SOIL CONDITIONS.
	Depth z (m)	Diam. 2R (m)	z/2R	(mm)	c_u (kN/m^2)	$\gamma z/c_u$	V_{exc} (m^3/m)	V_s (m^3/m)	V_s (%)	i (m)	i/R	3i (m)	w=2.5i (m)	
10. WASHINGTON D.C. METRO. PROJECT A-2 1st. TUNNEL.														Shield construction with bucket digger. Primary liner of steel ribs and timber lagging expanded during and after the shove. Partial de-watering with wells 60m apart on centre line. Medium dense silty and gravel, interbedded with sandy, silty clays.
C LINE	14.6	6.4	2.3	152	75	4		1.7		4.5	1.4	3.5	11.25 (β=28°)	
B LINE	14.6	6.4	2.3	139	75	4		1.5		4.2	1.3	12.6	11	
A LINE	14.6	6.4	2.3	76	75	4	4.0	1.0	3-5	5.4	1.7	16.2	14 (β=36°)	
11. WASHINGTON D.C.METRO. TREASURY YARD (Hansmire, 1975)	11.6	6.4	1.8	280	75	3	6.02	1.4	4.3	1.9	0.6	5.7	5 (β=9°)	Shield construction with ripper bucket digger. Primary liner or steel ribs (four-section) placed on 4 ft centres with full timber lagging. Lining expansion during and after shove. Medium dense silty sand and gravel interbedded with sand, silty clays.
12. WASHINGTON D.C. 1st TUNNEL														Articulated shield with bucket digger. Steel segments erected in tailskin and grouted before shove. Dense sand and gravel , very dense , slightly cemented sand.
SECTION A	20.9	6.4	3.3	6	-	-		0.1		5.1	1.6	15.3	12 (β=23°)	
SECTION B	23	6.4	3.6	3	-	-		<0.1	0.3					
13.FRANKFURT SHIELD, FONRGASSE(T-9) (Chambosse, 1972;Sauer & Lana,1973; Breth & Chambosse,1972)	12.4	6.5	1.9	70	-	-	2.23	0.86	2.6	4.9	1.5	14.7	12 (β=35°)	Shield construction. Bolted concrete segments. Sand with some limestone and clay marl lenses.
14.FRANKFURT SOMPLATZ (Authors as in 13)	15	6.5	2.3	23	130-550	0.6-2.5 (1.5 av.)	0.47	0.39	1.2	6.8	2.1	20.4	17 (β=42°)	Shield construction. Bolted concrete segments. Frankfurt clay marl with some limestone and sand lenses.

* Estimated value.

(Continued overleaf)

Table 2.1 Continued.

TUNNEL	TUNNEL DATA			SETTL.	GEOTECH. PROPERT.		VOLUMES			TROUGH				TUNNELLING METHOD AND SOIL CONDITIONS.
	Depth z (m)	Diam. 2R (m)	z/2R	(mm)	c_u (kN/m^2)	$\bar{\gamma}.z/c_u$	V_{exc} (m^3/m)	V_s (m^3/m)	V_s (%)	i (m)	i/R	3i (m)	w=2.5i	
15. FRANKFURT SHIELD DOMINIKANER-GASSE (Authors as in 13)	10.3	6.5	1.6	140	-	-	5.58	1.36	4.1	3.9	1.2	11.7	10 (β=33°)	Shield construction. Bolted concrete segments. Sand with some limestone and sand lenses.
16. FRANKFURT, NO SHIELD, BAULOS 17 (Authors as in 13)	13.3	6.5	2.1	13	130-550	0.6-2.5 (1.5 av.)	0.16	0.23	0.7	7.1	2.2	21.3	18 (β=48°)	Shieldless construction : heading and bench. Soil anchors; shotcrete and light steel ribs for support. Frankfurt Clay marl with some limestone and sand lenses.
17. FRANKFURT, NO SHIELD, BAULOS 18a TUNNEL 13 (Authors as in 13)	13.3	6.5	2.5	10	130-550	0.6-2.5 (1.5 av.)	0.09	0.18	0.5	7.1	2.2	21.3	18 (β=43°)	Shieldless construction : heading and bench. Soil anchors; shotcrete and light steel ribs for support. Frankfurt Clay marl with some limestone and sand lenses.
18. HEATHROW CARGO TUNNEL (Wood & Gibb, 1971; Smyth-Osbourne, 1971)	13.3	10.9	1.2	12	72-295	1-4 (2.5 av.)	0.04	0.19	0.2	6.5	1.2	19.5	16 (β=38°)	Shield construction and hand excavated. No tail to the shield - concrete segmental lining expanded behind shield. Upper section of London Clay with 3.6m of clay cover under wet gravel.
19. SAO PAULO METRO, BOA VISTA. (Costa, et al, 1974)	11.8	5.5	2.2	70	-	-	6.0	1.2	5	6.9	2.5	20.7	17 (β=50°)	Shield construction with compressed air. Sand and clay lenses.
20. BRUSSELS METRO. (Vinnel & Herman, 1969)	16	10	1.6	150	-	-	5.0	2.0	2.5	5.5	1.1	16.5	13 (β=26°)	Shield construction, hand excavated. Lining segments built in tail. Upper half of tunnel - uniform cohesionless sand; lower half of tunnel - clayey sand.

* Estimated value.

(Continued overleaf)

Table 2.1 Continued.

TUNNEL	TUNNEL DATA			SETTL.	GEOTECH. PROPERT.		VOLUMES			TROUGH				TUNNELLING METHOD AND SOIL CONDITIONS.
	Depth. z (m)	Diam. 2R (m)	z/2R	(mm)	c_u (kN/m²)	$\gamma z/c_u$	V_{exc} (m^3/m)	V_s (m^3/m)	V_s (%)	i (m)	i/R	3i (m)	w=2.5i (m)	
21. MEXICO CITY SYPHON II, GONZALEZ. (Tinajero & Vleitez, 1972)	11.7	2.9	4.0	105	40	5	78.9	2.1	38	7.8	5.4	23.4	20 (β=58°)	Shield with oscillating cutters. Steel lining. Lining grouted 8m behind shield. Cutters offer support to three - quarter of face. Ground dewatering before tunnelling. Plastic lacustrine clay.
22. LOWER MARKET ST., B.A.R.T., SAN FRANCISCO (Kuesel, 1972)	19.0	5.5	3.4	36	40	14	1.73	0.64	2.7	6.9	2.5	20.7	17 (β=37°)	Shield with a rotating cutter wheel. Compressed air support. Grouted segmental lining. Soft plastic clay.
23. WASHINGTON D.C. F2a-1 ROUTE TUNNELS. (Cording et al, 1976).														Articulated (3 segment) shield construction. Excavation by large, half moon shaped, hydraulically - operated digger spade. Tunnelling below the water table, but ground de- watered by deep well pumping in advance of tunnel construction. Segmental steel lining erected in tail of shield. Serves as both a primary and secondary or temporary support. Very variable medium stiff- to-hard clays ; clayey sands-sandy clays; coarse sand and gravel.
1 IB	20.3	5.5	3.7	5	-	-	0.06	0.12	0.5					
3 IB	20.3	5.5	3.7	3	-	-	0.02	0.07	0.3					
9 IB	22.5	5.5	4.1	8	-	-	0.16	0.2	0.8	8.52	3.1	25.56	21 (β=39°)	
10 IB	21.4	5.5	3.9	13	-	-	0.42	0.32	1.3				26	
11 IB	22.0	5.5	4.0	10	-	-	0.23	0.23	1.0	9.90	3.6	27.7	25 (β=45°)	
24. MISSION LINE. B.A.R.T. SAN FRANCISCO (Peck, 1969)	10.97	5.33	2.06	10.5 (9-12)	-	-	22.31	0.11	0.5	4.2	1.57	12.6	10.5	Mechanical shield tunnelling with 90 kN/m² compressed air. Dense, silty fine sand (N=30) with occasional thin lenses of peat. Dewatering by deep wells.
25. TORONTO SUBWAY (Peck, 1969)	11.89 (13.41 10.36)	30.5					21.07	0.21	1.0	2.7	1.04	7.1	6.7	Shield tunnelling, hand excavation. Medium-to-fine uniform dense sand (N=40 to 60) above the water table.
26. MISSION LINE. B.A.R.T. SAN FRANCISCO (Peck, 1969)	10.97	5.33	2.06	1.5	-	-	22.31	0.03	0.13	8.0	3.0	24.0	20.0	Mechanical shield tunnelling with 62 kN/m² air pressure. Slightly cemented dense silty fine sand (N=40 to 60). Dewatering by deep wells.

* Estimated value.

(Continued overleaf)

Table 2.1 Continued.

TUNNEL	TUNNEL DATA			SETTL.	GEOTECH. PROPERT.		VOLUMES			TROUGH				TUNNELLING METHOD AND SOIL CONDITIONS.
	Depth z (m)	Diam. 2R (m)	z/2R	(mm)	c_u (kN/m^2)	$\sigma \cdot z/c_u$	V_{exc} (m^3/m)	V_s (m^3/m)	V_s (%)	i (m)	i/R	3i (m)	w=2.5i	
27. WILSON TUNNEL. HAWAII. (Peck, 1969)	15.24	10.06	1.51	21.3	-	-	79.48							Horse-shoe shaped small drifts, hand excavated with ribs and lagging. Residual saprolitic tropically - weathered volcanic granular soil, readily cut by compressed air spades.
28. WILSON TUNNEL. HAWAII (Peck, 1969)	30.48	10.06	3.03	61.0	-	-	79.48							As for 27.
29. GARRISON TEST TUNNEL. (Burke, 1957)	36.88	10.97	3.36	18.29 (6.1-24.4)	958	0.77	94.51							Ribs and lagging support. Full-face blasting in a clay shale having an unconfined compressive strength of 958 kN/m^2.
30. SUBWAY CONTRACT D3, CHICAGO. (Peck, 1969)	23.47	7.31	3.2	36.6	38-78	8.09*	41.97	0.08	0.20	0.9	0.25	2.7	2.55	Hand excavated , horseshoe - shaped cross-section tunnel. Face benched and tunnel supported by ribs and liner plates. Compressed air pressure of 30 kN/m^2. Bottom half of tunnel in hard clay. Stiff clay (unconfined compressive strength=96-192kN/m^2) for 3m above crown. Soft-to-medium clay (u.c.s.=36-96 kN/m^2) above that.
31. G.N.R.R. SEATTLE (Hussey et al, 1915)	37.49	11.89	3.15	18.3	-	-	111.03	2.88	2.6	63.0	10.59	18).0	157.5	Hand excavated using small drifts with a central core. Timbered support for hard clayey till. Ravelling at the crown; poling bars used.
32. KYOTO TOKYO, SUBWAY (Shiraishi- personal communication to Peck)	22.55	7.01	3.22	12.2	77	5.85*	38.59	1.66	4.3	54.4	15.52	163.2	132	Hand excavated sectional shield. Face breated and lining segments erected in shield. Normally consolidated sensitive clay (u.c.s. = 72 kN/m^2) requiring no compressed air support.
33. B.A.R.T. SAN FRANCISCO (Peck, 1969)	17.98	5.48	3.28	46.0	77	4.67*	23.67	1.02	4.3	8.9	3.24	26.7	22.2	Shield tunnelling with breasted face. Liner segments erected in the shield. Moderately sensitive clay (u.c.s.= 77 kN/m^2) requiring no compressed air support.

* Estimated value.

(Continued overleaf)

Table 2.1 Continued.

TUNNEL	TUNNEL DATA			SETTL.	GEOTECH. PROPERT.		VOLUME			TROUGH				TUNNELLING METHOD AND SOIL CONDITIONS.
	Depth z (m)	Diam. 2R (m)	z/2R	(mm)	c_u (kN/m^2)	$\gamma z/c_u$	V_{exc} (m^3/m)	V_s (m^3/m)	V_s (%)	i (m)	i/R	3i (m)	w=2.5i (m)	
34. OTTAWA SEWER (Eden & Bozozuk, 1962)	1.29	3.05	6.00	6.1	354	1.03*	7.31	0.12	1.6	7.9	5.18	23.7	19.7	Mechanical shield excavation. Liner segments erected behind the shield. Sensitive Leda clay (u.c.s.=354kN/m^2) required 28-34 kN/m^2 compressed air support.
35. TORONTO SUBWAY. (Matish & Carling, unpublished)	13.11	5.33	2.46	22.0 (0.13-0.29)	67	3.91*	22.31	0.21 (0.13-0.3)	0.95	3.8	1.42	11.4	9.5	Shield tunnelling, hand excavation. Air pressure of 69-83 kN/m^2. Silty clay (u.c.s.=77kN/m^2) at invert level.
36. CHICAGO D-5 (Peck, 1969)	11.89	6.10	1.95	39.6 (18.3-61.0)	67	3.55*	29.22	0.28 (0.23-0.3)	0.95	2.8	0.92	8.4	7.0	Hand excavated benched heading with rib and liner plate support. Glacial lake clay (u.c.s.=57kN/m^2 at axis level and 33kN/m^2 at 3m depth). Nearer surface, ground is stronger.
37. TORONTO SUBWAY (Peck, 1969)														Dense sand above ground water level.
FIRST TUNNEL	10.36	5.33	1.94	85	-	-	22.31	0.42	1.9	1.9	0.73	5.7	4.7	
SECOND TUNNEL	13.41	5.33	2.52	140	-	-	22.31	0.85	3.8	2.4	0.92	7.2	6.0	
38. SAO PAULO (Terzaghi, 1950	30.48	2.74	11.12	204			5.9	2.97	50.39	5.8	4.2	17.4	14.5	Tunnelling in stiff clay with many construction difficulties.
39. AIRSHIRE JOINT DRAINAGE SCHEME TUNNEL (Wadie, 1976)														Shield tunnelling, hand excavation through water-bearing raised beach sands of Clyde Estuary, Scotland. Timber breasting with face jacks. Internal pressure 1.4 to 1.6 atmospheres absolute. Non-expanding concrete lining segments with cement-bentonite grout injected into void at end of each 12hr shift.
FIRST TUNNEL	6.3	2.59	2.43	13.5	-	-	6.89	0.06	0.87	1.41	1.09	4.23	3.52	
SECOND TUNNEL	6.2	2.59	2.39	16.0	-	-	6.89	0.06	0.87	1.60	1.23	4.80	4.00	
40. ACTON GRANGE SEWER, HARRINGTON														Slurry (bentonite) shield, machine excavated through a mixed face comprising mainly sand with some boulders but with a small proportion of Bunter Sandstone in the invert. Water table level is partway up face. Bolted precast concrete segm. lining.
SECTION C-C'	5.75	2.44	2.36	19.9	-	-	6.16	0.086	1.37	1.73	1.42	5.19	4.37	
SECTION D-D' (O'Reilly et al, 1982)	5.75	2.44	2.36	14.2	-	-	6.16	0.071	1.10	2.00	1.64	6.00	5.00	

* Estimated value.

(Continued overleaf)

Table 2.1 Continued.

TUNNEL	TUNNEL DATA			SETTL.	GEOTECH. PROPERT.		VOLUMES			TROUGH				TUNNELLING METHOD AND SOIL CONDITIONS.
	Depth z (m)	Diam. 2R (m)	z/2R	(mm)	c_u (kN/m^2)	$\gamma z/c_u$	V_{exc} (m^3/m)	V_s (m^3/m)	V_s (%)	i (m)	i/R	3i (m)	w=2.5i (m)	
41.WHITE MUD CREEK TUNNEL EDMONTON, ALBERTA (Thomson & El-Nahhas,1980	15.25	6.05	2.52		-	-								Two moles without shields (each 6.05m diam.). Poorly indurated clay shale interbedded with thin sandstone strata.Bolted steel segmental ribs in temporary lining and replaced by plain concrete lining.
42. 170 STREET TUNNEL, EDMONTON, ALBERTA. (As in 41)	21.5	2.56	8.40	12	-	-								Mole with shield. Temporary lining consisted of segmental steel ribs and later replaced by plain concrete lining. Major portion of the tunnel excavated through till.
43.NAGOYA SUBWAY. (Kawamoto & Okuzono, 1977)														Shield tunnelling. Twin circular tunnels of 6.4m diameter placed side by side. Tunnel constructed through the alluvium deposit.
SECTION A	17.4	6.4	2.72	48										
SECTION B	19.2	6.4	3.0	45										
SECTION C	16.5	6.4	2.58	46										
44.STOCKTON-ON-TEES.STAGE I INTERCEPTOR SEWER MEASUREMENT. SECTION C (McCaul, 1978)	6.28	1.26	4.98	43.7	30.5	2.7	1.25	0.38	30.4	3.48	3.47	5.51	8.70	Mini-tunnel system. Hand excavation from shield. Three-segment, smooth, precast concrete lining. Soft, silty, sandy clay.
45.STOCKTON-ON-TEES.STAGE IV INTERCEPTOR SEWER MEASUREMENT SECTION D (McCaul, 1978)	5.86	1.26	4.65	56.3	41.7	2.2	1.25	0.52	41.5	41.7	3.68	5.84	9.22	Mini-tunnel system. Hand excavation from shield. Three-segment, smooth, precast concrete lining. Soft,silty, sandy clay.
46.NEW CROSS L.T.S. EXPERIMENTAL TUNNEL. (Bodon & McCaul,1974)	10	4.15	2.4	21.5	-	-	13.52	0.27	2.0	5	1.82	15	12.5	Slurry (bentonite) shield. Sandy gravel.

* Estimated value.

(Continued overleaf)

Table 2.1 Continued.

TUNNEL	TUNNEL DATA			SETTL.	GEOTECH. PROPERT.		VOLUMES			TROUGH				TUNNELLING METHOD AND SOIL CONDITIONS.
	Depth z (m)	Diam. 2R (m)	z/2R	(mm)	c_u (kN/m^2)	$\gamma z/c_u$	V_{exc} (m^3/m)	V_s (m^3/m)	V_s (%)	i (m)	i/R	3i (m)	w=2.5i (m)	
47. HAMBURG-WILHELMSBURG COLLECTOR. (Jacob, 1978)	19.24	4.48	4.3	0-10	-	-								Well bedded, sharp sand and gravel (0.2-100 mm), boulders to 80 cm overlain by clay, peat and fill. Water table 16 m above invert. Hydro-shield. Reinforced concrete lining. Air pressure 1.6 m.
48. ANTWERP METRO. (Jacob, 1978)	24	6.56	3.7	6-7	-	-								Hydro - shield. Reinforced concrete lining. Fine alluvial sand, interlayers of clay, overlying overconsolidated clay. Water table 12m above invert, lowered to 10m before tunnelling.
49. AGASEGAWA SEWER MAIN No2 KATSUSHIKAKU, TOKYO. (Eng. News Record, 1974)	av.10	5.05	2.0	25-90	-	-								Slurry mole, concrete segmental primary lining. Mixed face of fine "quick" sand and silt and clay, N<20. Water table 7m above crown.
50. TAKUDO WATER MAIN, SUGUINAMI-KU, TOKYO. (Maki et al, 1977)	27.8	3.55	7.8	21.9 max. 1.4 av.	-	-								Slurry mole concrete segmental lining. Cemented dense sandy gravel (2 - 150 mm), N > 50, overlain by clay, sandy gravel and silty. Water table 11.5m above crown.
51. YOTSUGUI SEWER BRANCH, KATSUSHIKA-KU, TOKYO. (Miki et al, 1977)	7.4	2.40	3.1	20 max 15 av.	-	-								Slurry mole, steel segmental lining. Loose alluvial sand with silt; N=5-20. Water table 5.4m above crown.
52. SOUTHERN LINE PROPOSAL AMSTERDAM METRO. SECTION CHURCHILLHAM-SINGELGRACHT (Publ. Works Dept., 1975)	19.40-9.85 18.50 av.	6.2	3.1-1.6 3.0 av.	27.55	-	-		0.3-0.6	1-2	4.38	1.41	13.13	10.95	Fully mechanized shield with full face support. Medium to very dense sand and silt, overlain by clay, peat and fill. Water table 2.0m above invert.

*Estimated value.

(Continued overleaf)

Table 2.1 Continued.

TUNNEL	TUNNEL DATA			SETTL.	GEOTECH. PROPERT.		VOLUMES			TROUGH				TUNNELLING METHOD AND SOIL CONDITIONS.
	Depth z (m)	Diam. 2R (m)	z/2R	(mm)	c_u (kN/m^2)	$\gamma z/c_u$	V_{exc} (m^3/m)	V_s (m^3/m)	V_s (%)	i (m)	i/R	3i (m)	w=2.5i (m)	
53.CHICAGO S-6 (Peck, 1969)	10.97	6.10	1.8	25.6 (15.0-36.6)	5-7	3.85*	29.22	0.15	0.5	2.3	0.75	6.9	5.7	Hand excavated benched heading with rib and liner plate support. 83 kN/m^2 compressed air support. Glacial lake clay (u.c.s.=57 kN/m^2 at axis level and 33 kN/m^2 at 3m depth). Nearer surface, ground is stronger.
54.LINER PLATE TUNNEL,SABESP, BRAZIL.(Negro & Eisenstein, 1981)	8.0 appr.	3.6	2.22	25.0 av.	250	4.03	10.5	0.213	2.03	3.0	1.67	9.0	7.5	Full face hand excavation with circular steel segmental lining plates erected immediately behind the face. Tertiary soft porous clay and clayey dense sand.
55.HORSE-SHOE TUNNEL,SABESP, BRAZIL. (Authors as in 54)	9.00 appr.	3.6	2.5	15.5	250	4.03	12.5	0.171	1.37	2.5	1.38	7.5	6.25	Same as above.
56.MAIN TUNNEL SABESP,BRAZIL. (Authors as in 54)	8.5 appr.	3.96	2.14	5.0	250	4.28	12.8	0.048	0.37	3.0	1.52	9.0	7.5	Hand excavated in three stages : heading, bench and invert. Shotcrete 10-13 cm thick, with 10X10 cm steel wire mesh. Soil conditions as above.
57.ANGLIAN WATER AUTHORITY HAYCROFT RELIEF SEWER (O'Reilly & New, 1982)														Hand excavated in shield; lined with concrete segments ; compressed air applied about 20 days after excavation ; lower 60% of face stiff stony clay (Grimsby Marine Warp) overlain with 2.5 m of stiff clay.
a)	8.0	2.7	2.96	95	12	13.4	5.73	0.905	15.8	3.8	2.81	11.4	9.5	
b)	5.5	2.7	2.04	60	12	9.2	5.73	0.481	8.4	3.2	2.37	9.6	8.0	
c)	5.5	2.7	2.04	58	12	9.2	5.73	0.407	7.1	2.8	2.07	8.4	7.0	
d)	6.5	2.7	2.41	97	12	10.8	5.73	1.046	18.2	4.3	3.19	12.9	10.75	

*Estimated value.

(Continued overleaf)

Table 2.1 Continued.

TUNNEL	TUNNEL DATA			SETTL.	GEOTECH. PROPERT.		VOLUMES			TROUGH				TUNNELLING METHOD AND SOIL CONDITIONS.
	Depth z (m)	Diam. 2R (m)	z/2R	(mm)	c_u (kN/m^2)	$\gamma z/c_u$	V_{exc} (m^3/m)	V_s (m^3/m)	V_s (%)	i (m)	i/R	3i (m)	w=2.5i (m)	
58.THAMES WATER AUTHORITY, SUTTON SEWER. (O'Reilly & New, 1982)														Hand excavated; stiff fissured London Clay. Hand excavated; firm to stiff weathered London Clay. Full face machine (mini-tunnel) excavated; firm to stiff weathered London Clay.
a)	17.1	1.78	9.61	3.8	180	1.89*	2.49	0.096	3.86	10.0	1.12	30.0	25.0	
b)	3.4	1.78	1.91	3.7	90	0.76*	2.49	0.019	0.75	2.0	2.25	6.0	5.0	
c)	4.9	1.52	3.22	7.1	9	1.09*	1.81	0.054	2.98	3.0	3.95	9.0	7.5	
59.BRISTOL CITY ENGINEERS DEPT. AVONMOUTH 2, SEWERAGE SCHEME (Toombs, 1980)	6.0	3.4	1.76	20.0	18	6.67*	9.08	0.251	2.8	5.0	2.94	15.0	12.5	Hand excavated within shield with compressed air; soft to very soft alluvium overlain with fill for motorway embankment
60. LONDON TRANSPORT INTERCHANGE SUBWAY AT KINGS CROSS, LONDON. (West et al, 1981)	14.06	4.13	3.4	4.0	230	1.22*	13.46	0.078	0.6	7.8	3.78	23.4	19.5	Hand excavated (no shield); cast iron lining; London Clay.
61.THAMES WATER AUTHORITY OXFORD TRUNK OUTFALL SEWER. (O'Reilly & New, 1982)	11.7	2.82	4.15	2.2	200-400	0.78*	6.24	0.028	0.44	5.0	3.55	15.0	12.5	Full face machine in shield ; stiff heavily overconsolidated fissured clay (Oxford Clay).
62.WITOC LUMB BROOK SEWER. (O'Reilly & New, 1982)														Hand excavated within shield;loose to medium sand with some gravel. Hand excavated in medium to dense sand with some clay ; cover of very stiff sandy clay. Partially stabilized medium dense sand and gravel with a little clay. Fully stabilized sand and gravel.
a)	4.7	3.6	1.31	78.0	-	-	10.18	0.47	4.6	2.4	1.33	7.2	6.0	
b)	9.0	3.6	2.5	19.0	-	-	10.18	0.12	1.2	2.52	1.40	7.56	6.3	
c)	6.5	3.6	1.81	15.0	-	-	10.18	0.06	0.6	1.59	0.88	4.77	3.98	
d)	6.5	3.6	1.81	20.0	-	-	10.18	0.09	0.9	1.79	0.99	5.37	4.48	
e)	6.5	3.6	1.81	7.0	-	-	10.1	0.04	0.4	2.28	1.27	6.84	5.70	

* Estimated value.

(Continued overleaf)

Table 2.1 Continued.

TUNNEL	TUNNEL DATA			SETTL.	GEOTECH. PROPERT.		VOLUMES			TROUGH				TUNNELLING METHOD AND SOIL CONDITIONS.
	Depth z (m)	Diam. 2R (m)	z/2R	(mm)	c_u (kN/m^2)	$\gamma z/c_u$	V_{exc} (m^3/m)	V_s (m^3/m)	V_s (%)	i (m)	i/R	3i (m)	w=2.5i (m)	
63. NORTH WEST WATER AUTHORITY, JERSEY STREET TO HOWLEY SEWER. (O'Reilly & New, 1982)	8.4	2.0	4.2	28.0	-	-	3.14	0.23	7.1	3.2	3.2	9.6	8.0	Hand excavated within shield with compressed air; variable loose silty sand with some soft clay ; tunnelling about 4m below water table.
64. NORTHUMBRIAN WATER AUTHORITY SEWERAGE SCHEME OUSEBURN VALLEY (O'Reilly & New, 1982)	13.0	3.47	3.75	81.0	-	-	9.64	1.48	15.6	7.29	4.20	21.87	18.23	Hand excavated within shield ; recent fill materials , rubble , timber , household waste and ash in soft clay matrix.
65. BUDAPEST METRO (Ulrich,1974)														Shield tunnelling , hand excavated in Oligocene clay overlain by sandy silt. Bolted concrete segmental lining.
I) N-S LINE RUNNING TUNNEL	30.	5.5	5.45	26	-	-	23.76	0.83	0.29	9.23	3.35	27.66	23.05	
II) E-W LINE RUNNING TUNNEL	30.	5.5	5.45	37	-	-	23.76	2.2	0.11	30.25	11.00	90.75	75.62	
66. TYNE & WEAR PASSENGER TRANSPORT EXECUTIVE, RUNNING TUNNEL ELDON SQUARE, NEWCASTLE. (O'Reilly & New, 1982)	14.2	5.21	2.73	7.5	200	1.4*	21.32	0.132	0.6	7.0	2.69	21.0	17.5	Partial face machine excavated in shield with compressed air. Glacial till, firm/stiff clay with some sand and gravel lenses.
67. SEWAGE PIPELINE No. 352, UCHIKU-CHO IBARAKI. (Miki et al, 1977)	8.6	2.55	3.4	12.9 max 5 av.	-	-								Slurry mole , segmental lining. Cemented fine (0.4mm) clayey sand , overlain by sand, clay and silty. Water table 5.4m above crown.

* Estimated value.

(Continued overleaf)

Table 2.1 Continued.

TUNNEL	TUNNEL DATA			SETTL.	GEOTECH. PROPERT.		VOLUMES			TROUGH				TUNNELLING METHOD AND SOIL CONDITIONS.
	Depth z (m)	Diam. 2R (m)	z/2R	(mm)	c_u (kN/m^2)	$\gamma z/c_u$	V_{exc} (m^3/m)	V_s (m^3/m)	V_s (%)	i (m)	i/R	3i (m)	w=2.5i (m)	
68. BELFAST SEWERAGE SCHEME, CYDEHAM BELFAST. (Glossop & Farmer, 1977)	5	2.74	1.82	37.5	2.1	8.3	5.9	0.12	2.0	2.1	2.75	2.00	8.00	2.74m diameter shield, 2m long + 1m tailskin. Compressed air spade excavation. 41kN/m^2 compressed air pressure for ground support. Seven precast concrete lining segments, 0.6m long. Each ring grouted individually immediately after shield shove; 3-4 rings erected per shift. Belfast 'sleech' - soft organic silty clay with a high moisture content.

* Estimated value.

CHAPTER 3

APPLICATION OF THE FINITE ELEMENT METHOD.

3.1 INTRODUCTION.

The finite element method has found one of its major applications in the solution of geological/ geophysical problems. The versatility of the method facilitates the detailed treatment of many complex cases unapproachable by analytical methods, provided that the accuracy of the input data for the material involved in the analysis is acceptable for the degree of sophistication of the method.

3.2 THE FINITE ELEMENT METHOD.

The technique of the finite element method is also

well established within many engineering disciplines. Although there may be considerable diversity in the formulation, the method can be distinguished by four major features :

a) Representation of a body or a structure by an assemblage of discrete units called finite elements;

b) Derivation of expressions for the variation of the functions within each element and the relationship of unknown variables at junctions between neighbouring elements;

c) Establishment of a relationship between all the elements and the imposed mesh boundary conditions;

d) Solution of the constitutive simultaneous equations.

In the following Sections, the general procedure used in the finite element programming presented in Chapter 5 will be discussed briefly.

3.3 FORMULATION PROCEDURE.

The finite element displacement method of structural analysis was used. The governing equilibrium equations were obtained by minimising the total potential energy of the system, represented by the internal strain

energy and work contributions of the body forces and distributed surface loads. The displacement is assumed to have unknown values only at nodal points, so that nodal values are described by means of an interpolation function. The basic steps for deriving a finite element solution to an equilibrium problem can be summarised as : sub-division of the continuum, evaluation of the element stiffness matrix and load terms, assembly of element stiffness matrix and load terms into a global stiffness matrix and load vector, solution of the resulting linear equations for the unknown nodal variables, and finally, evaluation of additional element quantities.

3.3.1 IDEALIZATION OF THE CONTINUUM.

The discretization of the continuum is carried out in such a way that a number of finite elements represents the entire body or structure under analysis. If the geological conditions are relatively simple, it is possible to model the medium precisely. For complex conditions, it is necessary for the engineer, using his skill and his previous experience, to adopt a simplified model of the medium, taking into account every parameter and characteristic regarded as essential to the analysis. The final results depend largely on this idealization.

There are no general rules for determining the

exact number of nodes or elements required for a certain model to be adopted. Nevertheless, the depth and diameter of the tunnel and/or buried pipelines and the contours of different materials are well-defined parameters. The major difficulty of the idealization is to choose the appropriate number and size of elements, and the limits and boundary conditions of the mesh. In any case, it is always necessary to take into account the computing time, uniformity of material properties within each element, sequence and number of load increments to perform the calculation. The computing time is a particularly important factor in three-dimensional finite element analyses.

3.3.2 PRIMARY STATE OF STRESS.

The initial state of stress in the ground is a very important factor in simulating excavation process because it involves calculation of forces from the existing stresses on the surface to be exposed by the excavation. These initial stresses are generally specified in terms of vertical and horizontal components. At any point of the medium, the pre-tunnelling vertical stress is usually taken as a product of the soil unit weight, γ, and depth, z, of the point. The horizontal stress components at the same point are taken as a product

of the vertical stress and the coefficient of earth pressure, K (see Figure 3.1). An appropriate value of K must then be known. (K is here used without the subscript 'o' to denote the ratio of horizontal to vertical stress in situ.)

Tests to determine K have been derived both for the laboratory and in-situ. Often, the experimental determination of K is substituted by semi-empirical formulae which predict K from readily available data. Many expressions have been developed and K has been calculated from the effective friction angle, ϕ', or the plasticity index.

For normally-consolidated soft clays, the K values typically fall into the range 0.45 to 0.7. Overconsolidation significantly affects K, and values of 3 or more has been assumed for London Clay at ground surface (Burland et al, 1981).

3.3.3 MATERIAL PROPERTIES.

The basic material properties required in a finite element analyses are the modulus of elasticity (elastic modulus), E, and Poisson's ratio, ν. The main difficulty in the use of these parameters arises from the selection

of numerical values because soils are extremely complicated engineering materials. The soil response is influenced by a number of factors, including its density, water content, mineralogy, structure, particle size, stress history, confining pressure, drainage conditions, duration of loading, and so on. Because of this complexity, a simple and realistic constitutive relationship capable of describing the soil behaviour is still unavailable. This is also the reason why today, in spite of the sophisticated analytical procedures available, results obtained by theoretical means have in many instances remained rather poor.

The stress-strain behaviour of soils has been a subject of research for many years, and the advent of the finite element method of analysis has given additional impetus to this effort.

The finite element method has been applied to a wide range of geological problems, involving materials that obey linear or non-linear constitutive laws. The linear behaviour of material requires only one application of the solution process to obtain results for a particular loading case. Meanwhile, there are two common approaches for treating the soil as a non-linear material, characterizing it as piecewise linear or elastic-plastic.

Specific applications to non-linear problems include the use of hyperbolic formulation, spline functions, empirical equations, and tabular or digital forms. All these models have given satisfactory results if compared with field observations, but two common difficulties are revealed. The first one is the ability to predict accurately the initial value of Young's modulus, and the second is the ability of any particular function to describe adequately the soil response over the entire range of interest.

3.3.4 CHOICE OF THE ELEMENT AND ADVANTAGES OF THREE-DIMENSIONAL FINITE ELEMENT ANALYSIS.

Selection of the most suitable element for a particular problem is not an insignificant question. The complexity of programming, the accuracy of the solution, the total computation effort and its cost are strongly dependent on the element type. There are no well-defined rules for choosing the best element for a particular problem. All depends on the problem type, the boundary conditions, the computer capacity, the geometry of the boundaries, the accuracy desired, the maximum allowable computing time, as well as many other factors. The question of economy may generally dictate the choice of an appropriate element. The use of higher order elements

requires some justification because the additional complexity compared with simpler elements requires more computer time to perform calculations.

A further economy in computing time can be obtained by efficient calculations of the element stiffness matrix.

With the three-dimensional finite element method of analysis, the cost of computation is higher than for any other numerical method of calculation. It inherently involves a large number of degrees of freedom, and even with a reasonable number of elements the resulting system of equations can easily have several thousands of unknowns.

Although many difficulties exist it was felt that the three-dimensional finite element analysis would be essential to carry out the work presented in this thesis in order to simulate more realistically the tunnel excavation and the response of buried pipelines to ground movements. It is clear that both problems are inherently three-dimensional in character.

Several analyses have been performed over the past years using two-dimensional plane strain models, but they

do not model the true development of deformations and stresses during the process of tunnel construction. For instance, taking a transverse section to the tunnel centre line, as the tunnel face approaches and passes during the process of construction, there is a gradual development of deformations and stress variations. When a lining is installed at this section displacements have already taken place behind the face and prior to the onset of ground-lining interaction at the section in question. This effect cannot easily be taken into account in a two-dimensional formulation.

Another important effect which cannot be modelled in two-dimensional analyses is the fact that as the tunnel face advances, the excavation takes place in a zone ahead of the face in which the stress condition has already been modified by the approach of the face.

In summary, the three-dimensional finite element analysis is able to take into account all these effects although some limitations and difficulties exist.

One of the most popular three-dimensional finite element configurations available is the tetrahedral element, although occasionally it is difficult to subdivide a region into this type of element only. This

difficulty is aggravated, particularly in geotechnical problems, because of complex physical conditions involved in the analysis. For this reason, added to relative simplicity in programming and good numerical accuracy, the isoparametric hexahedral rectangular element, as shown in Figure 3.3, was chosen. Obviously, the choice was made on the grounds of economy, since more complex elements require correspondingly more calculation time and larger computer systems.

3.4 FACTORS AFFECTING FINITE ELEMENT CALCULATIONS.

Economical solution of problems by the finite element method is based on using the computer efficiently. In order to improve computational efficiency it is necessary to balance each process involved in the calculation. A rational approach to confirmation of the solution integrity in finite element analysis requires a categorization of the sources of error. A general scheme of such sources is presented in Figure 3.2.

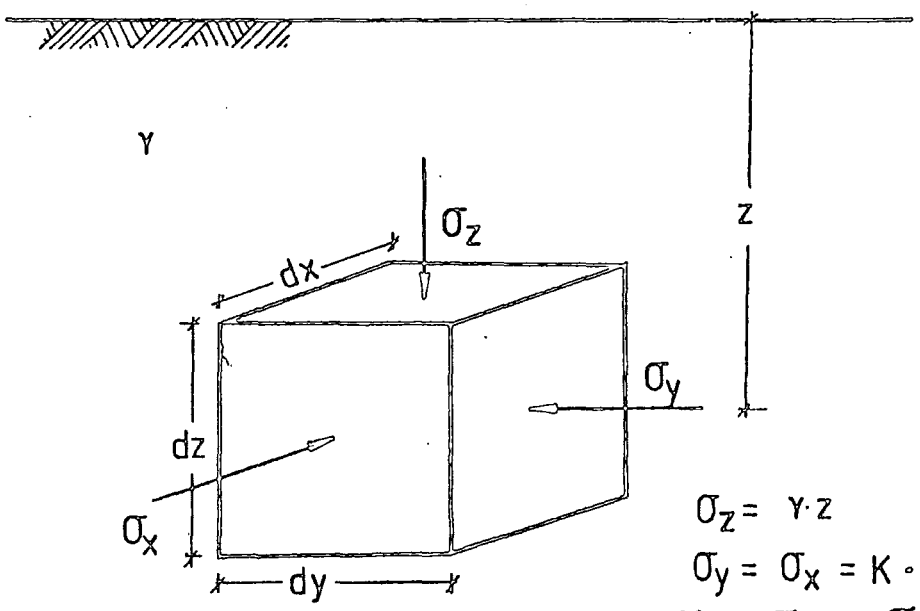

FIG.3.1) Initial stress in the soil.

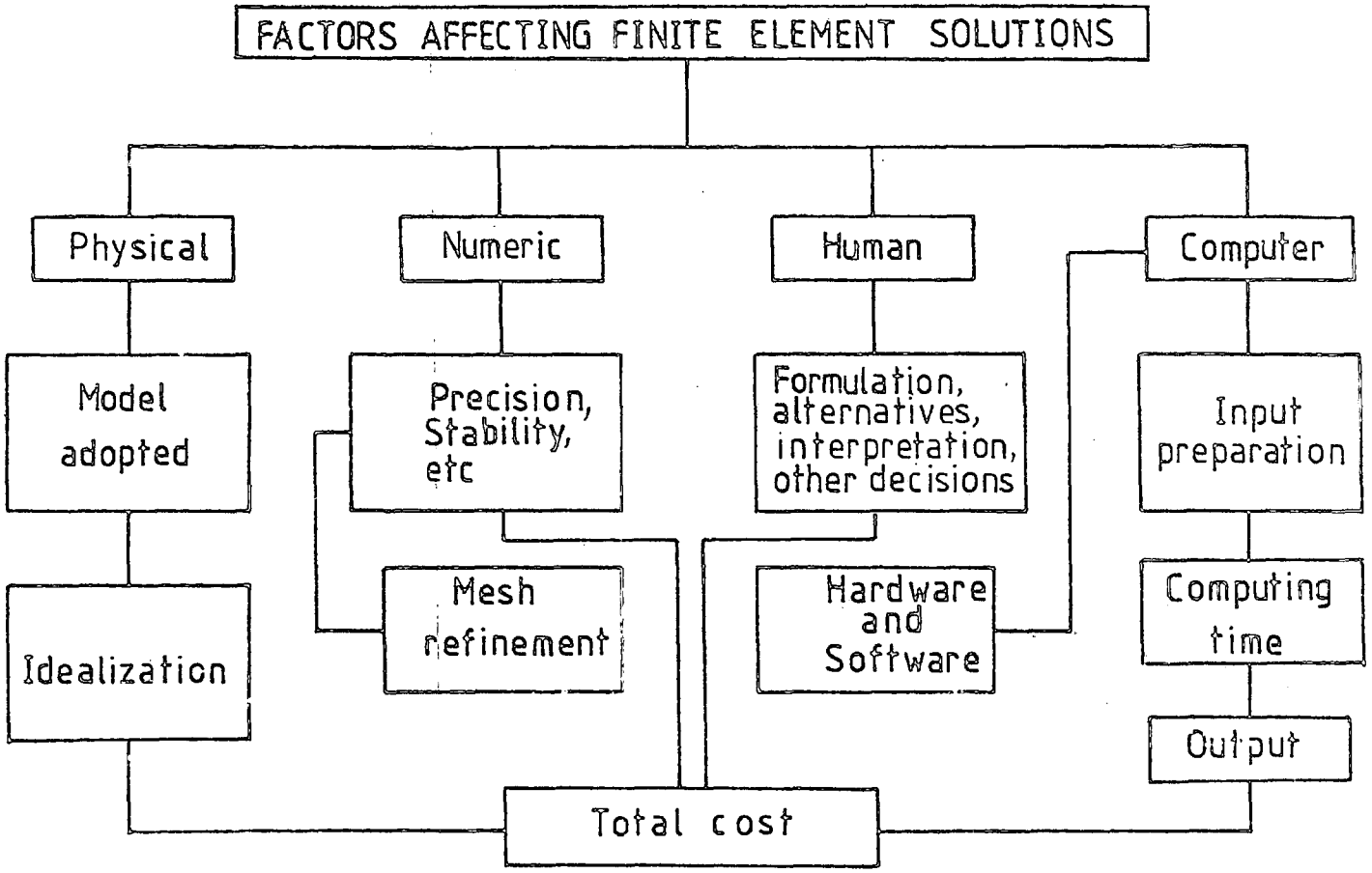

FIG. 3.2) The finite element scheme.

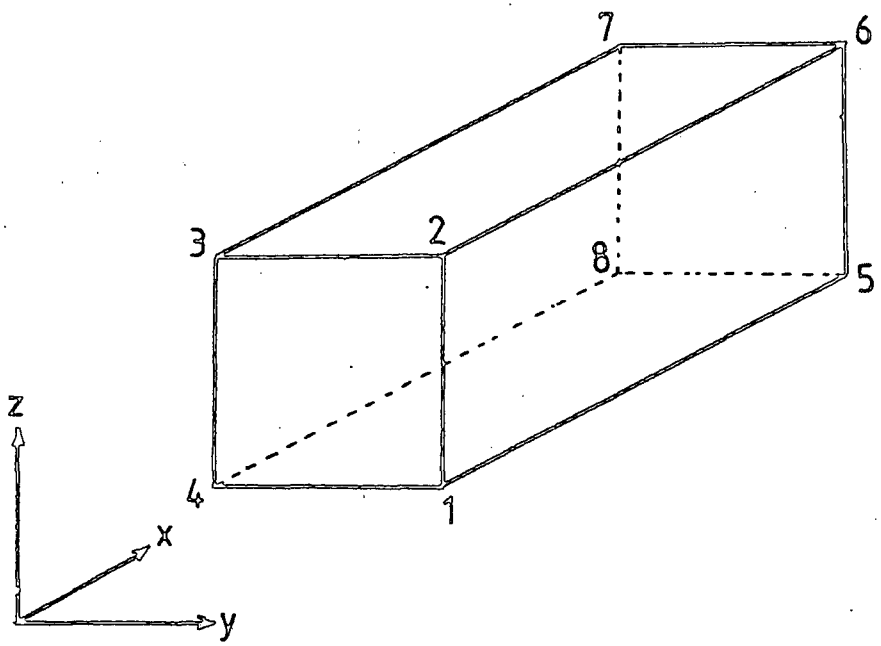

FIG. 3.3) The isoparametric hexahedral rectangular element.

CHAPTER 4

THE FINITE ELEMENT TECHNIQUE TO SIMULATE TUNNELLING.

4.1 INTRODUCTION.

The problem of predicting the actual ground deformation due to the tunnelling in soft ground provides a severe test for any method of calculation because, as noted earlier, conditions found in the field are quite different from those simulated in the analysis. It was realised at the beginning of this research that the finite element method could be more appropriate than any other analytical method because it accommodates specific actions involved in the tunnelling process that other methods cannot take into account. This Chapter presents the general procedure used in this work for modelling tunnel excavation.

4.2 SIMULATION OF EXCAVATION AND CONSTRUCTION.

During the tunnelling process, the ground around the tunnel is disturbed. If the magnitudes of the displacements exceed a certain limit they may damage the structures present in the area affected by the excavation. This potential damage is not only related to the maximum vertical movement, but is also significantly dependent on the distribution of horizontal movement.

In a finite element analysis, the actual tunnelling process starts with the in-situ stress condition and is followed by one or more stages of excavation and support installation, if and as necessary.

The excavation process is modelled by dividing the region of the soil to be removed into a number of parts. Each of these parts will represent one load increment, and it is assumed that after each sequence of simulation the stresses on surfaces exposed by excavation will be zero. In early techniques to simulate excavation, the loads required to create such conditions were obtained by multiplying the computed stresses at the nodes on the exposed surface by the projected area on which they act (Clough and Duncan, 1969). Then a cycle of finite element calculations is performed to find variations in stresses

due to the application of such loads. At the end of each cycle, the variations of stresses are added to the stresses computed in the previous stage. Often, the stresses for computing loads were found by interpolating stresses at the centroids of surrounding elements.

It was shown by the use of the foregoing procedure (Christian and Wong, 1973) that, for excavation in elastic soil, this procedure yielded different results for different numbers of load increments. The discrepancies were only reduced by using a least-squares extrapolation function to evaluate stresses on the boundaries between adjacent elements.

Later, an alternative technique was developed by the use of the displacements computed during the previous stages of excavation. This procedure does not require use of an auxiliary extrapolation model, and it has been shown that for excavations in an elastic medium the calculated stresses and displacements are independent of the number of steps employed to simulate the same stage of excavation process (Ishihara, 1970; Chandrasekaran and King, 1974). An approach based on this latter procedure is adopted in this work and will be presented in Section 4.3.

The aim of the finite element calculations used to

simulate excavation is to determine the change of state (displacements, stresses and strains) at specific points in the medium resulting from the removal of a stressed portion of the system. The excavation is simulated by the process of releasing forces calculated initially from the stresses acting on the surface which will form the boundary of the excavated region. The subsequent forces are calculated considering the effects of previous steps. Each stage of the excavation process is simulated by the application of nodal force relaxation in the model. Details of this procedure are explained in Section 4.3.

All the elements assigned to the internal portion of the tunnel are initially active. At a designated step when the excavation takes place these elements are deactivated, that is, the stiffness matrix of this element is not assembled in the global stiffness matrix of the system. The installation of a support system is simulated by the inverse operation : first, the stiffness matrix of elements representing the supporting structure is calculated by using an appropriate elastic modulus and then assembling it into the global stiffness matrix.

4.3 SIMULATION PROCESS.

The procedure was proposed by Chandrasekaran and

King (1974). One important feature of this procedure, when applied to linear analysis of geotechnical engineering problems, is the consistency demonstrated by the final results regardless of the number of load increments used. This is particularly important when loading history is an integral part of the problem.

To illustrate the simulation process, we consider that the tunnel excavation is carried out in N stages, corresponding to surfaces $S_1, S_2, S_3, S_4, \ldots, S_N$, respectively, as shown in Figure 4.1. Each excavation surface is defined by the face proper and the wall of the tunnel.

Initially the forces $\{F_1\}, \{F_2\}, \{F_3\}, \{F_4\}, \ldots, \{F_N\}$ are defined on the surfaces $S_1, S_2, S_3, S_4, \ldots, S_N$.

The first stage of an excavation process is carried out by applying the force $-\{F_1\}$ on the surface S_1, and deactivating the removed elements. Let $\{dF_2^1\}, \{dF_3^1\}, \{dF_4^1\}, \ldots, \{dF_N^1\}$ be the variation of $\{F_2\}, \{F_3\}, \{F_4\}, \ldots, \{F_N\}$, respectively, due to the first stage of excavation. Each component of these variations is obtained from the product of the stiffness matrix of elements located on the surfaces $S_2, S_3, S_4, \ldots, S_N$ and the corresponding first stage displacements.

The nodal forces on surfaces $S_2, S_3, S_4, \ldots, S_N$ can

now be expressed as :

$$\{F_2\}^* = \{F_2\} + \{dF_2^1\}$$
$$\{F_3\}^* = \{F_3\} + \{dF_3^1\}$$
$$\{F_4\}^* = \{F_4\} + \{dF_4^1\}$$
$$\vdots \qquad \vdots \qquad \vdots$$
$$\{F_N\}^* = \{F_N\} + \{dF_N^1\}$$

in which the first member of each expression represents the nodal forces equivalent to the stressed portion of the soil to be removed.

The second stage of excavation is carried out by applying forces $-\{F_2\}^*$ on nodes located on the surface S_2 and neglecting (or deactivating) the removed elements. At the end of this stage the forces acting on the remaining surfaces are given by,

$$\{F_3\}^{**} = \{F_3\}^* + \{dF_3^2\}$$
$$\{F_4\}^{**} = \{F_4\}^* + \{dF_4^2\}$$
$$\vdots \qquad \vdots \qquad \vdots$$
$$\{F_N\}^{**} = \{F_N\}^* + \{dF_N^2\}$$

in which $\{dF_3^2\},\{dF_4^2\},\ldots,\{dF_N^2\}$ are the variations of the respective forces due to the second stage of the excavation. They are now calculated by the use of corresponding second stage incremental displacements.

For the following stages, the procedure is applied successively as described above. At the end of each stage of the excavation process the incremental displacements, stresses and strains are added to the previous values.

4.4 FORMULATION.

For the initial opening, the releasing forces $\{F_1\}$ are simply calculated by integrating the virgin stresses along the faces of elements around the opening :

$$\{F_1\} = \int_{vol} [B] \cdot \{\sigma\} dV$$

in which, $[B]$ is the strain/displacement matrix and $\{\sigma\}$ is the stress vector for each node.

For subsequent analyses, the effects of previous loadings are considered by the use of the following equations to calculate the releasing forces $\{F_j\}$:

$$\{F_j\} = \{F_{j-1}\} - \{dF_j\}$$

and,

$$\{dF_j\} = [K] \cdot \{d_j\}$$

in which, j is the increment number, $\{dF_j\}$ the variation

of the force, [K] the stiffness matrix and $\{d_j\}$ the displacement vector calculated in increment j.

4.5 TUNNEL LINING INSTALLATION.

In practice,when the face advances during tunnel contruction, a certain length of the opening is left unsupported and this will change the stress field in the ground. Most of the load will be supported by the lining, particularly by the last ring. A significant part of the load is also transferred to the unexcavated ground ahead of the face, a process which cannot be accepted easily into a two-dimensional formulation. Then a new segment of lining is erected and the whole process is repeated cyclically. A pattern of movements always takes place between the installation of two consecutive lining segments.

The procedure used in the finite element method to simulate the lining placement involves the reactivation of the elements representing the support system. The nodal forces equivalent to the new portion to be excavated are applied and the response of both the ground and support system is obtained accordingly.

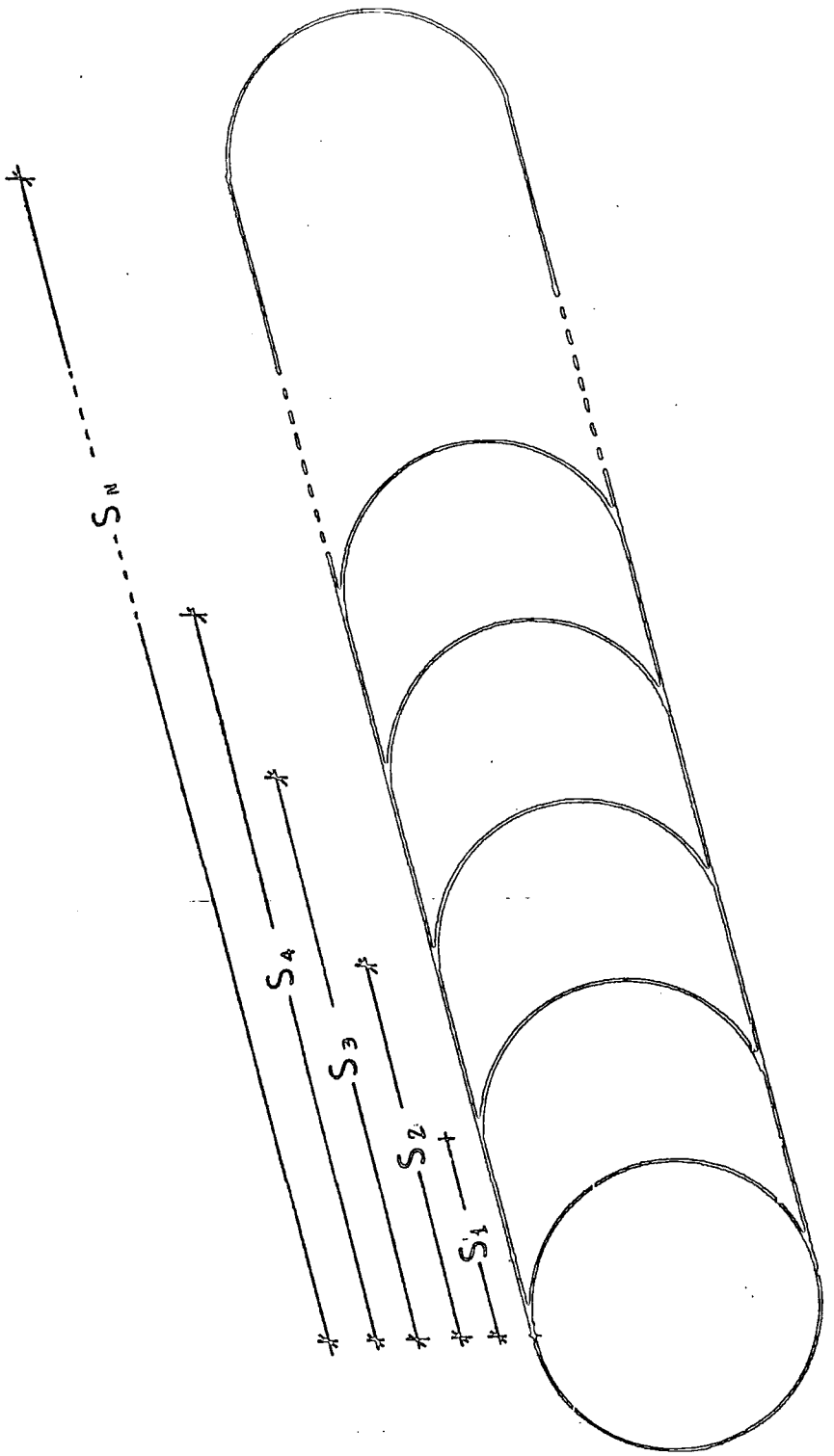

FIG.4.1) Model to simulate excavation process.

CHAPTER 5

THE THREE-DIMENSIONAL FINITE ELEMENT PROGRAM.

5.1 INTRODUCTION.

A Finite Element Program (see Appendix B) for 3-Dimensional Elastic Solution (FEP3DES) was written in the Fortran IV language, level G, using the University (NUMAC) IBM 370/168 mainframe computer with 2Mbytes core storage capacity.

A short program (GRAPH), (see Appendix C), was also written in order to select designated variables calculated by FEP3DES to be contoured using the General Purpose Contouring Package (GPCP) public program. GPCP is run separately from the FEP3DES and graphics subroutine.

The main program is comprehensive and automatic in many features such as generation of missing input data,

stiffness assembly, node fixing, solution of equations, stress and strain computations and output data. It was written taking into account a limit of computing time and the storage capacity of the computer used.

The following Sections present briefly some of main features, limitations and advantages of the program.

5.2 SCOPE OF THE PROGRAM.

As pointed out previously, a three-dimensional finite element method applied to tunnel construction analysis requires a large and fast computer. This was the reason for writing the program FEP3DES in as simple a manner as possible. The following features and scope of operation are included :

a) The program is intended for geotechnical applications.

b) Physical properties of materials are linear elastic, homogeneous and isotropic.

c) Loading can be in the form of discrete forces or prescribed displacements applied to selected nodes.

d) The simulation of tunnelling process is made by calculating initial releasing forces from the primary stress in the ground. For subsequent steps (if the incremental procedure is used) the releasing forces are

obtained from displacements calculated at the end of each step.

e) The finite element mesh is generated automatically.

g) Geometry and material properties do not change longitudinally.

h) Primary state of stress is expressed in terms of lateral, vertical and longitudinal stresses.

i) Elements representing the excavated portion of the soil are 'deactivated' to simulate the excavation process.

j) 'Deactivated' elements are 'reactivated' at a specified distance from the advancing face if tunnel support installation is simulated.

5.3 DESCRIPTION OF THE PROGRAM.

The program consists of a main routine and 25 subroutines. The action of these subroutines is described in Appendix A, the logic of the program is shown in Figure 5.1, and the program is listed at the end of this thesis.

5.3.1 MESH AND STORAGE DETAILS.

As indicated in Section 3.3.4, the finite element used in this program has 8 nodes located on corners of the

element as shown in Figure 3.3.

In order to reduce the input data to a minimum, coordinates, stresses, displacement conditions and element node numbers are given in a similar way to that in two-dimensional analysis. Associated with each node are numbers defining the displacement condition, coordinates and initial stresses. The maximum number of nodes and elements are 1122 and 840, respectively, and the permitted maximum semi-bandwidth of the global matrix is 351. Although the number of nodes and elements is considered adequate for most problems, this number may be increased if necessary.

5.3.2 EQUATION SOLUTION METHOD.

In order to minimize the required core storage, only the upper half of the banded global stiffness matrix is stored in the designated array. The equations are solved at each step using the Gauss elimination method. The displacements obtained by the solution of equations will generate the stresses and strains.

5.3.3 LOGICAL UNITS.

Four temporary files numbered 1, 3, 9 and 11, and one permanent file numbered 12 may be used in the program.

These units must be declared at the begining of the execution. File number 9 is only required if the lining placement during tunnel construction is simulated.

5.3.4 INPUT AND OUTPUT DATA.

Data for the FEP3DES program must be input in appropriate format using any set of consistent units. The values of displacements, stresses and strains calculated at the end of each step will correspond to the units adopted.

5.4 COMMENTS.

The finite element method of analysis not only has to be economically sound but also precise enough in its output information. This requirement can only be checked through careful comparison between calculated results and field measurements. The results will mainly depend on the implemented stress-strain behaviour of materials. As discussed briefly in Section 3.3.3, a general constitutive relationship describing this behaviour is still unavailable. At the present time, the most common procedure for approximating stress-strain properties of soils is based on results obtained from laboratory tests.

Although some limitations exist in this procedure, the relative simplicity and availability of the apparatus make it attractive for practical purposes.

Typically soil behaves non-linearly, but many workers have performed linear finite element analyses on actual cases. Linear elastic analyses were used in the present research, the reasons for this being discussed later in this thesis.

For many practical problems, particularly in three-dimensional analysis, too many elements and nodal points are involved so that the task of preparing the input data becomes extremely lengthy and tedious. Consequently, some unintentional human errors may be introduced during the preparation of thousands of data entries and may remain undetected in spite of the checks which are usually made. The presence of such errors will inevitably bring about incorrect results and, if detected at this stage, would require a further calculation on the computer after correcting the input data. However, if the errors remain undetected the consequences may be very serious because incorrect results lead to incorrect engineering decisions. The risk of introducing such input data errors can be reduced by the automatic mesh generation feature of the program. This consists of

generating the whole domain automatically by the computer using a minimum amount of information necessary to describe the mesh geometry and the requisite mesh divisions.

In addition to the two important factors discussed above, the following requirements were regarded as essential during the writing of the program :

a) The introduction of the stress-strain law in the analysis should not lead to high computing cost.

b) The applied mechanical properties of soils might be determined by common laboratory testing techniques.

c) The calculated results have to be close enough to reality for practical purposes.

d) There must be easy understanding of the program in order to allow further changes if necessary.

e) Realistic representation of the excavation and construction procedure is required.

f) The program should allow analysis of the response of buried pipelines to the ground movements caused by tunnel construction.

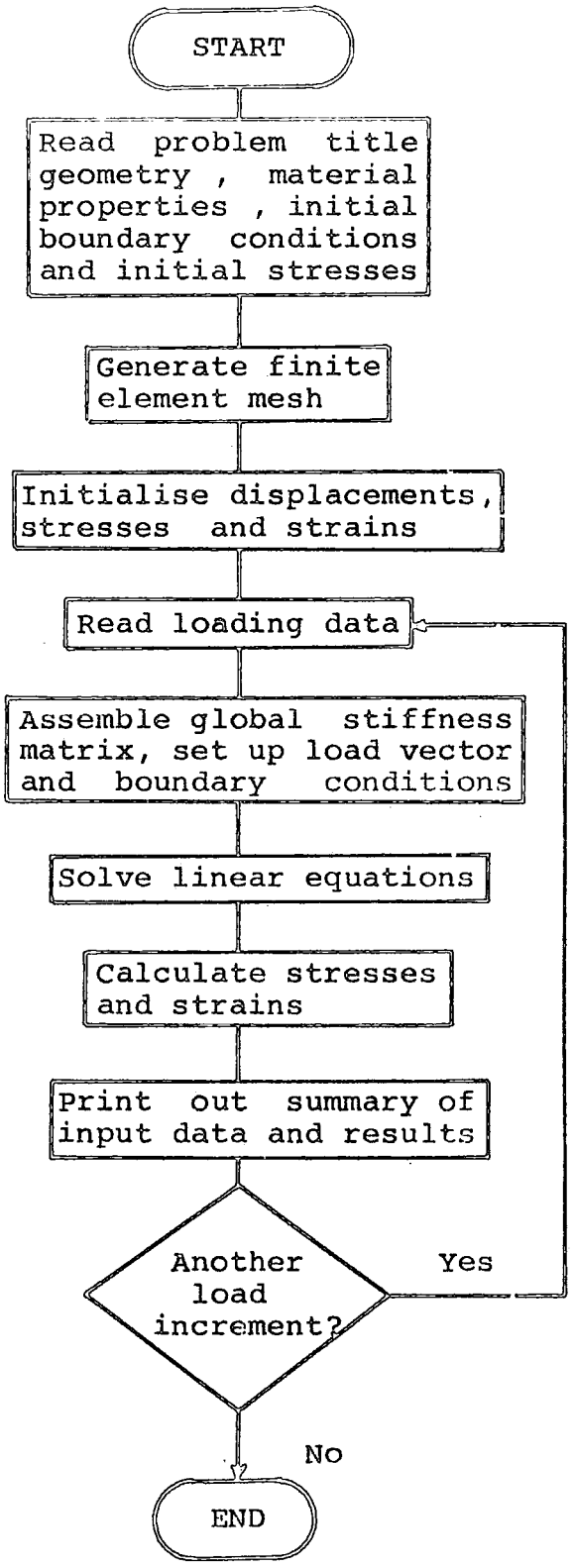

FIG. 5.1) Flow chart for the program FEP3DES.

CHAPTER 6

SITE AND MODEL USED IN THE ANALYSES.

6.1 INTRODUCTION.

The capabilities of the three-dimensional finite element technique for analysing stresses and deformations in engineering problems with complicated geometries have been well established in the past literature. However, the use of this analytical tool in geological problems has been resisted, partially because of its high cost, both in manpower and computer time.

It is attempted, with the following analyses, to put a more quantitative perspective on this objection by examining the advantages of a typical three-dimensional finite element study. An attempt has been made to investigate procedures which would avoid the great expense and some inefficiency inherent in the methods more

generally used.

The elastic approach has been used throughout the research to analyse the distribution of stresses, strains and displacements. Although it does not predict specific failure conditions, it does provide estimates of service behaviour and of possible failure mechanisms.

Even with the present state of finite element methodology and computer technology, three-dimensional analysis for simulation of tunnel construction and its effect on nearby structures can be quite expensive due to the size of the mesh and large number of steps required. While this approach may be feasible for studying on a case-by-case basis, parametric studies requiring several analyses of a general problem appear to be impractical at this time. A compromise has been attempted by combining the finite element method and an empirical approach using one set of material properties. In spite of these limitations, it has been considered that a simple three-dimensional linear elastic idealization could provide preliminary information when attempting to model ground movement caused by tunnel excavation and/or the possible response of buried pipes to these movements.

Simulation of the excavation process was performed

by varying the releasing forces at the tunnel surface until a 'best fit' between results calculated by the empirical method and the finite element approach was achieved.

It is not intended in this work to discuss fully all aspects of the tunnelling process in clay soil, nor the effect of tunnelling on buried pipelines. This presentation will concentrate on aspects of soil behaviour relevant to tunnelling, with or without lining installation, and the possible response of pipelines to ground movements, essentially as seen from the point of view of the engineer.

6.2 DETAILS OF THE SITE ANALYSED.

Figure 6.1 shows the plan of the area (Tyneside Sewerage Scheme at Collingwood Street, Newcastle upon Tyne) used in this study. The depth of the tunnel axis at this section varies between 13.36m and 13.72m. Three gas pipelines lie parallel to the tunnel centre line at depths varying from 0.8m to 1.7m . A 18" diameter pipeline lies under the pavement 6.5m from the tunnel centre line. The smallest diameter pipe (12") lies 1.7m from the centre line and the largest diameter pipe (24") lies directly

above the tunnel centre line. For ease of finite element idealization, it is assumed that all three pipes are located at a depth of 1.5m and the tunnel axis at a depth of 13.5m, as shown in Figure 6.4.

6.3 GEOLOGICAL CHARACTER OF THE SITE.

Ground investigations carried out in the area involved the putting down of boreholes as indicated in Figure 6.1. Four different types of deposit were found :

1) A variable depth of fill, comprising soft clay, stones, ashes, bricks, sand, gravel, timber and coal fragments, covers the whole area from a thickness of between 1.0m to about 12.0m.

2) Silty clays, often finely laminated with sand or silty intercalations. Clay thickness varies from about 1.0m to 6.0m.

3) Stiff to very stiff boulder clay, usually sandy or silty and containing cobbles, boulders and gravel in variable proportions; it underlies the laminated clay.

4) Sand and gravel horizons varying in thickness and depth and containing clay bands and pockets of clay.

From the analysis of the site investigation data Norgrove et al.(1979) suggested that most of the

tunnelling would take place in boulder clay. Because of the range of soil types they also suggested the convenience, for analytical purposes, of considering the deposits in three categories by grouping the sandy clays with the boulder clay.

6.4 SOIL PROPERTIES : TRIAXIAL TESTS.

Because of the large number of factors which influence the ground response, some simplifications and constant parameters have to be used in order to reduce computer time calculations. Values of Young's modulus (E) and Poisson's ratio (ν) for the ground were constant throughout the analyses. The value of E was based on triaxial tests while ν was assumed to be equal to 0.48 based on local geological conditions.

Figures 6.2 and 6.3 show the results of undrained triaxial tests carried out at the Northumbrian Water Authority's Central Site Office, Howdon on 15th September 1977. These tests were performed on 100mm diameter undisturbed soil samples described in both Figures, retrieved at depths of 4.0m and 10.0m from borehole G2C. Obviously, any number of possible secant or tangent moduli can be obtained from both stress-strain curves.

Choosing the best value of modulus applicable to the problem is a difficult task. The solution is to choose that modulus which best represents the stress changes which are expected to occur in the field. If the condition is to represent a very wide variety of stress levels, a secant modulus corresponding to one-half to one-third the failure stress is often used (Lee et al, 1983). The reasoning behind this is that a safety factor of 2 or 3 is usually applied to an assessment of strength, and hence on average the soil will be subjected to one-half to one-third the failure stress. However, Lee et al.(1983) pointed out that such an approach must be used with caution because the stress-strain curve is influenced by many factors such as the minimum principal stress. Bearing in mind the lack of test results and general uncertainty in estimating E, further refinement in obtaining the modulus value was considered unnecessary. Thus, values of 0.6 MN/m^2 and 1.0 MN/m^2 have been obtained from Figures 6.2 and 6.3, respectively, using one-half of the failure stress.

Because the tunnel at Collingwood Street was excavated below the water level, and the simulation of tunnelling is performed for an undrained condition, a Poisson's ratio value of 0.48 is used in the finite element analysis to simulate incompressibility.

A sketch of an idealized model of the site with values of the ground physical properties used in the analysis is shown in Figure 6.4.

6.5 PIPES : MATERIAL PROPERTIES.

The three pipes under investigation are made of cast iron and they are assumed to respond elastically to deformation. The tangent Young's modulus and Poisson's ratio were taken to be 65×10^3 MN/m^2 and 0.26, respectively. Table 6.1 shows the characteristics and symbols used for the pipes throughout the analyses.

6.6 'EQUIVALENT STIFFNESS' APPROACH.

At the interface of a pipe and foundation there can be a significant change in stiffness of the different elements. In order to illustrate the numerical problem which may develop, Wilson (1977) has presented a simple numerical example consisting of a small-size element having large stiffness connected to the other elements with comparatively small stiffness. He pointed out that although most modern digital computers normally operate with seven to fourteen significant figures, the numerical

sensitivity can still cause problems. To overcome such a problem, a logical and simple approach without affecting computer time requirements involves applying the 'equivalent stiffness' approach to the pipes. The idea of this method is to replace the original stiffness of the pipe with a reduced stiffness on a transformed cross section of the pipe in such a way that the response of the replaced pipe is the same in terms of deflections. If this approach is used, the bending and direct stresses output from the computations will have to the transformed back to actual values.

The following values have been used in the analyses :

a) PIPE A' : External diameter (De) = 0.650 m
Internal diameter (Di) = 0.610 m
Elastic modulus (E) = 65×10^{3} MN/m^2
Moment of inertia (I) = 19.925×10^{-4} m^4
Stiffness (EI) = 128.94 $MN.m^2$

Values of I or I^* have been obtained by using the following expression :

$$I = (\pi/64) \cdot (De^4 - Di^4)$$

Taking the wall thickness equal to 6-times the

actual thickness, the internal diameter of the transformed section is 0.4064m. Thus, the 'equivalent' moment of inertia (I^*) is :

$$I^* = 74.23 \times 10^{-4} \ m^4$$

if $EI = E^* I^*$, where E^* is the 'equivalent' Young's modulus. Then $E^* = 17.45 \times 10^3 \ MN/m^2$

Using a similar procedure for the remaining pipes, we have :

b) PIPE B' : $I^* = 1.86 \times 10^{-4} \ m^4$

$$I^* = 5.79 \times 10^{-4} \ m^4$$

Then $E^* = 20.88 \times 10^3 \ MN/m^2$.

c) PIPE C' : $I^* = 7.35 \times 10^{-4} \ m^4$

$$I^* = 25.66 \times 10^{-4} \ m^4$$

Then $E^* = 18.6 \times 10^3 \ MN/m^2$.

In addition to the primary reason for using such a procedure, this approach avoids the use of excessively distorted elements to represent the pipe.

6.7 DISPLACEMENT FIELD APPLIED TO FINITE ELEMENT MESH.

Because the dimensions of the pipelines relative to those of the idealised media of the site is too small,

the response of the buried pipes was analysed by isolating regions of design interest and applying to these regions the displacement fields calculated by the ground movement theory developed by Attewell and Woodman (1982). The input displacement field data were generated using a program run on an Exidy Sorcerer microcomputer at the University of Durham and written by Reeves (1982).

Clearly, the success of such a method totally depends on the realism and accuracy of the input displacements to the finite element program.

6.8 FINITE ELEMENT MODELS.

In constructing a finite element model for analysing the behaviour of a buried pipeline and/or the ground due to the tunnelling, careful consideration must be given to the number and the shape of the elements to be employed in the mesh. An important question arises as to what extent of the region should be discretized for the finite element solution. The idealization should be such that the accuracy of the solution is compatible with the precision with which the soil properties could be determined and to which the standards of the site practice could be controlled during construction. To model a semi-

infinite soil around the pipe and/or tunnel, a convenient boundary for the finite element model had to be chosen in order to duplicate as nearly as possible the stresses and deflections that would occur in the free field away from the region perturbed by the applied load.

Determination of the location of the external boundaries for the mesh was based on Figures 7.1.1 to 7.1.6, themselves derived from the analytical approach. Although the analysed system is not transversely symmetrical in the field, only one half of it is considered because the size of available computer core storage is incapable of accommodating data for the entire system discretized by finite elements.

Predicting the response of a buried pipe to ground movement is difficult because of the indeterminated nature of the soil-pipe interaction.

In the past, several assumptions have been made in order to formulate a simple theoretical model of the soil-pipe system for obtaining a practical method of design. These assumptions mainly relate to the distribution of load in the soil-pipe system. The finite element method, which does not require such an assumption, enables analyses to be carried out for a range of conditions to

which a soil-pipe system might be subjected. However, because of the reason pointed out previously, the behaviour of a buried pipe is analysed by applying a displacement field to two different finite element meshes: one considering the pipe and surrounding soil as a system, and the other considering the pipe alone.

The analyses of soil-pipe and soil-lining systems were performed assuming a perfect bonding between soil and structure.

6.9 GENERAL COMMENTS.

Although considerable study has been devoted to the analysis and design of both rigid and flexible buried cylinders, little attention has been given to the response of buried pipelines to the ground movements caused by tunnelling. The present investigation is aimed at improving the tools necessary for predicting their behaviour.

In all the cases studied and reported in this thesis, numerical techniques are used and presented as follows :

a) Simulation of a tunnel excavation without

lining installation. This represents the case in which the lining is installed after the full potential displacements have developed.

b) Simulation of the response of a soil-pipe system to the ground movement caused by tunnelling in soil without modelling the surrounding soil in the finite element mesh.

c) Simulation of the response of a soil-pipe system to the ground movement caused by tunnelling in soil.

d) Simulation of a tunnel excavation in a soft soil with lining installation.

Cases b) and c) have been analysed by applying a displacement field to the finite element mesh. The analyses of cases a) and d) were performed on finite element meshes without considering pipes lying parallel to the tunnel centre line.

The finite element meshes used in the analyses were defined in such a way that the geometry and material properties remained unchanged along the longitudinal direction. The transverse planes are parallel to each other and equally spaced.

The integration scheme used in this work is prone

to numerical instability beyond a certain range of finite element idealization. In the examples presented herein, the double precision statement was used in the program in order to overcome this problem. The general question of the choice of a best scheme having optimum economy and accuracy from among a large number of available finite element schemes is a difficult task, and further investigations were not carried out because this matter is out of the scope of this research.

As pointed out earlier, analyses were performed assuming the medium to be incompressible. This assumption may lead to numerical difficulties because stresses are related directly to the elasticity matrix [D]:

$$\{\sigma\} = [D].\{\varepsilon\}$$

For an elastic isotropic medium Poisson's ratio should be equal to 0.5, and for this value all terms in the appropriate elasticity matrix become infinite. Consequently, the solutions obtained by this numerical technique are unreliable if ν is too close to 0.5.

Although the tone of the discussions outlined in this Section may have appeared to emphasize the difficulties encountered in the accurate modelling of the

tunnelling process and the response of a buried pipeline to ground movements, it is nevertheless possible within the imposed limitations to examine various aspects of the problem and obtain information that can be useful for design purposes.

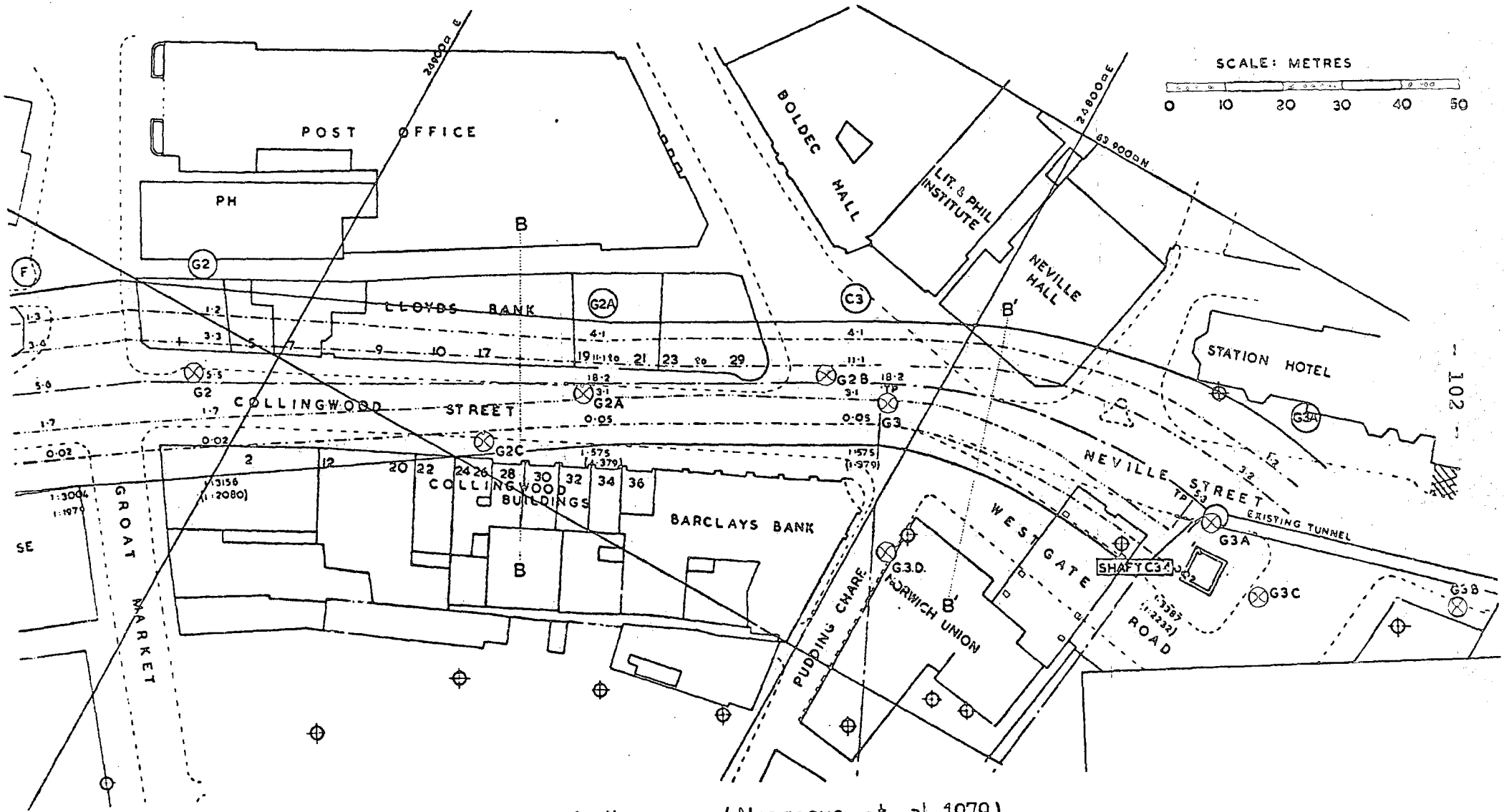

FIG. 6.1) Plan of the area (Norgrove et al, 1979)

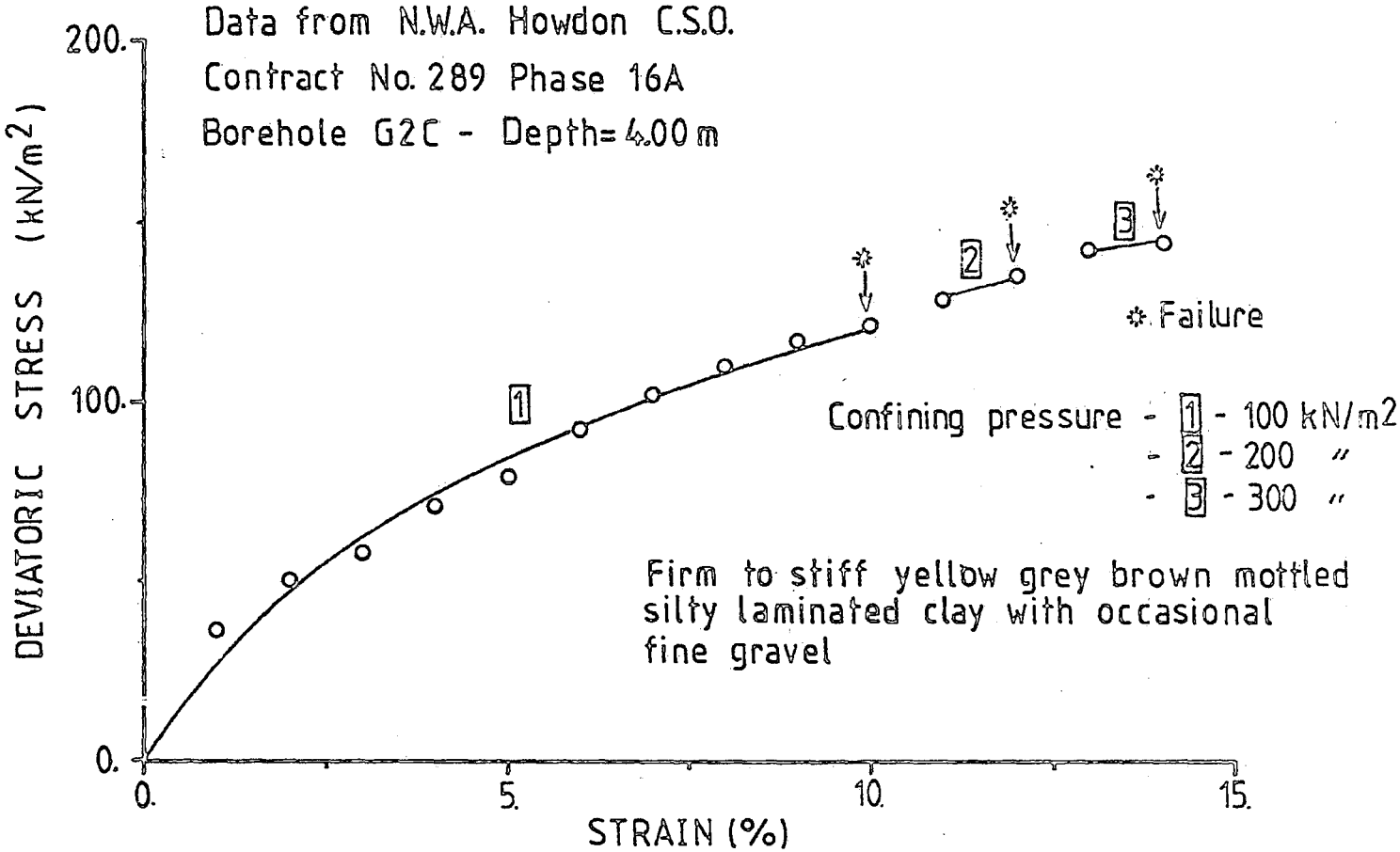

FIG.6.2) Undrained triaxial test on undisturbed sample at a depth of 4 m.

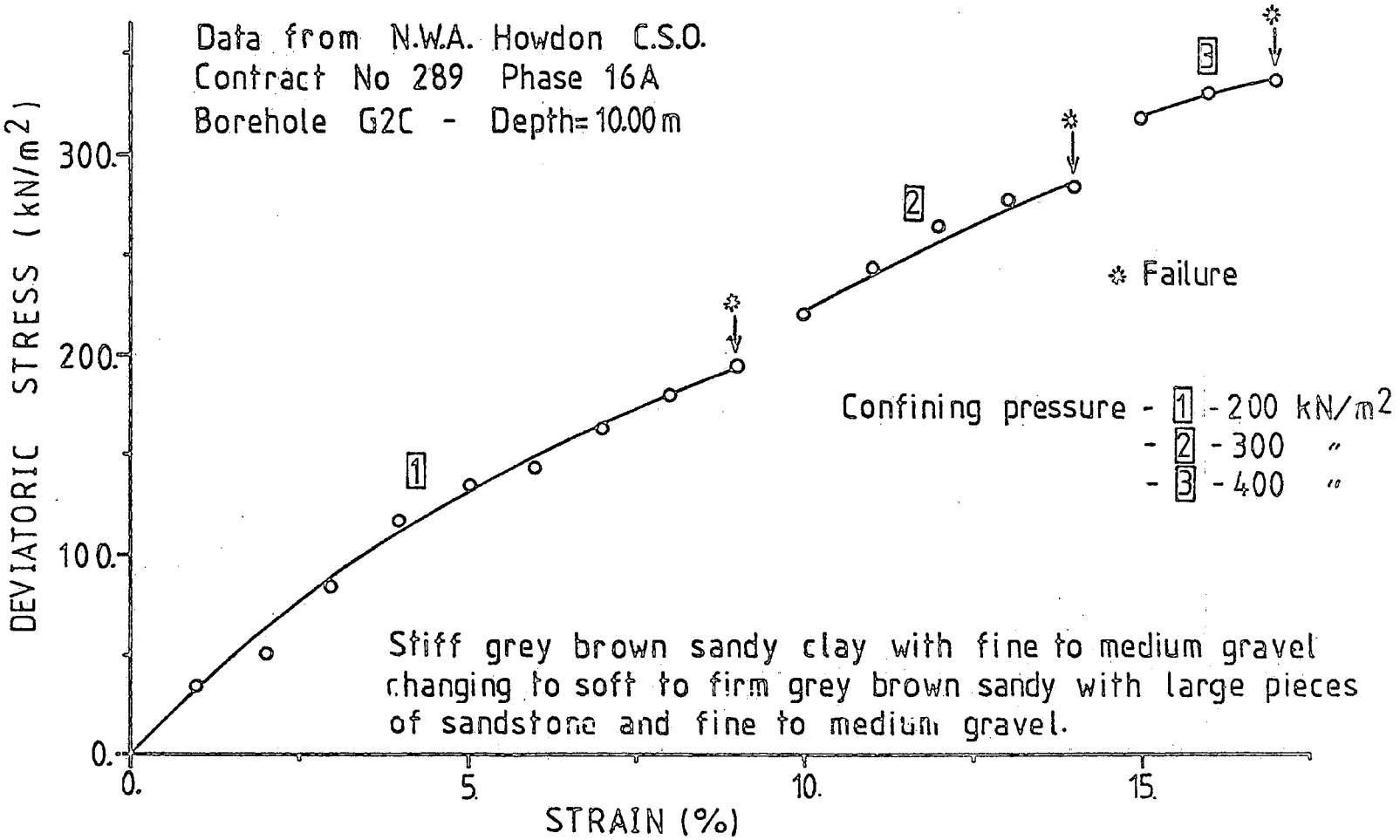

FIG. 6.3) Undrained triaxial test on undisturbed sample at a depth of 10 m.

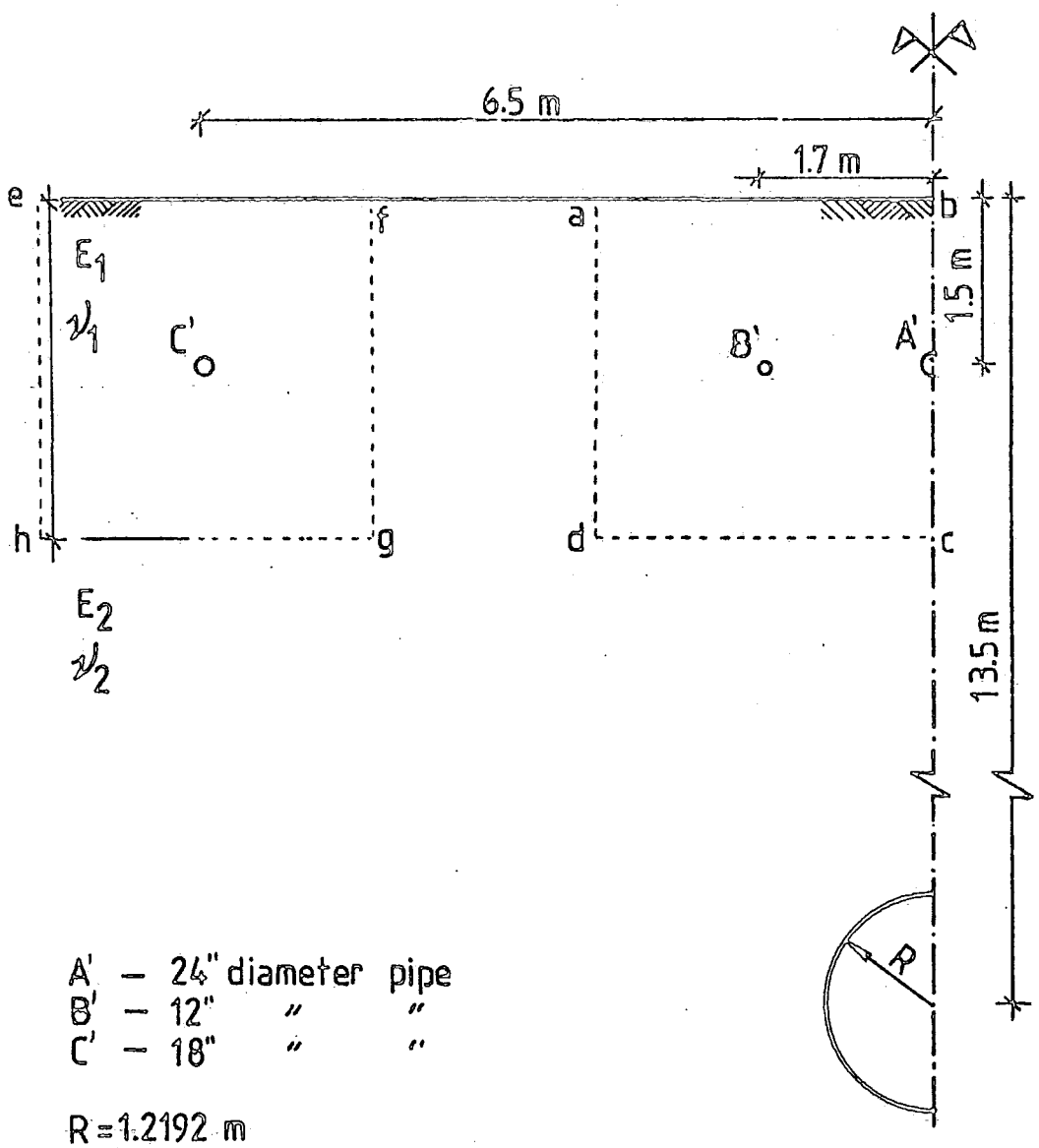

A' – 24" diameter pipe
B' – 12" " "
C' – 18" " "

R = 1.2192 m

E_1 = 0.6 MN/m^2
E_2 = 1.0 "
$\nu_1 = \nu_2 = 0.48$

FIG.6.4) Sketch of the idealized site profile.

TABLE 6.1 Characteristics of three pipes lying parallel to the tunnel centre line at Collingwood Street.

PIPE	INTERNAL DIAMETER (inch)	DISTANCE FROM CENTRE LINE (m)	EXTERNAL DIAMETER (m)	INTERNAL DIAMETER (m)	MOMENT OF INERTIA (m^4)
A'	24	-	0.650	0.610	19.92×10^{-4}
B'	12	1.7	0.334	0.305	1.86×10^{-4}
C'	18	6.5	0.492	0.457	7.35×10^{-4}

CHAPTER 7

FINITE ELEMENT CALCULATIONS AND DISCUSSION.

7.1 INTRODUCTION.

The computer code FEP3DES described in Chapter 5 has been used to carry out the analyses outlined in the previous Chapter. To illustrate the possible applications and difficulties in using the three-dimensional finite element linear analysis for predicting displacements, stresses and strains caused by tunnelling in soft ground, and its possible effects on buried pipelines, four examples are presented in the following sections.

As a prelude to evolving an incremental elastic-plastic analysis, the present work deals with the elastic analysis. In particular, various factors that affect calculated results are considered, including relative stiffness between soil and pipe, and the finite element mesh employed in the analyses. Each example is prefaced

by a summary of the assumptions employed in the analysis, and which outlines the essential problems in setting up reasonable models for behavioural studies of soil masses and/or nearby structures subjected to a programme of tunnel excavation. Only static deflection analysis is considered, and a summary of results discussed in this work is shown in Table 7.1.

7.2 TUNNELLING IN SOIL : DISPLACEMENTS, STRESSES AND STRAINS.

Given the factors outlined in the previous Section, it was decided to establish a rational criterion of analysis which could provide appropriate information for practical assessment and design purposes. A logical conclusion for this stage of study was that, with the present state of the art in tunnelling, the analysis cannot be expected to represent all the important factors influencing the ground displacements. Therefore, many researchers have performed reasonable analyses by assigning a Gaussian probability curve to the shape of the transverse settlement trough over tunnels, as discussed in Chapter 2. Thus, it was decided that the displacements calculated by the finite element method should be compared with displacements calculated by the approach of Attewell and Woodman (1982). Adoption of a Gaussian curve is supported by the literature survey reported in tabular

form in this dissertation (Table 2.1).

Before starting finite element calculations, the displacements and strains were calculated and plotted using an Exidy Sorcerer microcomputer, as noted above. The plots, comprising 10% (of maximum) contour lines, are shown in Figures 7.1.1 to 7.1.6 inclusive, and they were also used to limit the boundaries of the finite element meshes. These Figures have been obtained using a value of 5% for V_s, together with K_a and n values equal to unity, as suggested by Norgrove et al.(1979) for this site.

7.2.1 FINITE ELEMENT MODEL.

The finite element mesh is shown in Figure 7.2.1. This mesh was designed to represent only the major tunnel opening and giving smooth stress and displacement variations around the opening. Only one half of the system was considered and the three pipes lying parallel to the tunnel centre line were not taken into account because of the limitation of storage capacity of the computer used in the analysis.

Analysis of the excavation process was performed to include the following :

a) the soil mass was modelled as a linearly elastic, isotropic and homogeneous material.

b) the virgin stress field was simply assessed on the basis of stress for depth, with the horizontal stresses calculated by multiplying vertical stresses by the coefficient of earth pressure, K.

c) the lower boundary of the mesh is restrained from moving in any direction.

d) the vertical surfaces of the mesh, except for the frontal one, are prevented from moving perpendicularly to the surface considered.

e) all points in the interior, ground surface, and in the frontal surface, except those located on the edges of the mesh, were given no restrictions to movement.

f) no external loads or body forces were applied.

g) the only sources of deformation are the relaxation forces due to the excavation.

h) since only an elastic analysis was available, the simulation procedure was performed in one single step of excavation. The shaded portion of the mesh in Figure 7.2.1 represents the surface exposed by excavation.

i) no support structures were modelled in the analysis.

j) no in-ground structures were modelled in the analysis.

k) transverse sections of the mesh were equally spaced in the longitudinal (parallel to the tunnel centre line) direction in order to facilitate comparison between

results calculated by the finite element method and the normal probability curve assumption. This distance was taken to be equal to 3.375m (i/4).

l) output data were plotted once the 'best fit' between transverse settlement troughs calculated by the finite element method and the normal probability empirical approach was achieved.

m) three transverse sections were selected in order to achieve the previous objective : 3i behind the tunnel face, at the tunnel face, and i ahead of tunnel face, as indicated in Figure 7.2.2 by planes ABCD, EFGH and IJKL, respectively.

n) matching of surface settlement troughs was performed by varying the applied horizontal forces only.

o) the maximum settlement is assumed to be achieved above the tunnel centre line and 3i behind the face.

p) once the 'best fit' was assumed to be achieved using transverse sections indicated in m), the ground surface and longitudinal section, indicated respectively by planes MNOP and OPQR in Figure 7.2.3, were also consided.

7.2.2 COMPARISON BETWEEN FINITE ELEMENT AND NORMAL PROBABILITY CURVE RESULTS.

Included in this Section is a qualitative

discussion on the adjustment required to be made to the curves obtained by finite element calculations in order to give a more accurate approximation to a normal probability curve.

Four surface settlement troughs for each transverse section were calculated and plotted in terms of percentage of maximum settlement, as shown in Figure 7.2.4. The value of maximum settlement was taken at the point located on the surface above the tunnel centre line 3i behind the tunnel face.

Three finite element calculations were performed considering one case in which the horizontal forces were not reduced, and two cases reducing 5- and 10-times the values of the forces calculated from the virgin stresses. The resulting vertical displacements on the ground surface had to be adjusted based on the condition that no movement would occur on the vertical boundary parallel to the tunnel centre line. Thus, the displacements of nodes located on the upper edges of this boundary were set to zero and every node located on the same transverse section was reduced by the same amount of displacement. This is equivalent to a translation movement of each transverse settlement trough by an amount of corresponding vertical movement of the node located at the upper edge of the

vertical boundary parallel to the tunnel centre line.

Results are plotted in Figure 7.2.4. The dashed lines (1) represent the normal probability curve and solid lines (2, 3 and 4) represent results obtained by the finite element method.

The transverse settlement curves obtained by both approaches have shown the following :

a) Transverse section 3i behind the tunnel face.

- the maximum slope of curve 1 is steeper than those for curves 2,3 and 4.

- the maximum slope of curve 2 is the steepest of the finite element results.

- the inflexion points of all four curves are located approximately at the same distance from the centre line.

- the distance from the tunnel centre line of the interception point of curves 2, 3 and 4 with curve 1 increases with decreasing horizontal forces. This means that for distances smaller than i from the centre line, the difference in the percentage of maximum settlement is larger for smaller horizontal forces. The inverse applies for distances greater than i from the tunnel centre line.

b) Transverse section at the tunnel face.

- the maximum slope for the finite element models increases with the decrease in horizontal forces.

- the maximum discrepancy between curves 1 and 4 is approximately 2% for the same point.

- the percentage of maximum settlement on this section calculated by the finite element method is lower than 50%.

- the percentage of maximum settlement over the tunnel centre line increases with the decrease of horizontal forces.

c) Transverse section i ahead of tunnel face.

As expected, all four profiles have given lower percentages of maximum settlement if compared with both previous transverse sections. Comparatively, the discrepancies in terms of percentages between them are larger than in the other two transverse sections, but it seems that these differences are not significant for practical purposes because the magnitude of displacements developed in this section is small relative to the maximum settlement developed in the medium.

Bearing in mind all the limitations outlined in

previous Chapters and a lack of substantive geotechnical data, the succeeding finite element calculations to simulate tunnel construction were carried out based on the model adopted for obtaining curve 4 in Figure 7.2.4. The following observations can be made from the results obtained using the model outlined above and in Section 7.2.1.

7.2.3 DISPLACEMENTS.

7.2.3.1 LATERAL.

An attempt was made to define some of the mechanisms by which lateral displacements can accompany settlement, and to investigate the nature of such movements that develop when a tunnel is driven in soil under the conditions outlined in Chapter 6.

Contours of equal lateral displacements in millimetres for all five sections were plotted, and shown in Figures 7.2.5 through 7.2.8, where a positive sign means towards the tunnel centre line. The following observations can be made with respect to these Figures :

a) There is no lateral movement on the ground surface above the tunnel centre line (Figures 7.2.5 to 7.2.8).

b) At each location the direction of the lateral movement is toward the point of maximum settlement; that is, the displacements are always positive.

c) The point of maximum lateral movement on the ground surface (Figure 7.2.8) and the inflexion point of the fully-developed transverse settlement trough (Curve 4, Figure 7.2.4) are located at approximately equal horizontal distances from the tunnel centre line (1.5i).

7.2.3.2 VERTICAL.

The magnitude and distribution of vertical displacements calculated by the finite element method are shown in Figures 7.2.9 to 7.2.13. Contours of equal displacements are shown (positive sign means upwards), and the following can be observed :

a) The largest settlement of each transverse section is located above the tunnel centre line.

b) The maximum settlement may be taken at the point located not less than 3i behind tunnel face (Figure 7.2.13).

c) The magnitude of the maximum settlement is approximately twice as large as the magnitude of maximum settlement generated on the transverse section containing the tunnel face (Figures 7.2.9, 7.2.10, 7.2.12 and 7.2.13).

d) The vertical displacement beyond i ahead of the tunnel face (Figures 7.2.12) is less than 2% of the maximum settlement.

e) The magnitude of the vertical displacements decreases from the tunnel axis (centre) upwards, towards ground surface (Figures 7.2.9 and 7.2.10).

f) The springline of the tunnel moves slightly upwards (Figures 7.2.9 and 7.2.10).

7.2.3.3 LONGITUDINAL.

The distribution of longitudinal displacements in millimetres is plotted and shown in Figures 7.2.14 through 7.2.18. From these Figures, the following can be observed, taking the positive sign in the direction of the tunnel advance:

a) The ground surface moves in an opposite direction to that of the tunnel advance (Figure 7.2.17).

b) Longitudinal displacements on the ground surface increase towards the tunnel face (Figure 7.2.17).

c) The shape of the curves representing contours of equal longitudinal displacements above the tunnel face are approximately circular with the largest radius approximately equal to i (Figure 7.2.17).

d) The maximum longitudinal displacement is achieved on the tunnel springline (Figure 7.2.14).

7.2.4 STRESSES.

Distributions of all three normal (to each primary plane of section) stress components were plotted and shown in Figures 7.2.19 through 7.2.33, with a negative sign indicating compressive and a positive sign indicating tensile stresses. These Figures highlight the following points :

7.2.4.1 LATERAL.

a) Compressive and tensile lateral stresses develop on the ground surface (Figure 7.2.22).

b) There is no significant variation in lateral stresses beyond section i ahead of the tunnel face (Figures 7.2.21 and 7.2.23).

c) The transition line between compressive and tensile stresses on the ground surface runs parallel to and at about 2i distance from the tunnel centre line until a transverse plane including the tunnel face (Figure 7.2.22) is reached.

d) The absolute value of maximum compressive stress is greater than the absolute value of maximum tensile stress on the ground surface (Figure 7.2.22).

e) The tunnel excavation induces the same lateral stress pattern on soil sections located behind the tunnel face (Figures 7.2.19,7.2.20 and 7.2.23).

7.2.4.2 VERTICAL.

Although the ground surface is an unrestrained boundary of the finite element mesh, the normal vertical stresses develop on it because of the transverse displacement restriction imposed on the lateral boundary of this surface. Associated with this condition, there is another reason for such apparent ground surface behaviour. The finite element used in the program gives constant stress (also strain) on an entire volume of the element. This means that any point in the element, obviously including the nodal points, will have the same magnitude of stress (or strain). Then, the vertical stress distribution on any plane parallel to the ground surface intercepting the elements representing the ground surface will have the same pattern of distribution as shown in Figure 7.2.27, except for the plane common to the adjacent elements. Bearing in mind the limitations outlined above, the following observations may be made :

a) Compressive and tensile vertical stresses develop on the ground surface (Figure 7.2.27).

b) On the ground surface, the vertical stresses are tensile ahead of tunnel face and compressive behind tunnel face (Figure 7.2.27).

c) Observations b and d made for lateral stresses also apply for vertical stresses.

7.2.4.3 LONGITUDINAL.

Further comments on longitudinal stresses are considered unnecessary because observations made for lateral stresses also apply to longitudinal stresses.

7.2.5 STRAINS.

In a similar manner to the stresses, Figures 7.2.34 to 7.2.48 show the distribution of three components of normal strains in the transverse sections ABCD, EFGH and IJKL, ground surface section MNOP and longitudinal section OPQR.

A positive sign indicate tensile strain and a negative sign indicates compressive strain.

7.2.5.1 LATERAL.

a) Lateral strains on plane OPQR (Figure 7.2.3) are compressive (Figure 7.2.38).

b) The contour of zero lateral strain on the ground surface is sensibly parallel to the tunnel centre line (Figure 7.2.37).

c) The contour of zero lateral strain on the ground surface is located approximately 1.5i from the tunnel centre line (Figure 7.2.37).

d) On the ground surface the magnitude of maximum lateral strain in compression is greater than the strain in extension (Figure 7.2.37). The approximate respective values are 0.075% and 0.025%. This ratio is larger than the theoretical ratio according to normal probability curve theory.

7.2.5.2) VERTICAL.

Observations made for vertical stresses on the ground surface also apply to vertical strains. Then, the following can be observed :

a) The maximum tensile vertical strain on the ground surface is located above the tunnel centre line and behind the tunnel face (Figure 7.2.42).

b) The maximum compressive vertical strain on the ground surface is located laterally 2.5i from the tunnel centre line and i behind the face (Figure 7.2.42).

c) The patterns of vertical strair distributions on any transverse planes distant more than i/2 behind the tunnel face are similar (Figures 7.2.39, 7.2.40 and 7.2.43).

7.2.5.3) LONGITUDINAL.

a) Contours of equal longitudinal strains on plane

OPQR developed within 2i ahead and 2i behind the tunnel face are approximately symmetric relative to the vertical transverse plane located i/2 ahead of the tunnel face (Figure 7.2.48).

b) The magnitudes of longitudinal strains on the transverse section at the tunnel face are much smaller than on sections 3i behind the tunnel face and i ahead of the face (Figures 7.2.44 to 7.2.46).

c) The patterns of the longitudinal strain distribution contours shown in Figures 7.2.44 and 7.2.46 are similar, but a contour representing compressive strain in one of the Figures (Figure 7.2.44) corresponds to a tensile contour in the other (Figure 7.2.46).

7.2.6 DISCUSSION.

From the example of numerical analysis presented above, some relations may be predicted between displacements, stresses and strains that are likely to develop on pipelines buried in an area disturbed by the tunnelling process.

From contours of results calculated by the finite element approach for the model adopted, and presented in Figures 7.2.5 through 7.2.48, the following can be deduced :

a) A pattern of differential vertical movements always exists with the magnitude of settlement increasing from near zero at the outer edges of a settlement trough to a maximum at some point behind and on the line of a moving disturbance source.

b) The point of maximum lateral movement corresponds to the point of zero lateral strain (Figures 7.3.8 and 7.2.37)

c) The pattern of movements and strain distributions on the ground surface obtained by the finite element and normal probability approaches are similar.

d) The position of the maximum extensional strain and zero strain are predicted to be approximately the same by the finite element and normal probability approaches.

e) The prediction that the maximum lateral displacement, zero lateral stress and zero lateral strain on the ground surface should occur approximately at the same point was not confirmed in the finite element calculations (Figures 7.2.8, 7.2.22 and 7.2.37). This situation may well be caused by the boundary conditions adopted for the finite element mesh.

f) The mesh boundary conditions adopted for the finite element calculations may cause the development of spurious normal stresses on the ground surface.

Additional information relating to the analysis performed above can be found in Chapter 8.

TABLE 7.1 SUMMARY OF THE RESULTS PRESENTED.

	TUNNELL. WITHOUT LINING INSTALL.					SOIL-STRUC SYST.			SOIL-STRUC SYST.			PIPE A°				PIPE B°				PIPE C°				TUNNELLING WITH LINING INSTALLATION																			
												Fibre				Fibre				Fibre				Step 1					Step 2					Step 3					Step 4					Step 5					Step 6					Step 7				
	ABCD	EFGH	IJKL	MNOP	OPQR	ABCD	EFGH	IJKL	ABCD	EFGH	IJKL	UPPER	LOWER	RIGHT	LEFT	UPPER	LOWER	RIGHT	LEFT	UPPER	LOWER	RIGHT	LEFT	ABCD	EFGH	IJKL	MNOP	OPQR	ABCD	EFGH	IJKL	MNOP	OPQR	ABCD	EFGH	IJKL	MNOP	OPQR	ABCD	EFGH	IJKL	MNOP	OPQR	ABCD	EFGH	IJKL	MNOP	OPQR
u	X	X	X	X		X	X	X	X	X	X																X								X								X				
v	X	X	X	X	X	X	X	X	X	X	X																X	X							X	X							X	X			
w	X	X	X	X	X	X	X	X	X	X	X																X	X							X	X							X	X			
σ_x	X	X	X	X	X																																											
σ_y	X	X	X	X	X																																											
σ_z	X	X	X	X	X							X	X	X	X	X	X	X	X	X	X	X	X																											
τ_{xy}																																																
τ_{yz}																																																
τ_{zx}																																																
ε_x	X	X	X	X	X	X	X	X	X	X	X	X	X														X	X							X	X							X	X			
ε_y	X	X	X	X	X	X	X	X	X	X	X																X	X							X	X							X	X			
ε_z	X	X	X	X	X	X	X	X	X	X	X	X	X			X	X			X	X						X	X							X	X							X	X			
γ_{xy}																																																
γ_{yz}																																																
γ_{zx}																																																

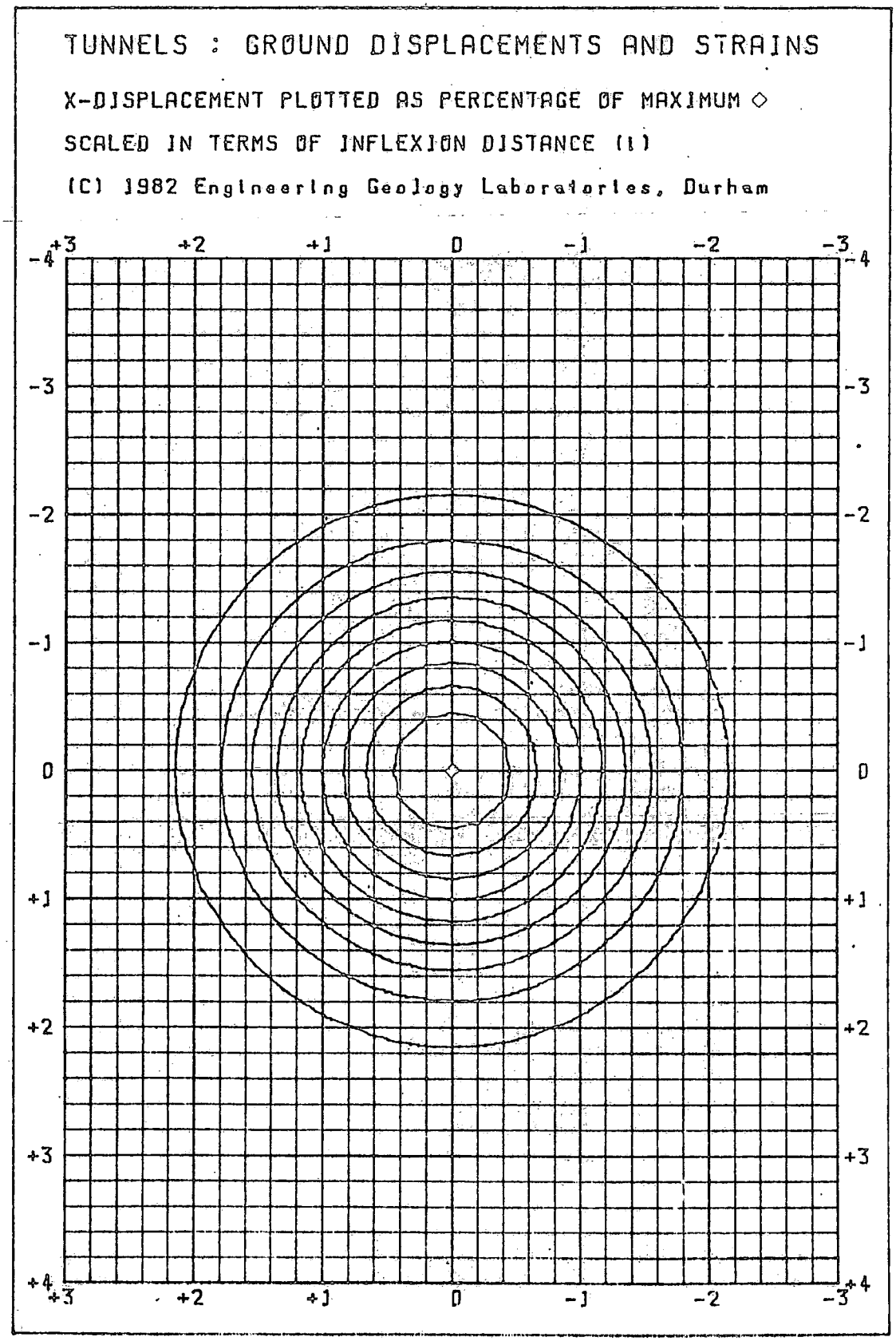
TUNNELS : GROUND DISPLACEMENTS AND STRAINS
X-DISPLACEMENT PLOTTED AS PERCENTAGE OF MAXIMUM ◇
SCALED IN TERMS OF INFLEXION DISTANCE (i)
(C) 1982 Engineering Geology Laboratories, Durham
+3 +2 +1 0 -1 -2 -3
-4
-3
-2
-1
0
+1
+2
+3
+4

FIG. 7.1.1

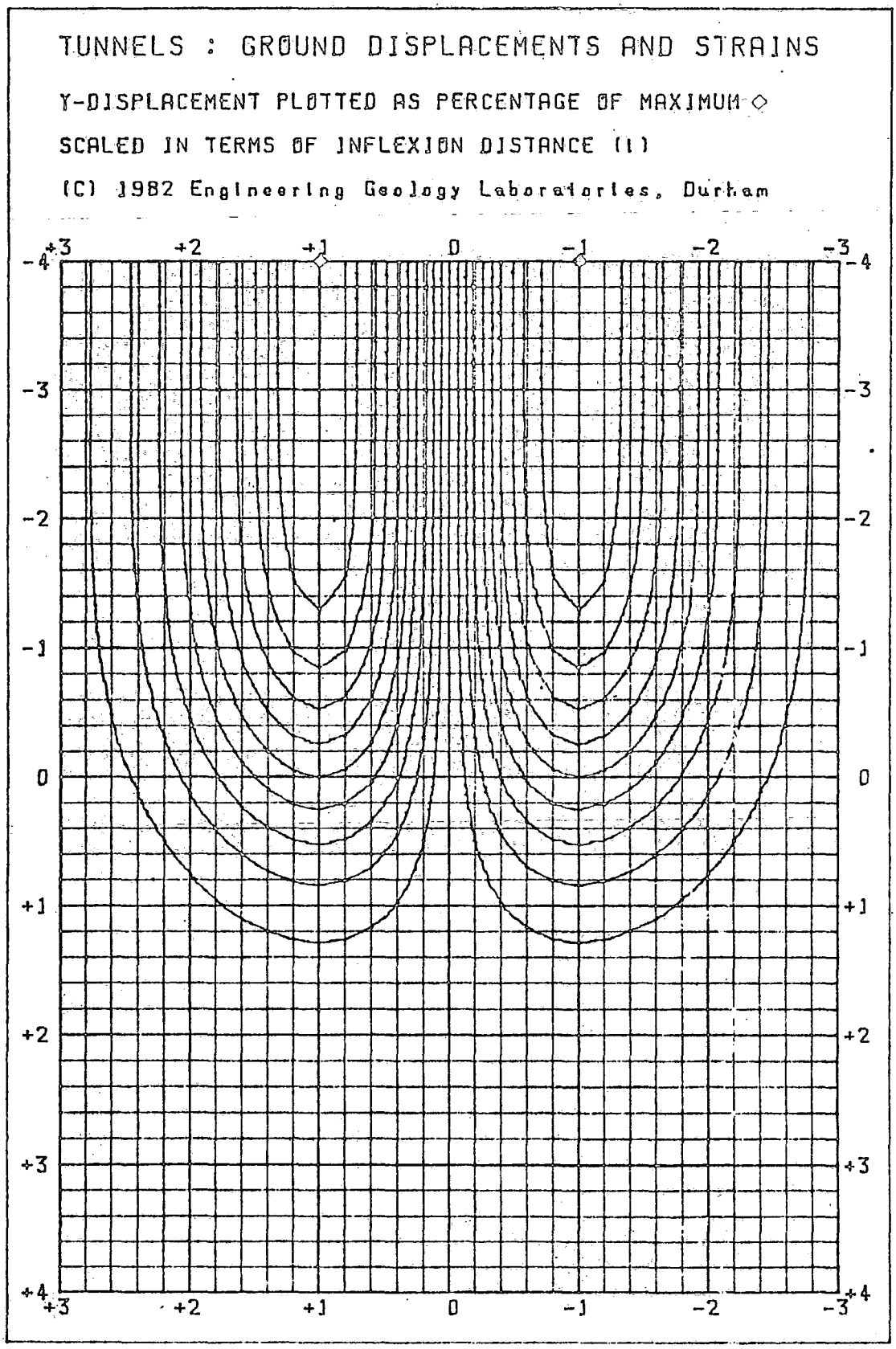
TUNNELS : GROUND DISPLACEMENTS AND STRAINS
Y-DISPLACEMENT PLOTTED AS PERCENTAGE OF MAXIMUM ◇
SCALED IN TERMS OF INFLEXION DISTANCE (i)
(C) 1982 Engineering Geology Laboratories, Durham
+3 +2 +1 0 -1 -2 -3
-4
-3
-2
-1
0
+1
+2
+3
+4

FIG. 7.1.2

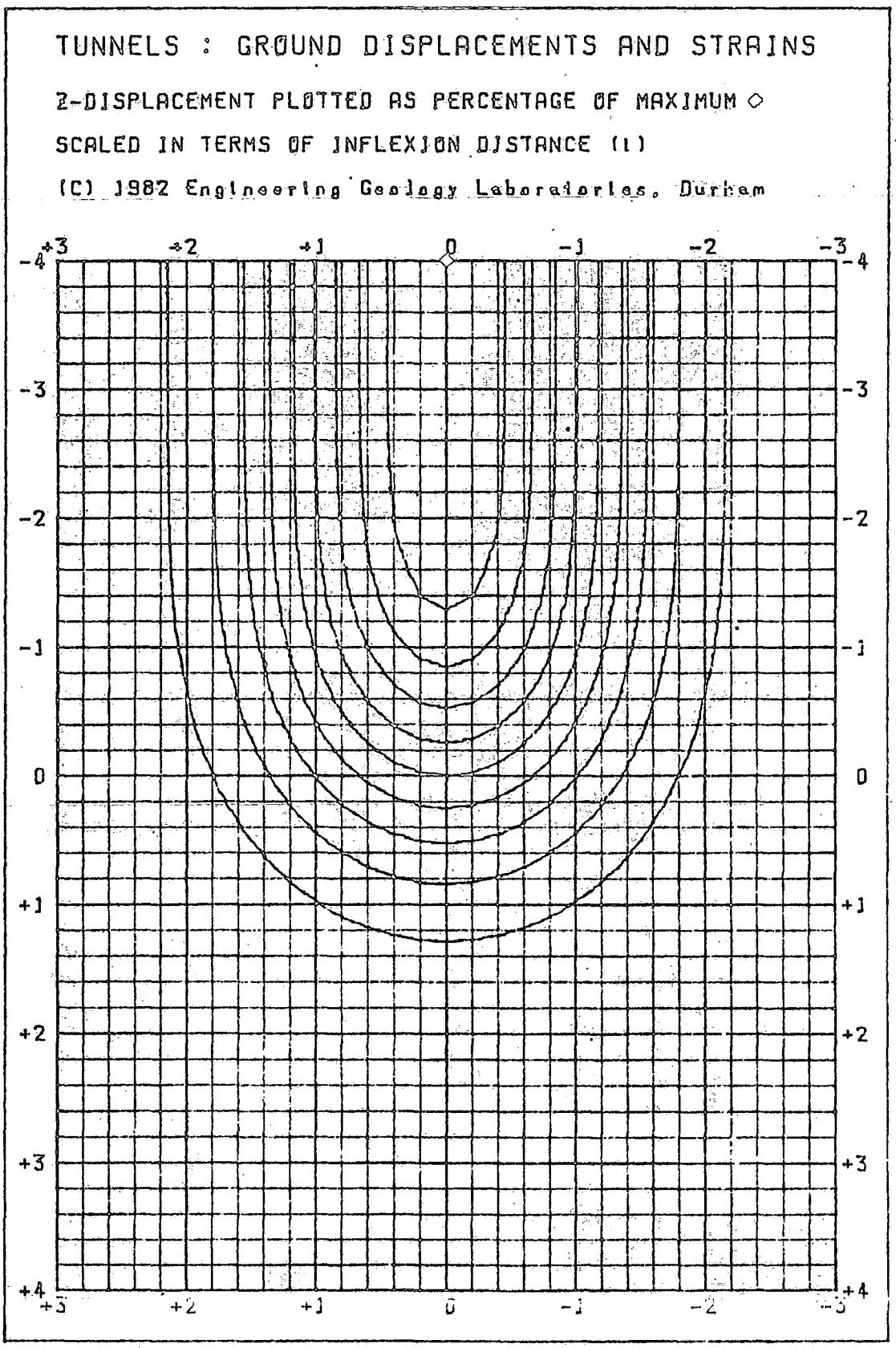
TUNNELS : GROUND DISPLACEMENTS AND STRAINS
Z-DISPLACEMENT PLOTTED AS PERCENTAGE OF MAXIMUM ◇
SCALED IN TERMS OF INFLEXION DISTANCE (i)
(C) 1982 Engineering Geology Laboratories, Durham
+3
+2
+1
0
-1
-2
-3
-4
+4

FIG. 7.1.3

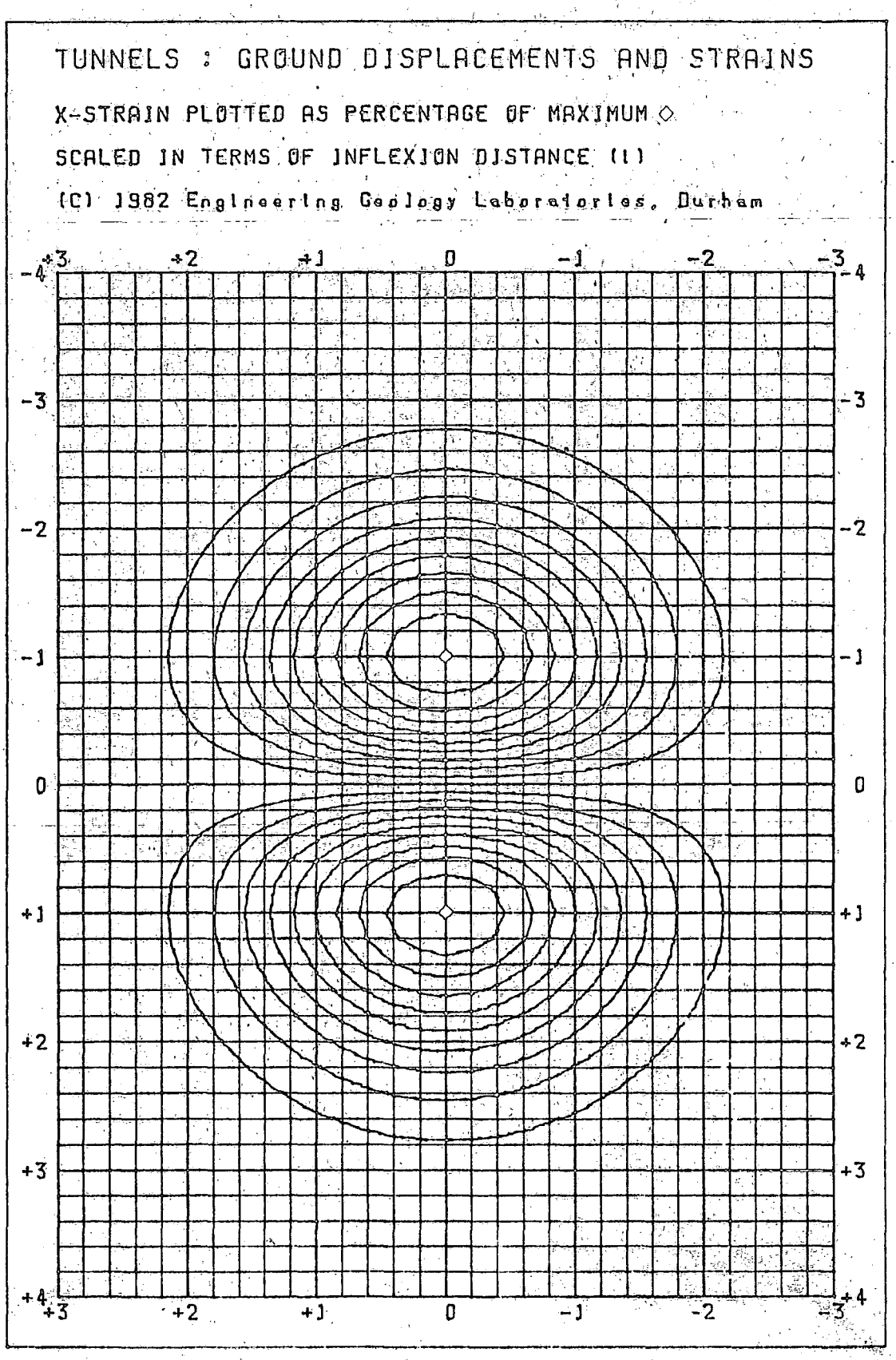
TUNNELS : GROUND DISPLACEMENTS AND STRAINS
X-STRAIN PLOTTED AS PERCENTAGE OF MAXIMUM ◇
SCALED IN TERMS OF INFLEXION DISTANCE (i)
(C) 1982 Engineering Geology Laboratories, Durham
+3 +2 +1 0 -1 -2 -3
-4
-3
-2
-1
0
+1
+2
+3
+4

FIG. 7.1.4

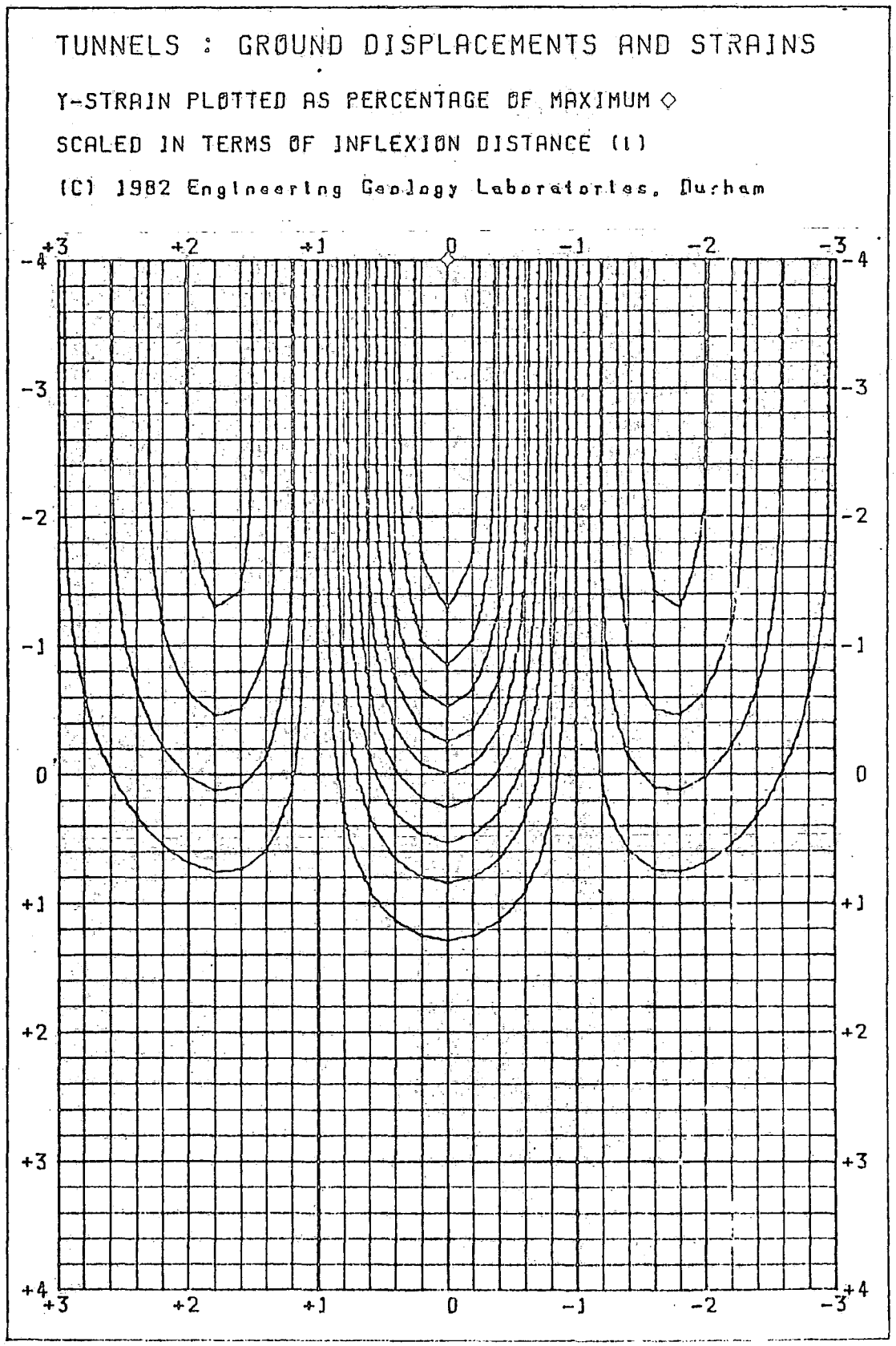
TUNNELS : GROUND DISPLACEMENTS AND STRAINS
Y-STRAIN PLOTTED AS PERCENTAGE OF MAXIMUM ◇
SCALED IN TERMS OF INFLEXION DISTANCE (i)
(C) 1982 Engineering Geology Laboratories, Durham
+3 +2 +1 0 -1 -2 -3
-4 -3 -2 -1 0 +1 +2 +3 +4

FIG. 7.1.5

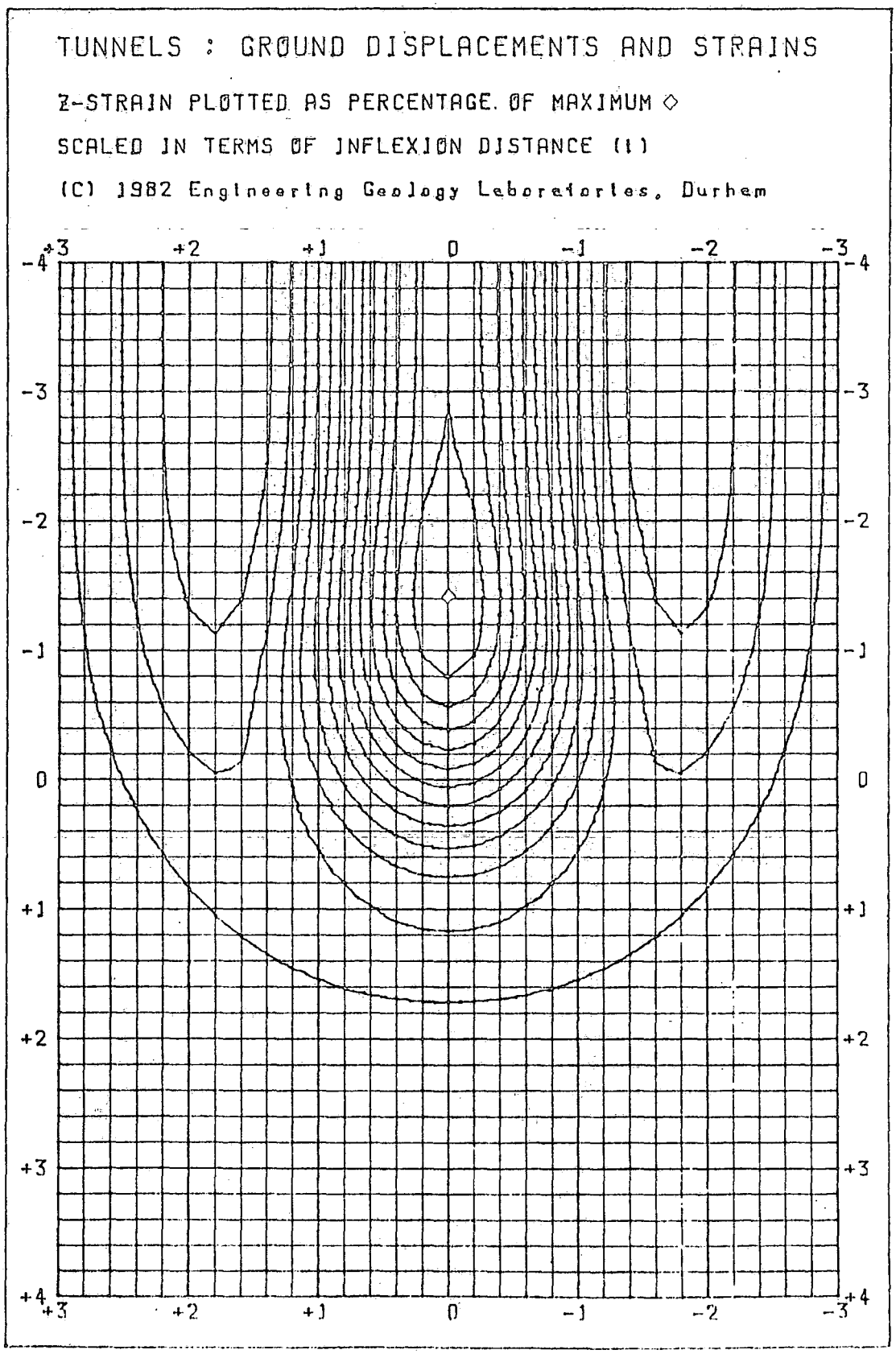
TUNNELS : GROUND DISPLACEMENTS AND STRAINS
Z-STRAIN PLOTTED AS PERCENTAGE OF MAXIMUM ◇
SCALED IN TERMS OF INFLEXION DISTANCE (i)
(C) 1982 Engineering Geology Laboratories, Durham
+3
+2
+1
0
-1
-2
-3
-4

FIG. 7.1.6

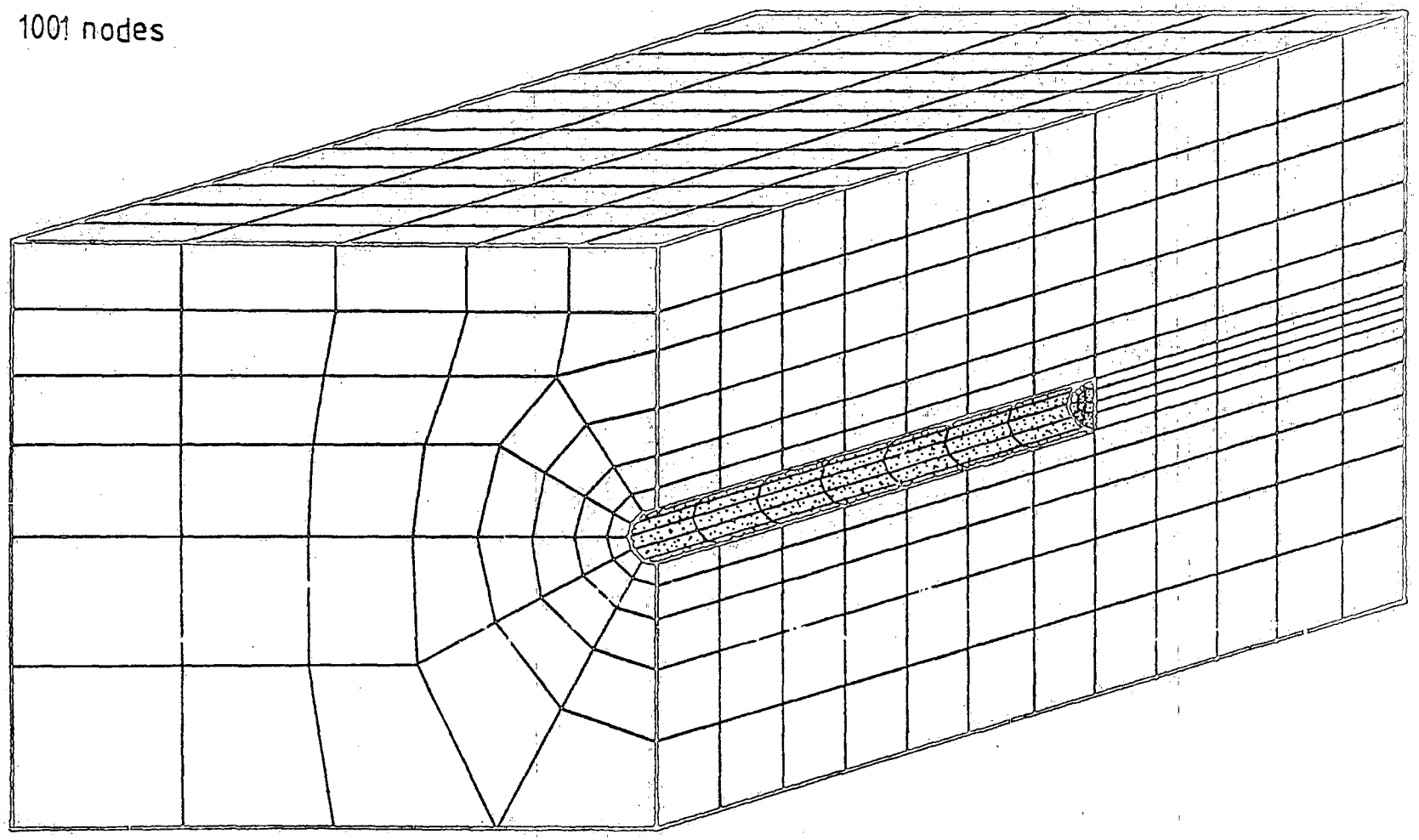

FIG. 7.2.1) 3-D finite element mesh to simulate tunnel excavation.

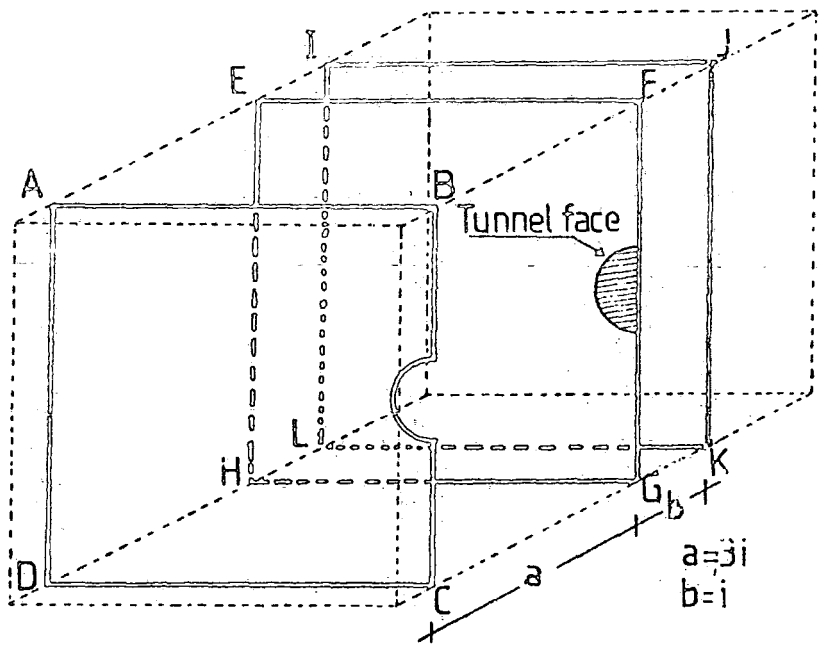

FIG. 7.2.2) Tranverse sections.

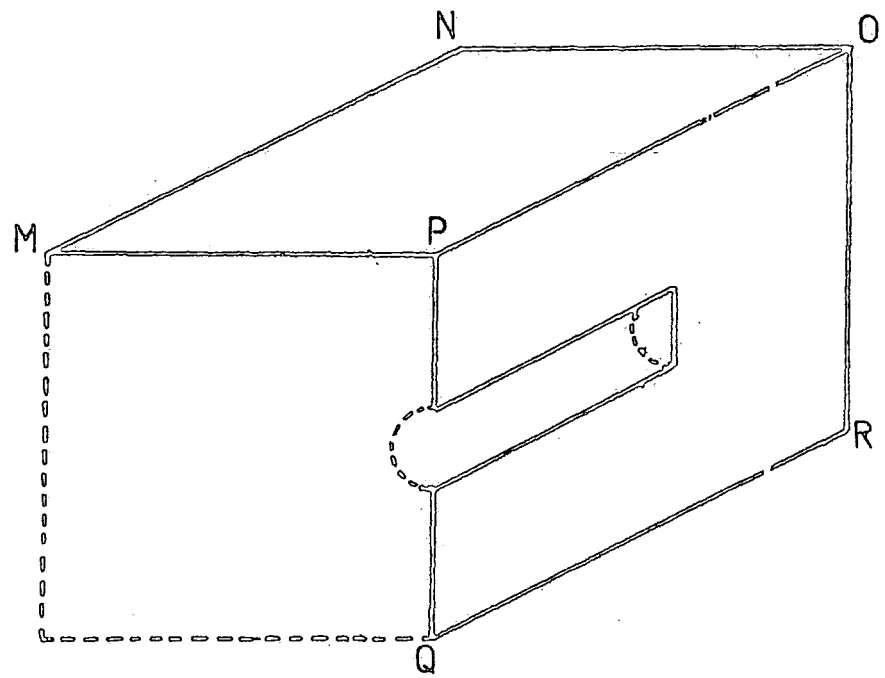

FIG. 7.2.3) Longitudinal section & ground surface.

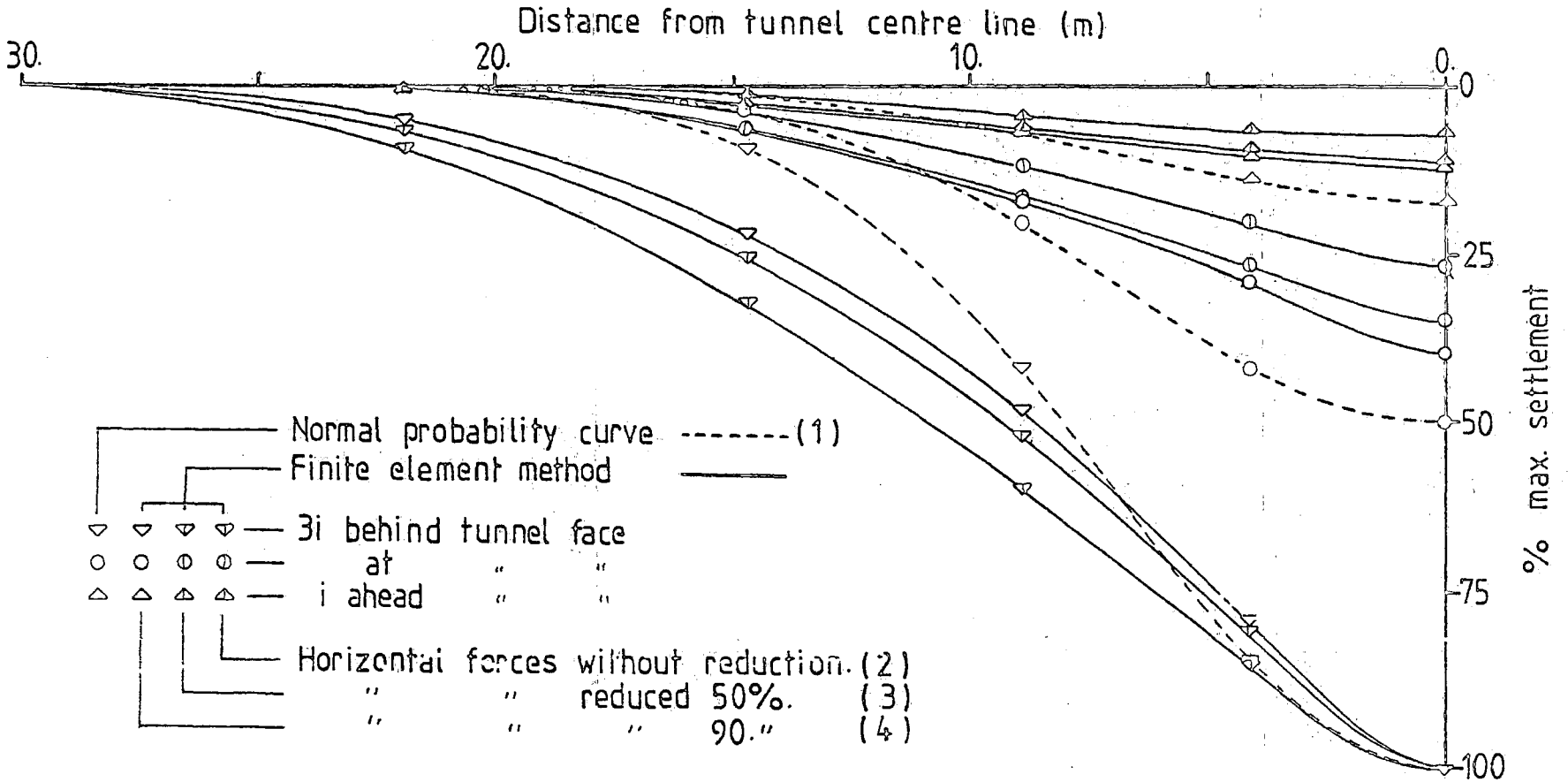

FIG.7.2.4) Transverse settlement trough.

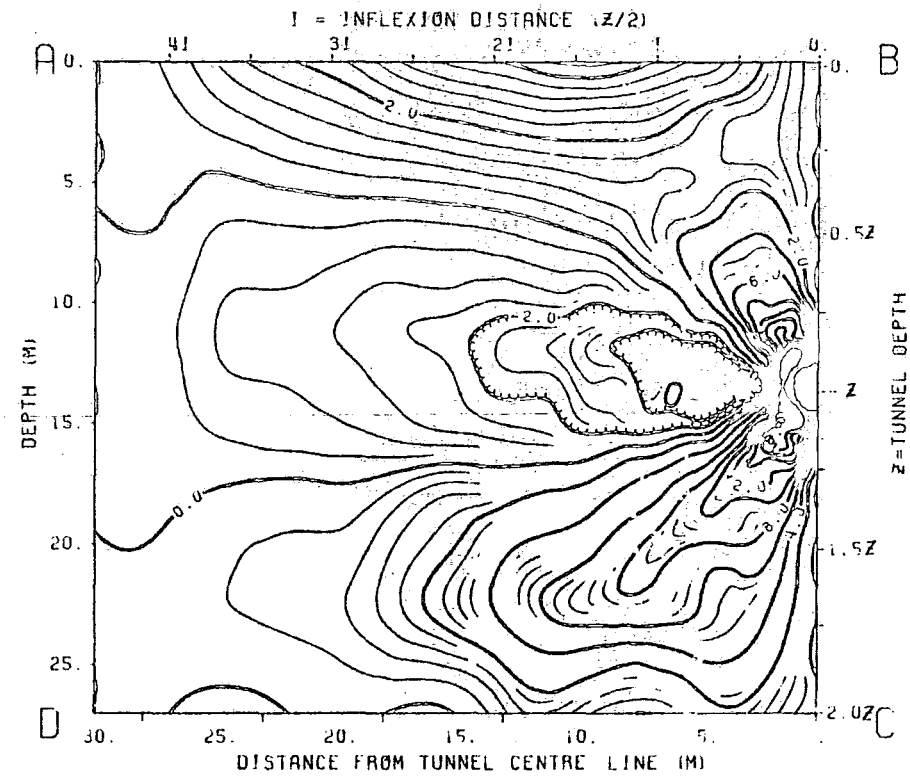

FIG. 7.2.5) Contours of equal lateral displacements (mm). Transverse section 3i behind tunnel face.

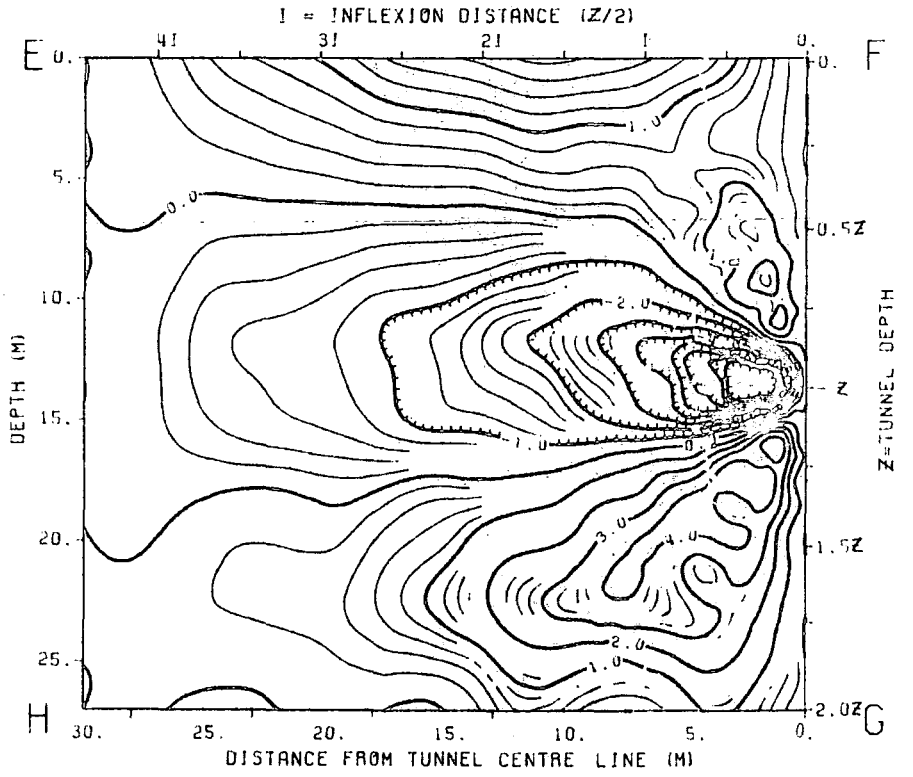

FIG. 7.2.6) Contours of equal lateral displacements (mm). Transverse section at tunnel face.

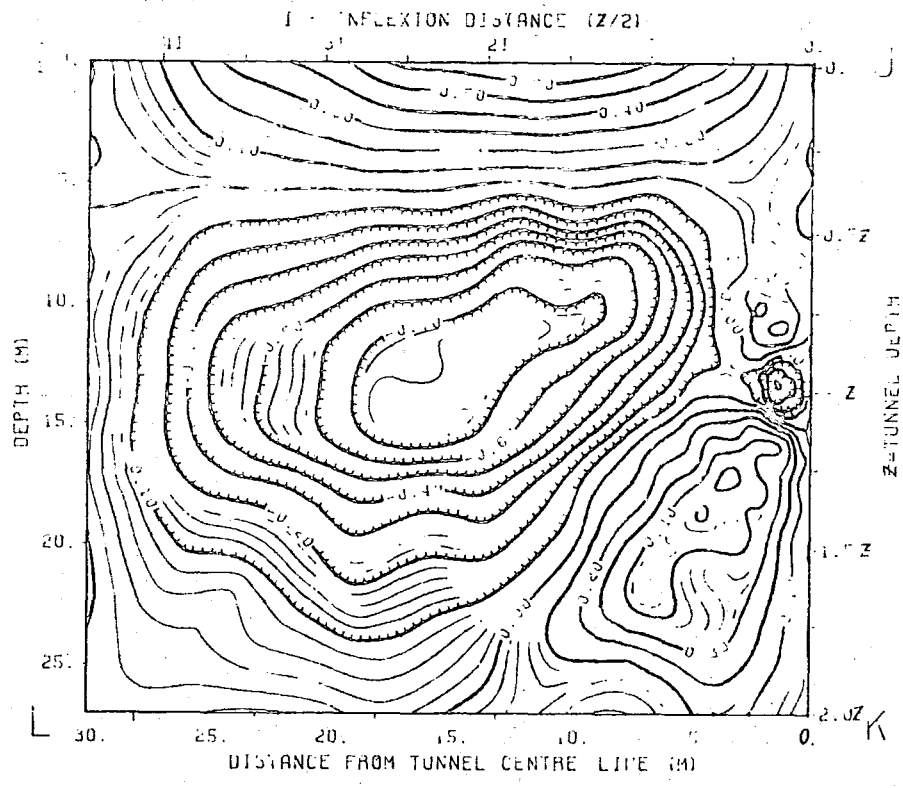

FIG. 7.2.7) Contours of equal lateral displacements (mm). Transverse section i ahead tunnel face.

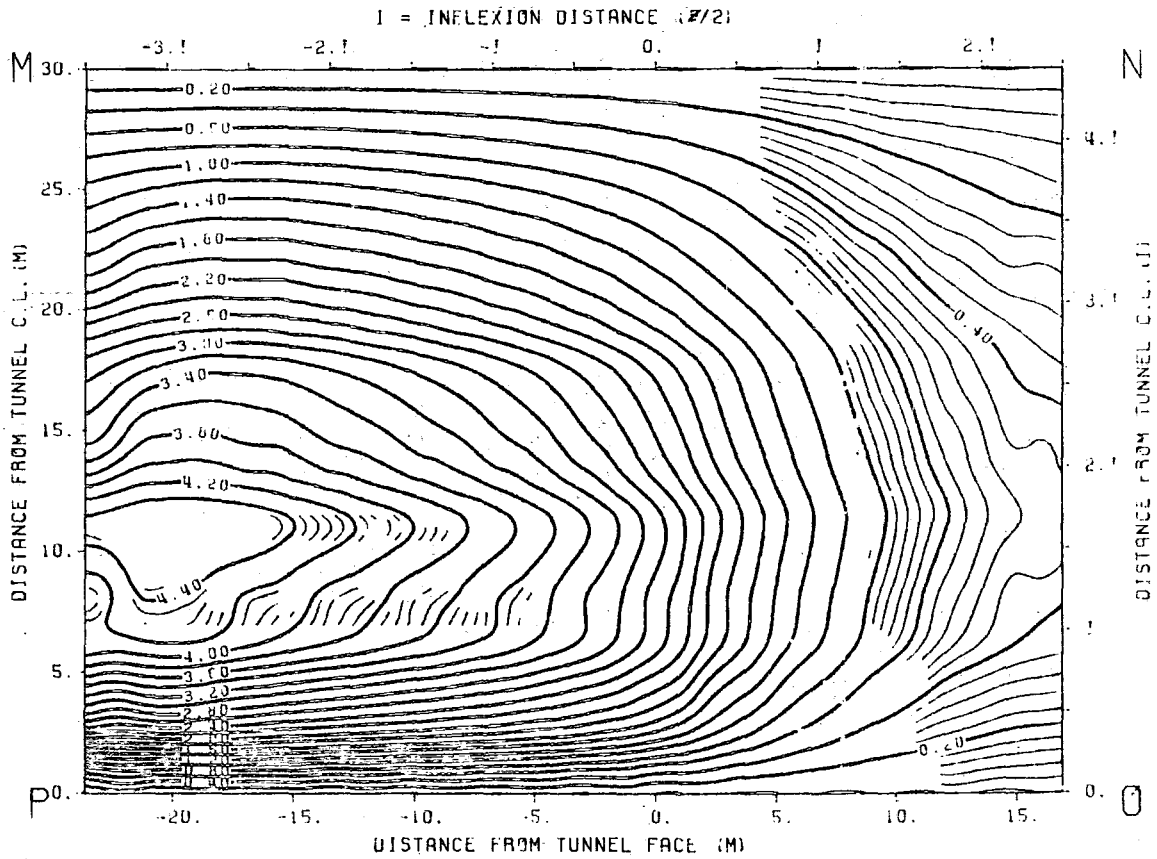

FIG. 7.2.8) Contours of equal lateral displacements (mm). Ground surface.

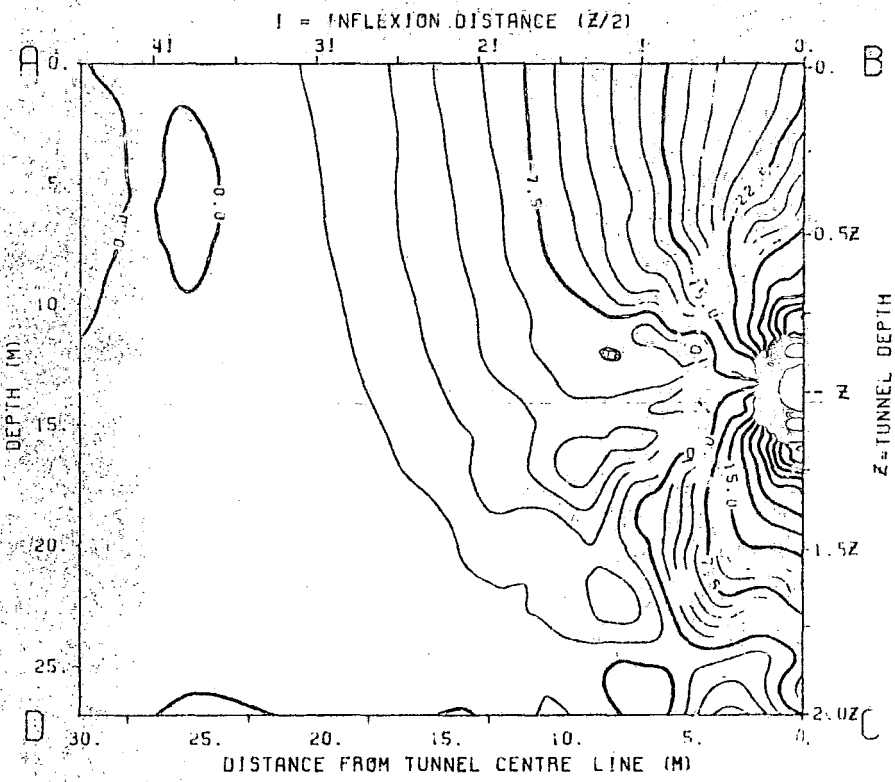

FIG. 7.2.9) Contours of equal vertical displacements (mm). Transverse section 3i behind tunnel face.

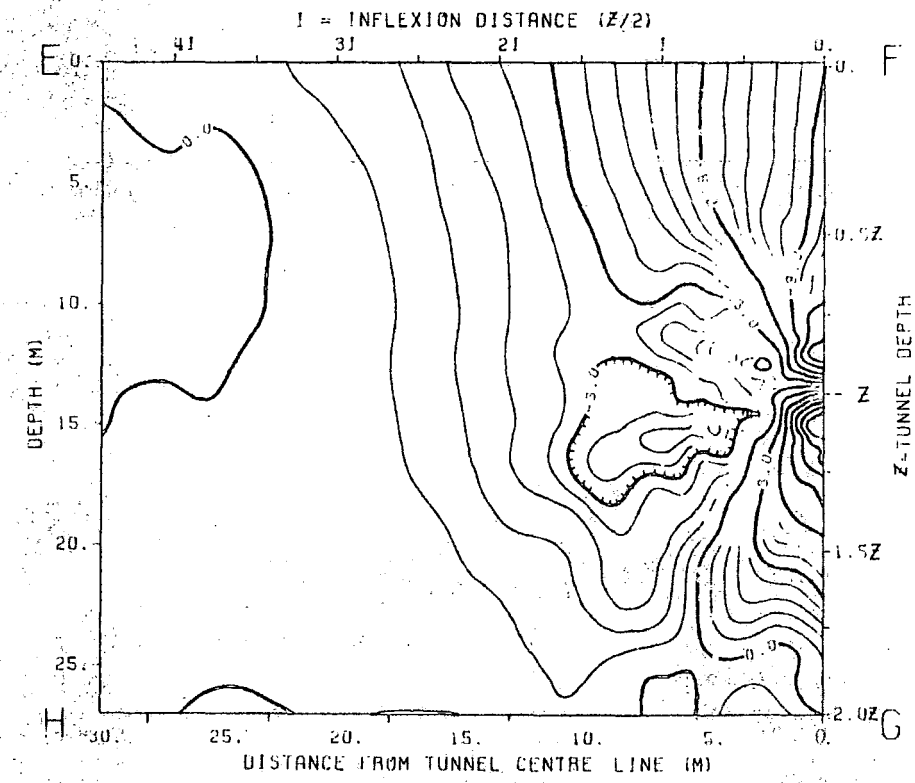

FIG. 7.2.10) Contours of equal vertical displacements (mm). Transverse section at tunnel face.

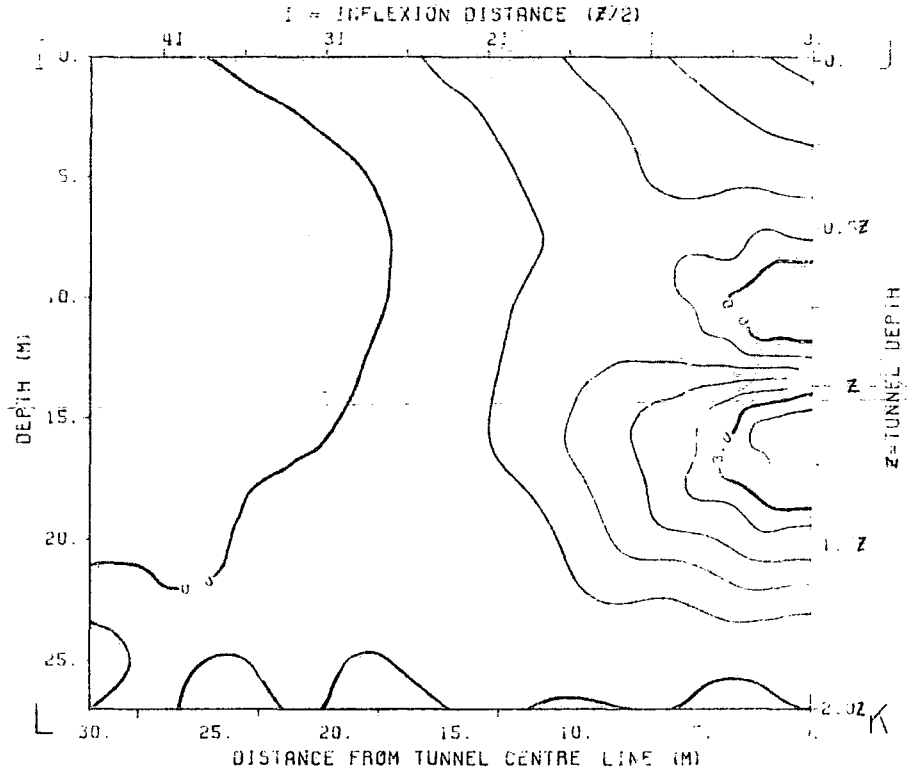

FIG. 7.2.11) Contours of equal vertical displacements (mm). Transverse section i ahead tunnel face.

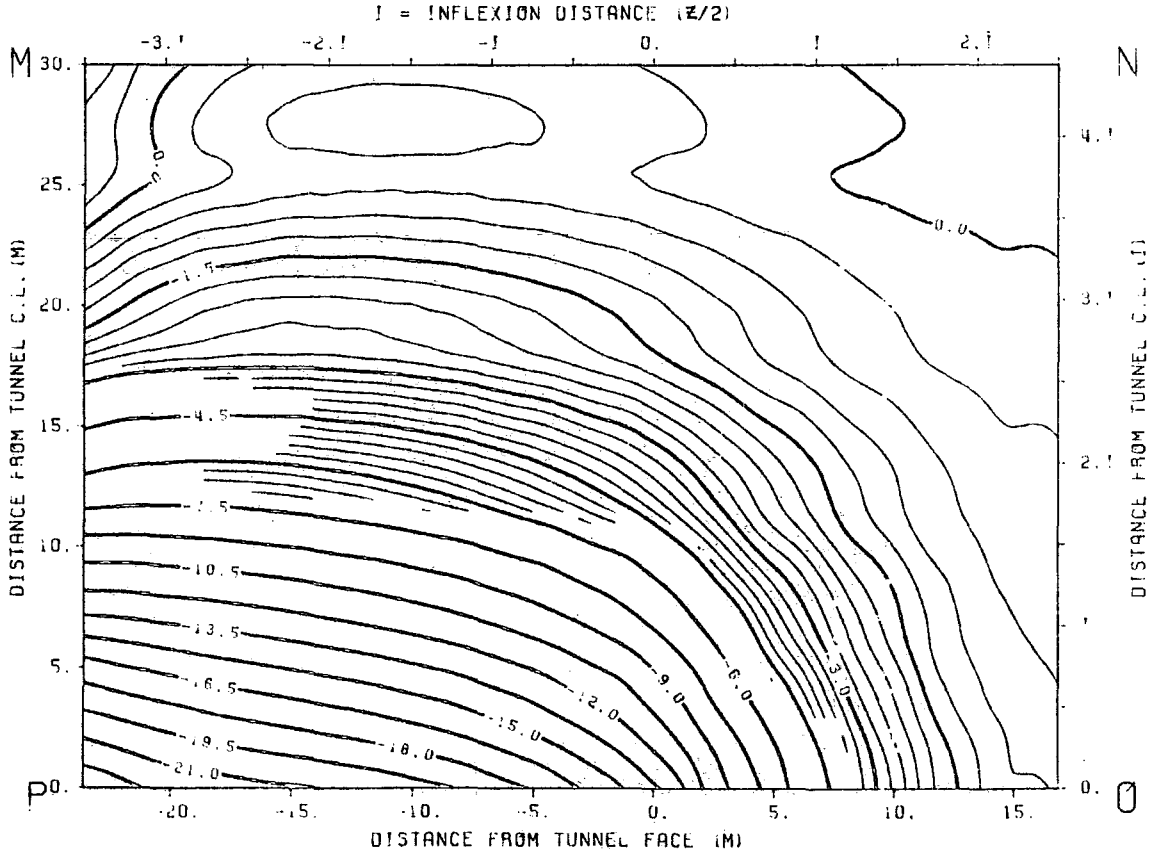

FIG. 7.2.12) Contours of equal vertical displacements (mm). Ground surface.

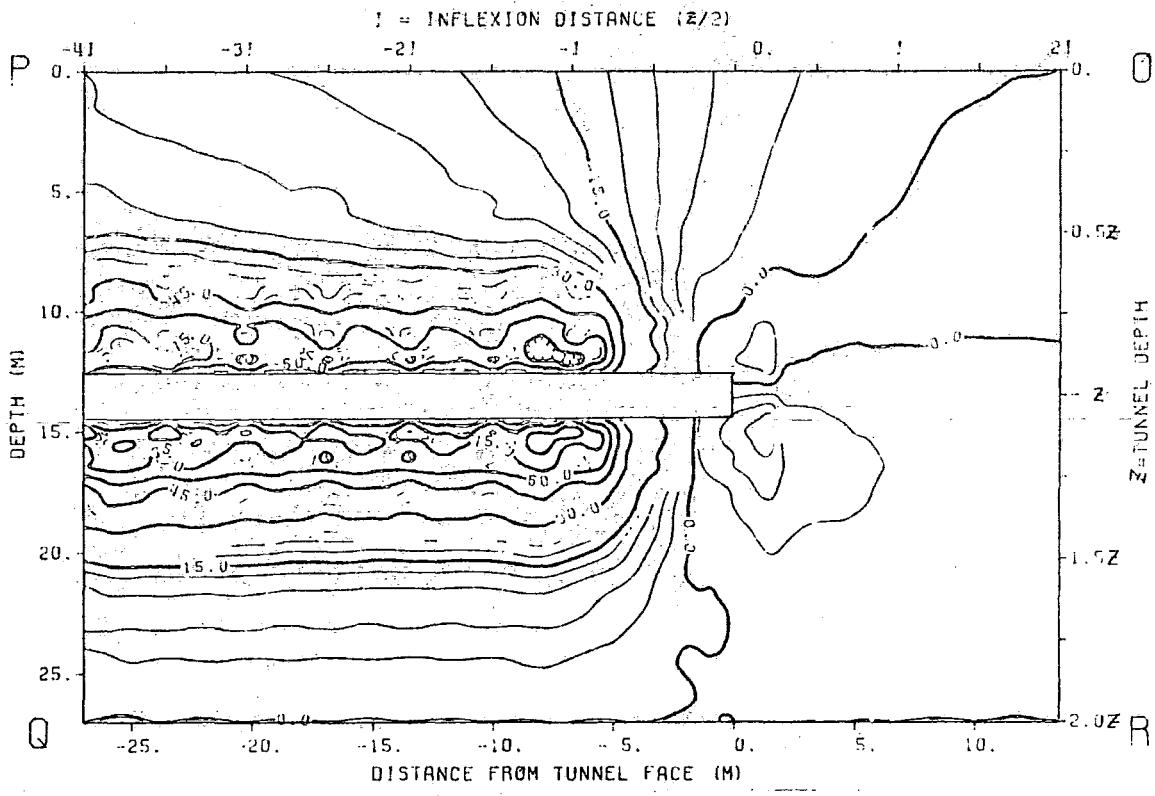

FIG. 7.2.13) Contours of equal vertical displacements (mm). Longitudinal section.

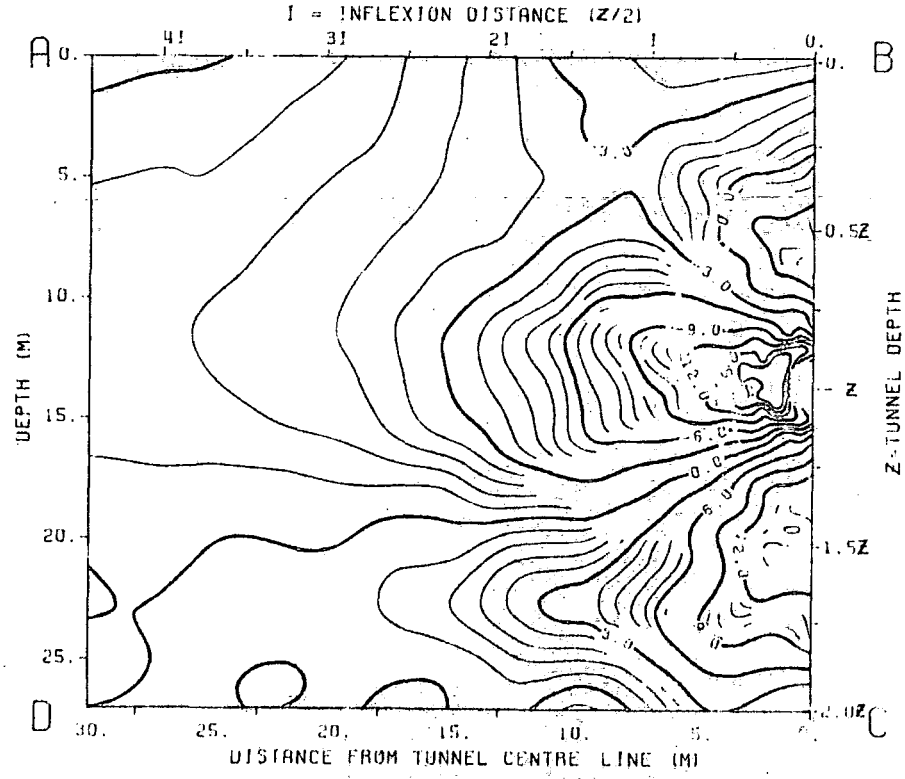

FIG. 7.2.14) Contours of equal longitudinal displacements (mm). Transverse section 3i behind tunnel face.

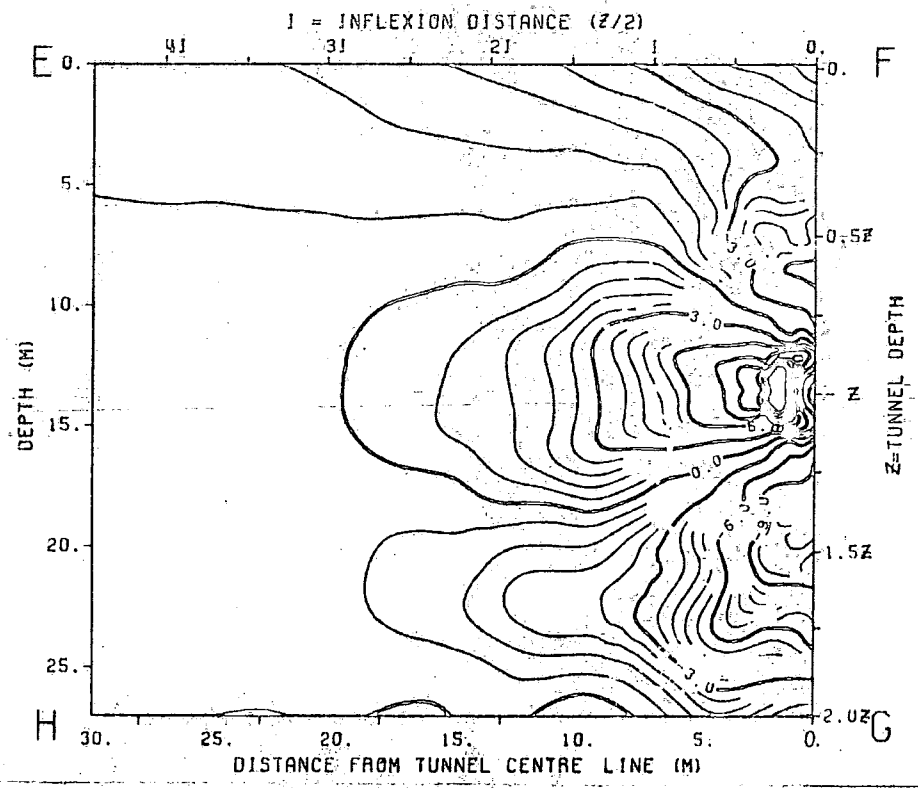

FIG. 7.2.15) Contours of equal longitudinal displacements (mm). Transverse section at tunnel face.

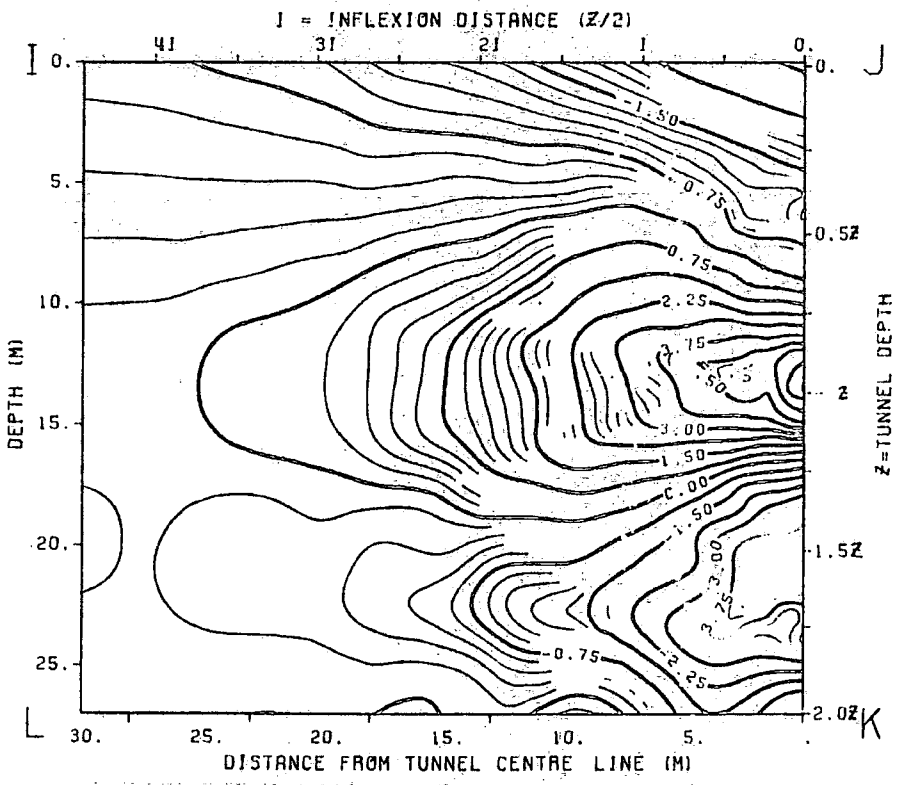

FIG. 7.2.16) Contours of equal longitudinal displacements (mm). Transverse section i ahead of tunnel face.

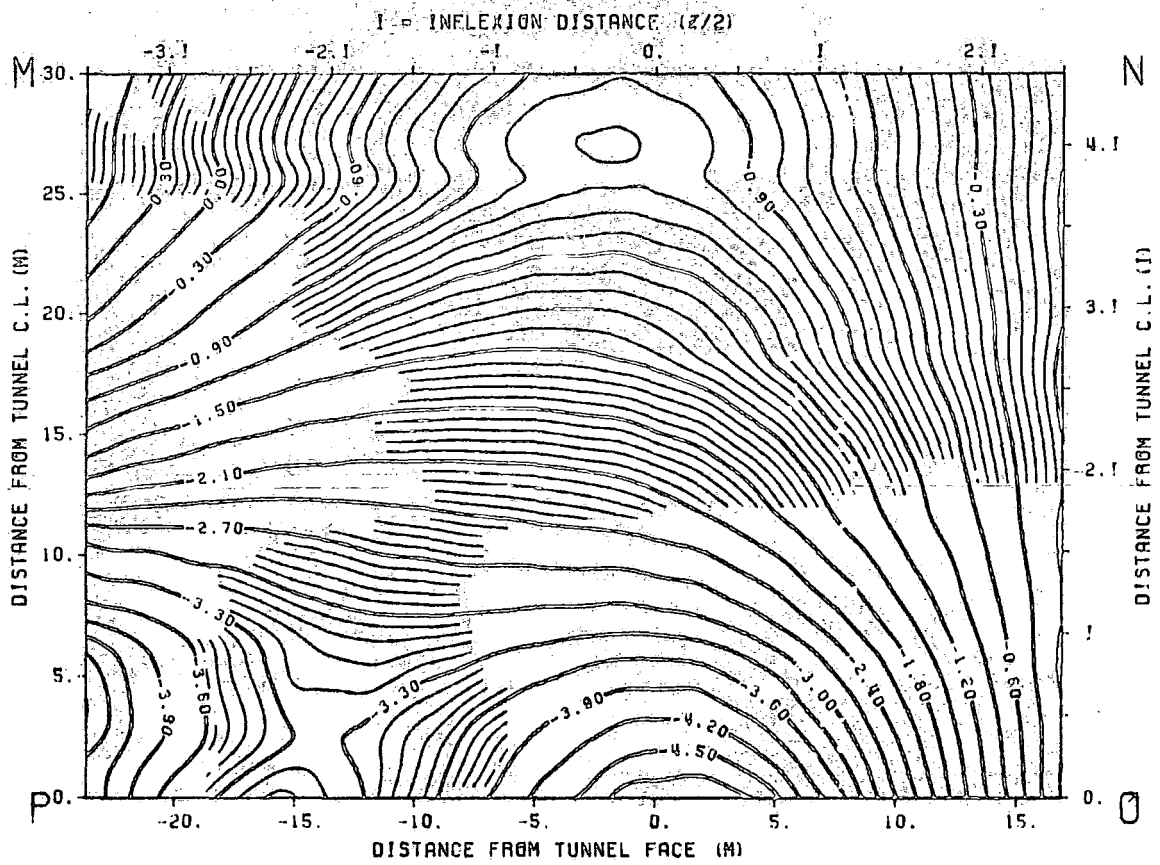

FIG. 7.2.17) Contours of equal longitudinal displacements (mm). Ground surface.

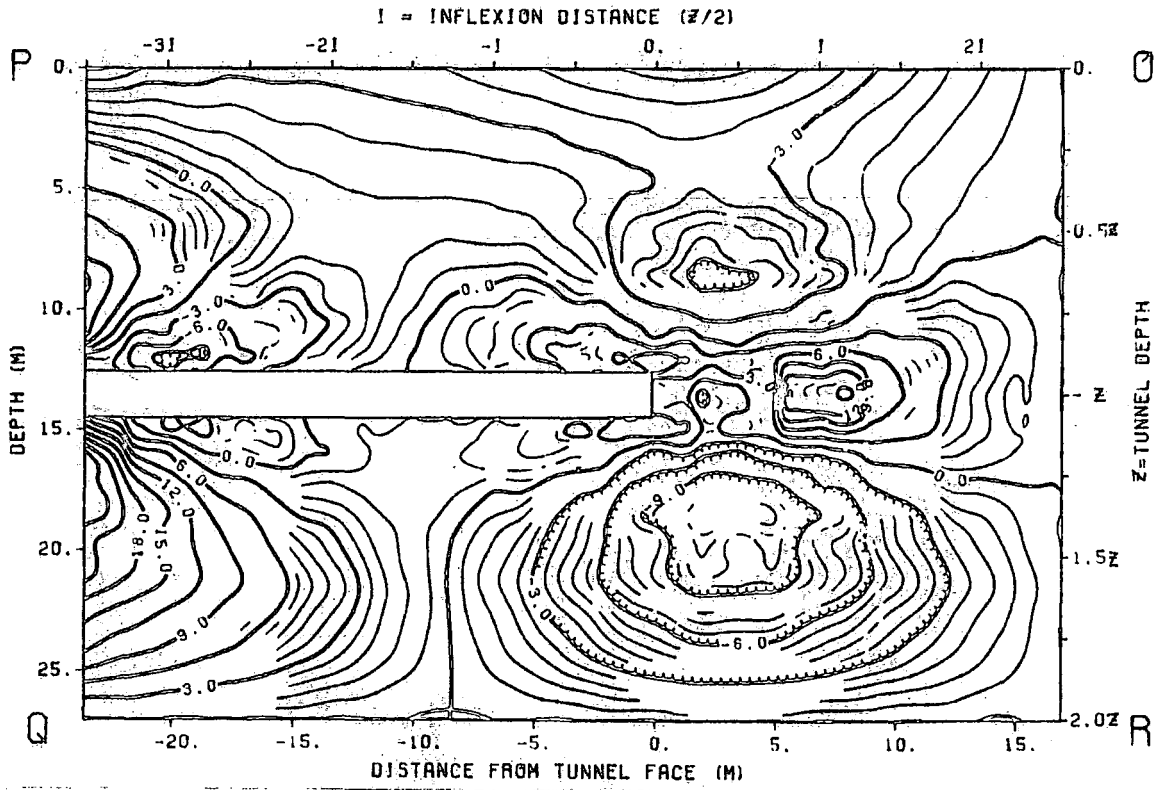

FIG. 7.2.18) Contours of equal longitudinal displacements (mm). Longitudinal section.

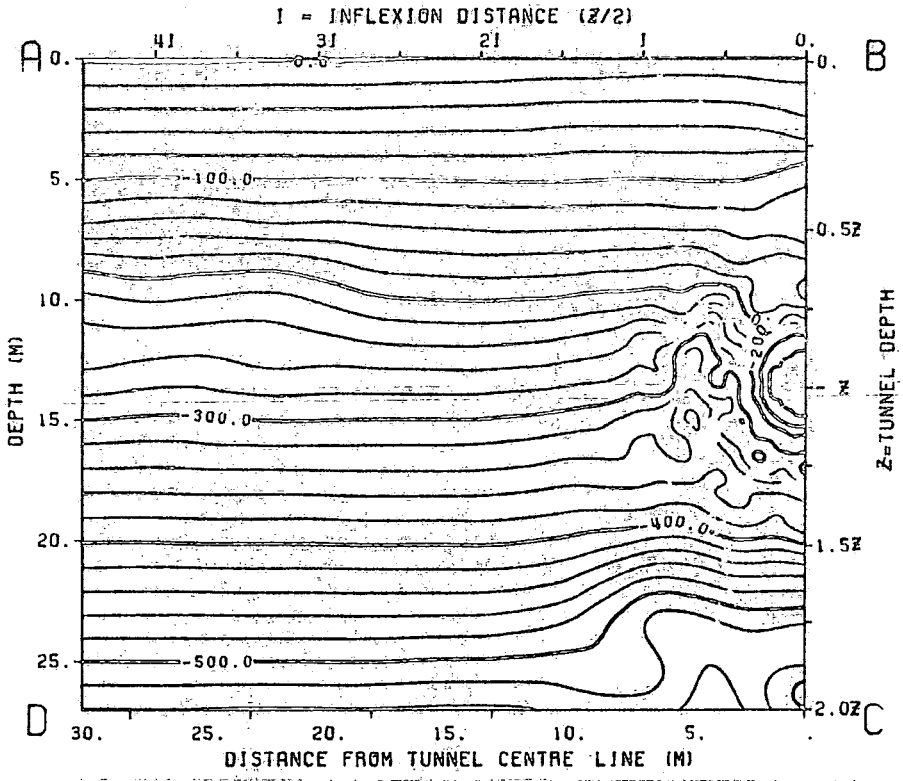

FIG. 7.2.19) Contours of equal lateral stresses (kN/m^2). Transverse section 3i behind tunnel face.

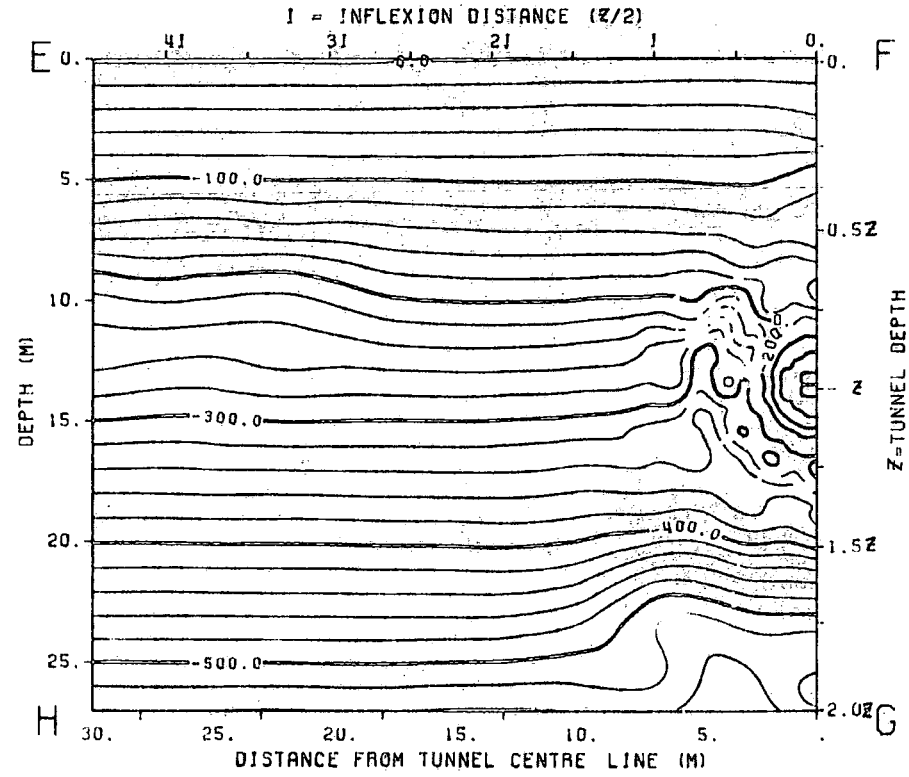

FIG. 7.2.20) Contours of equal lateral stresses (kN/m^2). Transverse section i ahead of tunnel face.

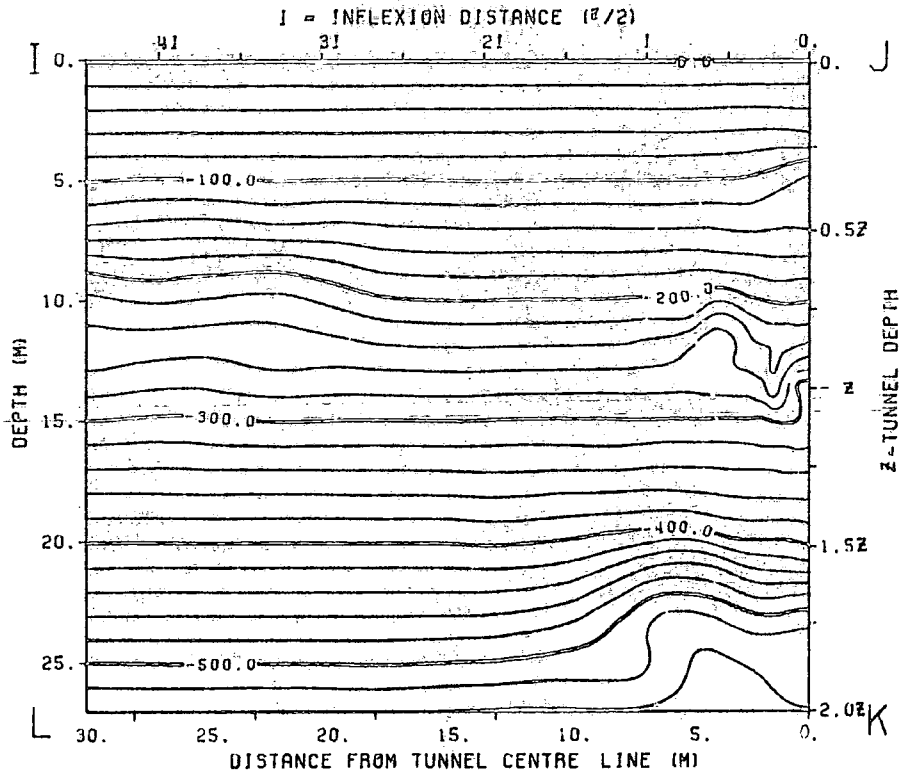

FIG. 7.2.21) Contours of equal lateral stresses (kN/m^2). Transverse section i ahead of tunnel face.

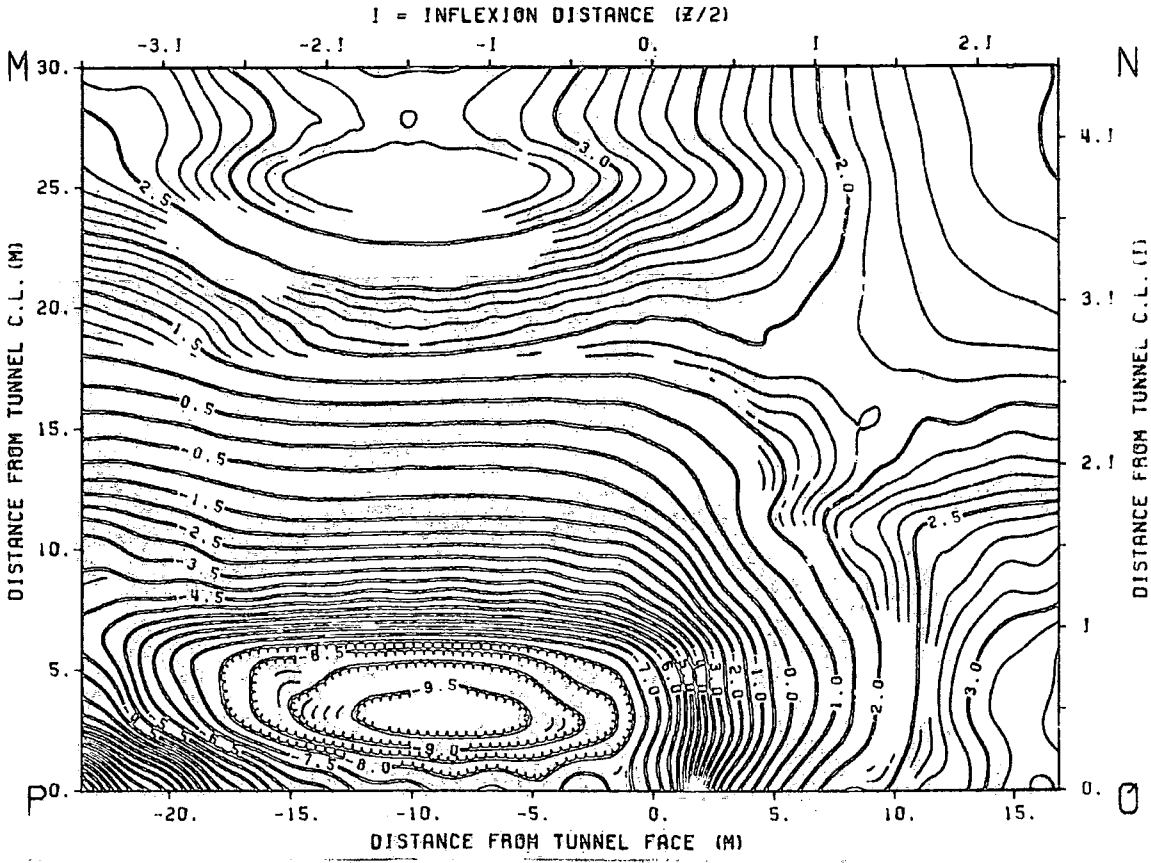

FIG. 7.2.22) Contours of equal lateral stresses (kN/m^2). Ground surface.

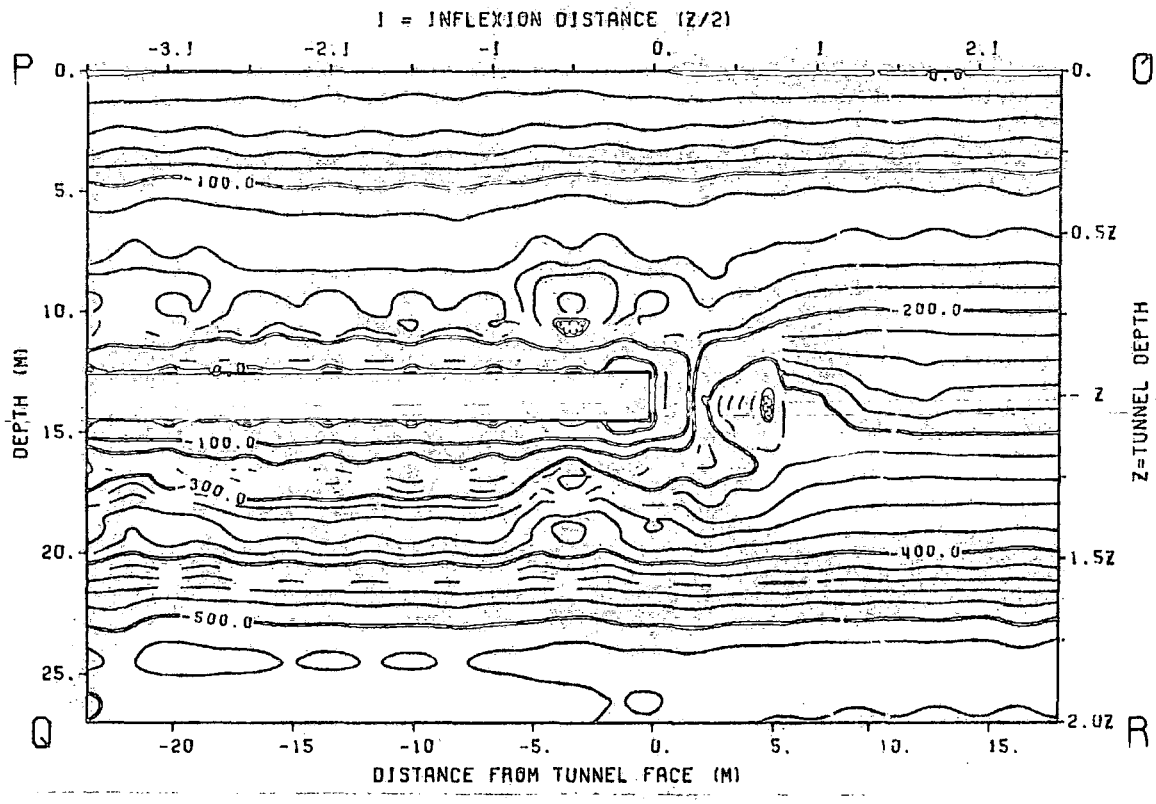

FIG. 7.2.23) Contours of equal lateral stresses (kN/m^2). Longitudinal section.

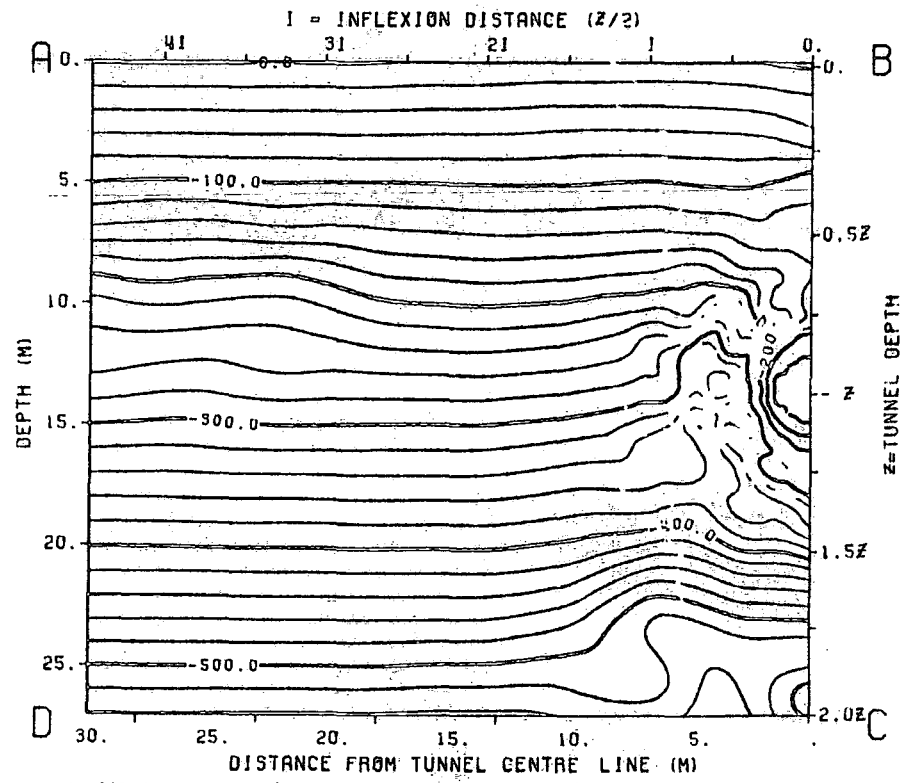

FIG. 7.2.24) Contours of equal vertical stresses (kN/m^2). Transverse section 3i behind tunnel face.

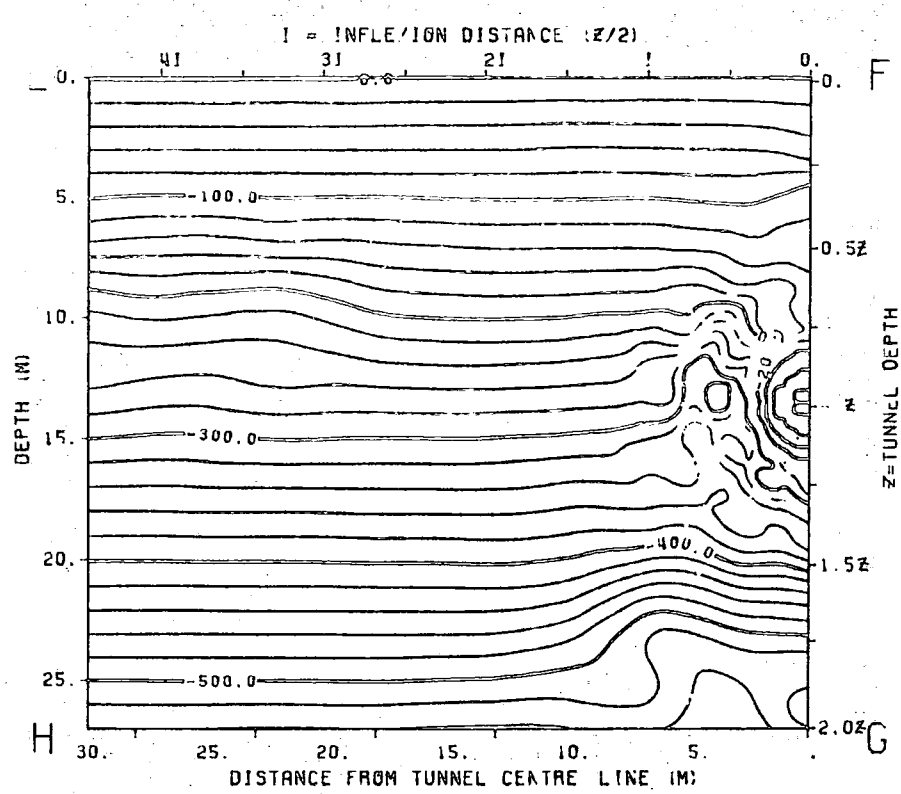

FIG. 7.2.25) Contours of equal vertical stresses (kN/m^2). Transverse section at tunnel face.

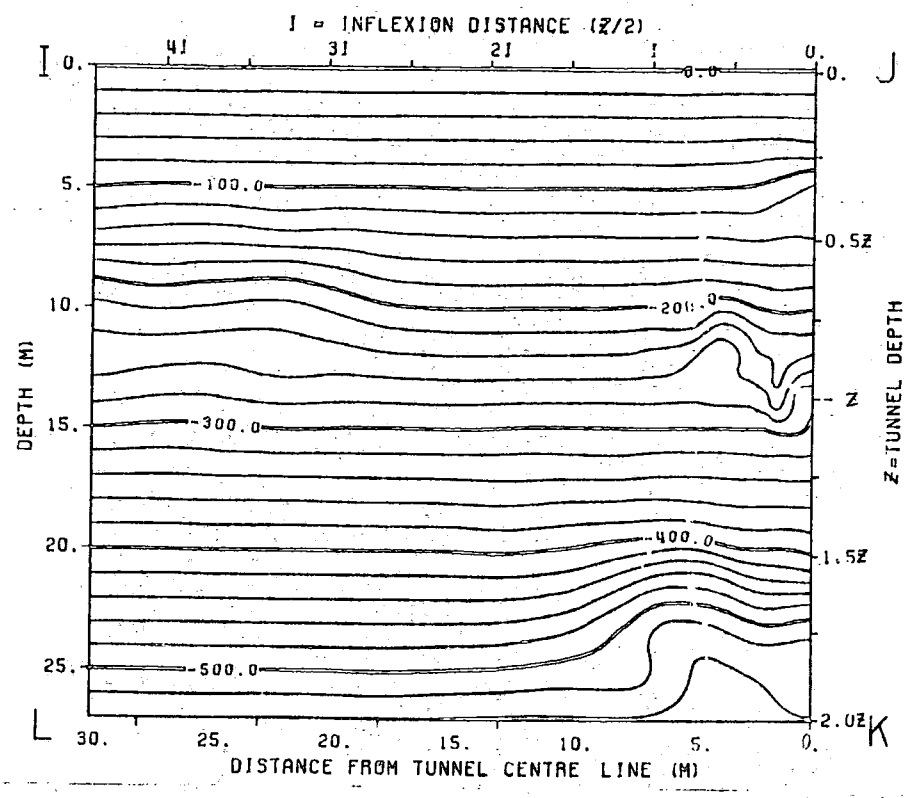

FIG. 7.2.26) Contours of equal vertical stresses (kN/m^2). Transverse section i ahead tunnel face.

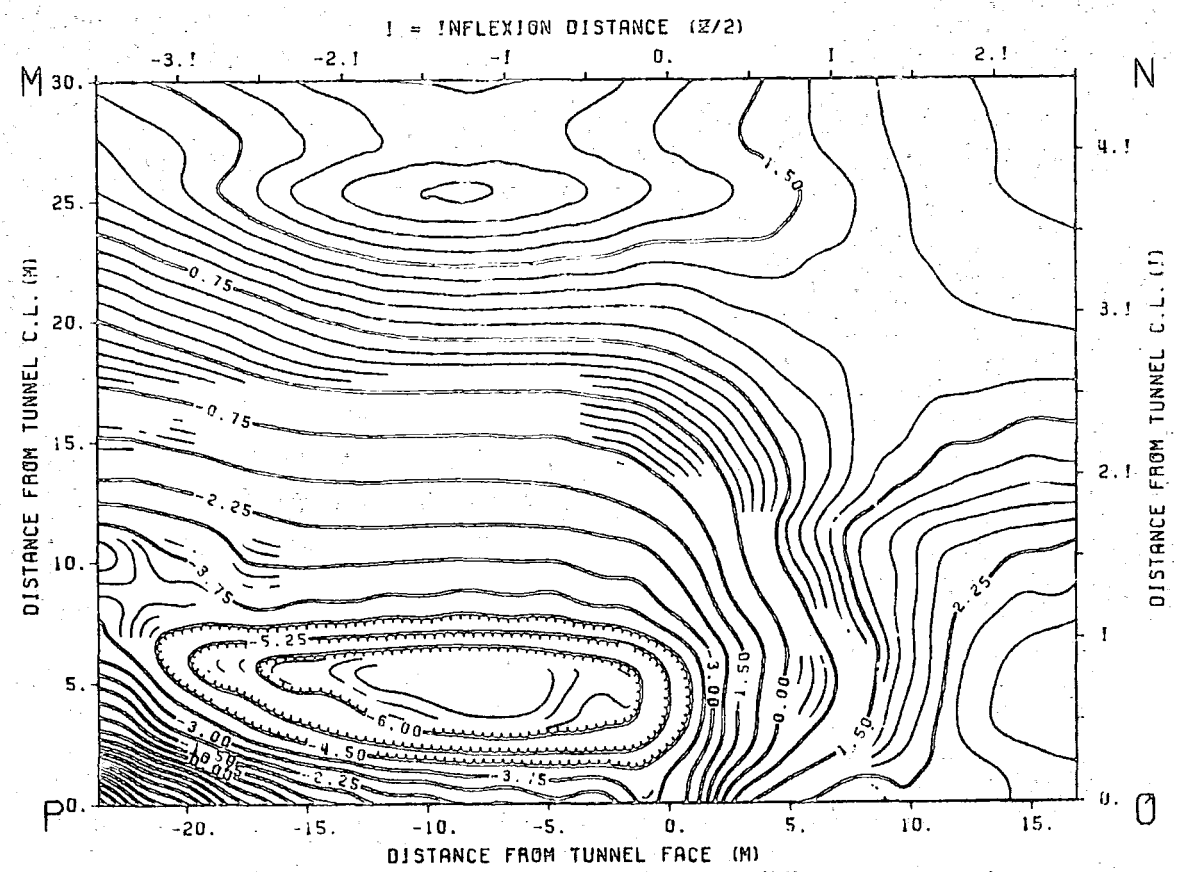

FIG. 7.2.27) Contours of equal vertical stresses (kN/m^2). Ground surface.

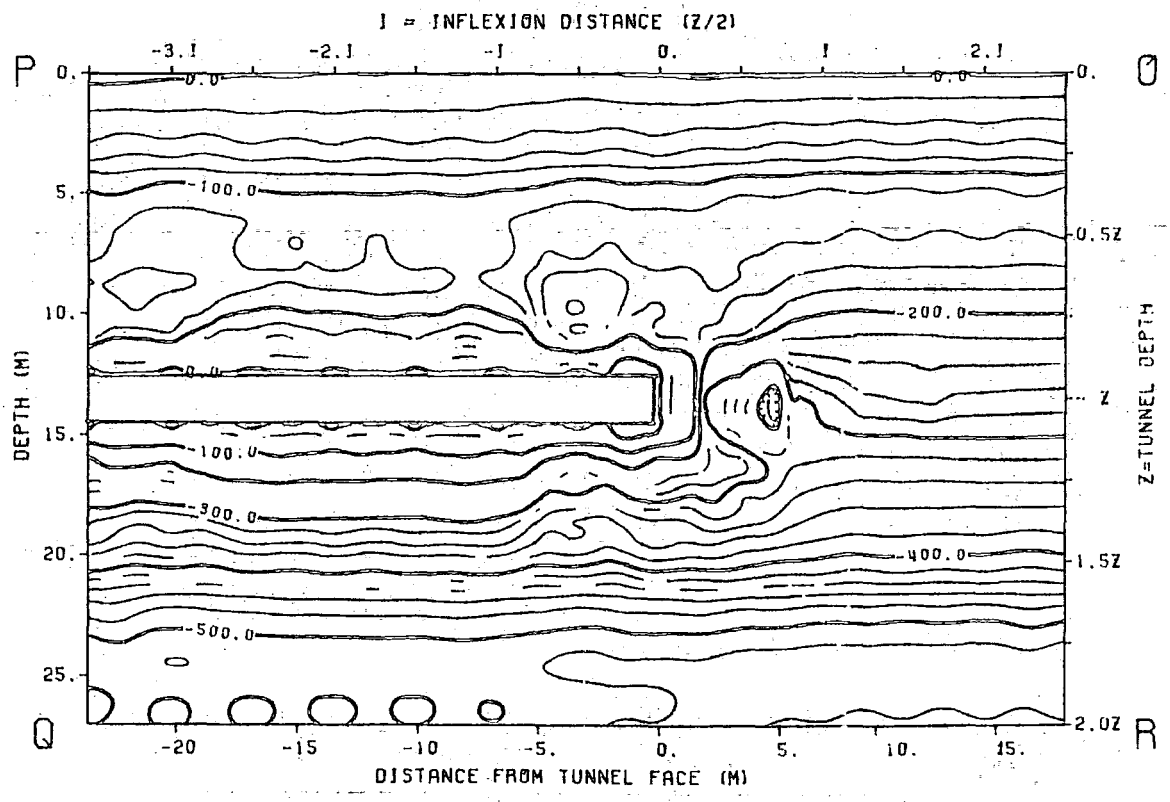

FIG. 7.2.28) Contours of equal vertical stresses (kN/m^2). Longitudinal section.

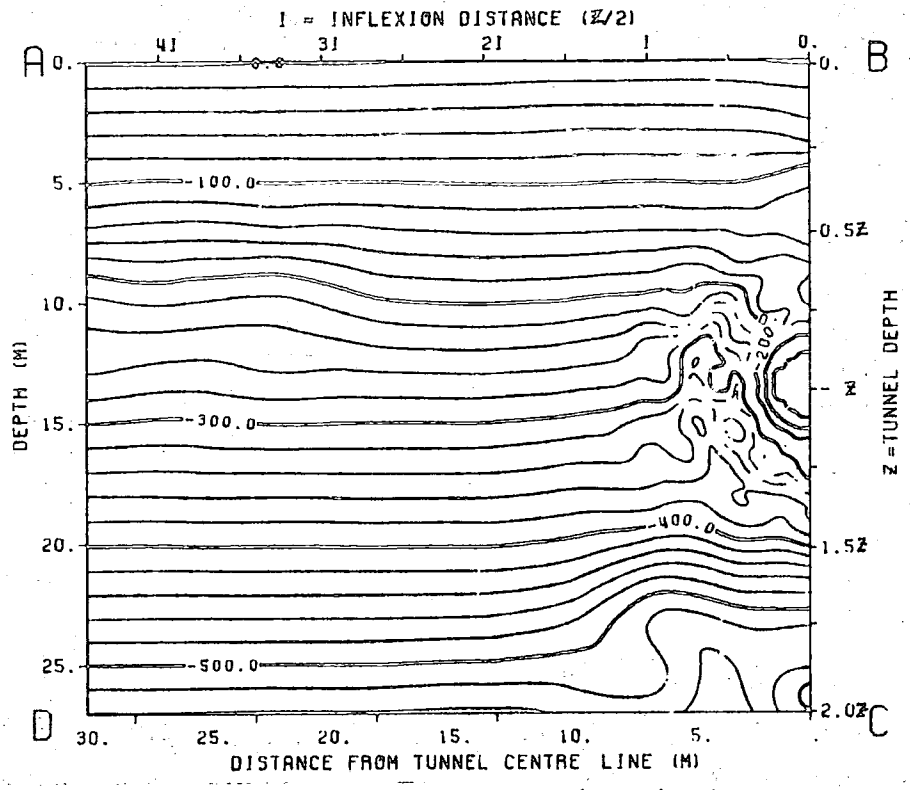

FIG. 7.2.29) Contours of equal longitudinal stresses (kN/m^2). Transverse section 3i behind tunnel face.

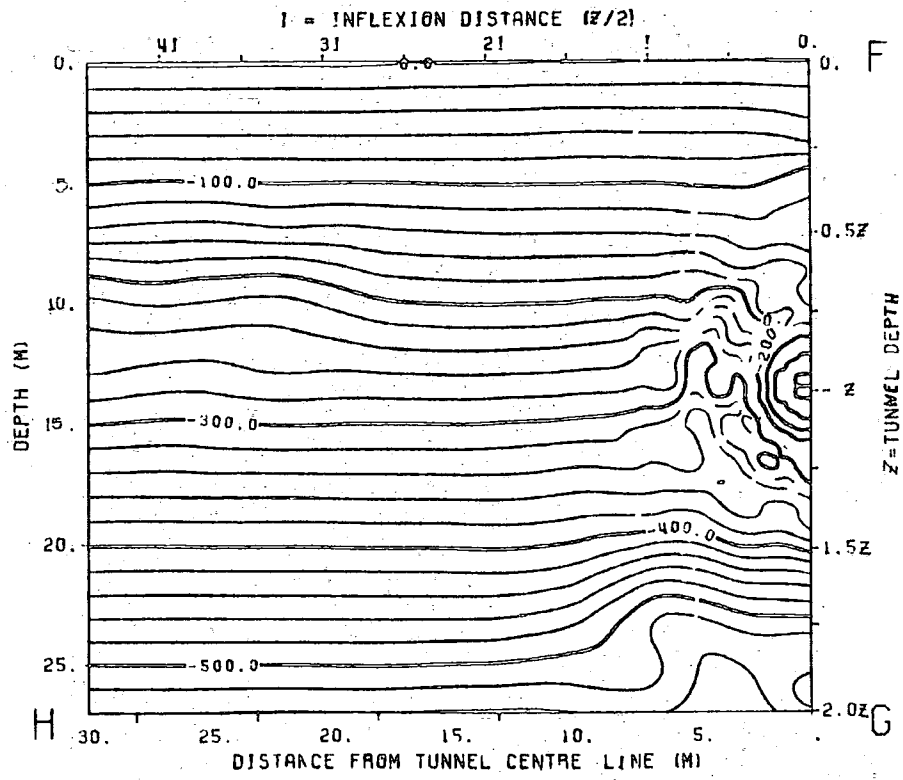

FIG. 7.2.30) Contours of equal longitudinal stresses (kN/m^2). Transverse section at tunnel face.

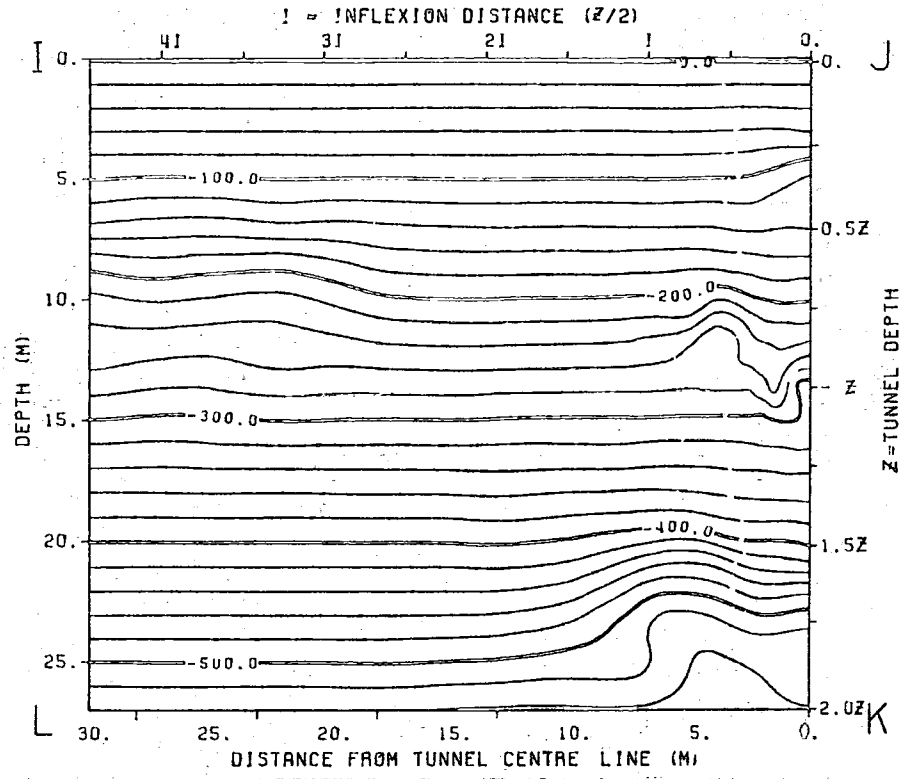

FIG. 7.2.31) Contours of equal longitudinal stresses (kN/m^2). Transverse section i ahead tunnel face.

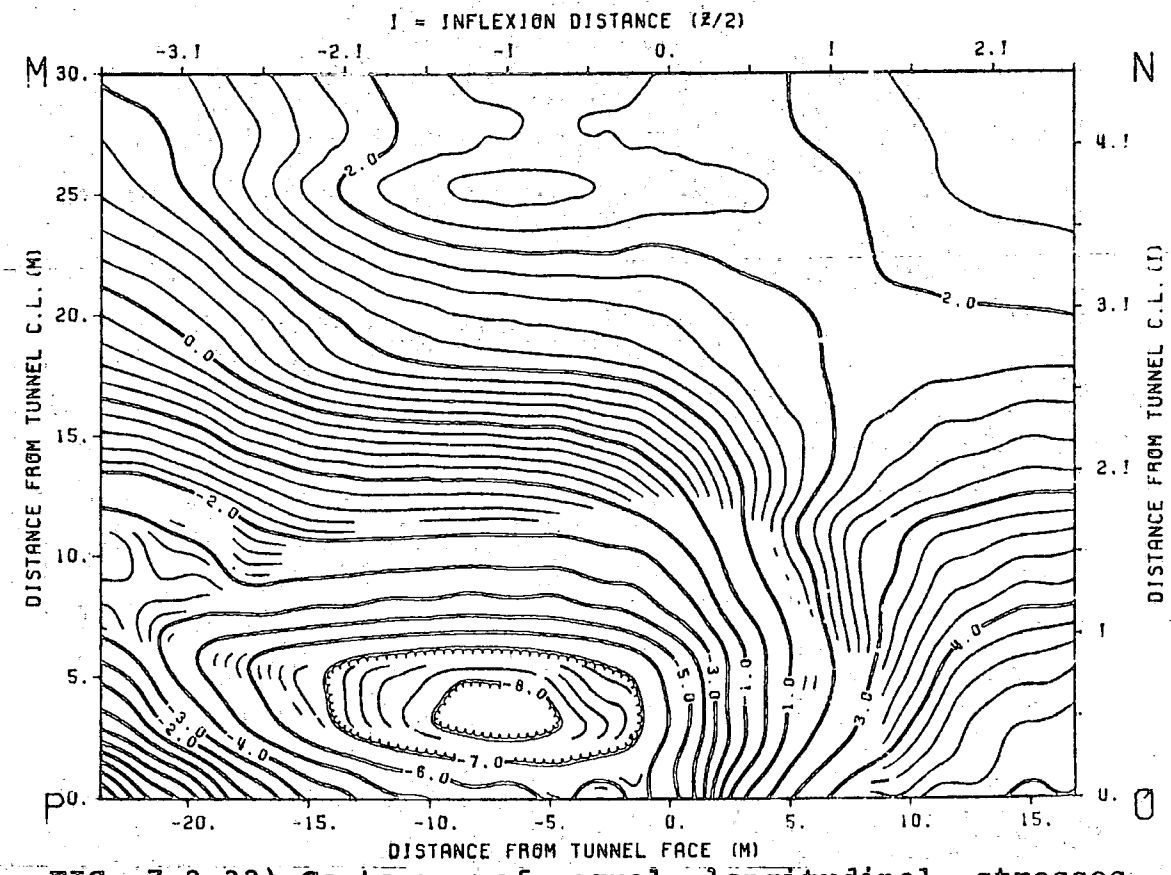

FIG. 7.2.32) Contours of equal longitudinal stresses (kN/m^2). Ground surface.

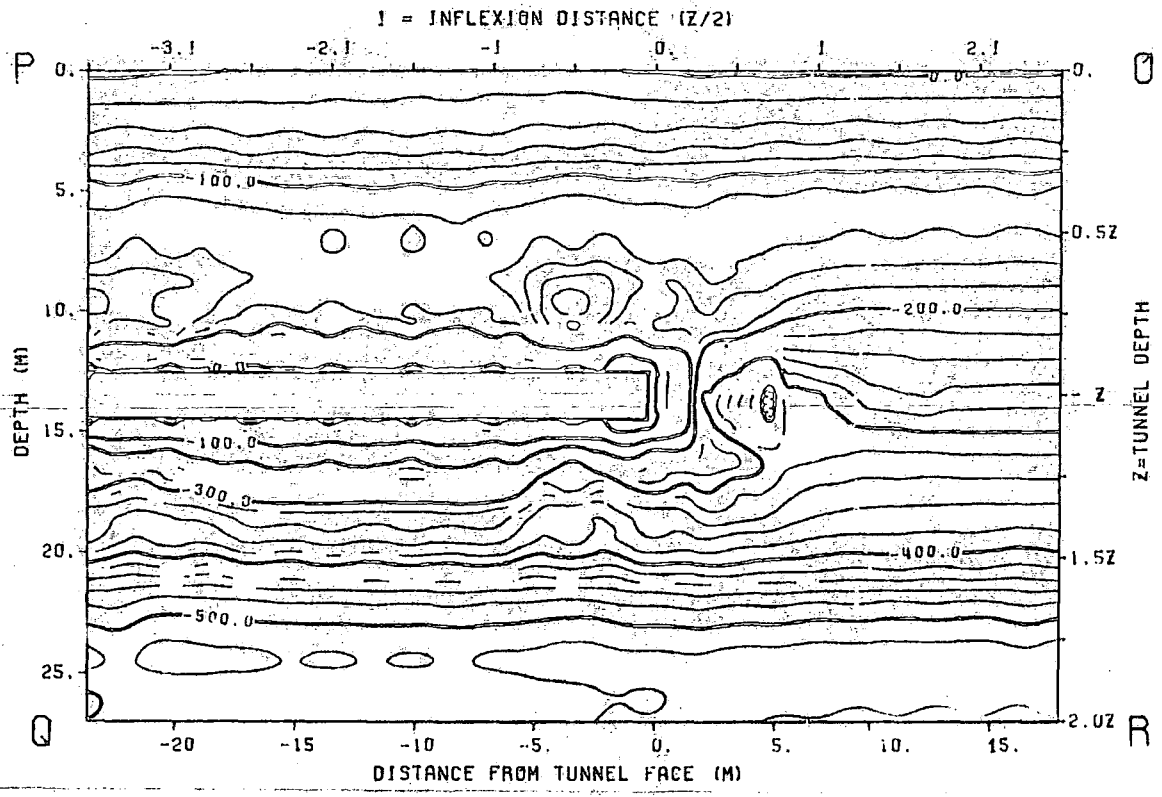

FIG. 7.2.33) Contours of equal longitudinal stresses (kN/m^2). Longitudinal section.

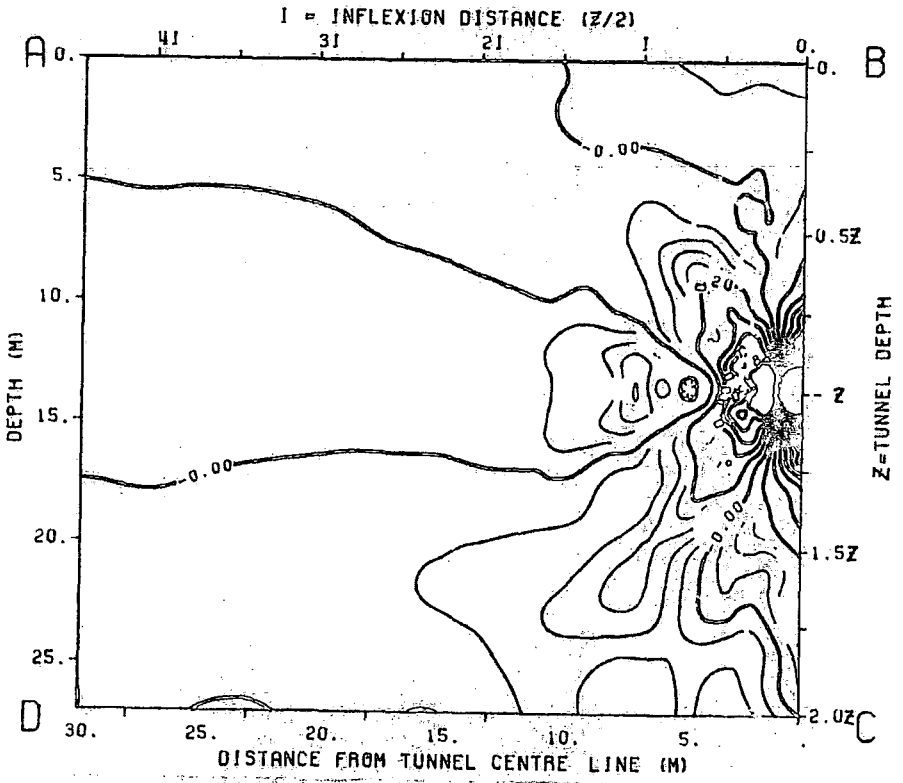

FIG. 7.2.34) Contours of equal lateral strains (%). Transverse section 3i behind tunnel face.

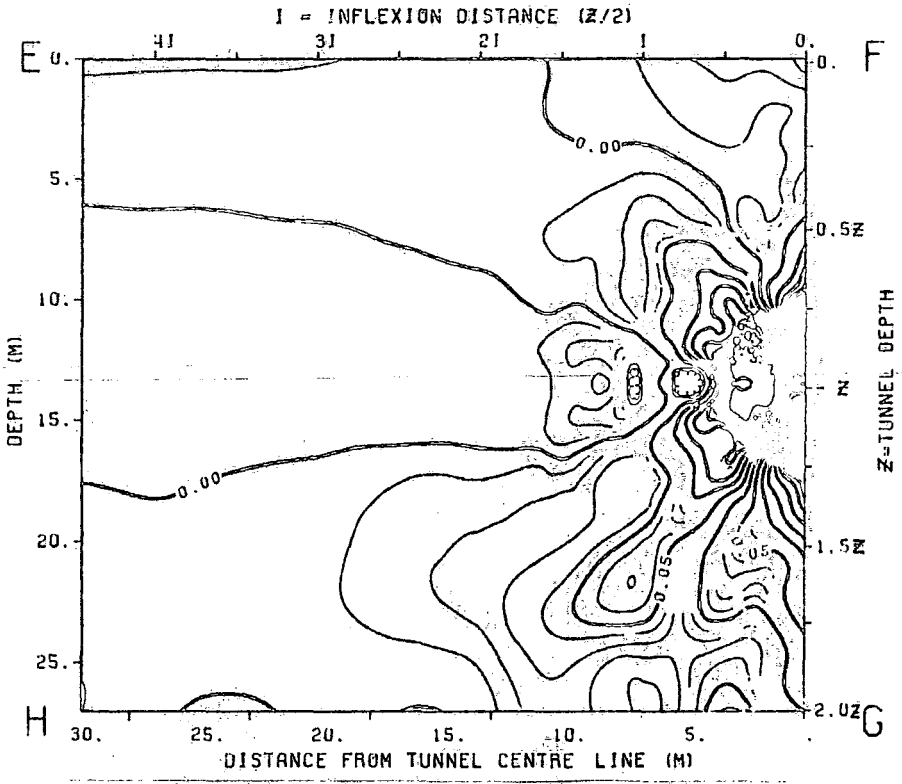

FIG. 7.2.35) Contours of equal lateral strains (%). Transverse section at tunnel face.

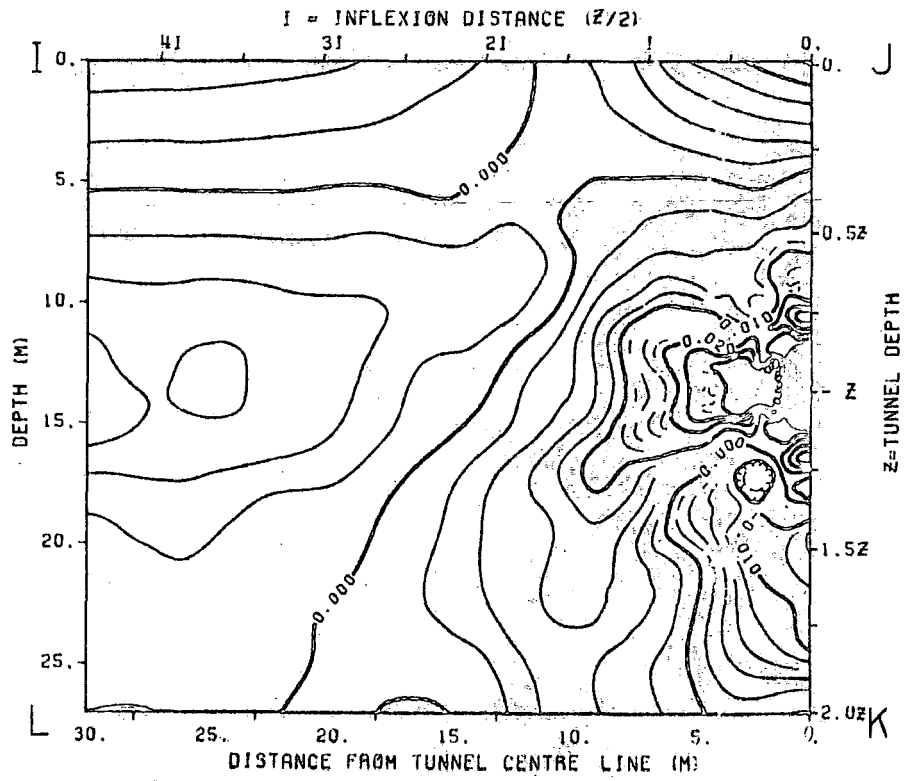

FIG 7.2.36) Contours of equal lateral strains (%). Transverse section i ahead of tunnel face.

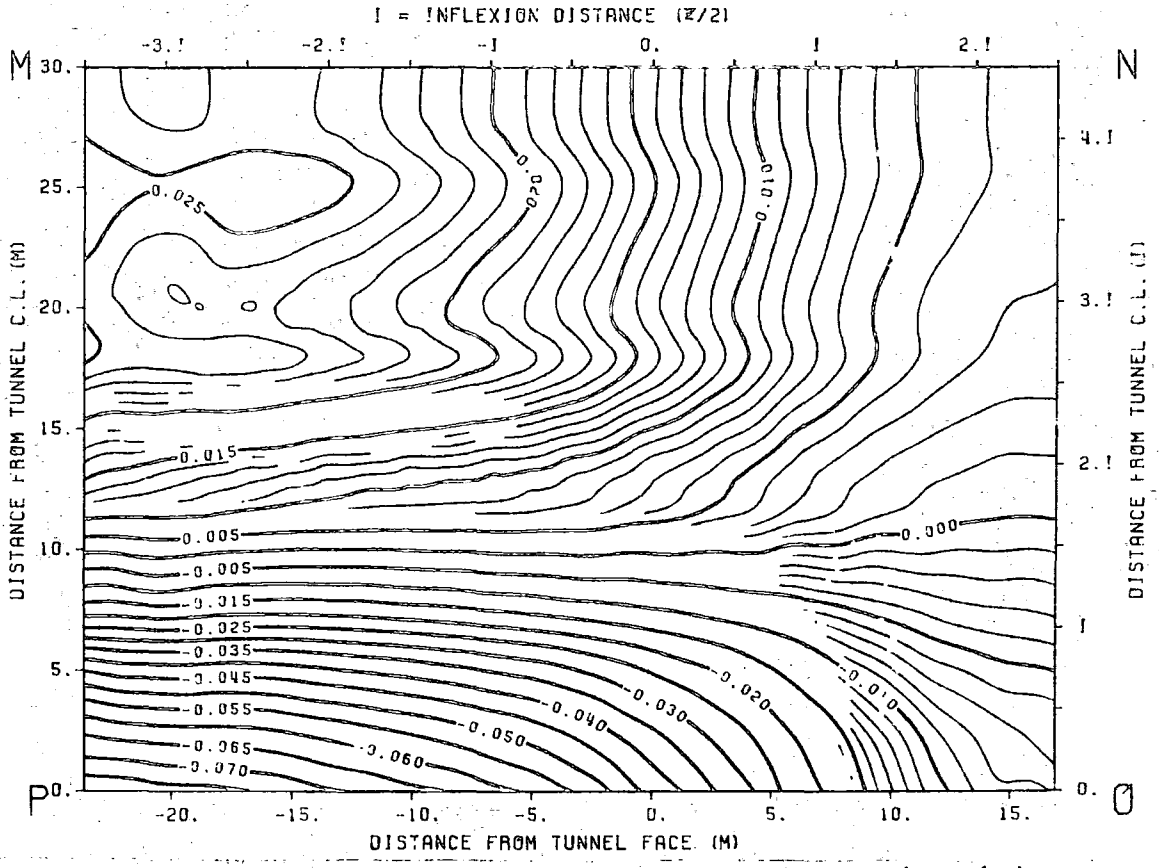

FIG. 7.2.37) Contours of equal lateral strains (%). Ground surface.

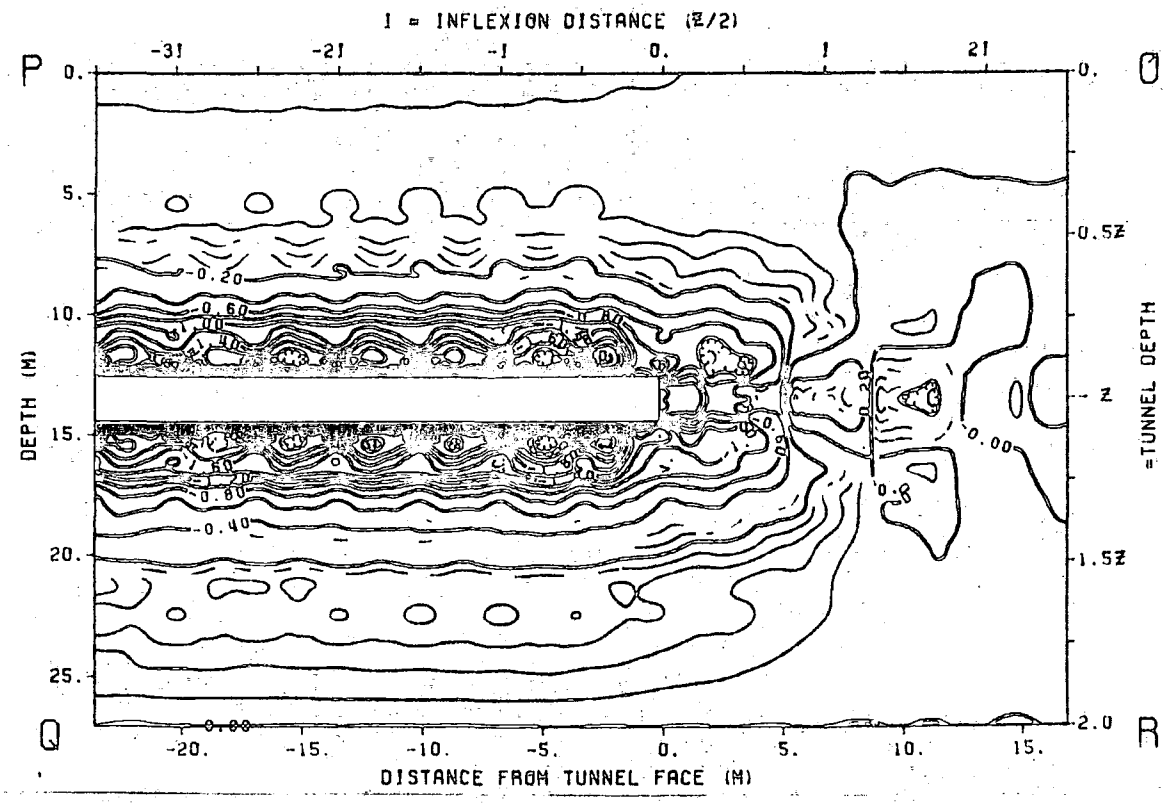

FIG. 7.2.38) Contours of equal lateral strains (%). Longitudinal section.

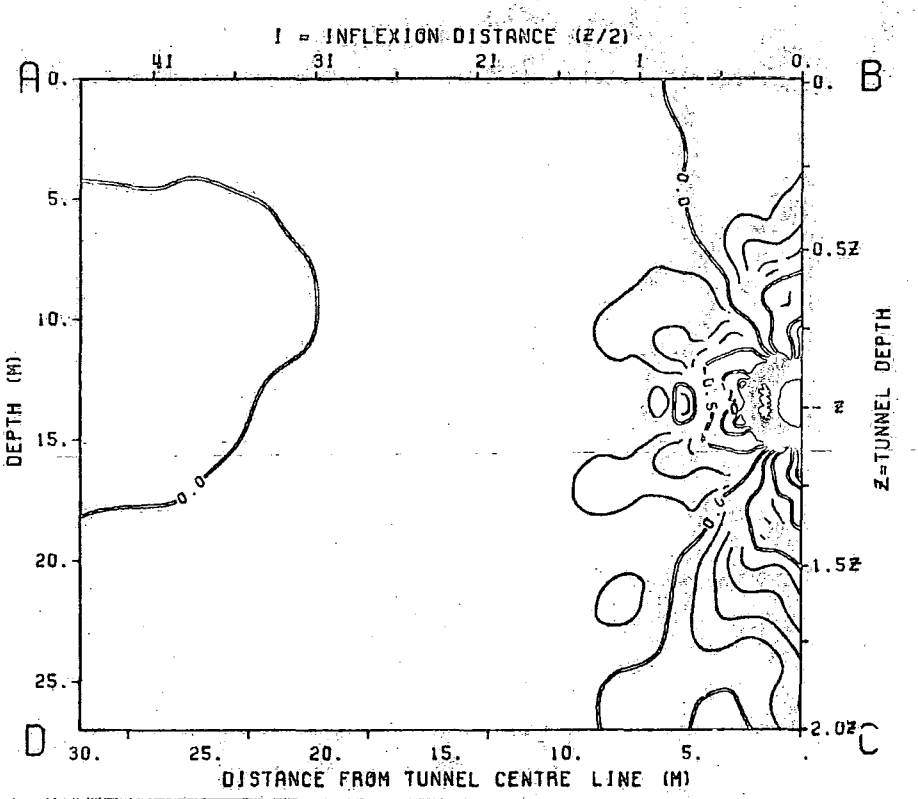

FIG. 7.2.39) Contours of equal vertical strains (%). Transverse section 3i behind tunnel face.

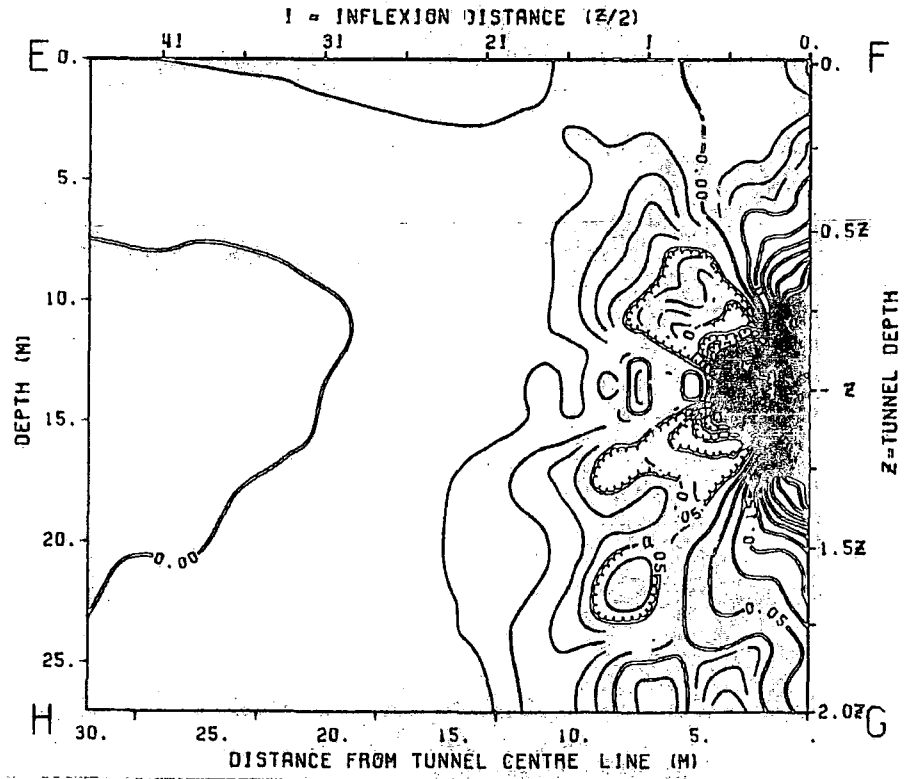

FIG. 7.2.40) Contours of equal vertical strains (%). Transverse section at tunnel face.

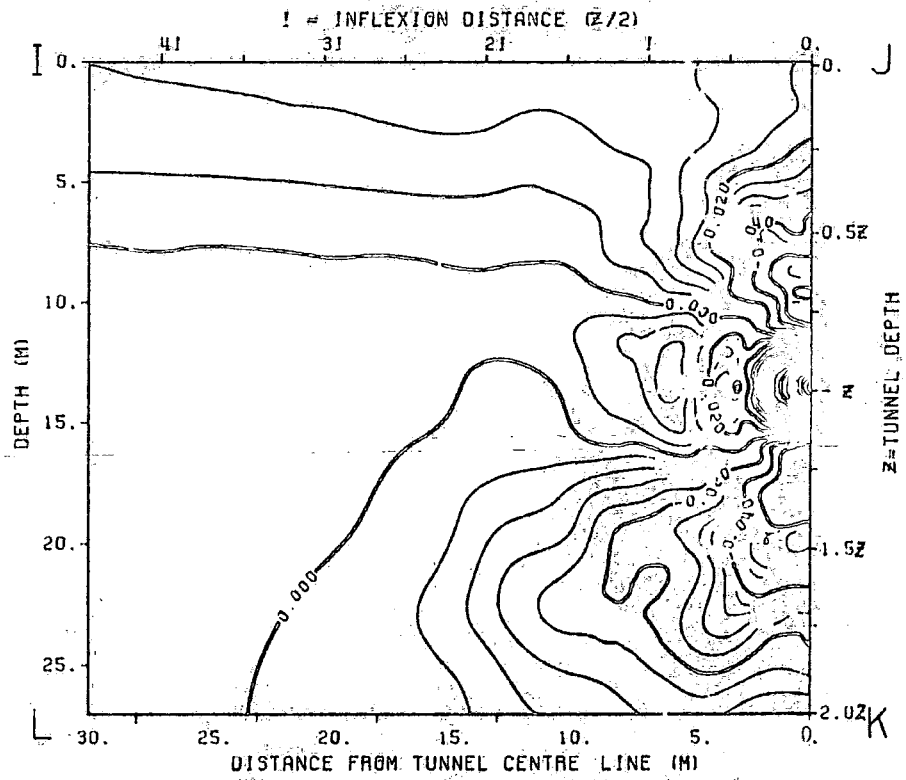

FIG. 7.2.41) Contours of equal vertical strains (%). Transverse section i ahead tunnel face.

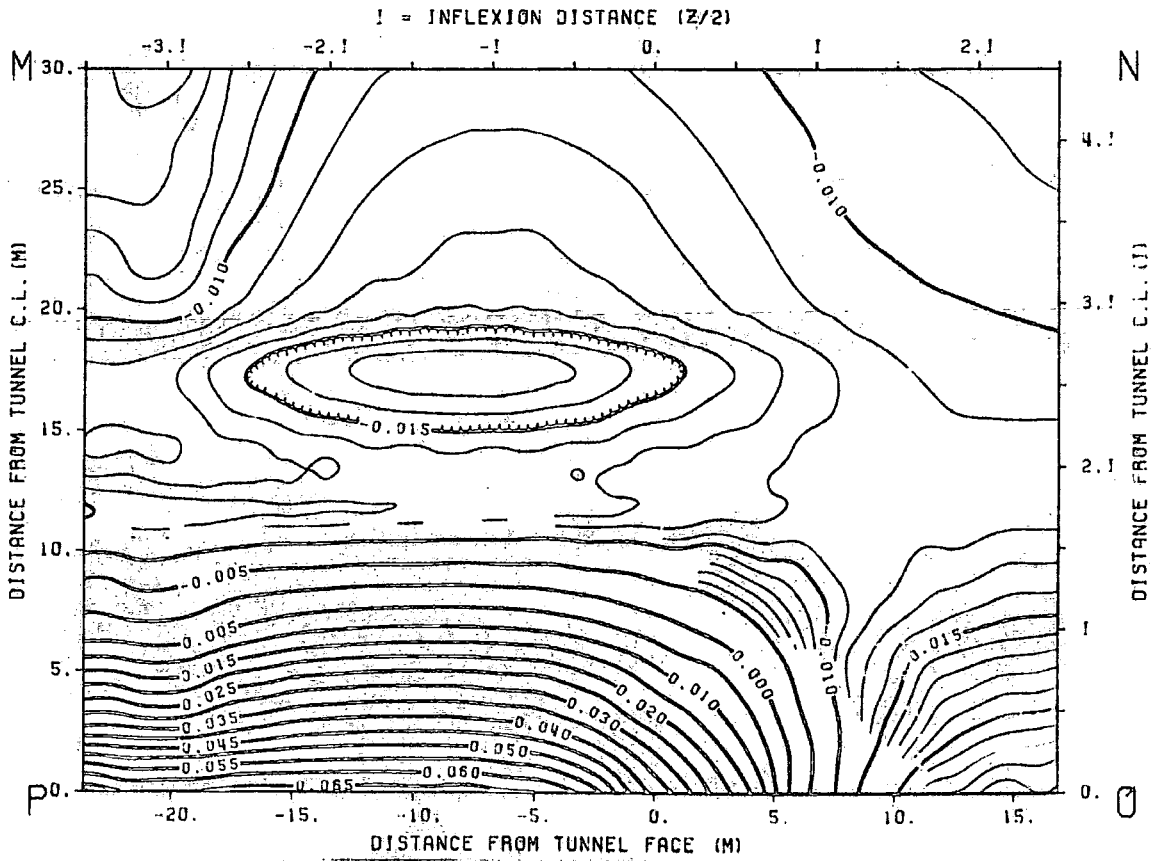

FIG. 7.2.42) Contours of equal vertical strains (%). Ground surface.

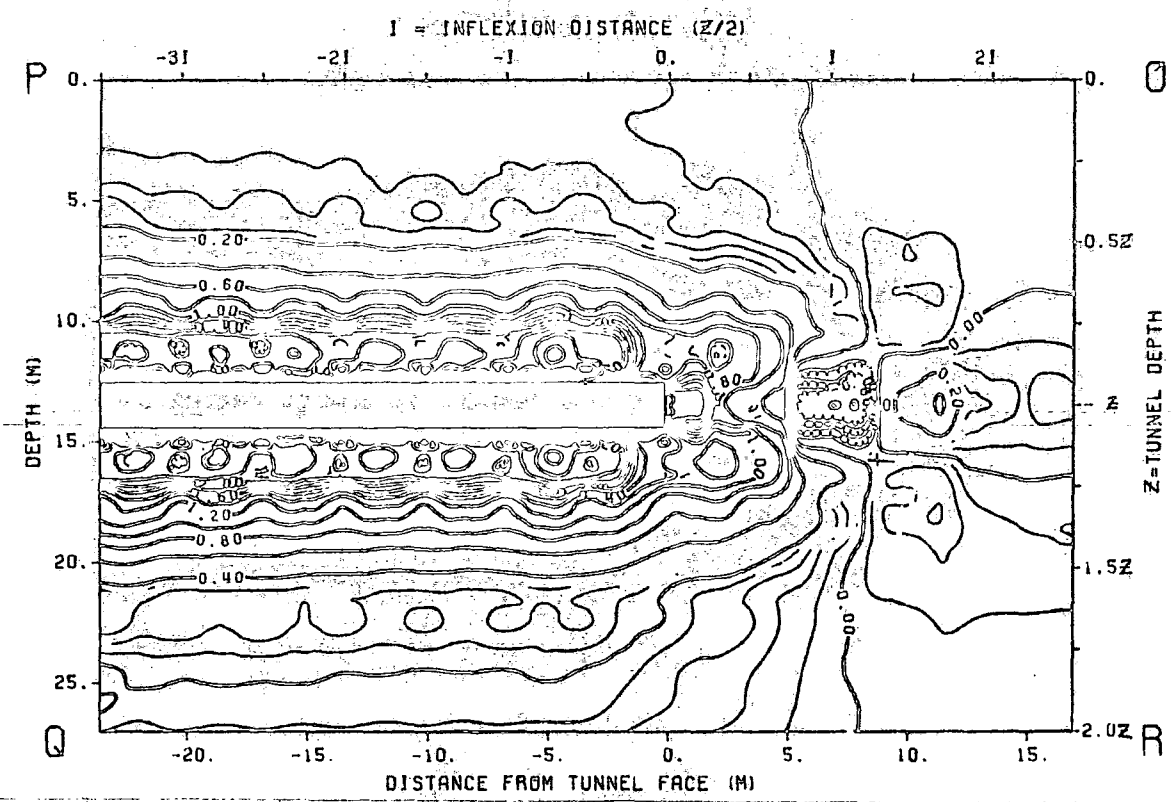

FIG. 7.2.43) Contours of equal vertical strains (%). Longitudinal section.

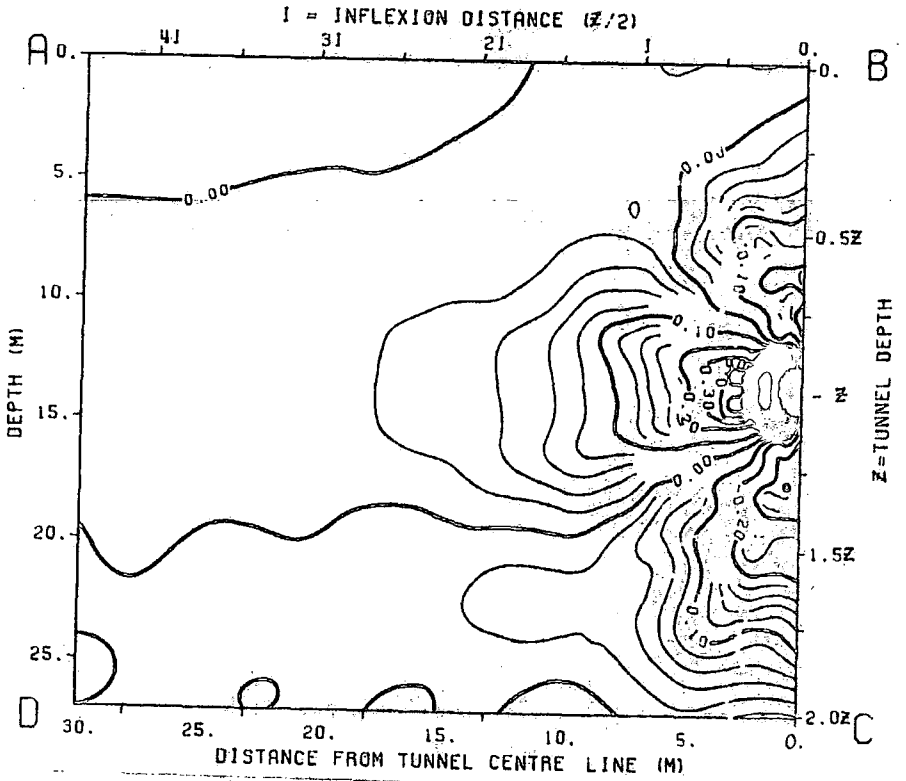

FIG. 7.2.44) Contours of equal longitudinal strains (%). Transverse section 3i behind tunnel face.

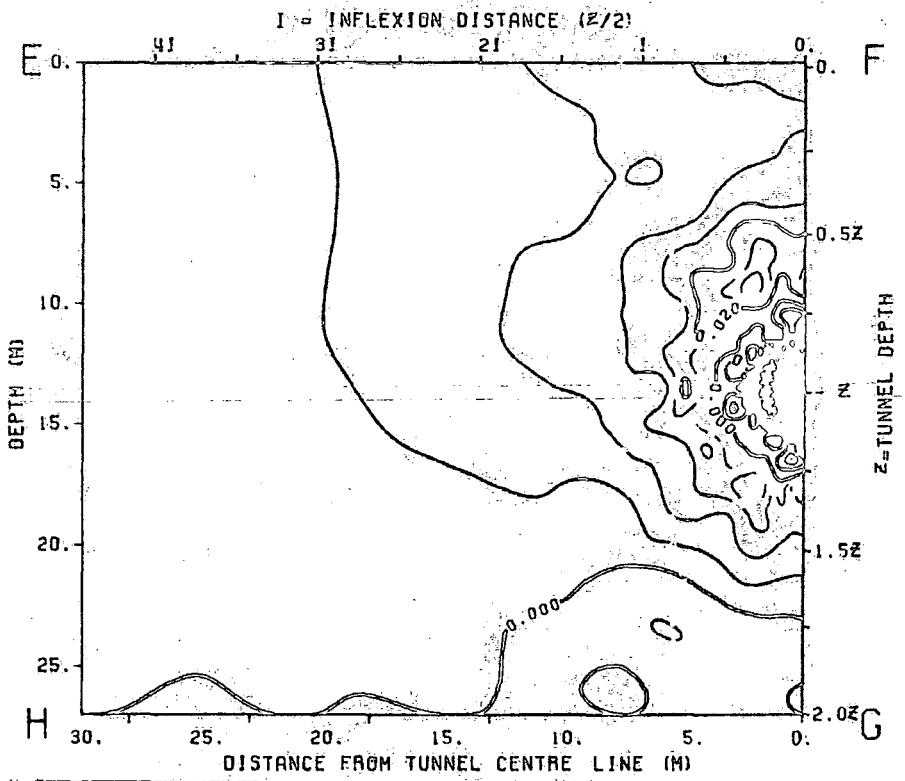

FIG. 7.2.45) Contours of equal longitudinal strains (%). Transverse section at tunnel face.

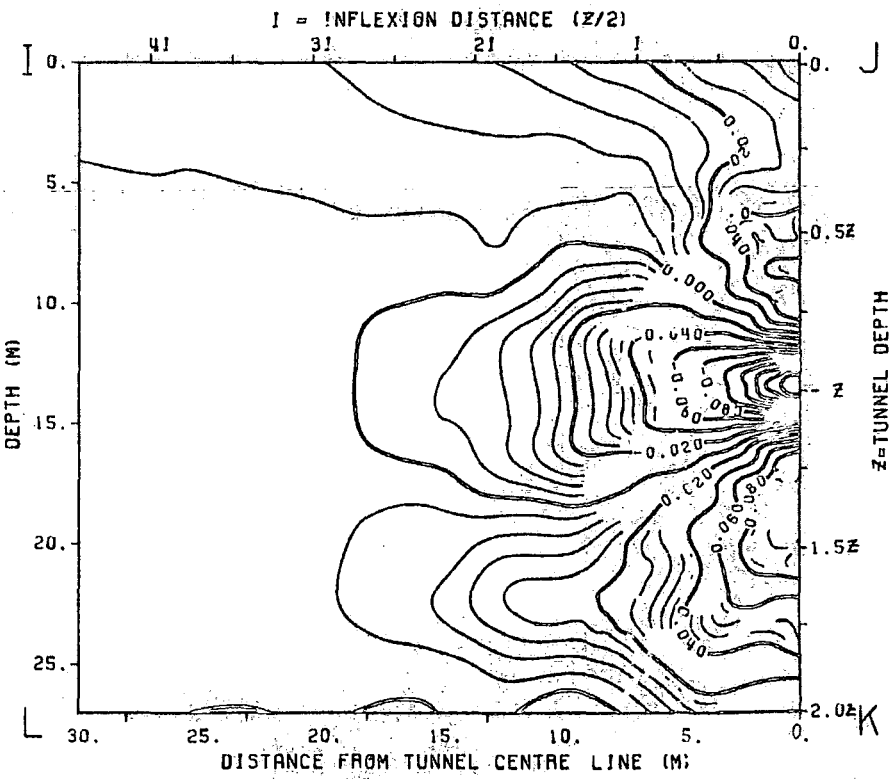

FIG. 7.2.46) Contours of equal longitudinal strains (%). Transverse section i ahead tunnel face.

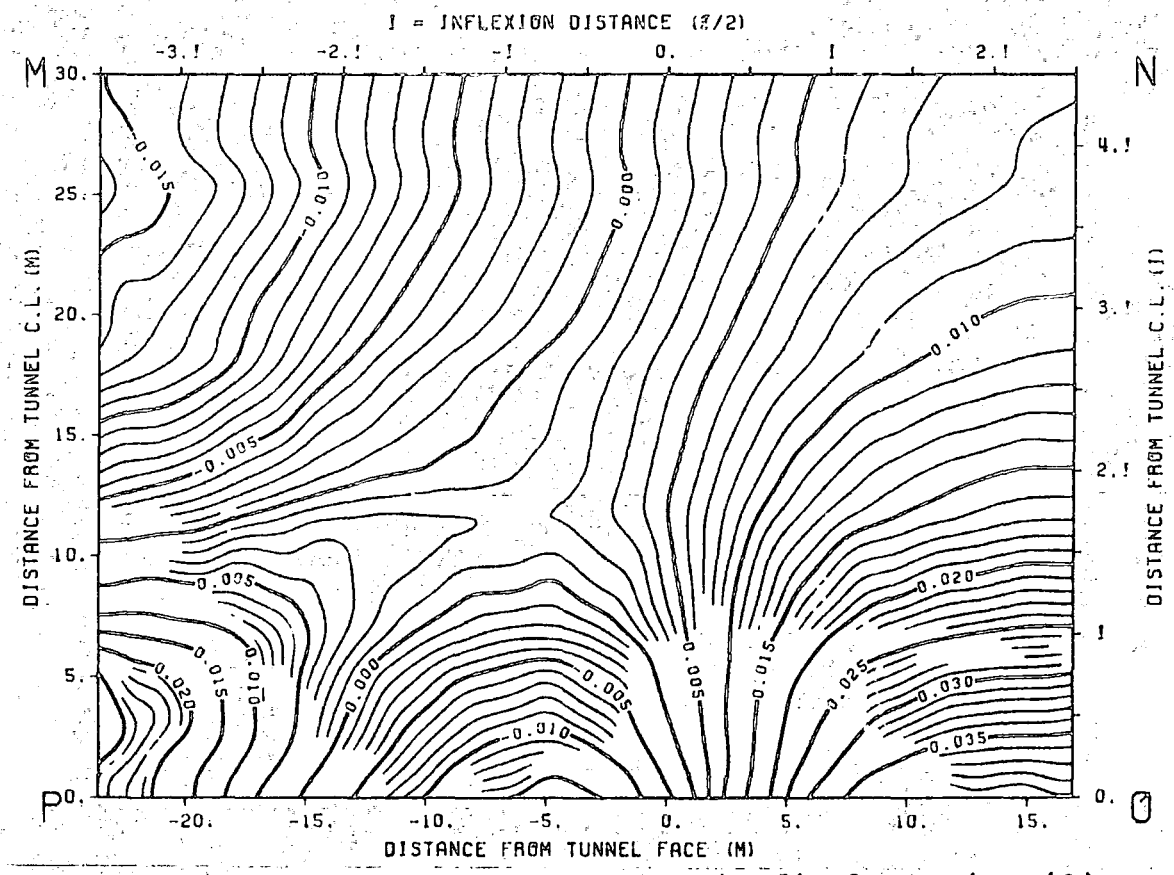

FIG. 7.2.47) Contours of equal longitudinal strains (%). Ground surface.

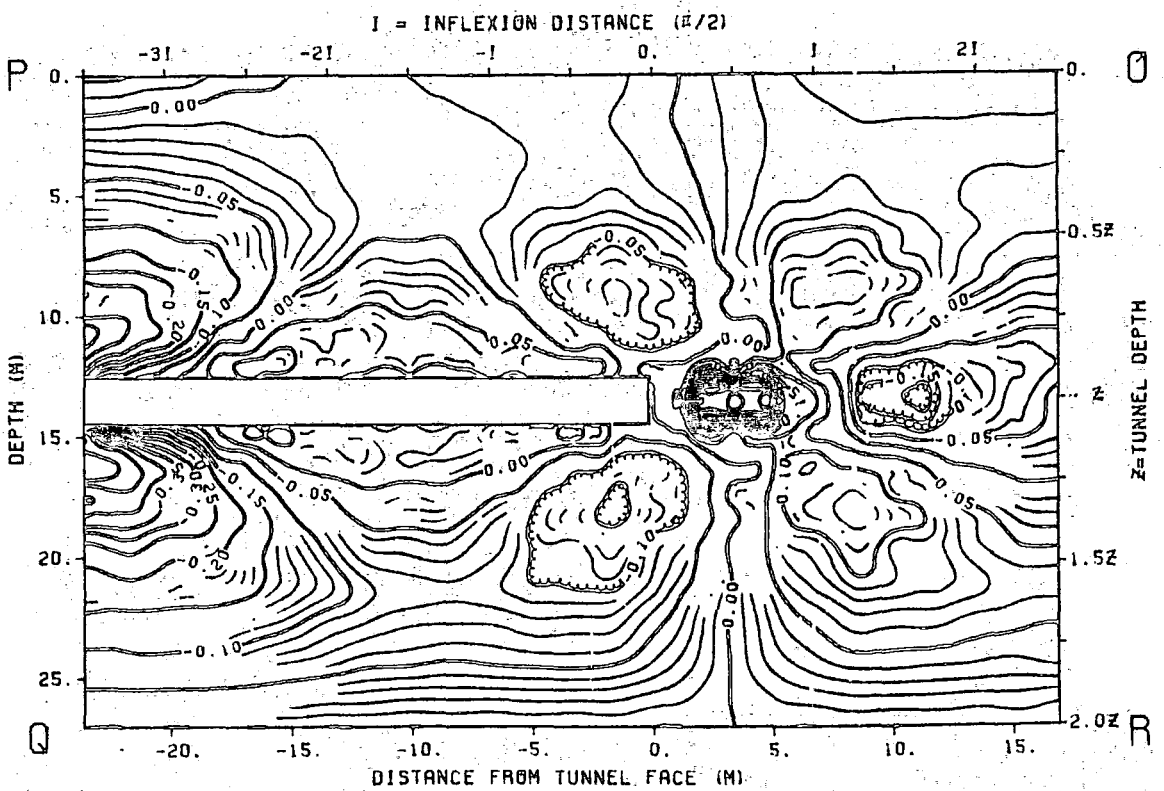

FIG. 7.2.48) Contours of equal longitudinal strains (%). Longitudinal section.

7.3 EFFECT OF GROUND MOVEMENTS ON BURIED PIPELINES.

An attempt was made to analyse a possible response of buried pipelines to the ground movement caused by tunnelling in soil. All three pipes studied in this example lie parallel to the tunnel drive.

7.3.1 THE FINITE ELEMENT MODEL.

The basic configuration of all three pipe meshes used in the analysis is presented in Figure 7.3.1. As shown in the Figure only the pipe is modelled in the finite element mesh in order to attempt to overcome the problem of a high stiffness ratio between pipe and surrounding soil. The positions of the pipes relative to the tunnel axis are shown in Figure 6.4.

The procedure used to find stresses and strains in the pipe is to apply a specified ground displacement field on the boundaries of the mesh of the pipe (Figure 7.3.1). Displacement field data for the soil alone (pipe inclusions at that stage being absent) were first generated by using a program, based on the normal probability approach, on an Exidy Sorcerer microcomputer and then inputting all the data manually to the finite element program through the mainframe computer terminal. It is noted that, in effect, this operation generates a

pessimistic strain condition in the pipe since, with the pipe in place, the soil displacements at the pipe boundary would be less than those displacements at the same point without the pipe being present.

As the differential displacements in the x, y and z directions in the pipe cause variations in pipe stresses and strains, the finite element program conveniently adjusts these displacements before transforming them into equivalent forces. This adjustment is equivalent to a rigid body translation movement which is made by setting to zero the smallest nodal displacement in one direction and subtracting the same amount from the remaining nodal displacements in the same direction. After the removal of such a translation movement, the resulting displacements are transformed to equivalent forces by applying the following expression :

$$\{F\} = [K] \cdot \{d\}$$

where [K] is the element stiffness matrix and {d} is the adjusted displacement.

The input displacements calculated by the empirical approach, as outlined in Section 6.7, were obtained by assuming that the tunnel face is located halfway along the pipe length (that is, the length between

the cross-section boundaries of the finite element mesh) with the total length (27m or 4i) taken to be equal to twice the depth of the tunnel axis (13.5m or 2i).

The length of the pipes was determined by analysing Figures 7.1.1 to 7.1.6. As can be seen in these Figures, the longitudinal components of displacements and strains may be assumed to be predominant parameters to determine the appropriate position of the boundaries. This predominance is related to the ground surface ahead of the face affected by the tunnelling process, assuming that the contour of 10% of maximum longitudinal strain is an appropriate value to limit the pipe length of interest. In retrospect, it would have been preferable to have adopted boundaries beyond the 10% (of maximum) strain contour.

The secant elastic modulus and Poisson's ratio were taken to be 94×10^3 MN/m^2 and 0.26, respectively, for all three pipes.

7.3.2 RESULTS OF THE FINITE ELEMENT ANALYSIS.

7.3.2.1 DISPLACEMENTS.

Values of soil displacements at the levels of all three pipe axes calculated in the last example are plotted

in Figures 7.3.2 through 7.3.4 in terms of percentage of maximum settlement, which was taken from the point located on the ground surface over the tunnel centre line and 3i behind the tunnel face. Values of each point plotted in these Figures represent the average displacement of four nodes surrounding the pipe axis at each transverse section used in the finite element mesh.

As expected, these Figures show that the soil lateral displacements at pipe axis levels are smaller for pipes located near to the tunnel centre line. On the other hand, and again as expected, the vertical and longitudinal displacements are greater.

In Figure 7.3.4, the effect of the boundary conditions are considerable, but the Figure shows that the maximum value of longitudinal displacement is located at the tunnel face.

7.3.2.2 STRESSES.

Values of stresses on pipes A', B' and C' were derived and plotted through Figures 7.3.5 to 7.3.7. Four fibres : upper fibre, lower fibre, outer right-hand side fibre and outer left-hand side fibre were chosen in order to analyse the longitudinal stresses likely to develop on such pipelines due to the tunnel excavation. In the

following discussions, the term 'longitudinal stress' refers to the sum of longitudinal bending stress and direct stress in the x direction.

The information provided by Figures 7.3.5 to 7.3.7 indicates that the vertical differential movement in the longitudinal direction is a predominant factor conditioning the longitudinal bending response of pipes. As the pipes experience larger differential movements in the vertical direction it was expected that the fibres located on the crown and invert of the pipes would experience higher (tensile or compressive) longitudinal stress levels than in any other position. This prediction was confirmed and can be observed in all three pipes (Figures 7.3.5 to 7.3.7) where the upper fibre is subjected to the absolute highest and lowest longitudinal stress levels ahead of and behind the tunnel face, respectively.

Figures 7.3.5 to 7.3.7 show that the outer right-hand side and left-hand side fibres are subjected approximately to the intermediate longitudinal stress levels between stresses on the upper and lower fibres in each cross-section of the pipe. Figure 7.3.7 shows that fibres located at the springline of pipe C' present different characteristics from those shown in Figures 7.3.5 and 7.3.6. The magnitude of the longitudinal

stresses on the outer right-hand side fibre are closer to the magnitude of longitudinal stresses on the upper fibre, and those for the outer left-hand side fibre are closer to the magnitude of longitudinal stresses on the lower fibre.

Although longitudinal bending compressive stresses must be induced on the lower fibre of the pipe ahead of the tunnel face as a result of the vertical differential displacements, the finite element results have shown that all points ahead of the tunnel face are subjected to total longitudinal tensile stress. Similarly, all points behind the tunnel face are subjected to total longitudinal compressive stress even though bending tensile stresses must be induced on the lower fibres. This pipe behaviour may be caused by the boundary displacement conditions imposed on the finite element mesh, great rigidity of the pipe in the x direction and an assumed perfect bonding at the interface between soil and pipe.

The contributions of displacement boundary conditions and rigidity of the pipe in the x direction are related to each other. Then, any force acting in the x direction will induce development of high stress levels (direct stress) in the x direction. The magnitude of direct compressive (or tensile) stress at one point is greater than the magnitude of longitudinal bending tensile (or compressive) stress at the same point, so causing an

entire cross-section of the pipe to be subjected to the total longitudinal compressive (or tensile) stresses.

If perfect bonding between soil and pipe is assumed in the finite element model, any movement in the x direction of the soil located adjacent to the pipe will contribute to an increase in longitudinal stresses on the pipes. If the load is such that no significant amount of relative slip occurs between soil and pipe, it may be admissible to assume that those materials remain perfectly in contact. However, in practice and in some instances there may be relative slip, leading to local de-coupling between soil and pipe and a wave of closing and opening of the soil at the soil-pipe interface.

Besides these factors, there are others that may also contribute to the response of pipes as discussed above, such as flexibility of pipelines in the zx plane, diameter of the pipe, depth and diameter of the tunnel.

It is obvious that the magnitude of the deformations induced by the tunnelling process on flexible pipes would be greater than on rigid pipes having equal dimensions and occupying the same position in the ground relative to that of the tunnel. Consequently, greater longitudinal bending deformations would tend to be induced on flexible pipes. In a similar manner (and now assuming

that both pipes are made of the same material and experiencing same magnitude of deformations at axis levels), larger diameter pipelines will be subjected to greater bending stresses than those having smaller diameters.

The magnitude of the deformations introduced to the ground by tunnel excavation are obviously related to the diameter and the depth of the tunnel, and these deformations control the behaviour of the pipes. The effect of both these tunnel parameters on the ground movements are not described here because they have already been discussed in Chapter 2.

In all three cases analysed, the output data have shown that the maximum compressive and the maximum tensile stresses are located behind and ahead of the tunnel face (Figures 7.3.5 to 7.3.7), respectively, both at a distance approximately equal to half the depth of the tunnel axis (13.5m).

Variations in direct and bending stresses in the upper fibres of the pipes are shown in Figures 7.3.8 and 7.3.9, respectively. As expected, these Figures indicate that pipes located closer to the tunnel centre line experience higher levels of stress in both direct traction and bending.

The longitudinal stresses in the soil at pipe axis levels, calculated in the example presented in Section 7.2, are shown in Figure 7.3.10. The graph shows that the longitudinal stress varies according to the relative position of the pipes in the excavated region. Thus, a pipe located on the centre line is expected to experience greater longitudinal stress (longitudinal bending and direct stress) disturbance, and this was confirmed and shown in the Figure.

7.3.2.3 STRAINS.

In a similar manner to the longitudinal stress, longitudinal strain refers to the sum of longitudinal bending strain and direct strain in the x direction.

As predicted, the patterns of longitudinal strain distributions on pipes are similar to those for longitudinal stresses. The reasons for this similarity lie in those same factors discussed in Section 7.3.2.2.

Figure 7.3.11 shows the longitudinal strains on the upper and lower fibres of pipes A', B' and C'. The maximum compressive and maximum tensile longitudinal strains develop behind and ahead of the tunnel face, respectively. This Figure also shows that both maximum direct and maximum bending strains take place on a pipe

located above the tunnel centre line because at this location the ground experience larger differential movements than in any other position. According to the graph, the points of maximum longitudinal compressive and maximum longitudinal tensile strains are located 6m behind and 6m ahead of the tunnel face, respectively. This distance corresponds approximately to 90% of the assumed inflexion distance i (6.75m).

Predicted longitudinal strains in the soil at pipe axis levels, also calculated in last example, were obtained in a similar manner to displacements and shown in Figure 7.3.12. This graph also shows that the maximum strains are located above the tunnel centre line and approximately 6m from the tunnel face.

7.3.3 DISCUSSION.

The results obtained from the three-dimensional finite element analyses of displacement, stress and strain in three pipes along Collingwood Street, Newcastle upon Tyne, promote several observations. However, the results must be interpreted with respect to the limitations of the approach adopted. Nevertheless, information provided by this study may be useful for practical purpcses.

One important conclusion drawn from the analyses

is that the total longitudinal stress at any point behind (or ahead) the tunnel face is compressive (or tensile) despite the bending deformation induced by vertical differential displacements and the introduction of bending tensions (or compressions) to the lower fibre of the pipe. For the particular model adopted in this analysis, the following may contribute to such pipe behaviour :

a) Great rigidity of the pipe in the longitudinal (x) direction.

b) Assumed (for the model) perfect bonding between pipe and soil.

c) Depth of the tunnel axis.

e) Diameter of the tunnel.

f) Diameter of the pipe.

h) Boundary displacement conditions of the finite element mesh.

i) Length of the pipe.

Actual ground movements, and their effects on these pipes, have been monitored at this location on Collingwood Street, Newcastle upon Tyne. Recorded values of direct (longitudinal) strains, vertical bending strains and horizontal bending strains for the particular location shown in Figure 7.3.13 are presented in Figure 7.3.14. Analysing the field data, Hurrell (1983) pointed out that, although ground movements measured in Collingwood Street

were in fact negligible, a definite response of the pipe to these movements has been observed. From strain measuments on the pipeline there are signs of a tensile direct strain wave developing some 18m in advance of the tunnel face, becoming compressive and then tending to zero as the face moved forward.

From comparison with the actual field measurements, the finite element results have provided useful qualitative information on the response of a buried pipeline to the ground movements induced by a moving disturbance source. The basic difference between the field measurement results and finite element calculations shown, respectively, in Figures 7.3.11 and 7.3.14, is the position of the tunnel face relative to the point (line) representing zero strain. Several factors may contribute to this difference: unavoidable simplifications made for the finite element model (such as the length of pipe, the finite element mesh boundary conditions, no consideration of the effect of adjacent buildings on induced ground displacements), the assumed input displacement field data based on the normal probability approach, material properties used in the analysis, and so on.

256 elements
544 nodal points

Pipe A' - R = 0.650 m
" B' - R = 0.325 m
" C' - R = 0.492 m

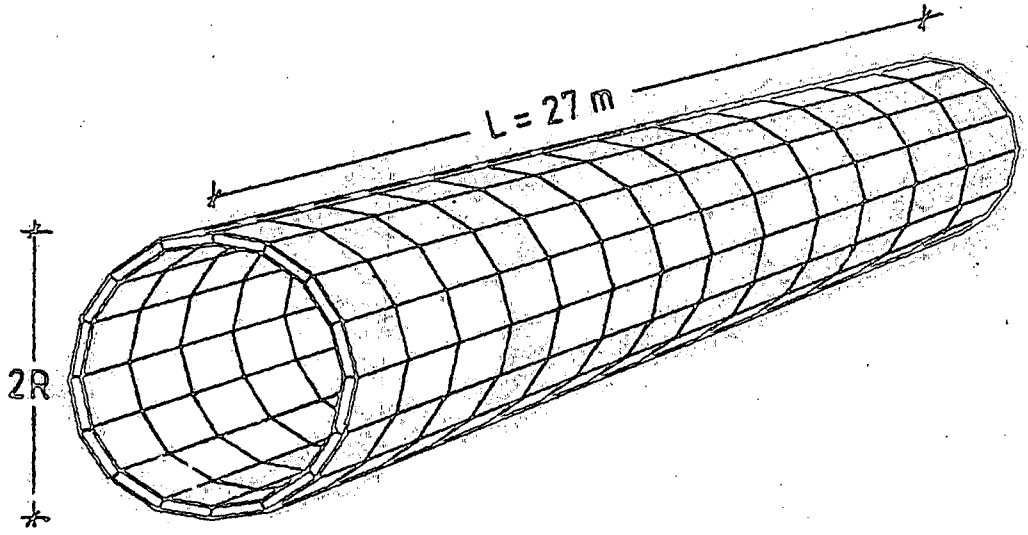

FIG. 7.3.1) Finite element idealization of the pipe.

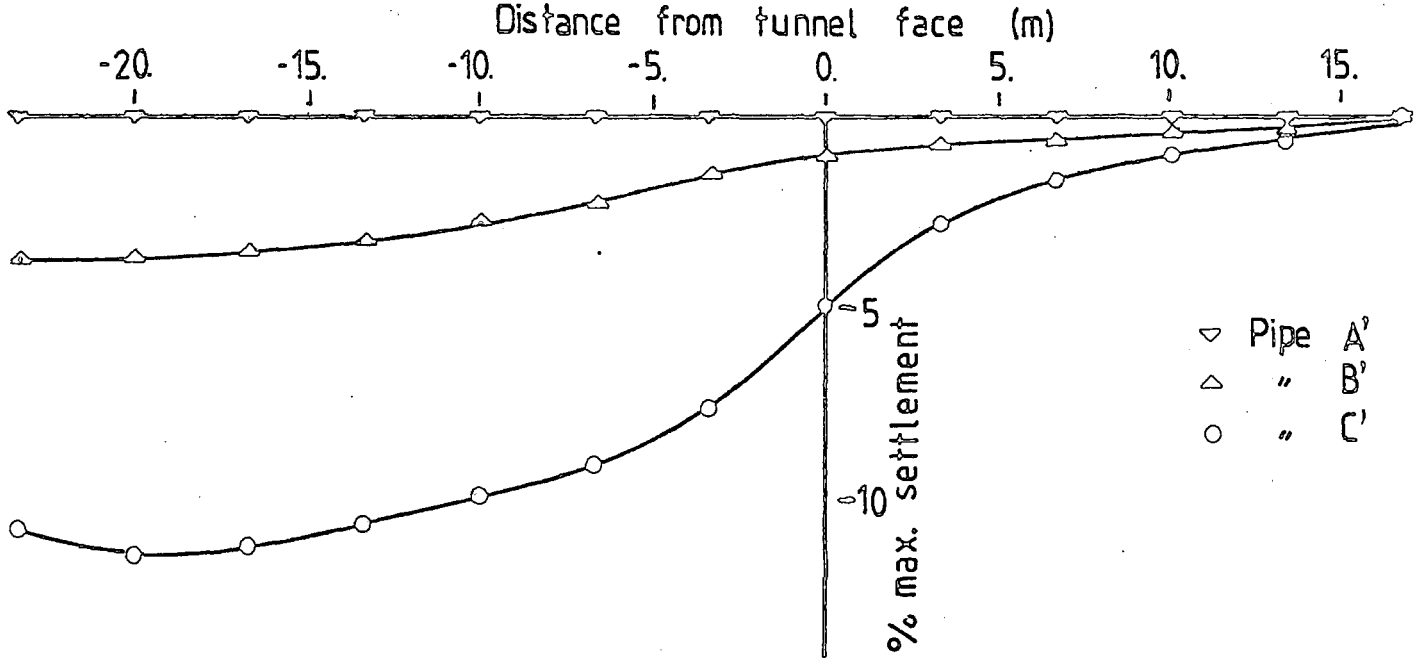

FIG. 7.3.2) Predicted lateral movements in the soil at pipe axis level.

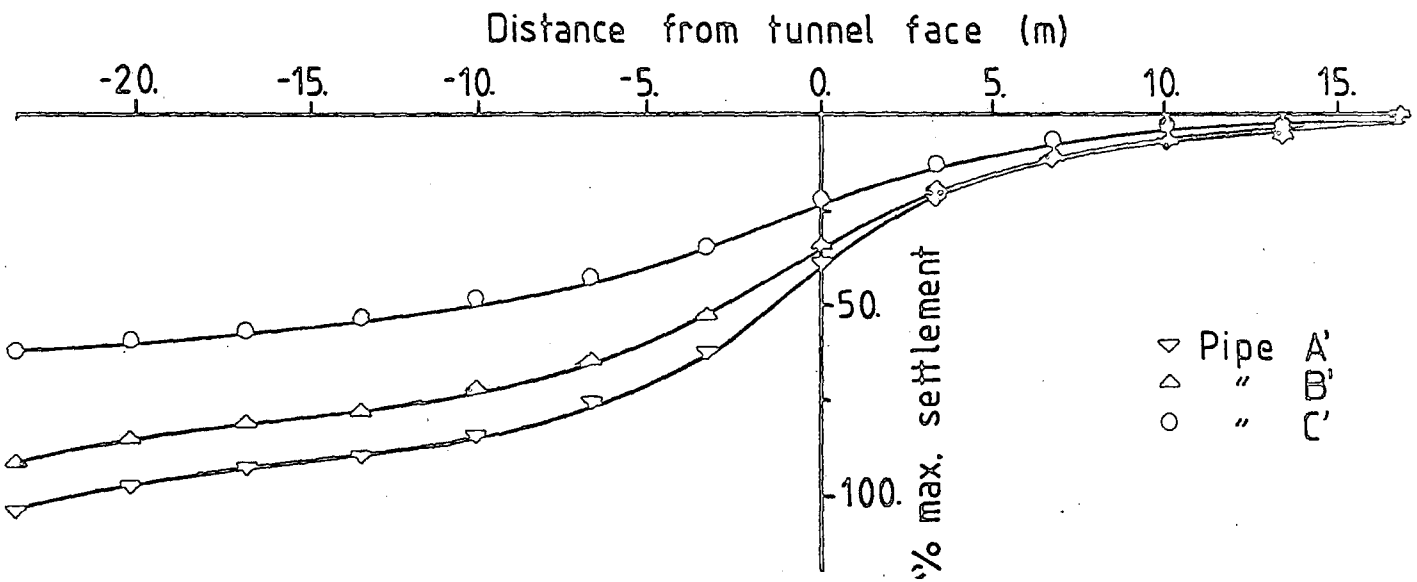

FIG. 7.3.3) Predicted vertical movements in the soil at pipe axis level.

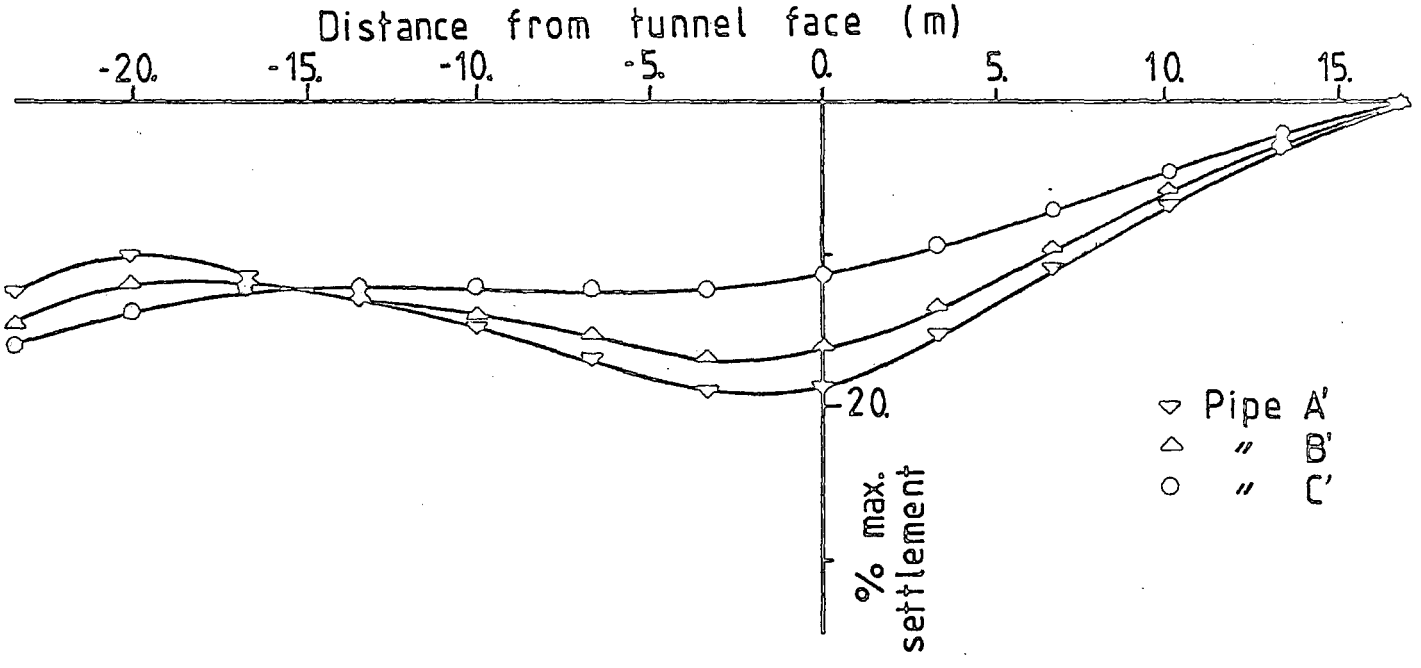

FIG. 7.3.4) Predicted longitudinal movements in the soil at pipe axis level.

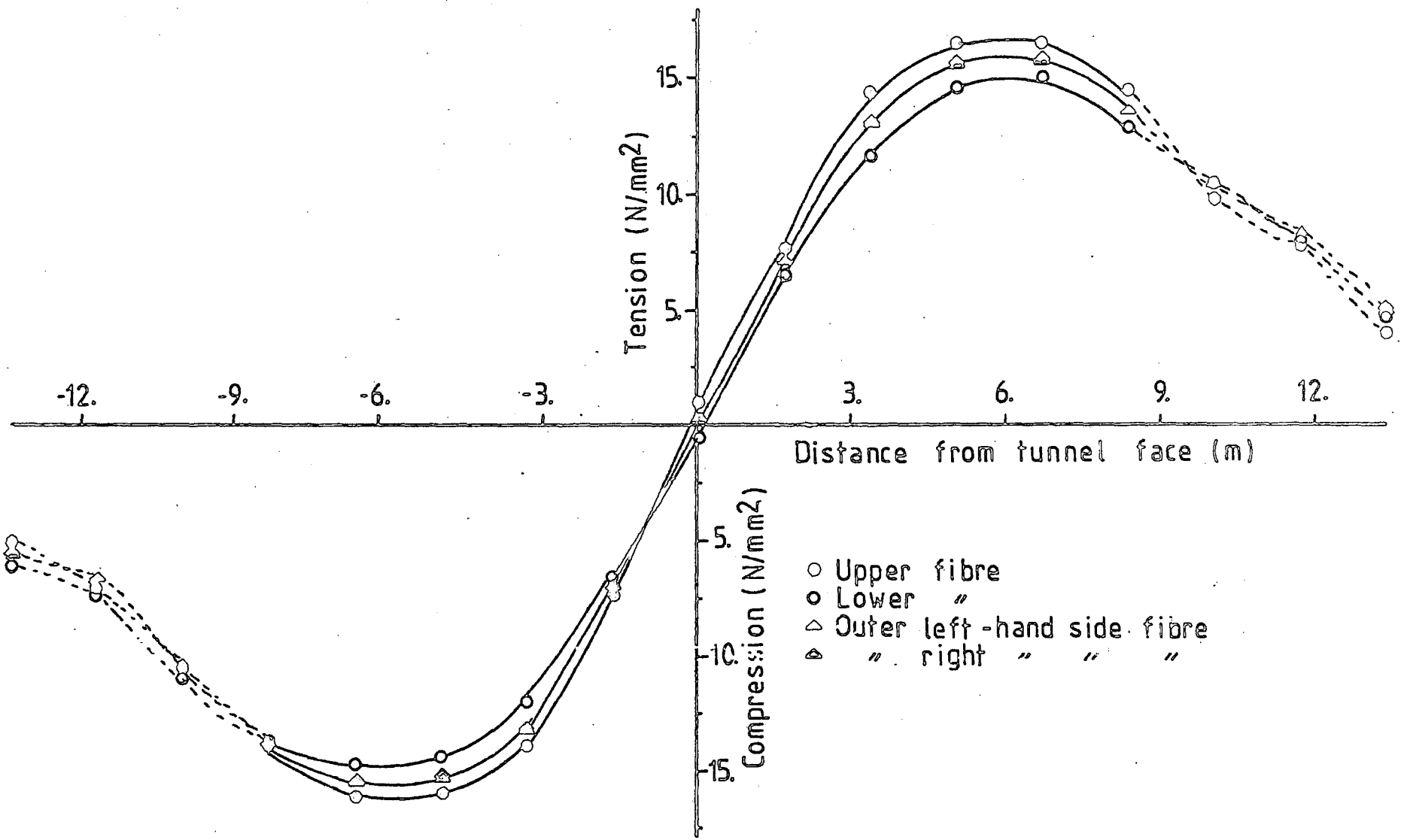

FIG. 7.3.5) Longitudinal stresses on pipe A'.

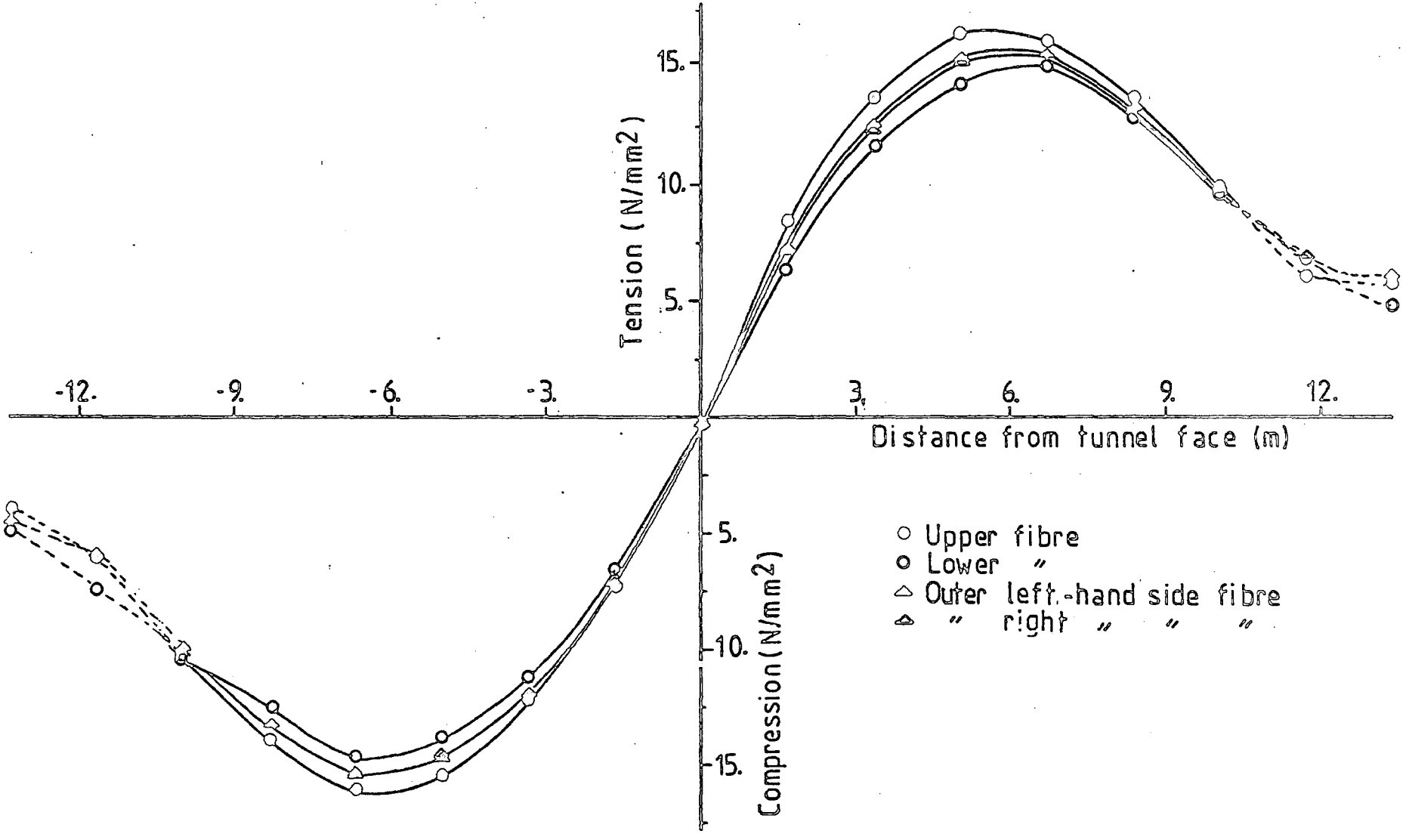

FIG. 7.3.6) Longitudinal stresses on pipe B'.

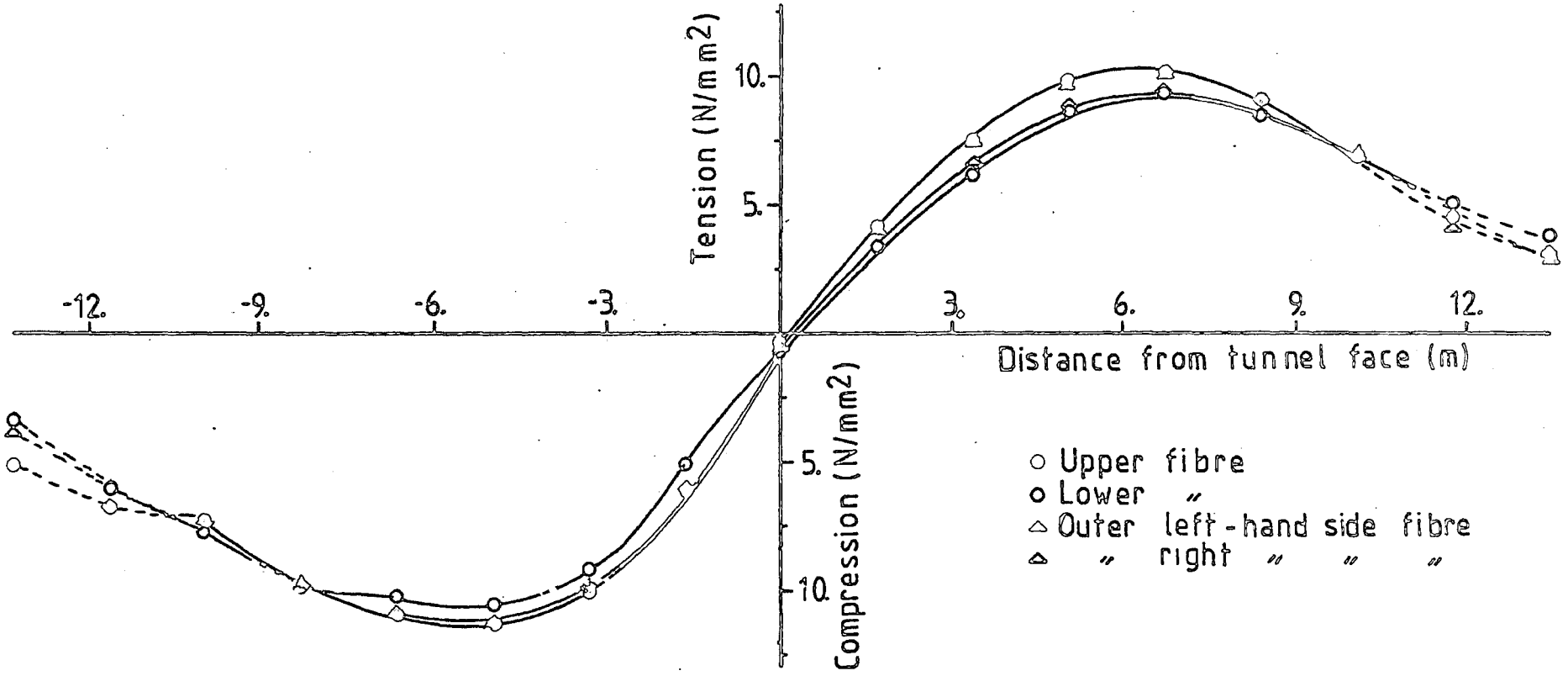

FIG 7.3.7) Longitudinal stresses on pipe C'.

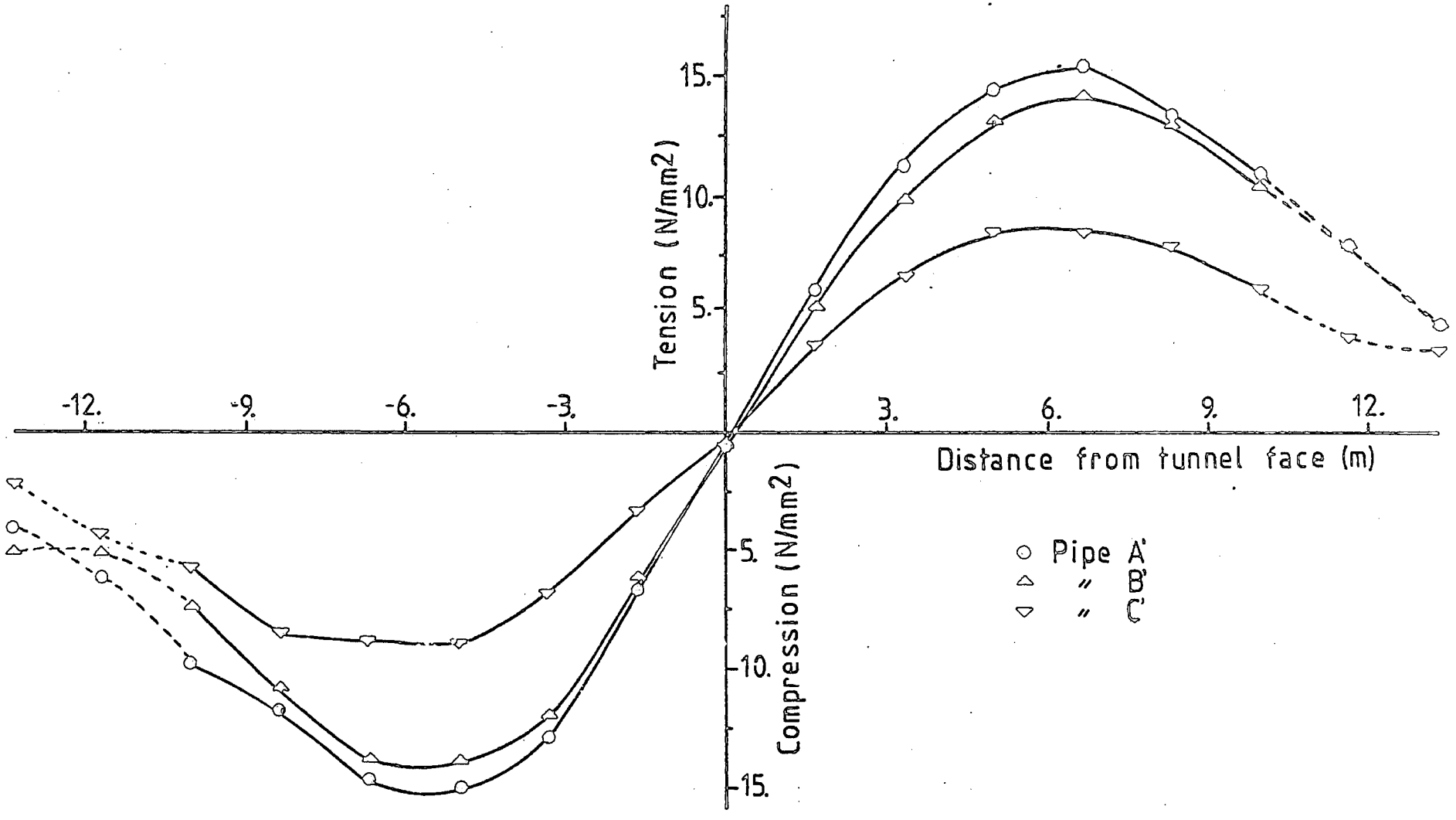

FIG 7.3.8) Direct stresses on upper fibre.

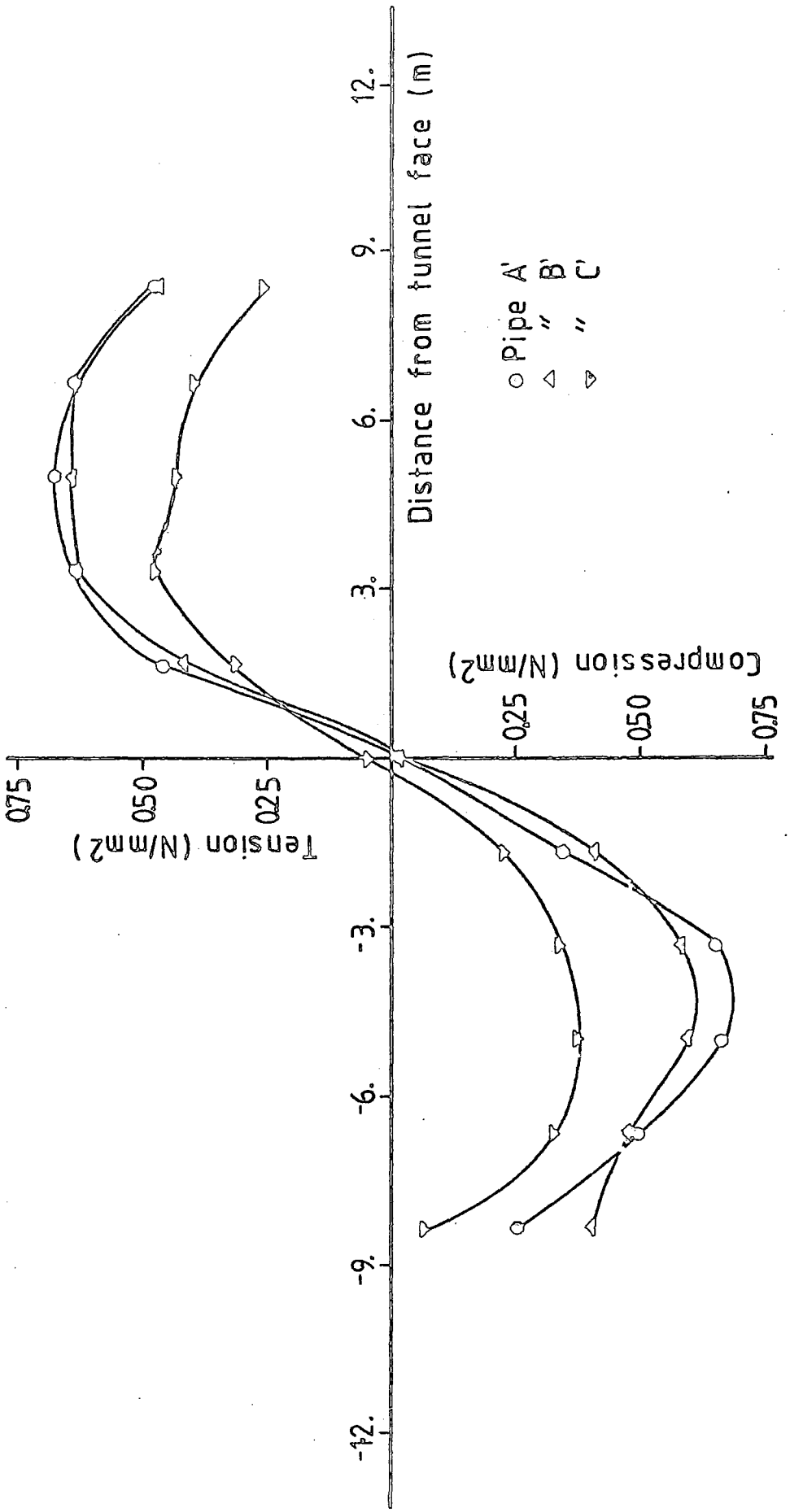

FIG 7.3.9) Bending stresses on upper fibre.

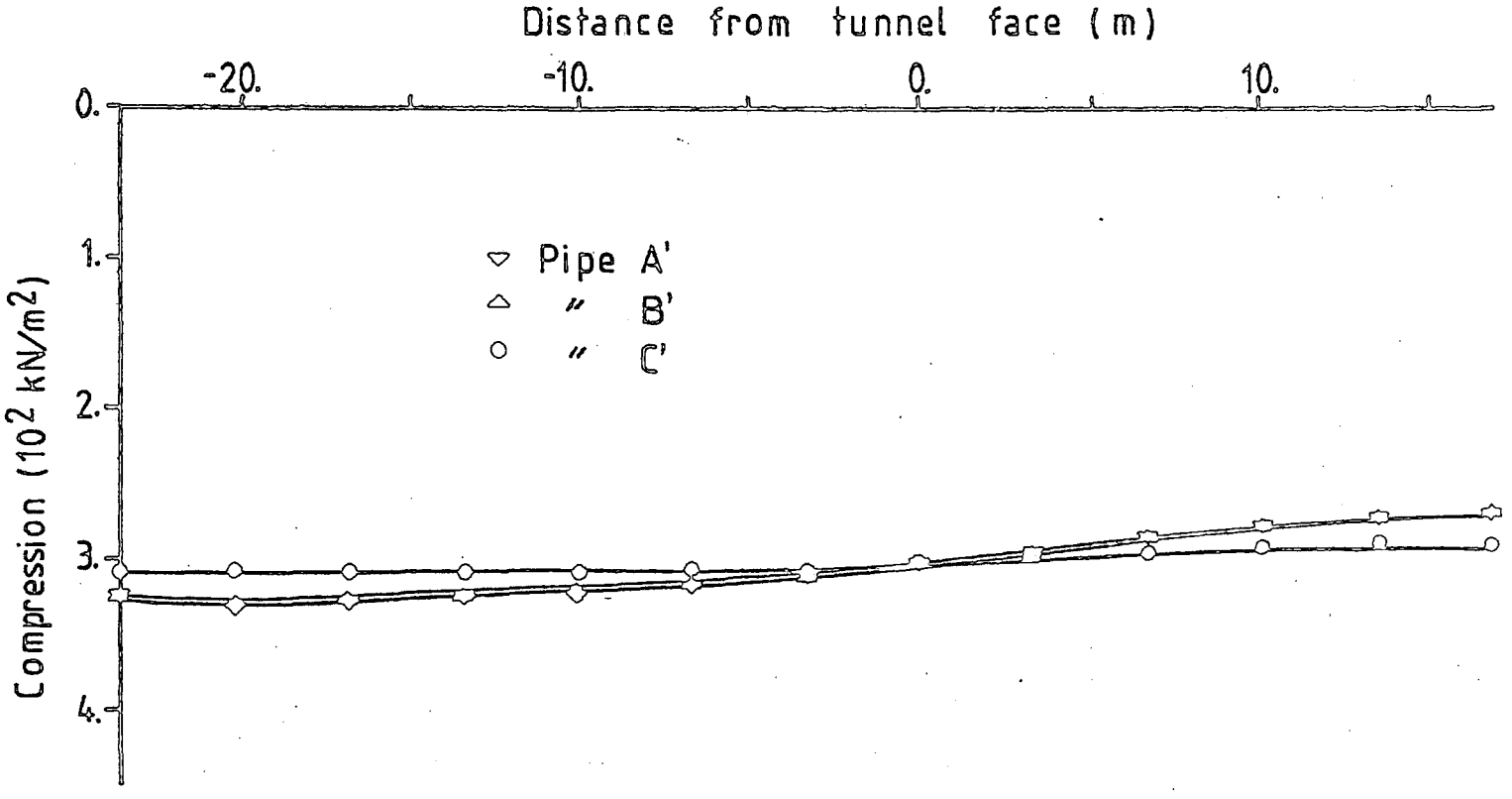

FIG. 7.3.10) Predicted longitudinal stresses in the soil at pipe axis level.

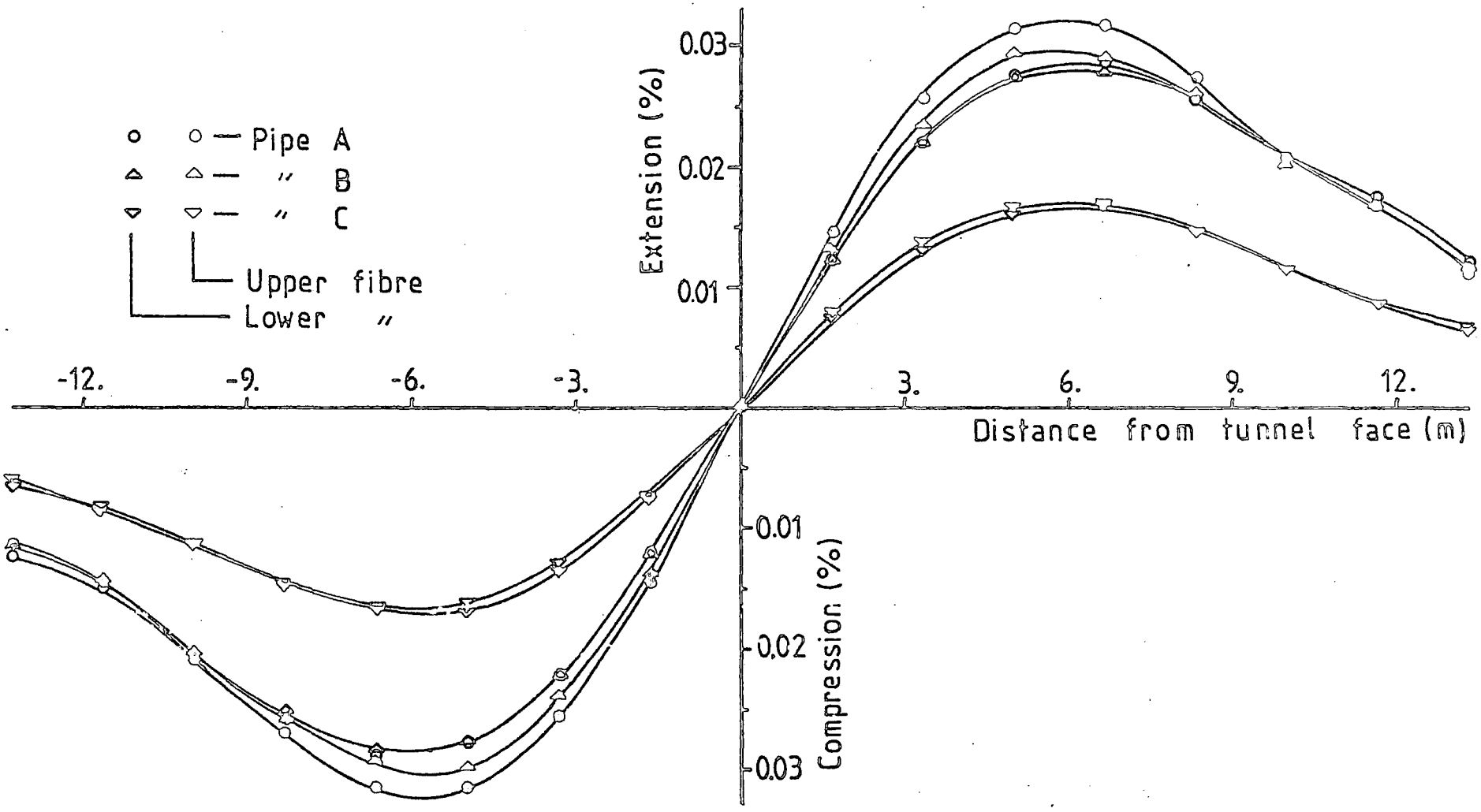

FIG. 7.3.11) Longitudinal strains on pipes A', B' and C'.

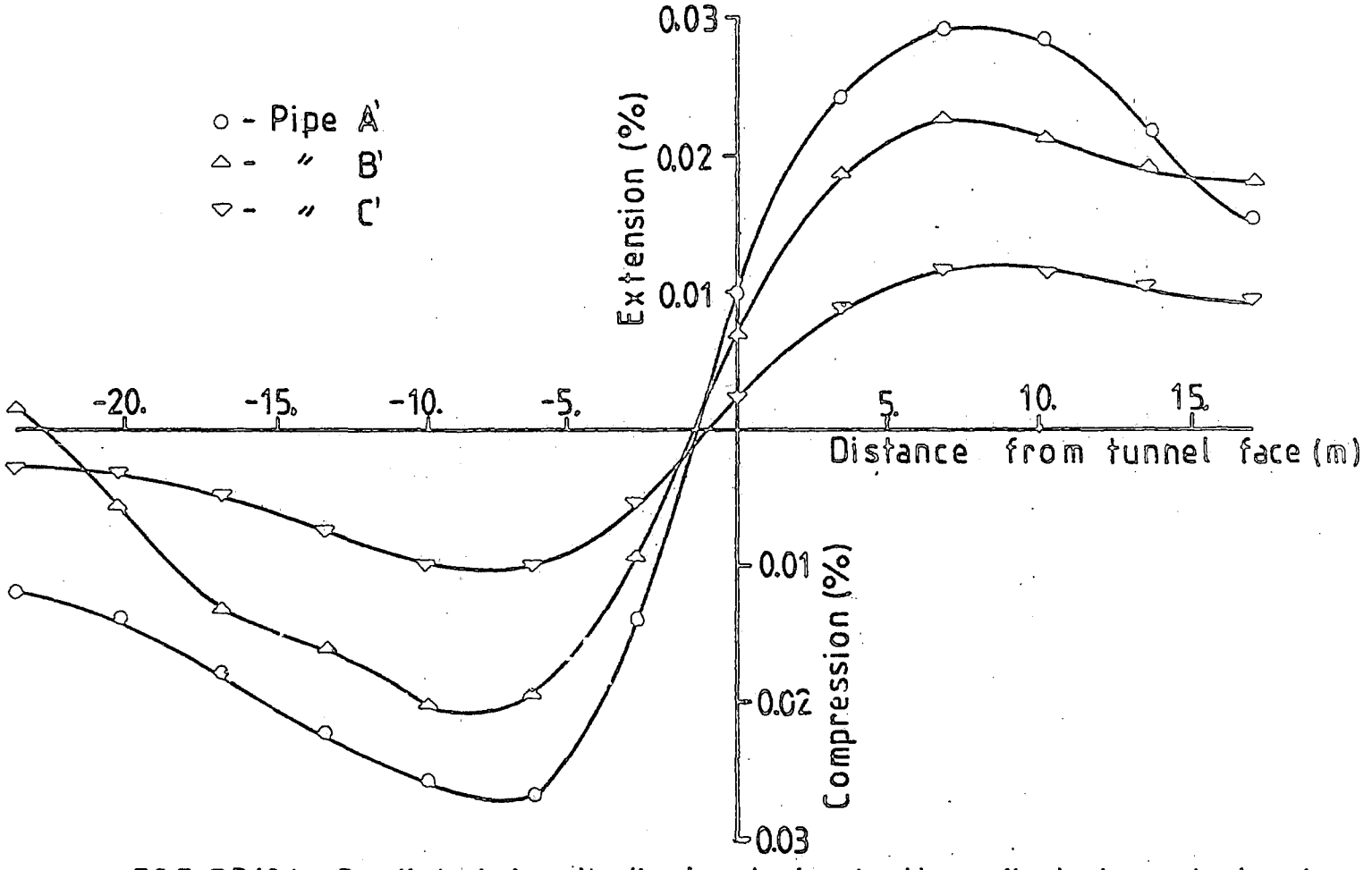

FIG. 7.3.12) Predicted longitudinal strains in the soil at pipe axis level.

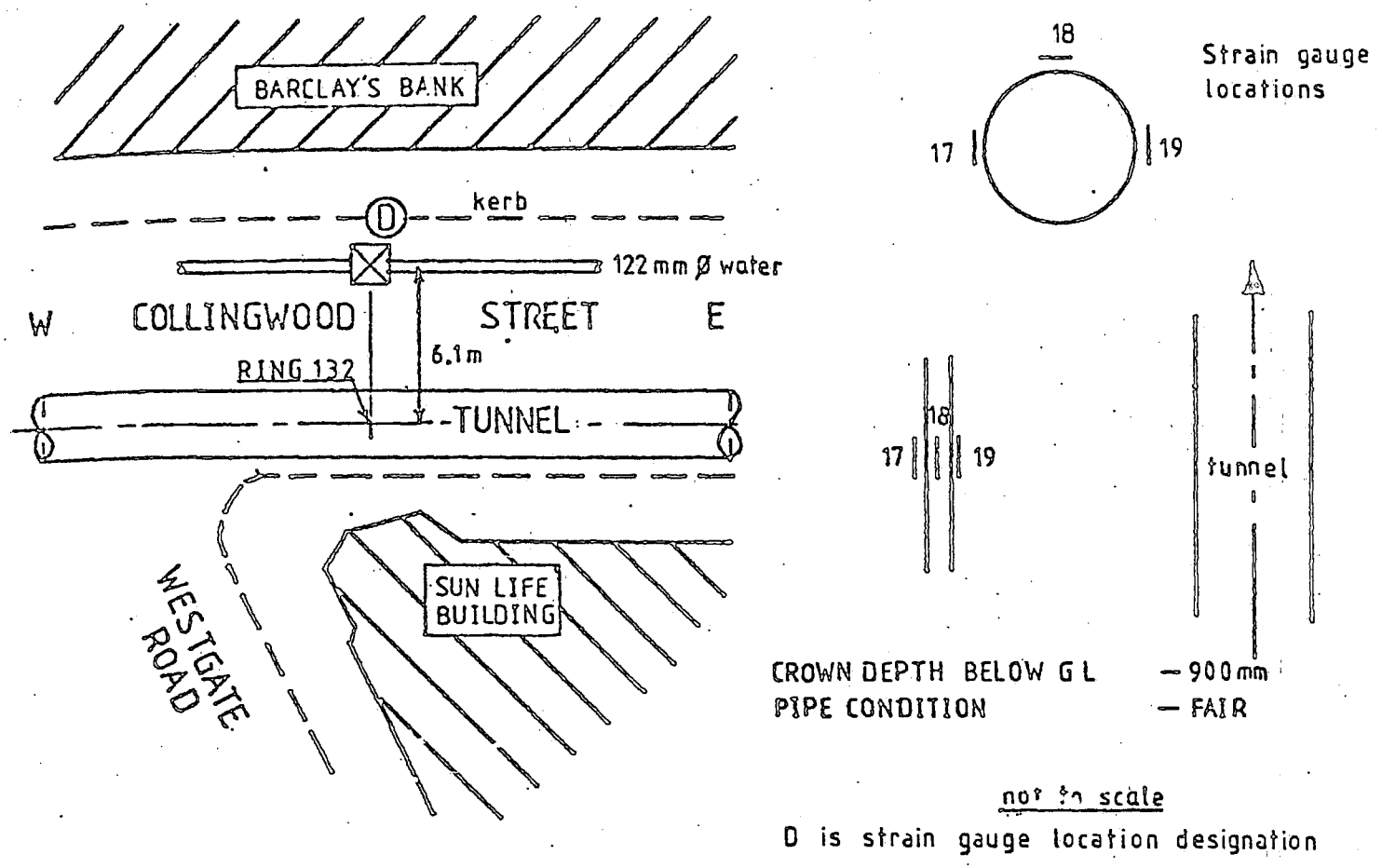

FIG. 7.3.13 Vibrating wire strain gauge installation.

Array D (after Hurrell, 1983).

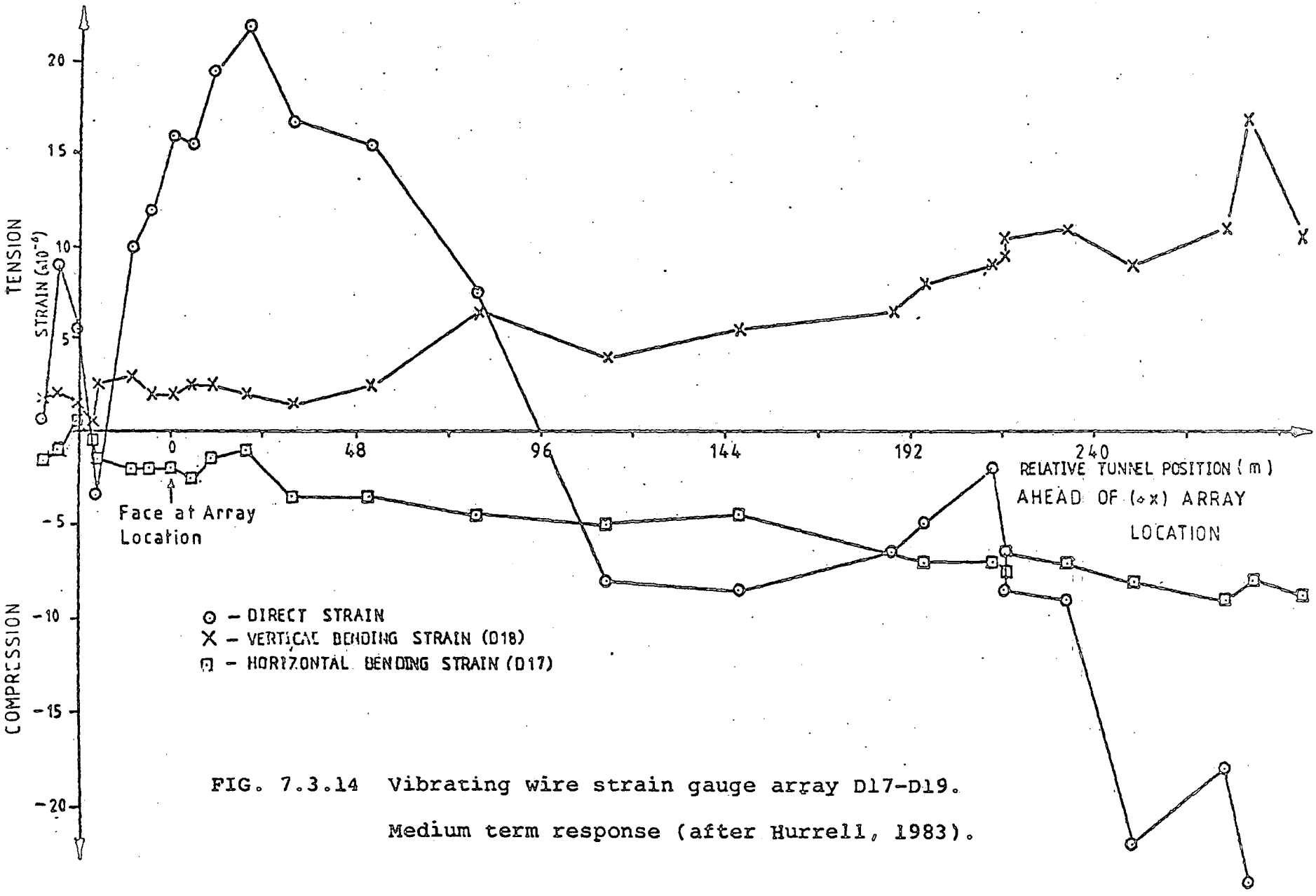

FIG. 7.3.14 Vibrating wire strain gauge array D17-D19.
Medium term response (after Hurrell, 1983).

7.4 EFFECT OF PIPE STIFFNESS ON SOIL MOVEMENT.

In this example, an attempt has been made to analyse the effect of pipe stiffness on the ground movements caused by the tunnelling process.

A general procedure for analysing, by means of a finite element mesh, the interaction behaviour of a soil-pipe system with a tunnelling operation, is to model the entire medium disturbed by the excavation. In this example, it was not possible to apply this technique because of the small size of the pipes relative to the scale of the ground section, and so an alternative approach had to be used for studying the problem. Accordingly, a displacement field was applied to an isolated region of design interest, that is, the region(s) in the vicinity of the pipe(s).

Two meshes shown in Figures 7.4.1 and 7.4.2 were used because using a single finite element mesh to represent all three pipes would not be feasible.

One of the meshes (Figure 7.4.1) includes pipes A' and B', because it was considered that interaction between them could be more significant than that between pipes B' and C'. This consideration stemmed from the fact that the distance between pipe A' and pipe B' is smaller than that

between pipes B' and C'. Figure 7.4.2 shows the mesh which considers pipe C' isolated from the others. Contours of typical transverse sections for both meshes are indicated in Figure 6.4 by dashed lines abcd (MESH 2) and efgh (MESH 3). Also the positions of pipes A', B' and C' relative to the tunnel axis are indicated in the same Figure.

Using the procedure outlined in Section 6.6, Young's moduli adopted in this example were 17.4×10^3 MN/m^2 20.9×10^3 MN/m^2 and 18.6×10^3 MN/m^2 for pipes A', B' and C', respectively. One single value of Poisson's ratio, 0.26, is used for all three pipes. For the soil, the parameters used in both models were 0.6 MN/m^2 and 0.48, respectively, for E and ν.

The displacement fields, plotted by means of the GPCP package program on the NUMAC computer system, are related to three transverse sections 1.5i behind the tunnel face (plane ABCD), at the tunnel face (plane EFGH), and i ahead of the tunnel face (plane IJKL), for both meshes. Perfect bonding at the interface between soil and pipe was assumed in the finite element model. However, some additional observations are made related to this assumption.

The pipe (the strength of which is much higher

than that of the surrounding soils) and soil materials are assumed to be linearly elastic in this analysis. When two or more linearly elastic structural elements couple to share a common load, the portion supported by each of them depends on the relative stiffness of the coupled elements. The stiffer elements attract a greater portion of the load. If one of structural elements is linear and elastic and the other is non-linear and inelastic, then the concept of relative stiffness loses meaning in a quantitative sense. However, in a qualitative sense the concept of relative stiffness is still valid.

The above observations indicate that, at the present time, the forces acting at the soil/pipe interface cannot reasonably be analysed. In addition, a finite element idealization of a three-dimensional soil-pipe system which takes full account of the soil-pipe interface behaviour would not be practical for the present study because the cost of computer time requirements would be too high. A mesh finer than that shown in Figures 7.2.2 and 7.2.3 would be required in a soil region close to the pipes together with additional elements at the interface between the soil and the pipes.

7.4.1 RESULTS.

Contours of three component (u, v and w)

displacements on the transverse sections described above were plotted and shown in Figures 7.4.3 to 7.4.20, inclusive. In all these Figures, the effect of boundary conditions on the ground movements can clearly be noticed on the bottom and left-hand side of the Figures, mainly on the sides where larger displacements take place. Obviously, the soil adjacent to the pipe is expected to experience smaller displacements because of the presence of the stiffer pipe material. This was confirmed and can be seen in Figures 7.4.3 to 7.3.20.

Attention should be drawn to the fact that the magnitudes of the computed displacements in the soil adjacent to the pipe could, in practice, be larger than shown in the graphs because perfect bonding between soil and pipe has been assumed to apply in the finite element model. The effect of this factor on soil behaviour will not be discussed in this example because it has already been covered in the last example.

As expected, contours of equal displacements have shown that perturbations due to the presence of pipes, on the trends of the soil displacements, are more significant where the soil mass experiences larger displacements. This can be observed in Figures 7.4.3 through 7.4.20. The effect of the presence of pipe A' on the soil lateral

movements cannot be noticed in Figure 7.4.3 because this pipe is located above the tunnel centre line (the point of transverse symmetry where there is no lateral displacement of the ground). On the other hand, the presence of pipe C' in the medium considerably affects the soil lateral movements because it is located close to the soil region where the largest lateral displacements are induced by the tunnelling process. Again, as expected, the effect of pipe B' on the ground lateral displacement is not as large as with pipe C', because it is located closer to the tunnel centre line. These observations can be applied to all three transverse sections ABCD (1.5 behind the tunnel face), EFGH (at the tunnel face) and IJKL (i ahead of the tunnel face).

For vertical displacements shown in Figures 7.4.9 to 7.4.14, the predicted behaviour of all three pipes was confirmed qualitatively. Pipes located closer to the tunnel centre line affect more strongly the soil vertical displacements than do pipes located at greater distances from the centre line.

Further comments on longitudinal displacements (Figures 7.4.14 to 7.4.20) were considered unnecessary because observations made for vertical displacements also apply to movements in the x direction.

7.4.2 DISCUSSION.

The results obtained in this example indicated that soil displacements around (in close proximity to) pipes would be larger if the presence of the pipes is not taken into account during computations. This fact is more significant in a soil region where larger displacements take place.

As shown in Figures 7.4.3 to 7.4.20, the differential displacements are caused by the high stiffness ratio between soil and pipe materials, which is particularly great in the x coordinate direction. These differential movements may be reduced if the behaviour of soil-pipe interface is modelled in a finite element mesh.

Figures 7.4.3 to 7.3.20 also indicate that future analyses must more comprehensively model the interfacial behaviour of pipe and soil, accommodating the fact that slippage may well occur, and thus substantially affect the movements in both ground and pipe.

From the results obtained in this example the following conclusions may be drawn :

a) Movements in the soil adjacent to a pipe are

reduced by the presence of a pipe.

b) The relative stiffness of the soil-pipe system dictates its performance.

c) It may be overly conservative to design buried structures based on the strains developed in the free field.

d) The approach used can be expanded to analyse the response of different soil-structure systems.

e) If a buried pipeline is subjected to large displacements, and perfect bonding is assumed to exist between soil and pipe, potential errors may be introduced.

f) The magnitude and distribution of displacements, particularly in the longitudinal (x) direction, may be affected by the boundary displacement conditions associated with the distance from the source of soil disturbance.

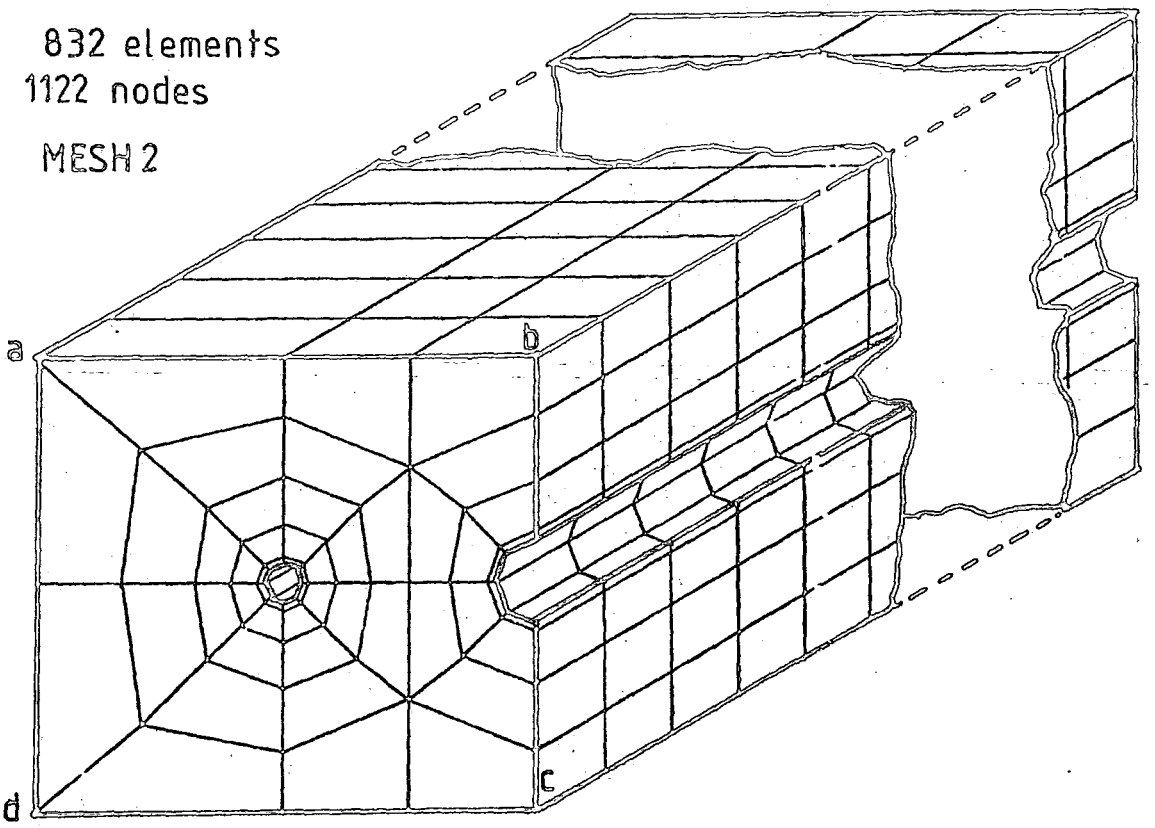

FIG.7.4.1) Soil-structure system idealization (pipes A' & B').

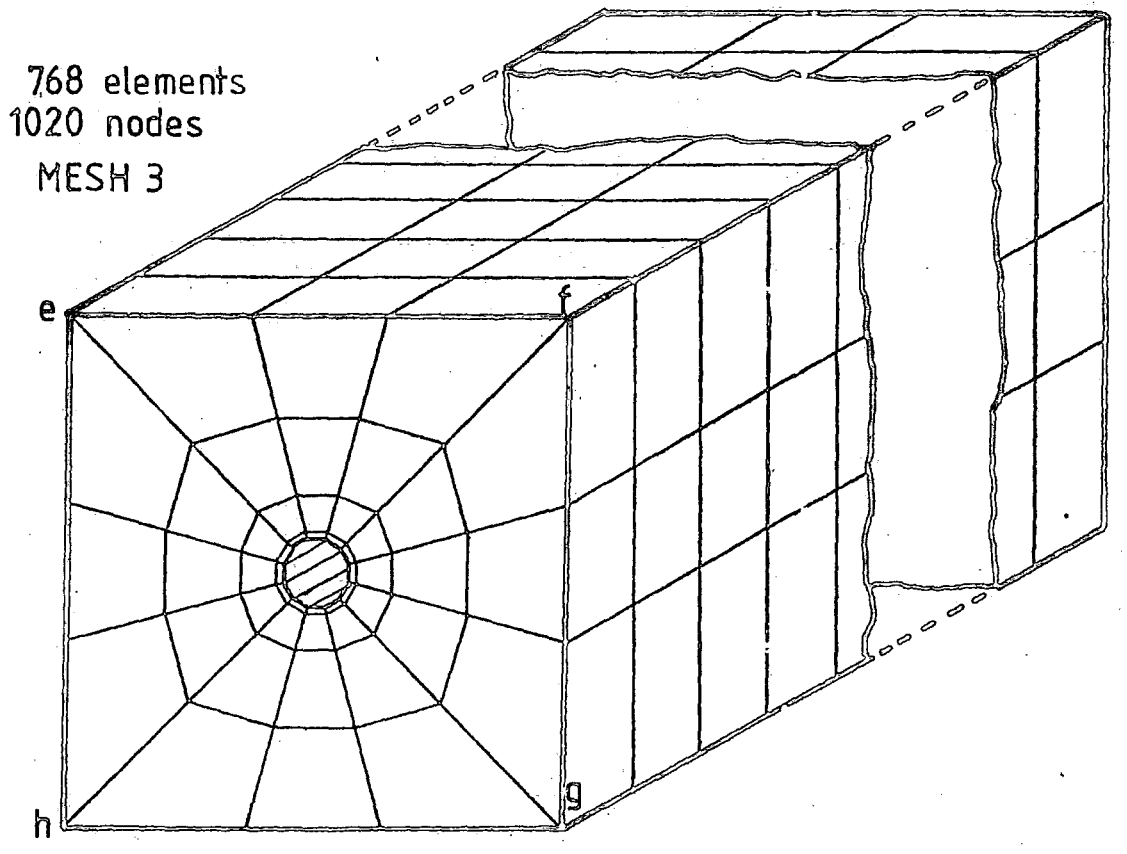

FIG.7.4.2) Soil-structure system idealization (pipe C').

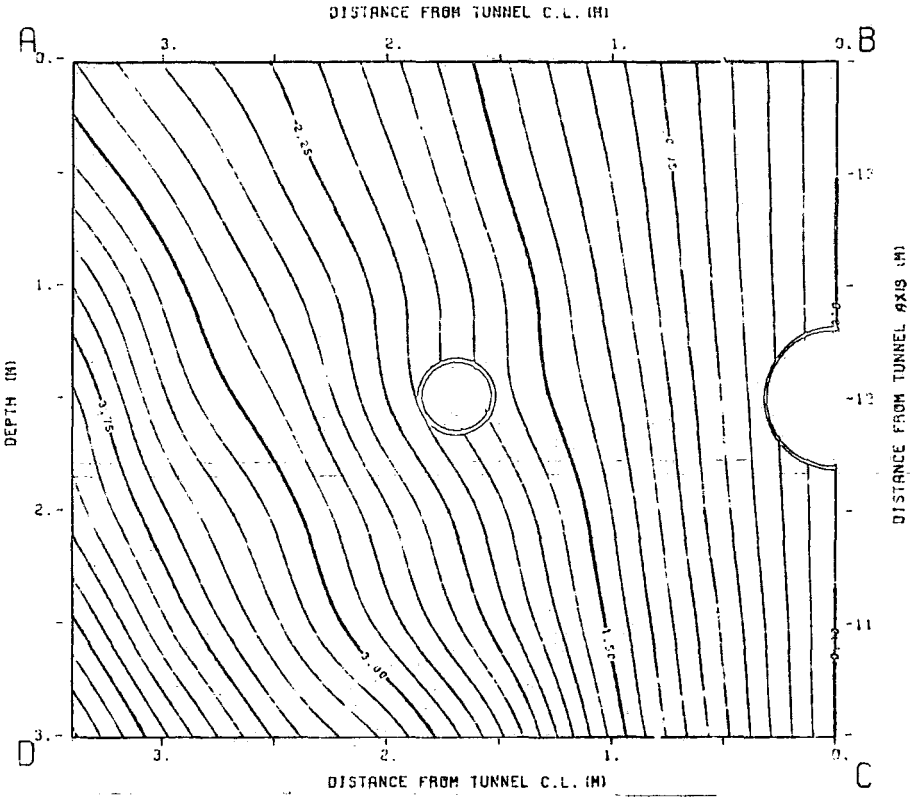

FIG. 7.4.3) Contours of equal lateral displacements (mm). Transverse section 1.5i behind tunnel face. (MESH 2 - Pipes A' & B').

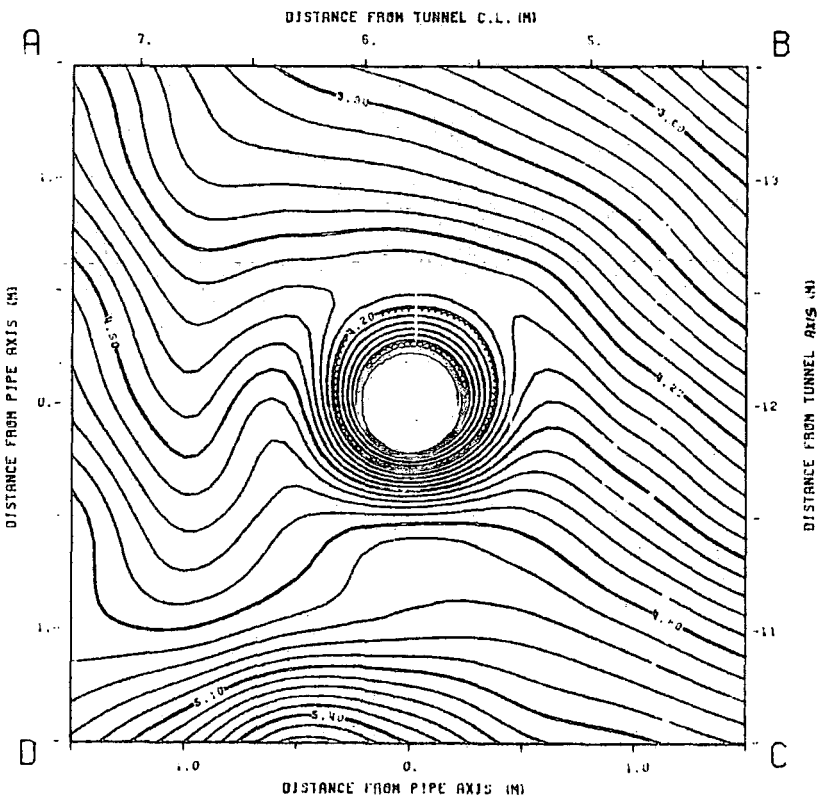

FIG. 7.4.4) Contours of equal lateral displacements (mm). Transverse section 1.5i behind tunnel face. (MESH 3 - Pipe C').

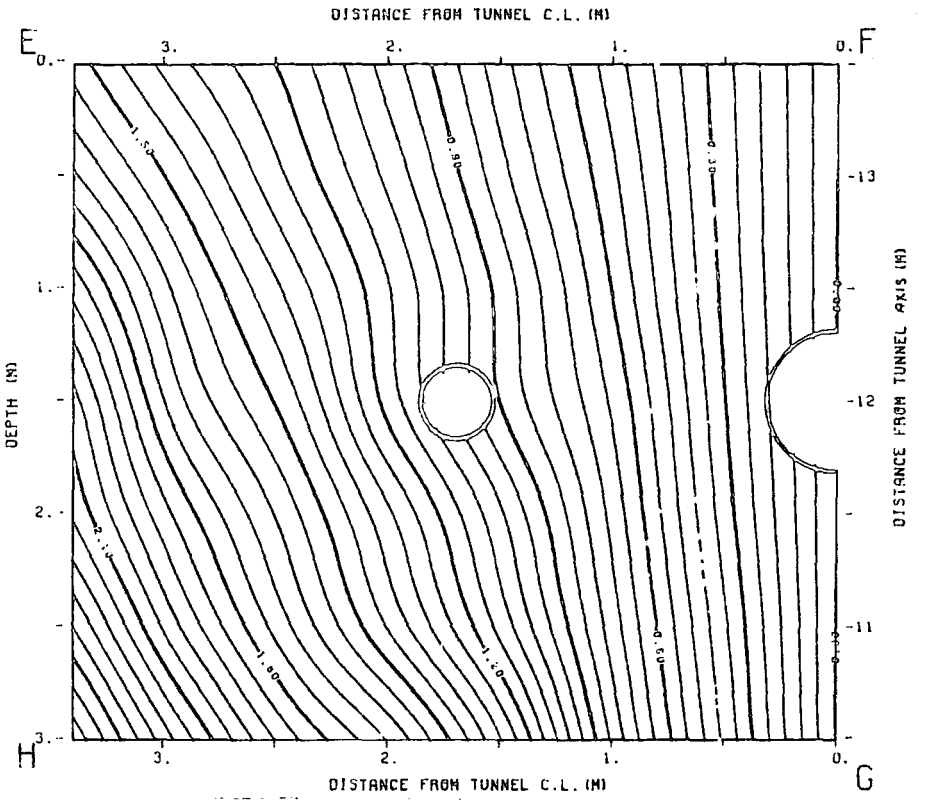

FIG. 7.4.5) Contours of equal lateral displacements (mm). Transverse section at tunnel face. (MESH 2 - Pipes A' & B').

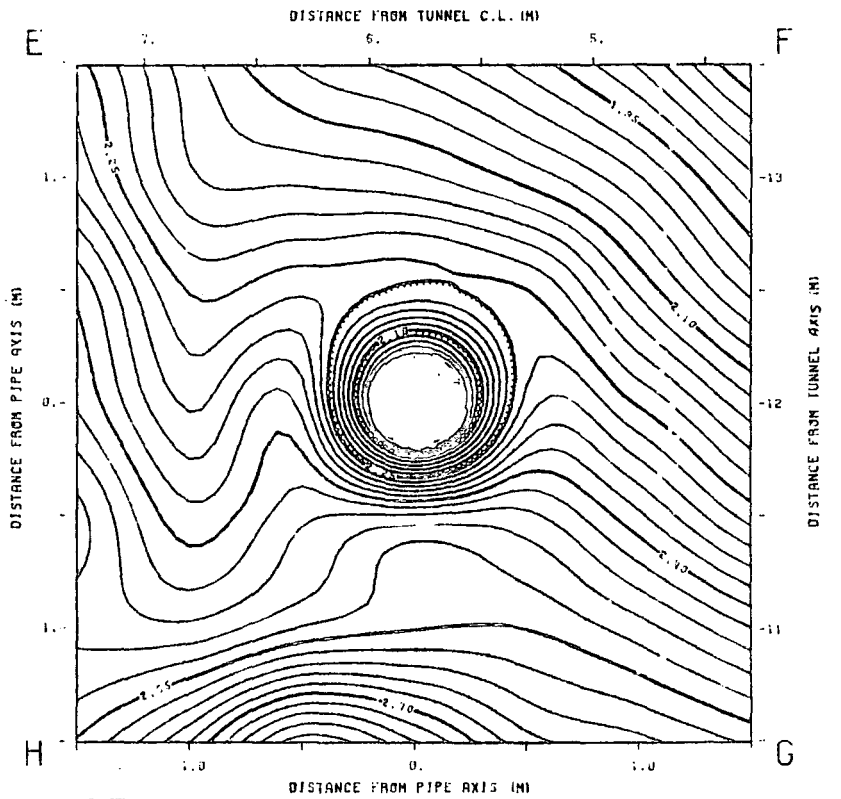

FIG. 7.4.6) Contours of equal lateral displacements (mm). Transverse section at tunnel face. (MESH 3 - Pipe C').

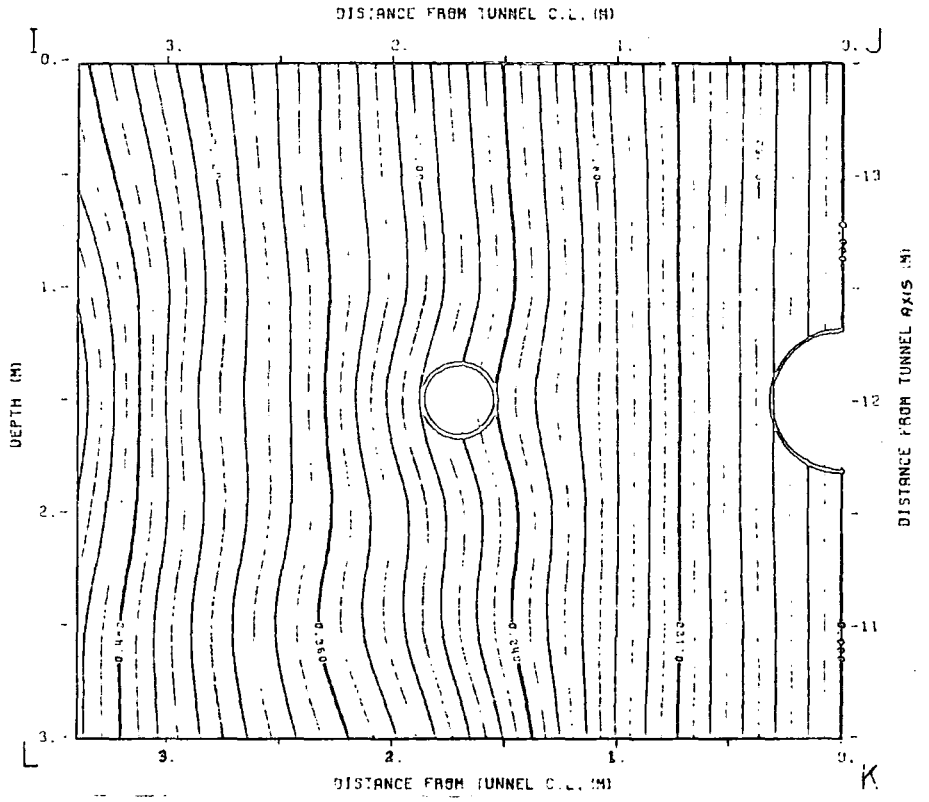

FIG. 7.4.7) Contours of equal lateral displacements (mm). Transverse section i behind tunnel face. (MESH 2 - Pipes A' & B').

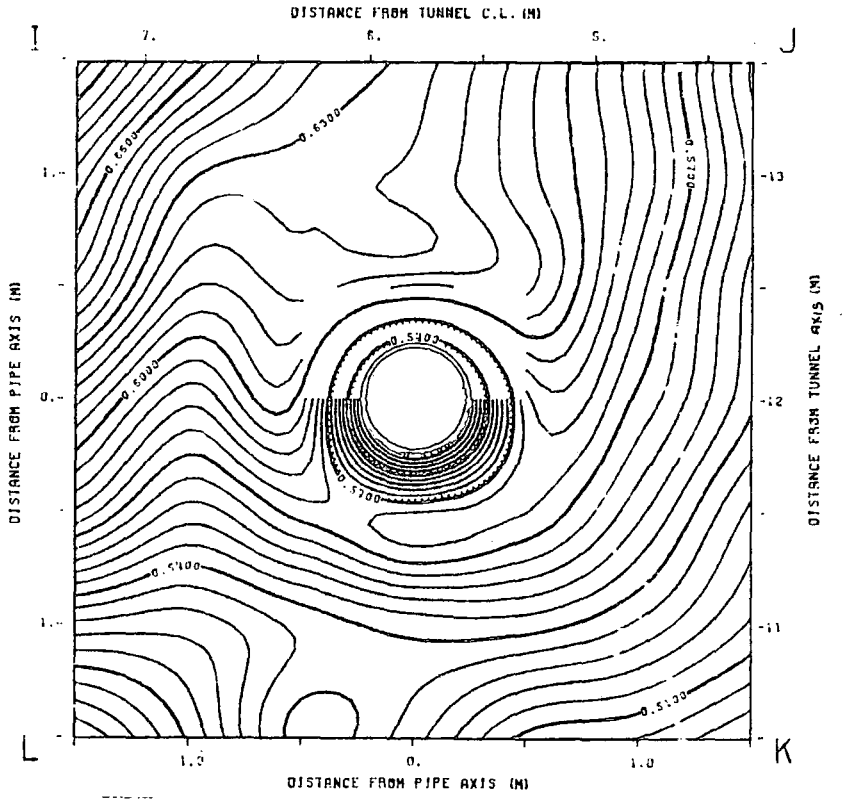

FIG. 7.4.8) Contours of equal lateral displacements (mm). Transverse section i behind tunnel face. (MESH 3 - Pipe C').

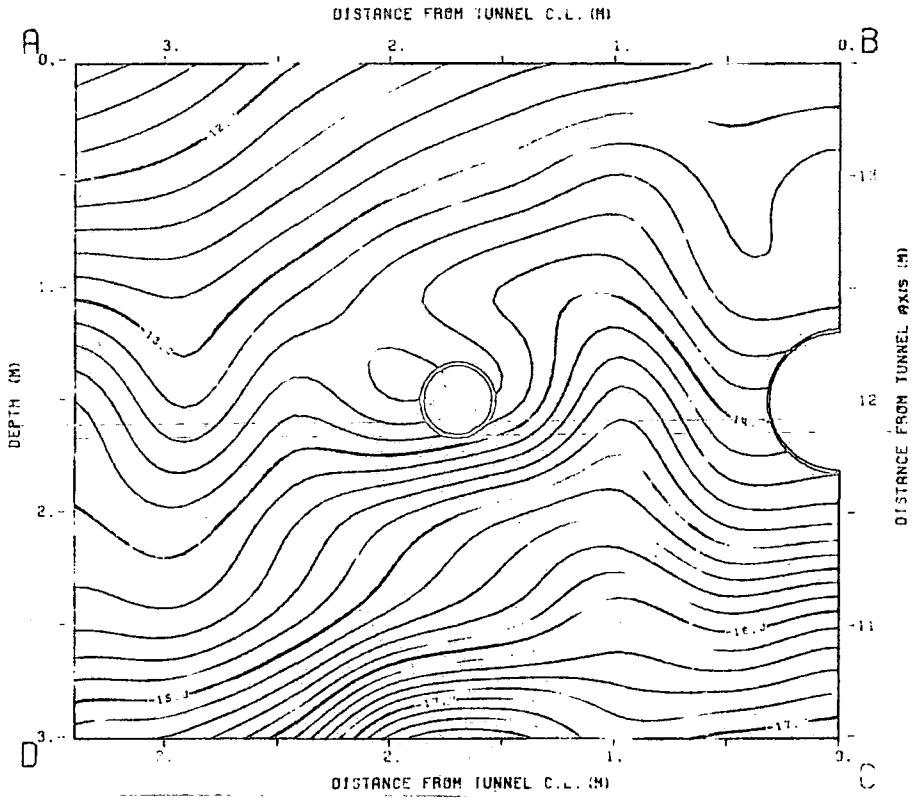

FIG. 7.4.9) Contours of equal vertical displacements (mm). Transverse section 1.5i behind tunnel face. (MESH 2 - Pipes A' & B').

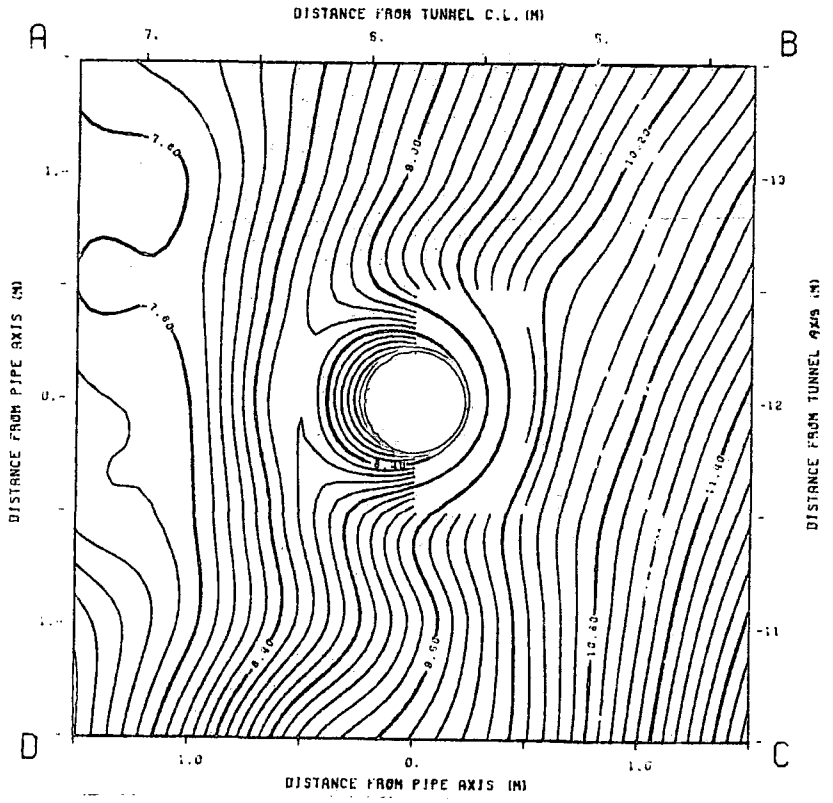

FIG. 7.4.10) Contours of equal vertical displacements (mm). Transverse section 1.5i behind tunnel face. (MESH 3 - Pipe C').

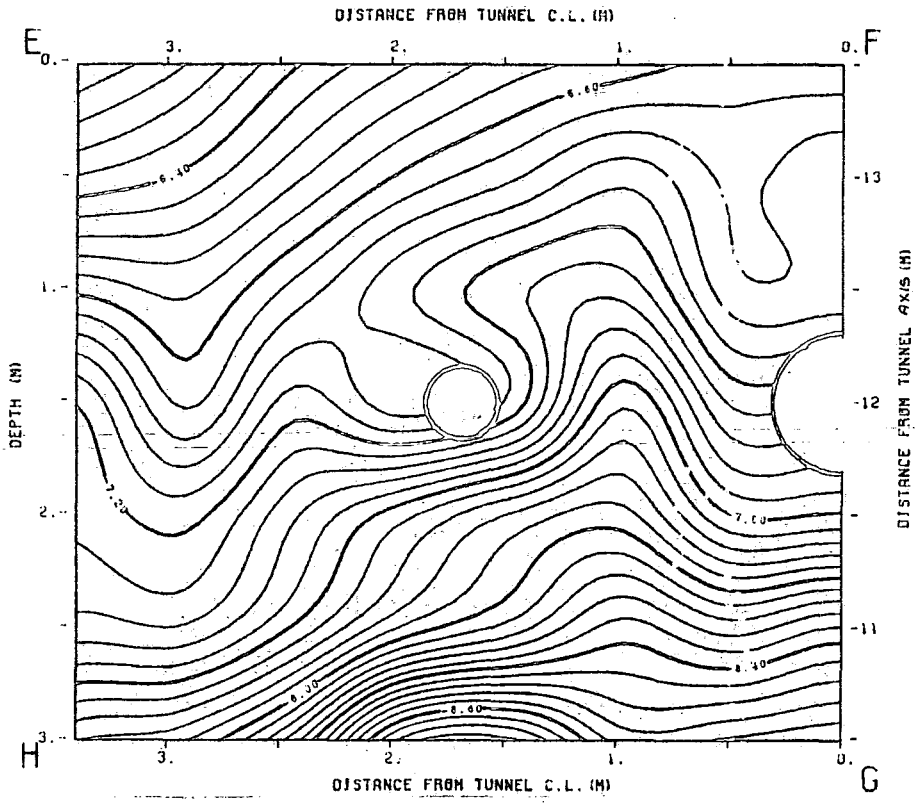

FIG. 7.4.11) Contours of equal vertical displacements (mm). Transverse section at tunnel face. (MESH 2 - Pipes A' & B').

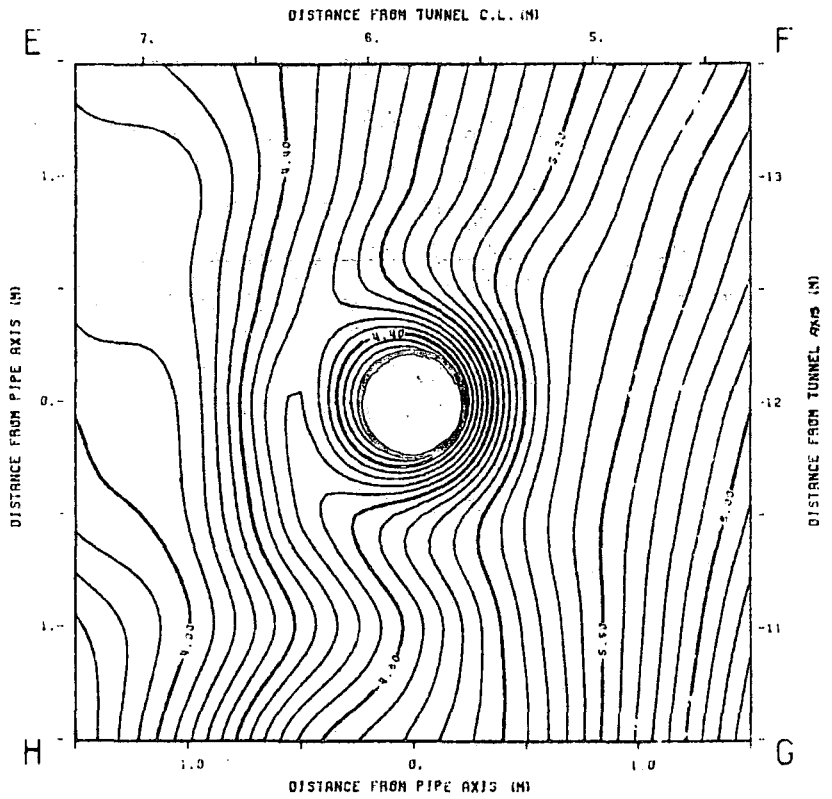

FIG. 7.4.12) Contours of equal vertical displacements (mm). Transverse section at tunnel face. (MESH 3 - Pipe C').

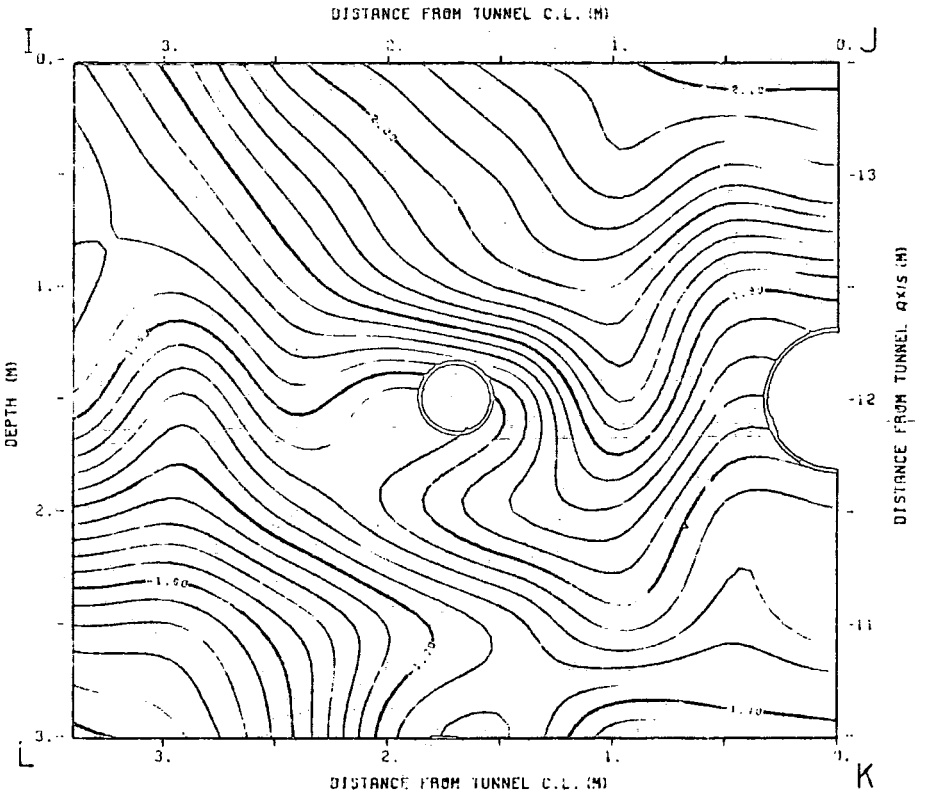

FIG. 7.4.13) Contours of equal vertical displacements (mm). Transverse section i ahead tunnel face. (MESH 2 - Pipes A' & B').

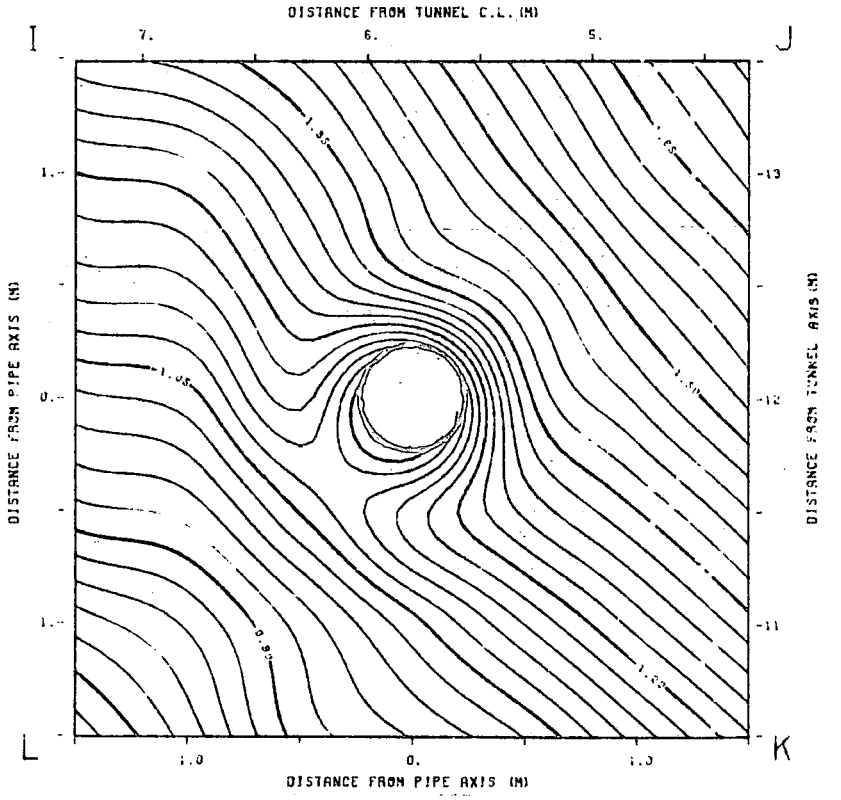

FIG. 7.4.14) Contours of equal vertical displacements (mm). Transverse section i ahead tunnel face. (MESH 3 - Pipe C').

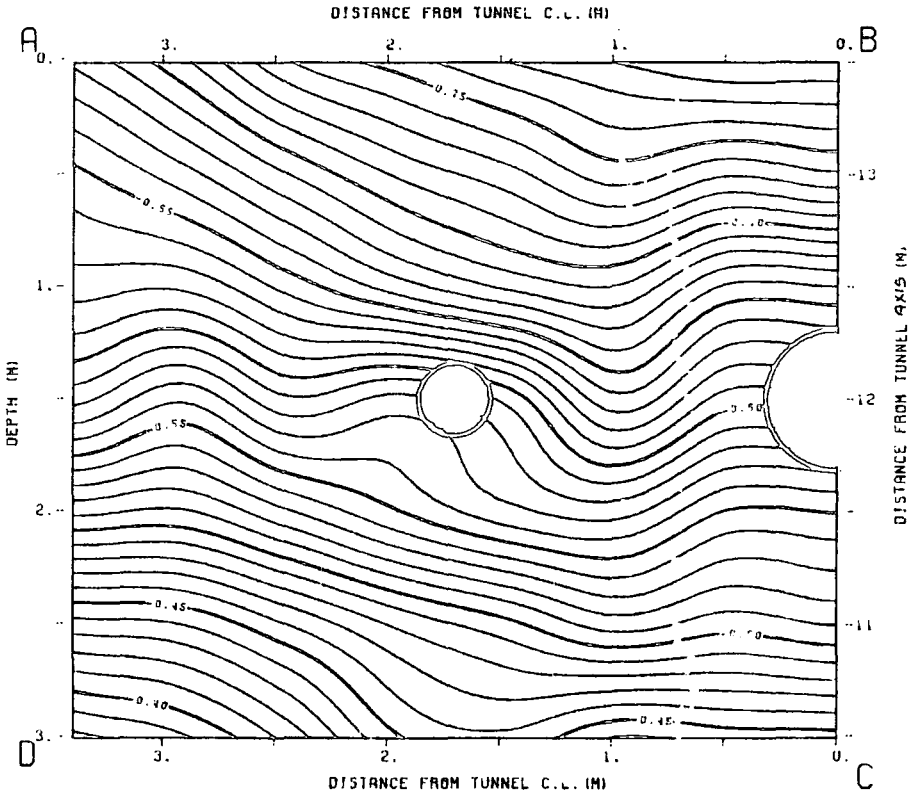

FIG. 7.4.15) Contours of equal longitudinal displacements (mm). Transverse section 1.5i behind tunnel face. (MESH 2 - Pipes A' & B').

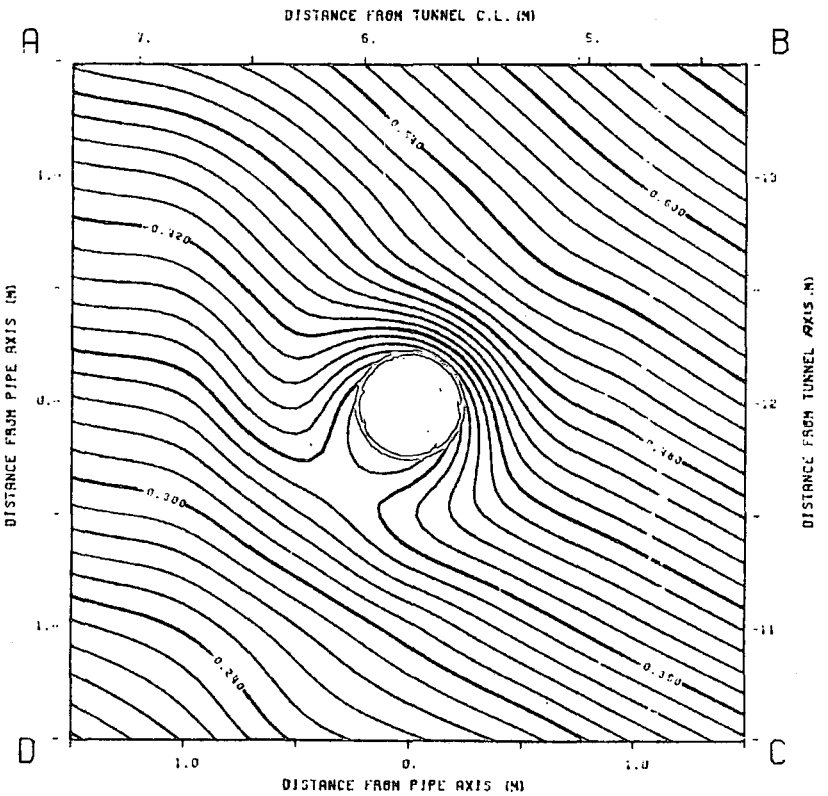

FIG. 7.4.16) Contours of equal longitudinal displacements (mm). Transverse section 1.5i behind tunnel face. (MESH 3 - Pipe C').

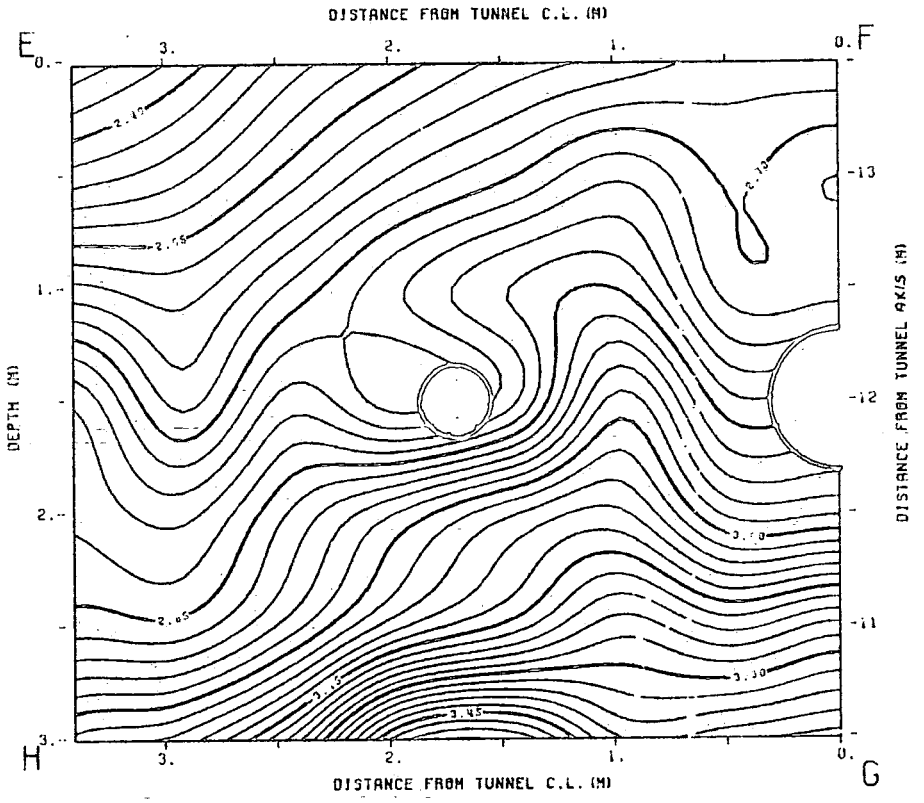

FIG. 7.4.17) Contours of equal longitudinal displacements (mm). Transverse section at tunnel face. (MESH 2 - Pipes A' & B').

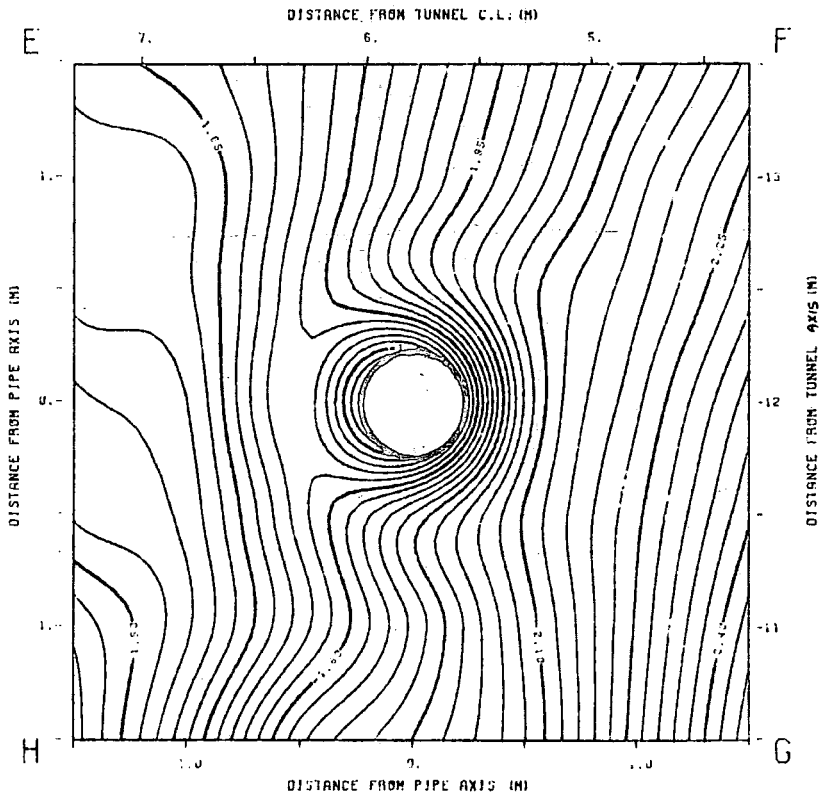

FIG. 7.4.18) Contours of equal longitudinal displacements (mm). Transverse section at tunnel face. (MESH 3 - Pipe C').

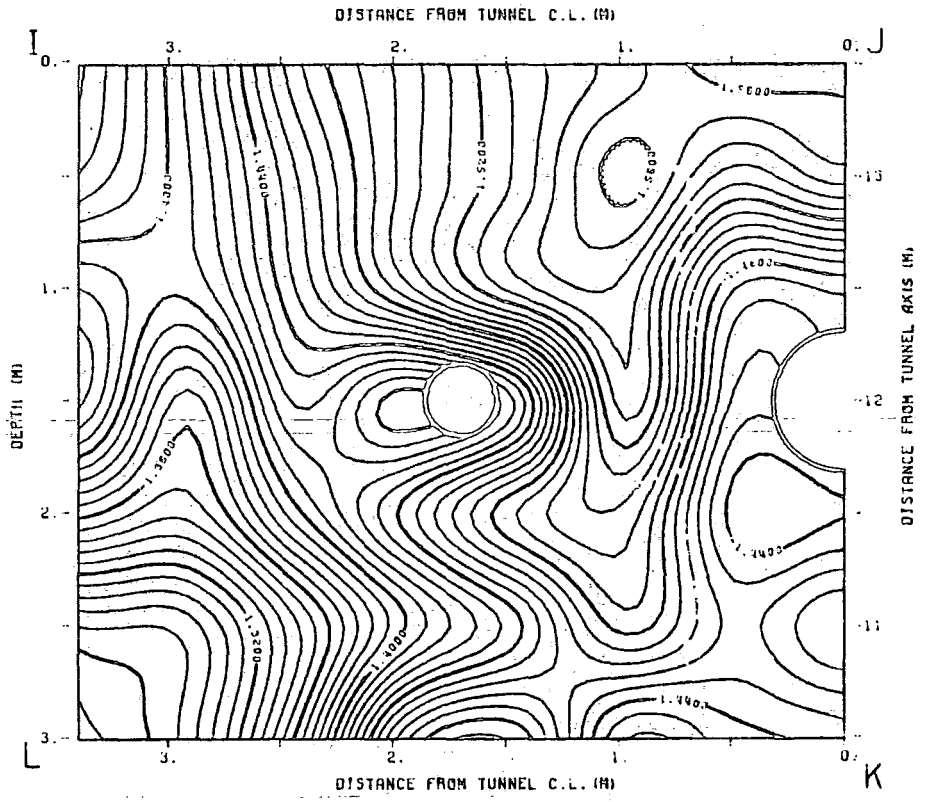

FIG. 7.4.19) Contours of equal longitudinal displacements (mm). Transverse section i ahead tunnel face. (MESH 2 - Pipes A' & B').

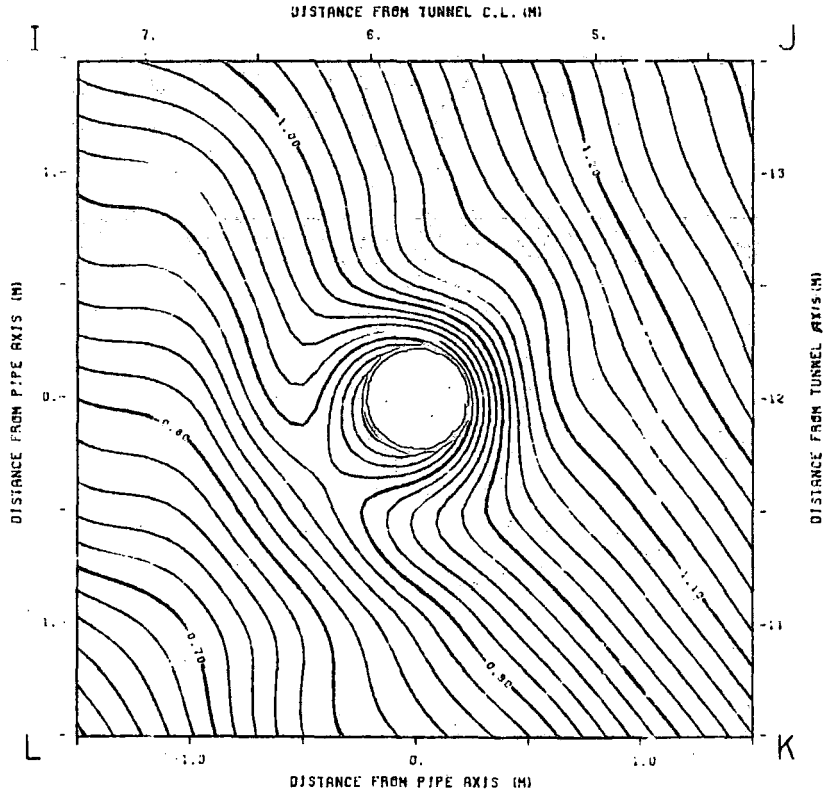

FIG. 7.4.20) Contours of equal longitudinal displacements (mm). Transverse section i ahead tunnel face. (MESH 3 - Pipe C').

7.5 SIMULATION OF AN ADVANCING EXCAVATION FACE AND LINING INSTALLATION.

7.5.1 INTRODUCTION.

This example is concerned with the three-dimensional finite element simulation of the short-term effects that develop when a tunnel is driven in a soft ground and a lining is installed.

The excavation process is simulated by applying seven sequences (or steps) of load increment, which values are obtained as outlined in Section 4.3. The element stiffness matrices are calculated accordingly and assembled into the global stiffness matrix as described in Section 4.2. Again, all three pipes lying parallel to the tunnel centre line are assumed not be present in the analysis.

The presence of an unsupported zone between the face of the excavation and the leading edge of the lining is considered. The length of this unsupported zone is assumed to be equal to half of the inflexion distance, i, (3.375 m) for this particular tunnel depth configuration. The concrete lining is assumed to be monolithic, so this

does not strictly replicate the actual concrete segmental lining which does permit slight articulation about the longitudinal joints. Such articulation tends to shed a little vertical load and mobilize a little horizontal load, thereby creating a more uniform radial stress distribution in the immediate vicinity of the tunnel extrados. Clearly, this effect is not replicated under the present modelling conditions.

The first step of the analysis consists of calculating stresses and deformations in the medium without the presence of a lining. In the following steps of the simulation process (or loading increment) the lining is considered in the manner outlined in Section 4.5.

The geometry of the idealized medium and soil properties (Figure 6.4), the finite element mesh (Figure 7.3.1), the ground surface and the longitudinal section (Figure 7.2.3) used in this analysis are same as those used in the example presented in Section 7.2.

Young's modulus for the concrete lining was taken to be equal to 1.4×10^3 MN/m^2, obtained by using the equivalent stiffness approach (see Section 6.6).

7.5.2 RESULTS.

Although a large number of output results has been obtained, only those results considered to be particularly important are presented for selected surfaces.

Components of displacement and normal strain, calculated in steps 3, 5 and 7 for the ground surface (plane MNOP) and longitudinal section (plane OPQR), are shown in Figures 7.5.1 to 7.5.3, inclusive. Typical variations of three components of displacement and strain, calculated between two consecutive steps, are shown in Figures 7.5.34 through 7.5.44. These results correspond to those obtained between steps 4 and 5. Before plotting them, each of the variables was multiplied by 1000 to make the results suitable for use as input data for the GPCP package program. Thus, the note on the Figure captions '(10^{-3} mm)' and '(10^{-3} %)' is an intruction to the reader to multiply each contour value by that number.

7.5.2.1) DISPLACEMENTS.

All the Figures presented in this example show clearly that the ground disturbance wave follows the tunnel face advance concordantly.

The maximum lateral displacement on the ground surface located behind the tunnel face, and 1.5i from the tunnel centre line, is shown in Figures 7.5.1 to 7.5.3. Figure 7.5.1 shows that no lateral movement takes place on the ground surface for distances greater than 3.5i ahead of tunnel face.

Contours of equal vertical movements on the ground surface, shown in Figures 7.5.4 to 7.5.12, indicate that the maximum vertical displacement is located above the tunnel centre line and approximately 3i behind the tunnel face. From Figures 7.5.4, 7.5.5 and 7.5.6 the vertical displacements may be considered negligible for the soil mass 2i ahead of tunnel face; they may also be considered negligible for the soil mass located beyond the line 3.5i parallel to the centre line.

The vertical movement on the ground surface and above the tunnel face is less than 50% of the maximum settlement (Figures 7.2.13, 7.2.14 and 7.2.15). The point above the tunnel centre line showing 50% of the maximum settlement is located approximately i/2 behind the tunnel face.

The ground surface affected by the tunnelling process moves longitudinally in the opposite direction to

that of tunnel advance, and its maximum value occurs behind the tunnel face (see Figures 7.5.7, 7.5.8 and 7.5.9).

Figures 7.5.10, 7.5.11 and 7.5.12 show that there is no significant vertical movement in the soil region below the tunnel axis and ahead of the tunnel face.

Figures 7.3.7, 7.3.8 and 7.3.9 related to ground surface movements have shown that the boundary conditions adopted for the present analysis strongly influence the longitudinal displacements calculated for nodal points located on the edge of the finite element mesh behind the tunnel face. This effect may arise from the installation of the lining which replaces the removed soil with much stiffer material than existed previously.

The longitudinal movement distribution on section OPQR is shown in Figures 7.5.13 to 7.5.15. These Figures indicate that the magnitude and distribution of longitudinal displacements in the soil region located above the tunnel centre line and between vertical lines i behind and 2i ahead of tunnel face are similar for steps 3, 5 and 7. These Figures also show the distinct behaviour of the ground close to the tunnel face. At the tunnel axis level, results have shown that the soil moves

forward while the soil above and below the face moves backwards. This behaviour may be caused by the assumption made in the analysis that the soil is incompressible, and, perhaps, by numerical instability (too-small displacements in front of the tunnel face) caused by excessive distortion of the elements used to model the tunnel.

7.5.2.2) STRAINS.

Contours of lateral strains on the ground surface, plotted in Figures 7.5.16 through 7.5.18, have shown that the boundary line between compressive and tensile strains runs parallel to and 1.5i from the centre line with the tunnel face advance. The strong influence of mesh boundary conditions can also be observed on the edge opposite to the longitudinal section OPQR.

Vertical strains on the ground surface, as calculated in steps 3, 5 and 7, have been plotted in Figures 7.5.19, 7.5.20 and 7.5.21, respectively. The distribution of vertical strains ahead of tunnel face is similar for all three steps. Basic differences in contour configurations between these Figures is to be found behind the tunnel face and close to the tunnel centre line. As the face advances, contours of equal vertical strains tend to become parallel to the tunnel centre line. If the

maximum vertical strain is assumed to be equal to 0.0004%, taken from Figures 7.5.20 or 7.5.21, this maximum tensile vertical strain has already been developed in step 3 (Figure 7.5.19).

Figures 7.5.19 to 7.5.21 also show that the vertical strain on the ground surface over the tunnel face is compressive and smaller than 50% of the maximum compressive strain.

Longitudinal strains on the ground surface are shown in Figures 7.5.22 to 7.5.24. The effect of mesh boundary conditions on these strains is strong, particularly on the edge of the mesh towards which the tunnel face is advancing (Figure 7.5.24).

Figures 7.5.25 to 7.5.27 show the lateral strains developed on longitudinal section OPQR. In these Figures lateral strains on large areas are compressive and the magnitude of these strains is not significant for soil regions ahead of the tunnel face. It is also demonstrated that contours of equal strain become parallel to the tunnel centre line with the face advance.

From Figures 7.5.19 and 7.5.21, it can be observed that the maximum vertical strain has already been

maximum vertical strain is assumed to be equal to 0.0004%, taken from Figures 7.5.20 or 7.5.21, this maximum tensile vertical strain has already been developed in step 3 (Figure 7.5.19).

Figures 7.5.19 to 7.5.21 also show that the vertical strain on the ground surface over the tunnel face is compressive and smaller than 50% of the maximum compressive strain.

Longitudinal strains on the ground surface are shown in Figures 7.5.22 to 7.5.24. The effect of mesh boundary conditions on these strains is strong, particularly on the edge of the mesh towards which the tunnel face is advancing (Figure 7.5.24).

Figures 7.5.25 to 7.5.27 show the lateral strains developed on longitudinal section OPQR. In these Figures lateral strains on large areas are compressive and the magnitude of these strains is not significant for soil regions ahead of the tunnel face. It is also demonstrated that contours of equal strain become parallel to the tunnel centre line with the face advance.

From Figures 7.5.19 and 7.5.21, it can be observed that the maximum vertical strain has already been

developed on the ground surface for increment 3, and little change take place in the soil mass behind the point of maximum strain as a result of subsequent load increments. Similar behaviour can be observed on the longitudinal section OPQR, as shown in Figures 7.5.28 to 7.5.30.

With respect to longitudinal strains on the ground surface, the strong influence of boundary conditions on edges MP, MN and ON can be perceived in Figures 7.5.22 to 7.5.24. However, the distribution contour of longitudinal strains around the tunnel face, say between -i and i on both sides of the face, presents a constant shape and follows the tunnel face advance.

Contours of longitudinal strain on longitudinal section OPQR (Figures 7.5.31 to 7.5.33) show that the line (surface) separating compressive and tensile strain passes close to the tunnel face. Generally, the longitudinal strains behind this line are compressive and ahead of it are tensile, except in a small portion of the soil mass located approximately at the tunnel axis level and i ahead of the tunnel face. This ground response can be observed in all three Figures.

Figures 7.5.34 to 7.5.44 show the three components

of displacement and strain on ground surface section MNOP and longitudinal section OPQR. The values plotted in these Figures were calculated for a single load increment, and correspond to those obtained between the 4th and 5th steps as mentioned earlier. Values shown in these Figures represent typical variations of displacement and strain, which values are added to those calculated in previous steps.

7.6 GENERAL DISCUSSION.

This Section considers, in a general way, the information obtained from the examples presented in the present Chapter. Difficulties faced during development of this work, together with limitations and advantages of the approaches used will be discussed in general terms in the following paragraphs.

The finite element method which was used in all four examples discussed above, should replicate, with adequate precision, the field prototype situation. The quality of this replication can only be checked through comparison of the finite element results with measurements on site. With any real problem, the input data are not usually available in their entirety, and the missing data have to be estimated.

In practice, any appraisal of calculated results is made by comparison with measured data available for only a few points (limited areas). Although complete and precise measured data are not always available, judgement of the computed model output is necessarily augmented by input engineering experience. If the results of the modelling do not coincide with those expected, the mechanical laws are modified empirically. This much-used and popular method may not always be academically legitimate, but is often apparently unavoidable.

The results obtained by the finite element calculations are subject to certain limitations because the geometry and the material properties in the model remain the same along the longitudinal direction. This will rarely be the case in practice. Therefore, in view of a lack of ideal conditions for computer calculations, the author believes that the use of such a representation is (must be) satisfactory as a first approximation.

The method of combining structure and soil as one unit has been shown to provide some answers for some particular factors involved in the analysis. But the major advantage of the approach used in this work is its flexibility in being able to analyse practical problems without needing to make assumptions far from the usual

practice in finite element calculations such as for loading, material properties, structural shape, and so on.

The examples presented above have been chosen to illustrate a few of the many tunnelling process and soil-pipe interaction problems that occur in practice. There are other processes that could be modelled using the system developed by the writer.

Although a simple form of pipeline has been studied (the presence and effect of joints, for example, have not been considered), the response of a pipe to the ground movement is clearly a complex problem, particularly if related to the tunnelling process, which itself generates numerous ground response complexities. It is obvious that if such complex behaviour has to be understood, detailed field measurements for the acquisition of suitable input parameter values and also for checking model conclusions must be considered essential.

The effectiveness of any finite element analysis, and particularly any three-dimensional analysis, may not be considered by some tunnel designers to be particularly useful in view of the high cost and time required to prepare input data, conduct analyses and interpret

results, when compared with other numerical methods. These designers are correct if only the preliminary design stage is considered. However, the cases analysed and presented in this work provide examples of problems in which finite element analysis can be used effectively. In other cases, for example if the non-linear behaviour of soil and if more complex excavation and support installation sequences are simulated, the cost would obviously be higher. But, in the present author's opinion, the costs of these analyses will not be generally prohibitive, especially if compared to the total cost of the tunnelling project.

A combined (hybrid) analytical and numerical (finite element) approach for studying the effect of ground movements caused by tunnelling on buried pipeline has been described. This technique was used because field data for the site used in the analysis were not available at the time of development of this work and also in view of the difficulties of modelling an entire region of interest in a single finite element mesh. In view of the difficulties associated with predicting ground movements in the context of soil/pipe interaction in a realistic manner, it was thought that the simpliest initial method of predicting the ground movements involved the use of the now-accepted normal probability approach.

An 'equivalent stiffness' approach has also been described and used in this work. The reason for using this procedure lies in the fact that excessively distorted and stiff (representing pipes) elements coupled with much softer (representing soil) elements induce numerical instability during computations.

In the case where the tunnel excavation was simulated without lining installation, and without modelling the pipes in the mesh, the vertical displacements calculated by the empirical approach formed the basis of comparison with the finite element results. The normal probability method was also used to generate the displacement input data as outlined in Section 6.7.

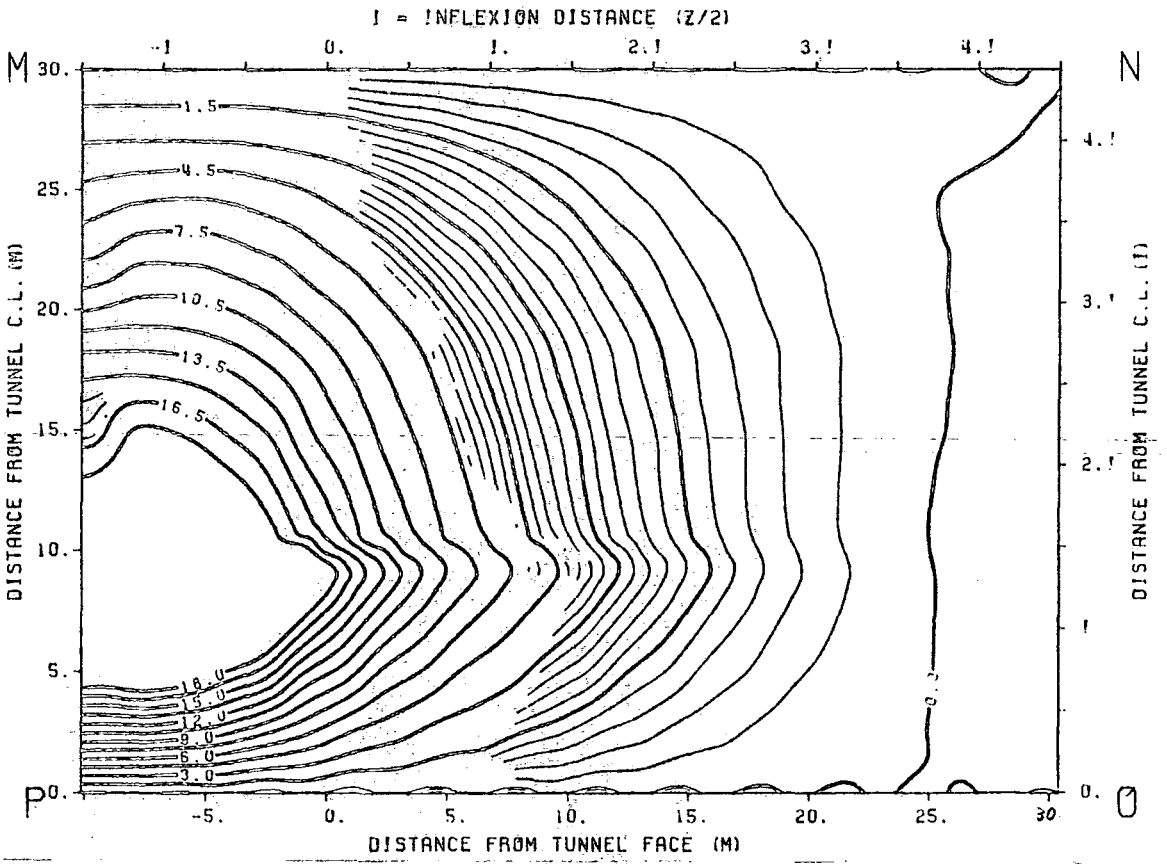

FIG. 7.5.1) Contours of equal lateral displacements (10^{-3}mm). Ground surface. Step 3.

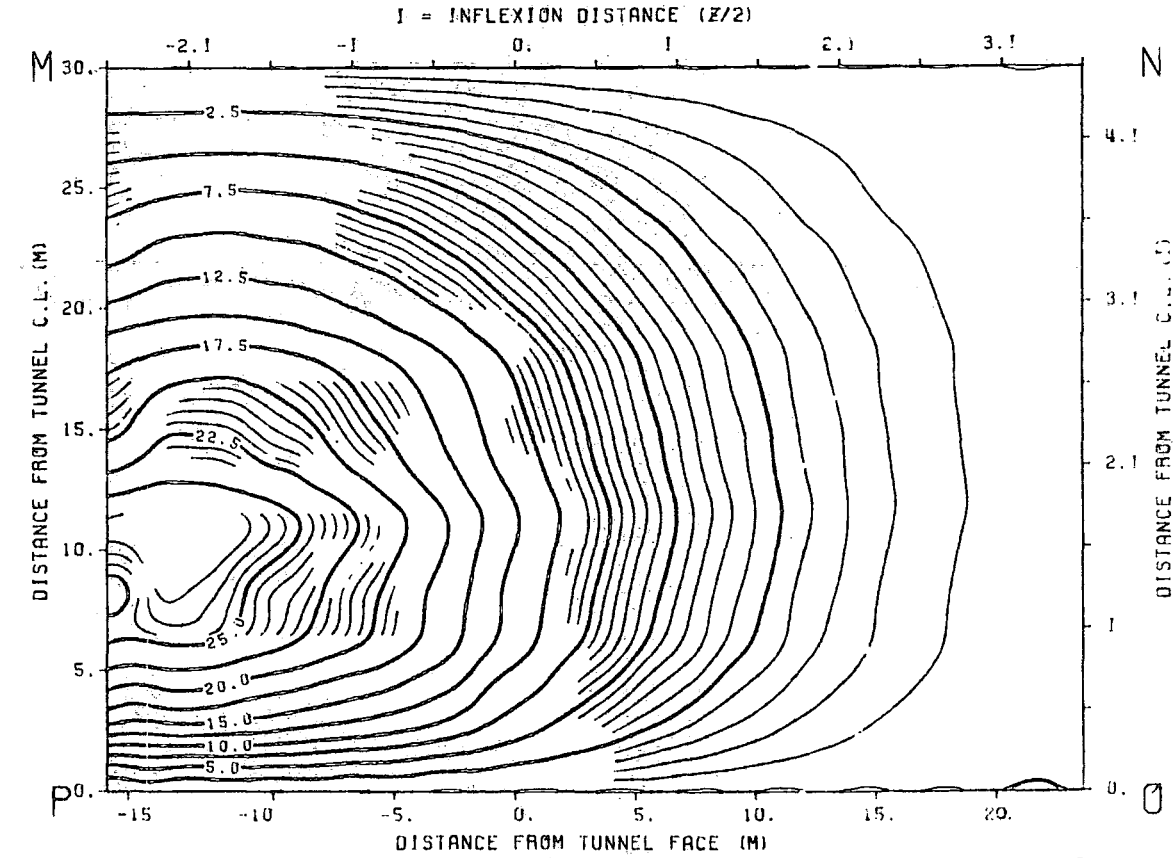

FIG. 7.5.2) Contours of equal lateral displacements (10^{-3}mm). Ground surface. Step 5.

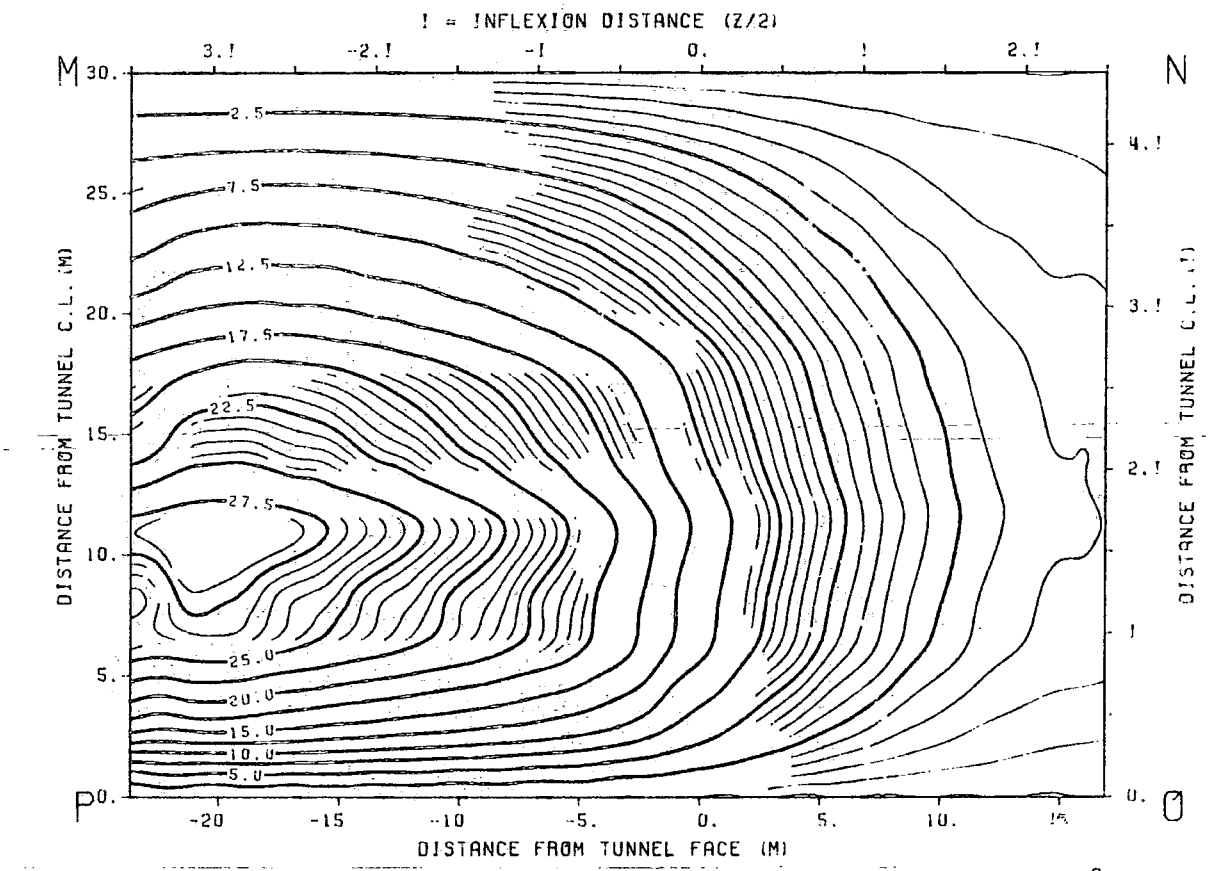

FIG. 7.5.3) Contours of equal lateral displacements (10^{-3}mm). Ground surface. Step 7.

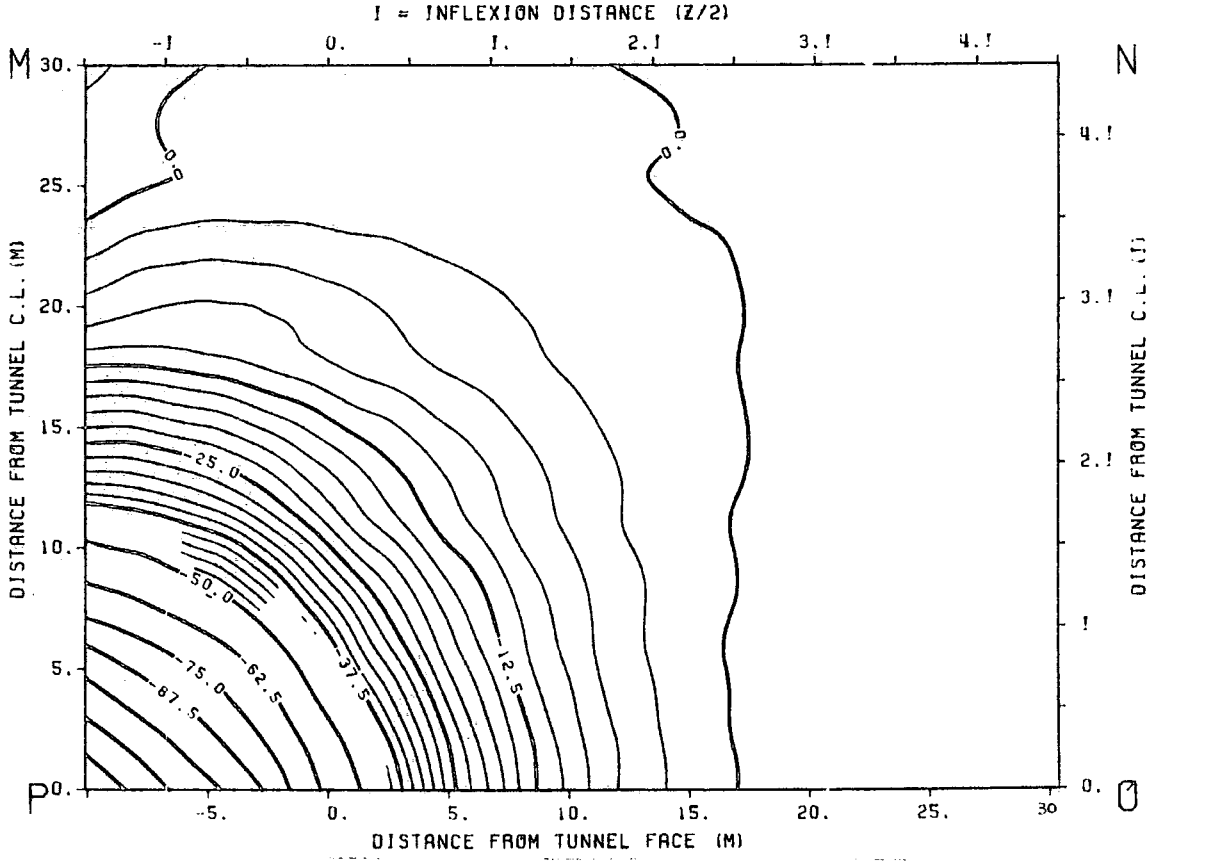

FIG. 7.5.4) Contours of equal vertical displacements (10^{-3}mm). Ground surface. Step 3.

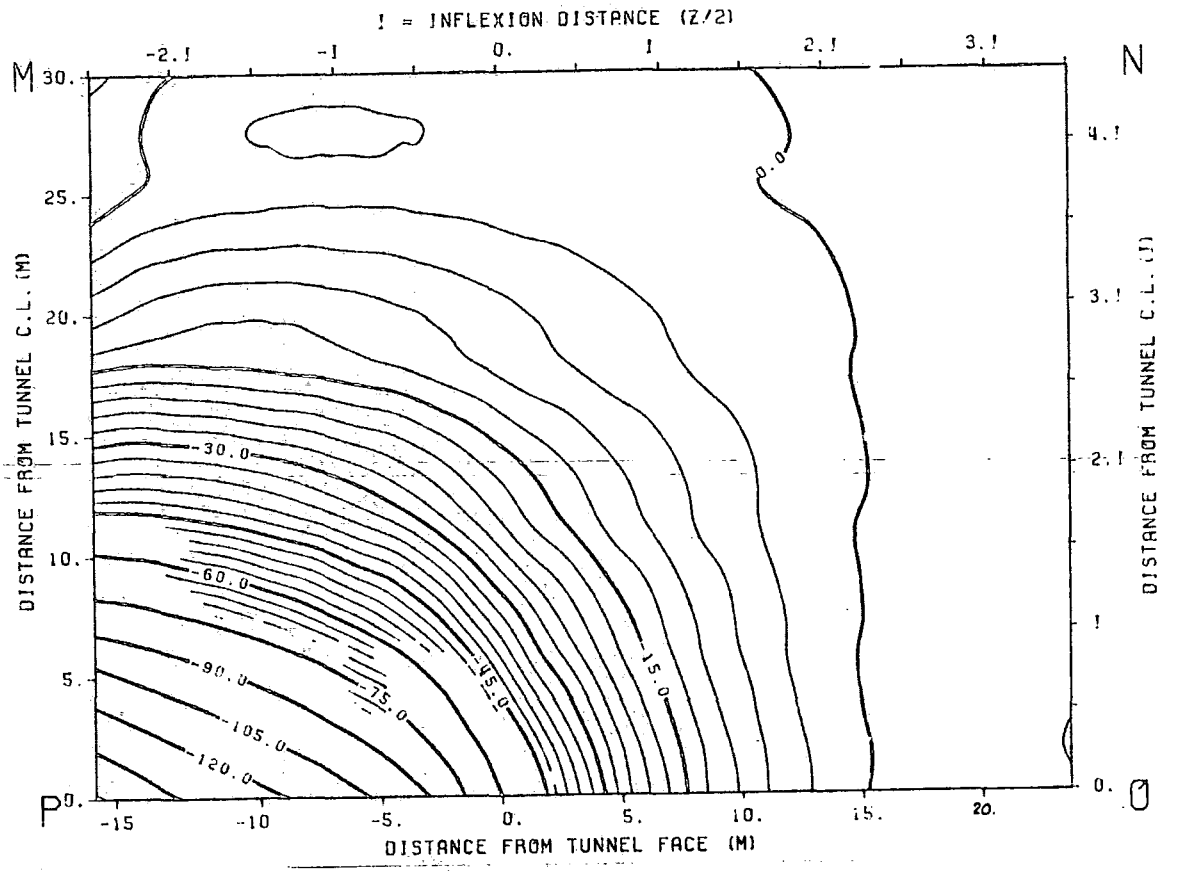

FIG. 7.5.5) Contours of equal vertical displacements (10^{-3} mm). Ground surface. Step 5.

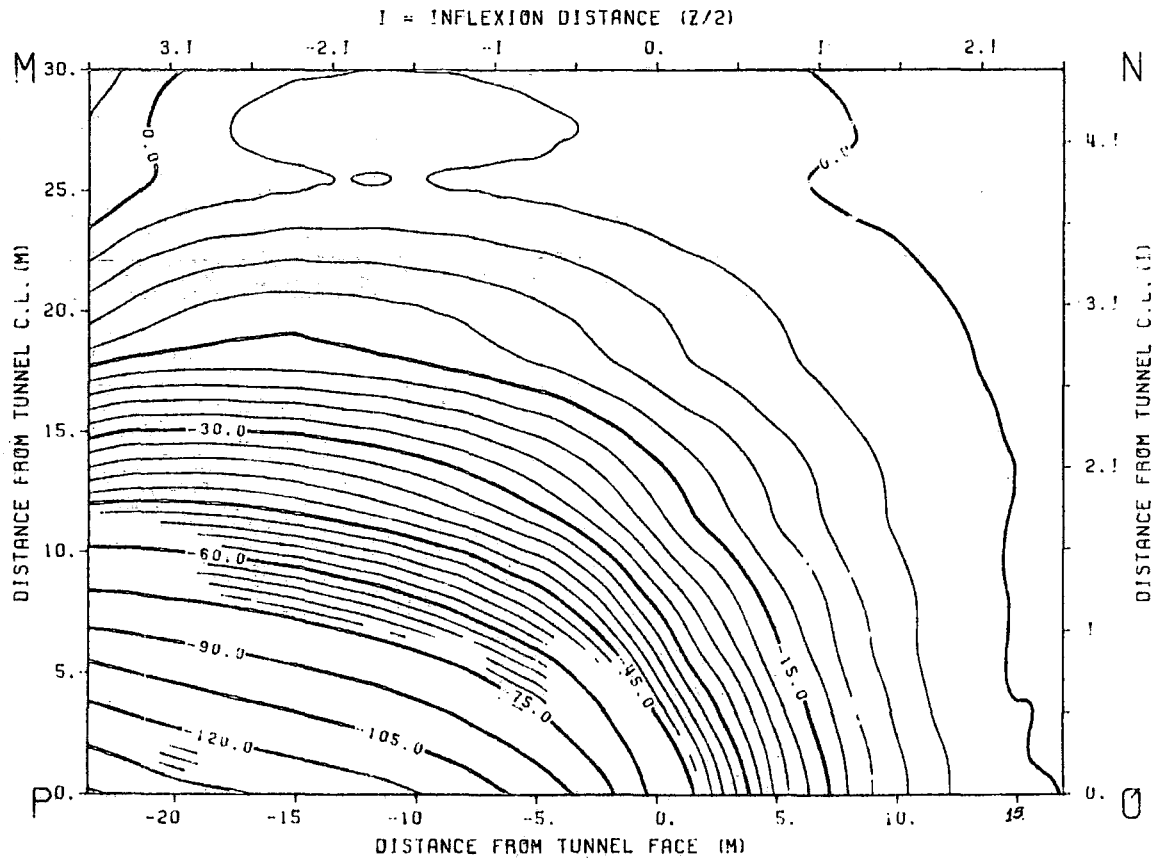

FIG. 7.5.6) Contours of equal vertical displacements (10^{-3} mm). Ground surface. Step 7.

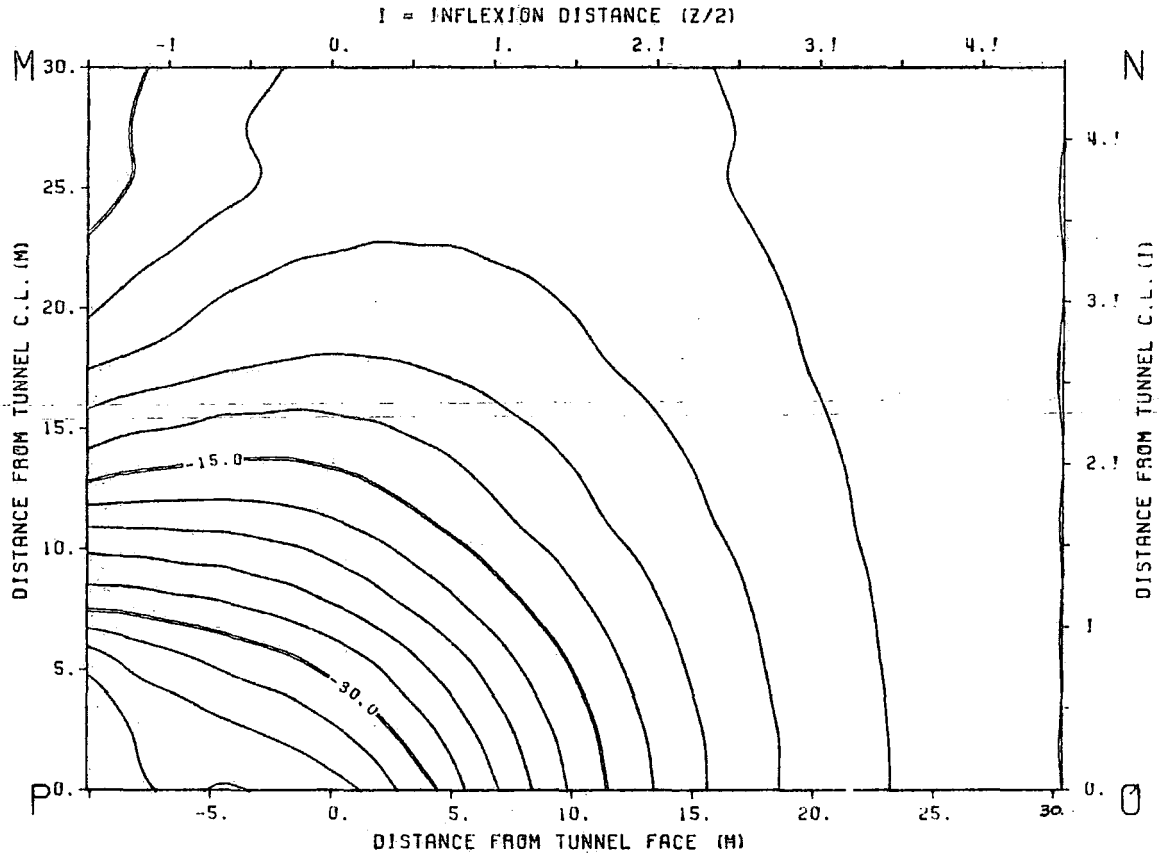

FIG. 7.5.7) Contours of equal longitudinal displacements (10^{-3} mm). Ground surface. Step 3.

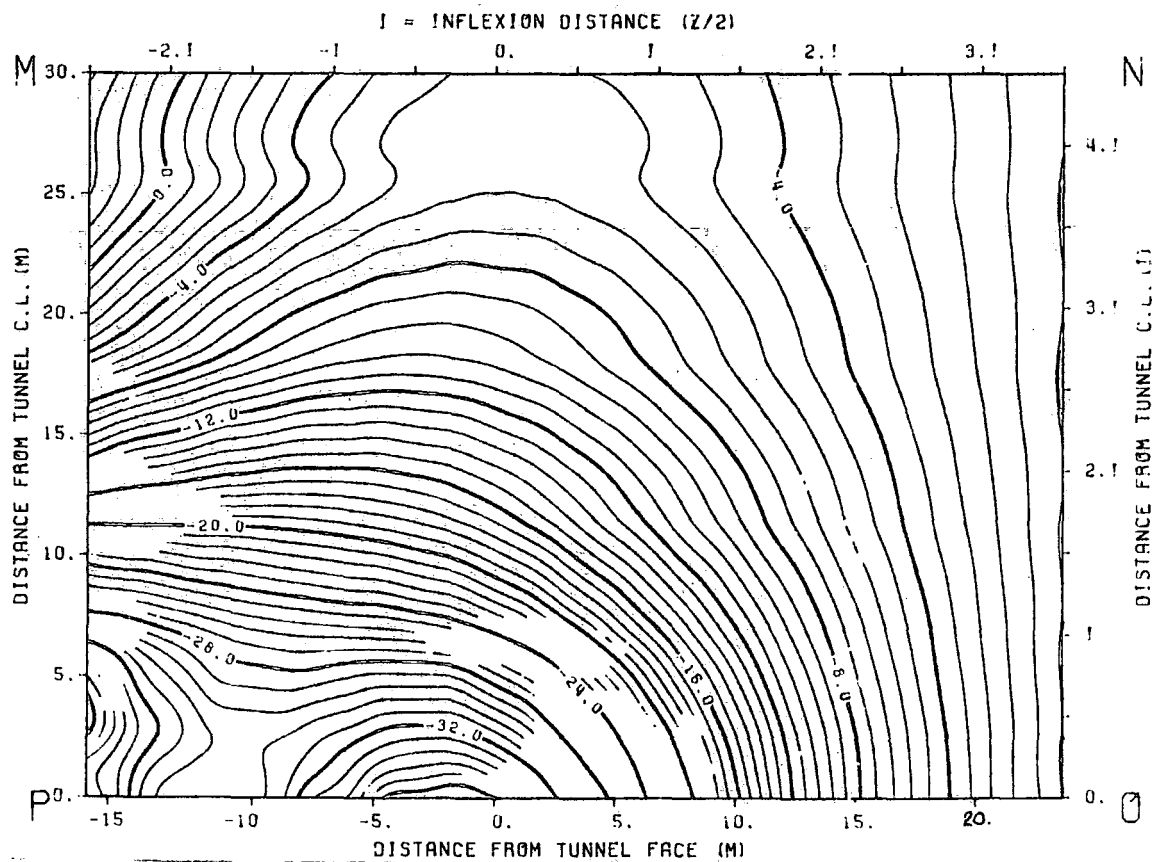

FIG. 7.5.8) Contours of equal longitudinal displacements (10^{-3} mm). Ground surface. Step 5.

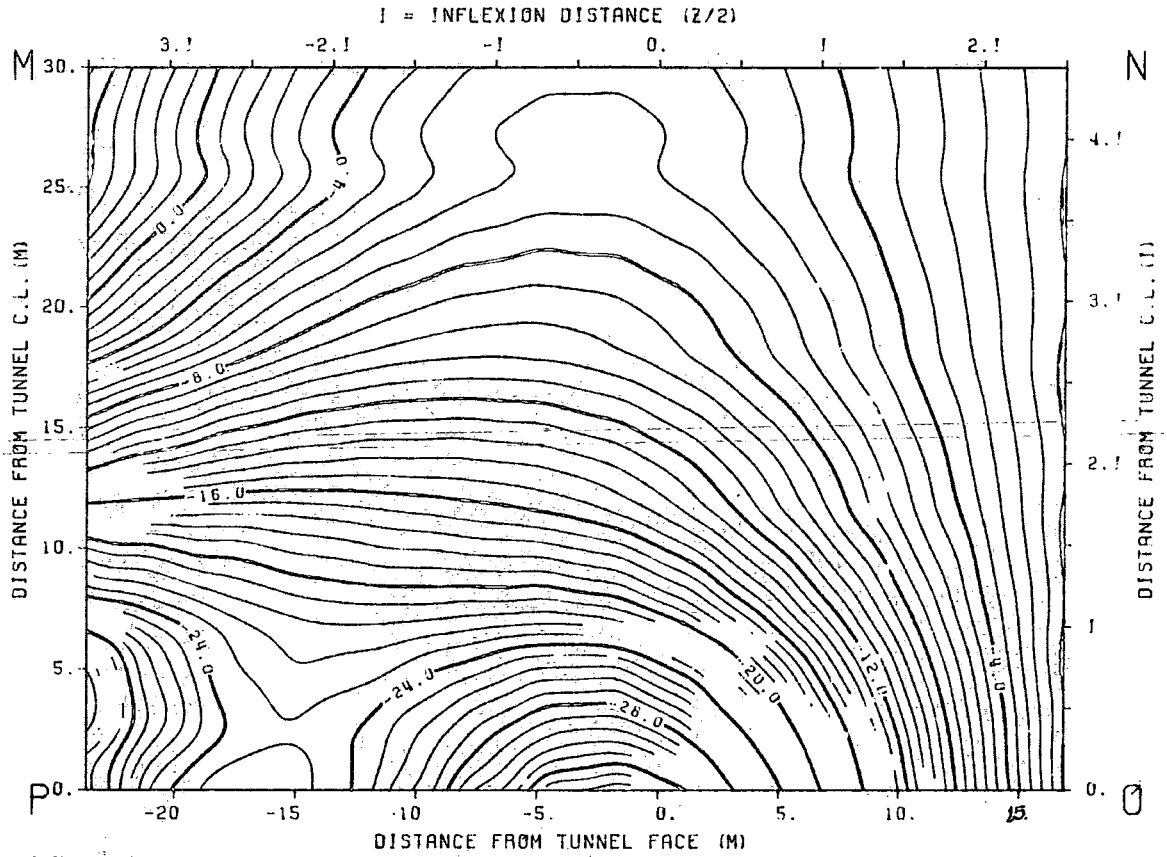

FIG. 7.5.9) Contours of equal longitudinal displacements (10^{-3} mm). Ground surface. Step 7.

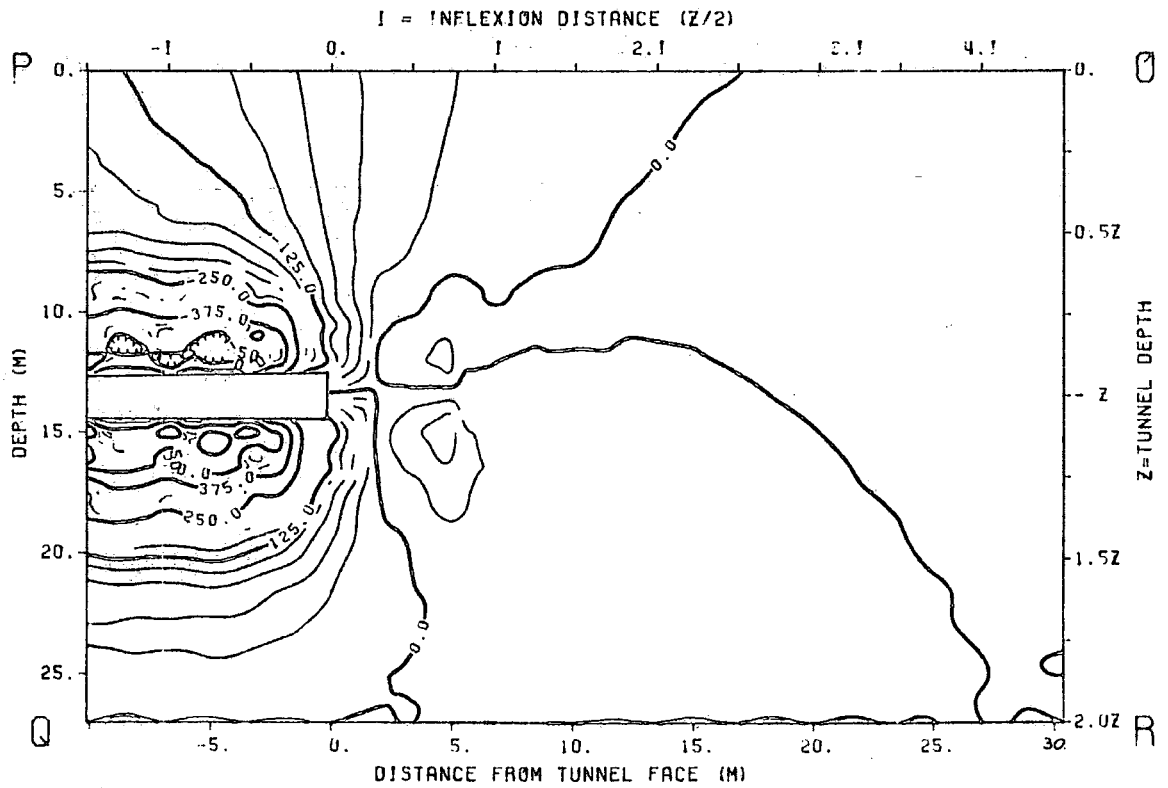

FIG. 7.5.10) Contours of equal vertical displacements (10^{-3} mm). Longitudinal section. Step 3.

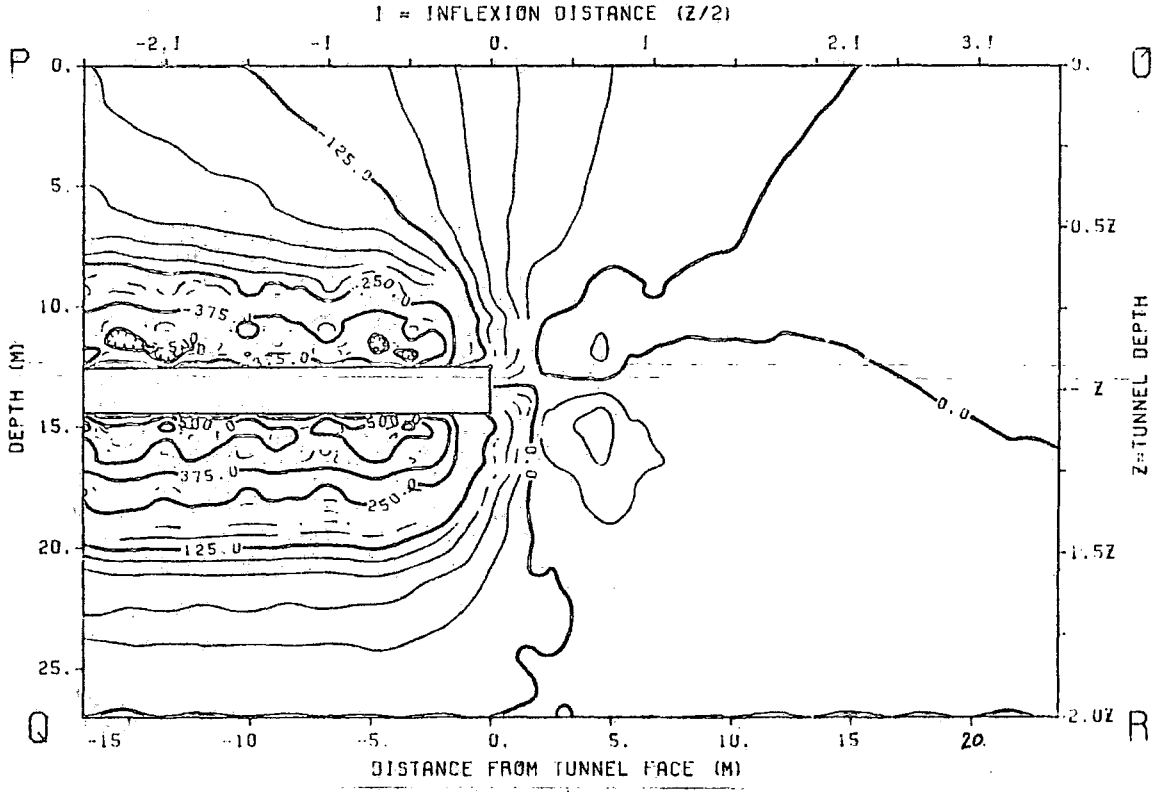

FIG. 7.5.11) Contours of equal vertical displacements (10^{-3} mm). Longitudinal section. Step 5.

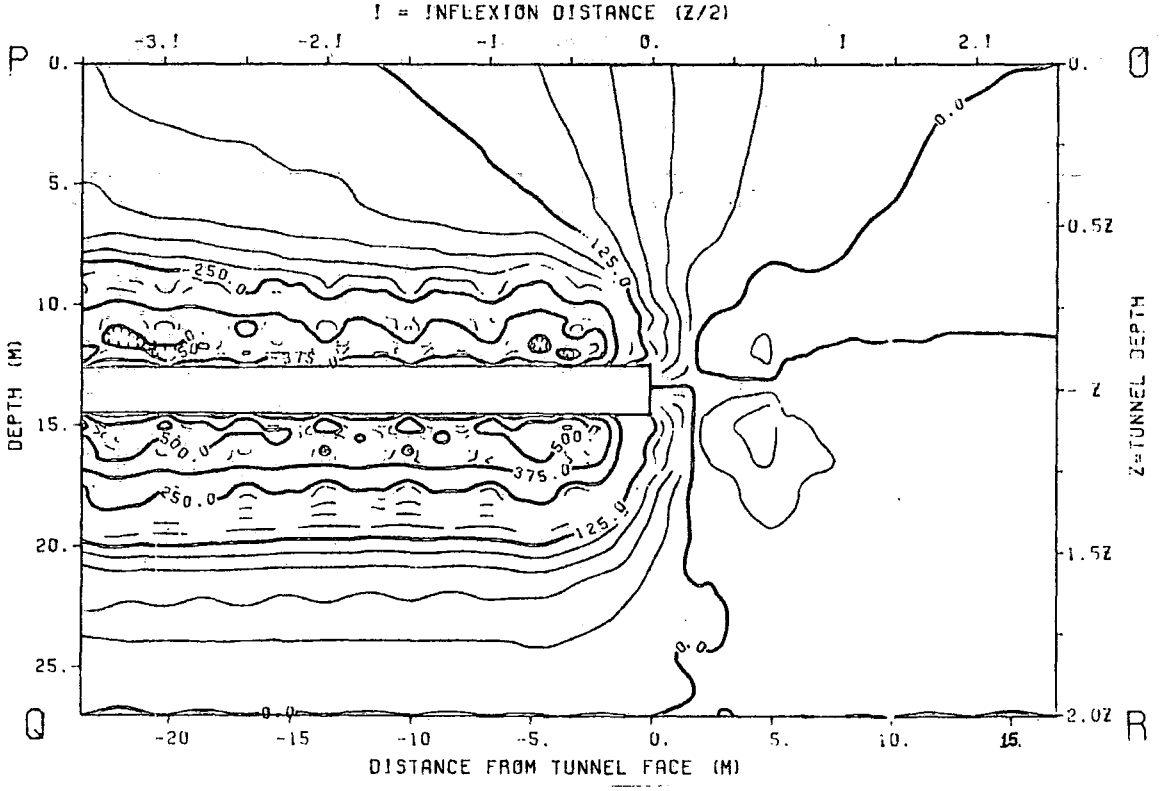

FIG. 7.5.12) Contours of equal vertical displacements (10^{-3} mm). Longitudinal section. Step 7.

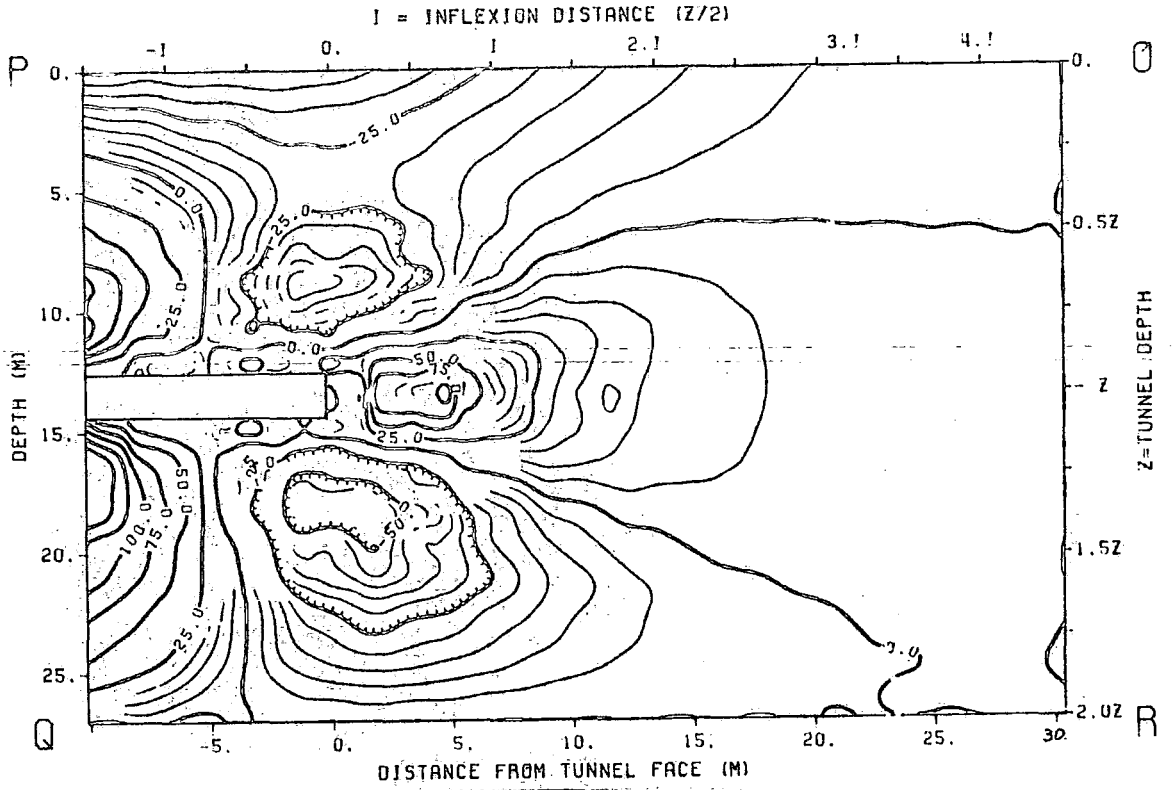

FIG. 7.5.13) Contours of equal longitudinal displacements (10^{-3} mm). Longitudinal section. Step 3.

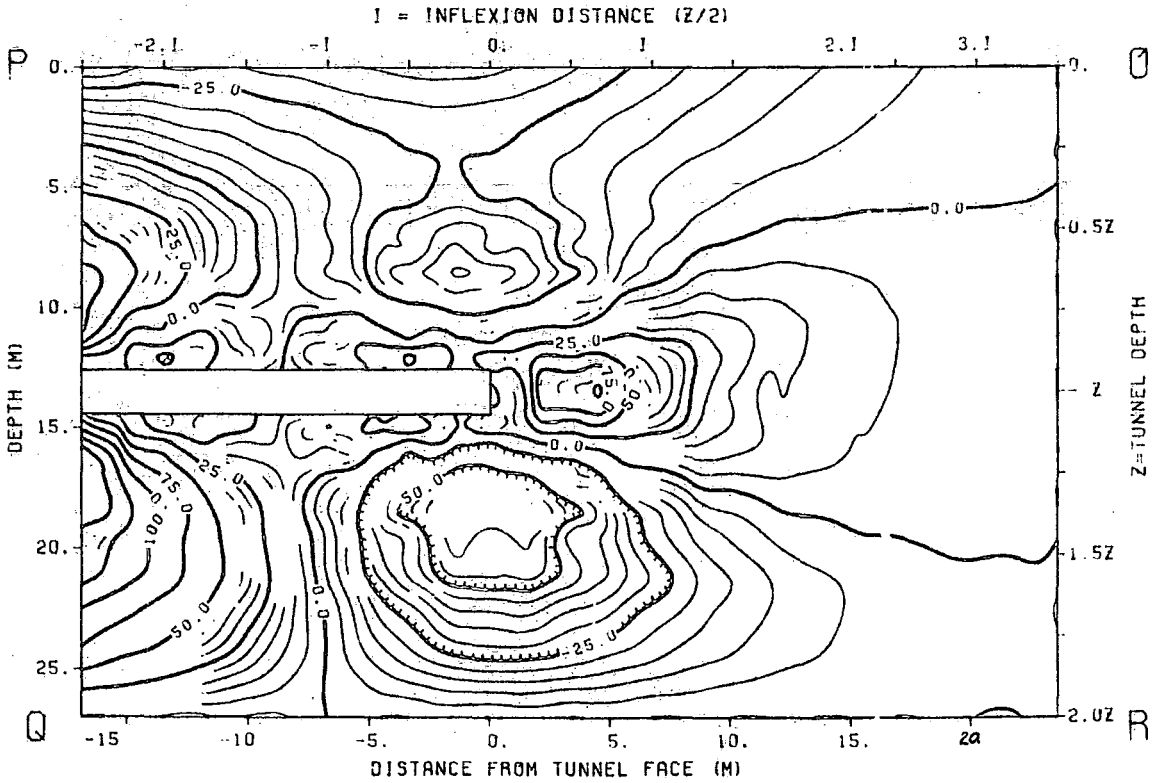

FIG. 7.5.14) Contours of equal longitudinal displacements (10^{-3} mm). Longitudinal section. Step 5.

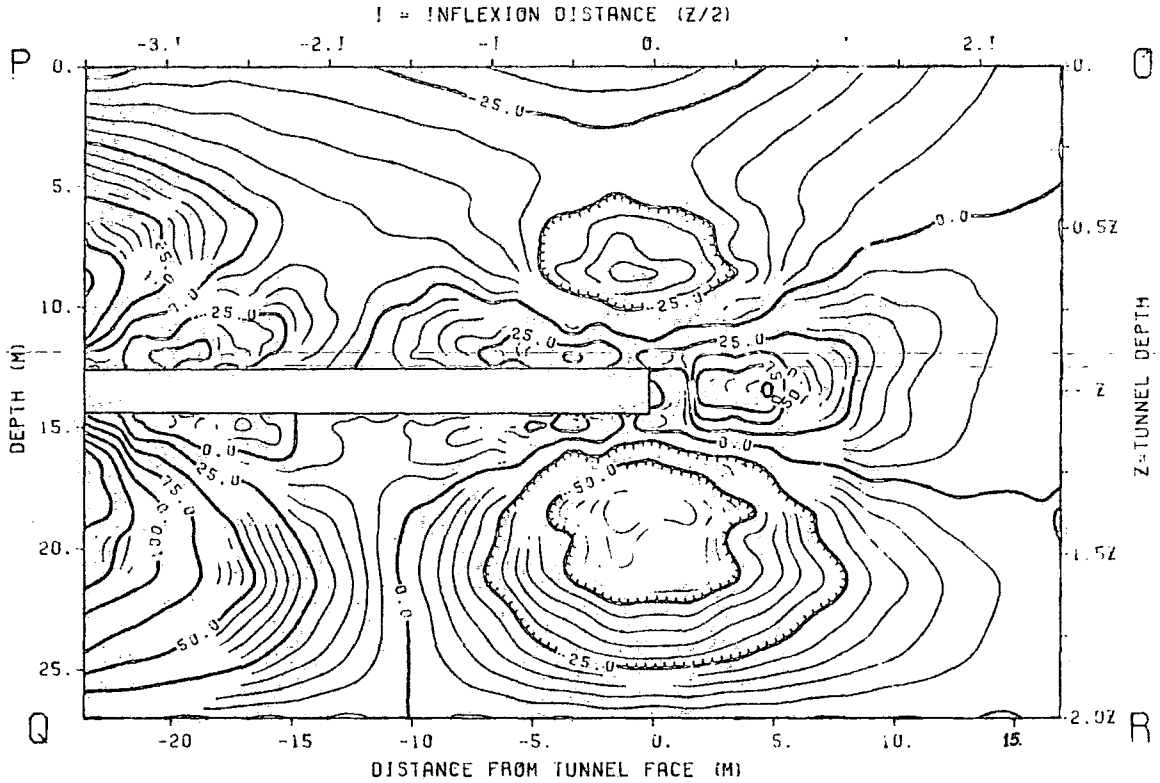

FIG. 7.5.15) Contours of equal longitudinal displacements (10^{-3} mm). Longitudinal section . Step 7.

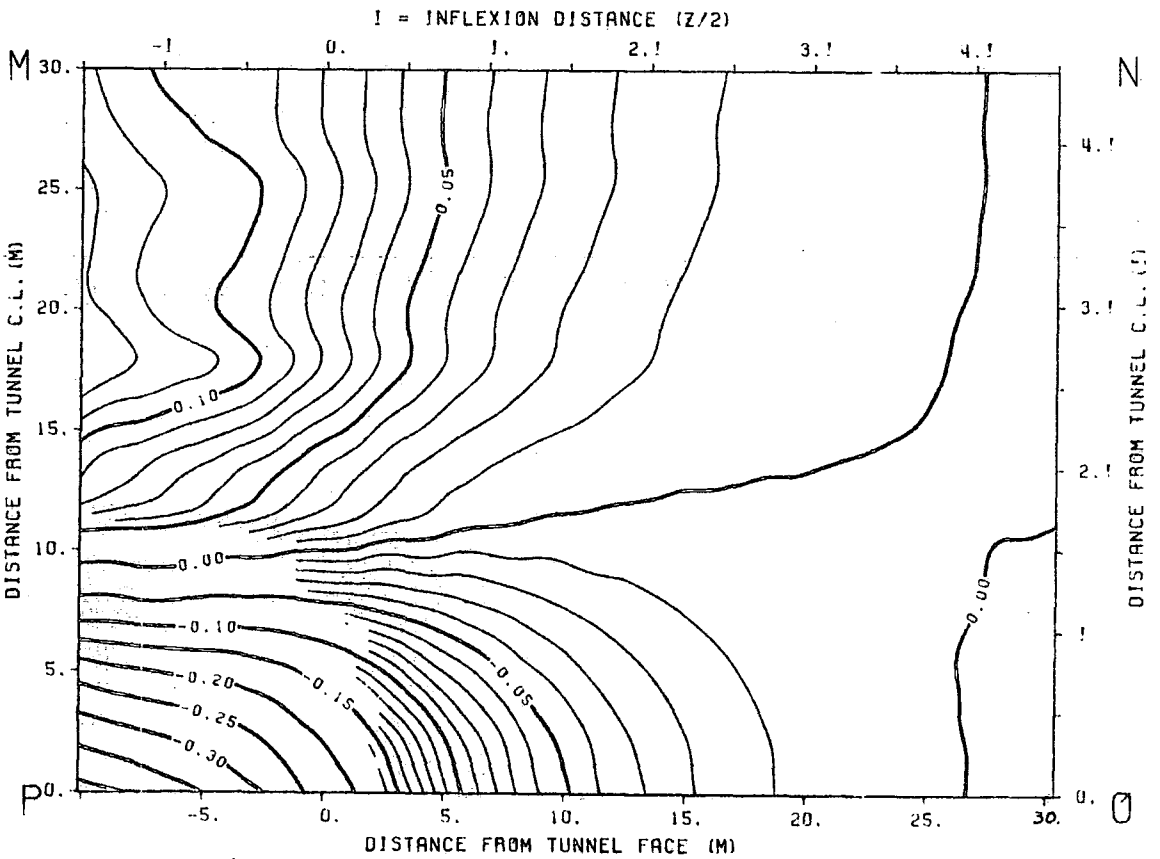

FIG. 7.5.16) Contours of equal lateral strains (10^{-3} %). Ground surface. Step 3.

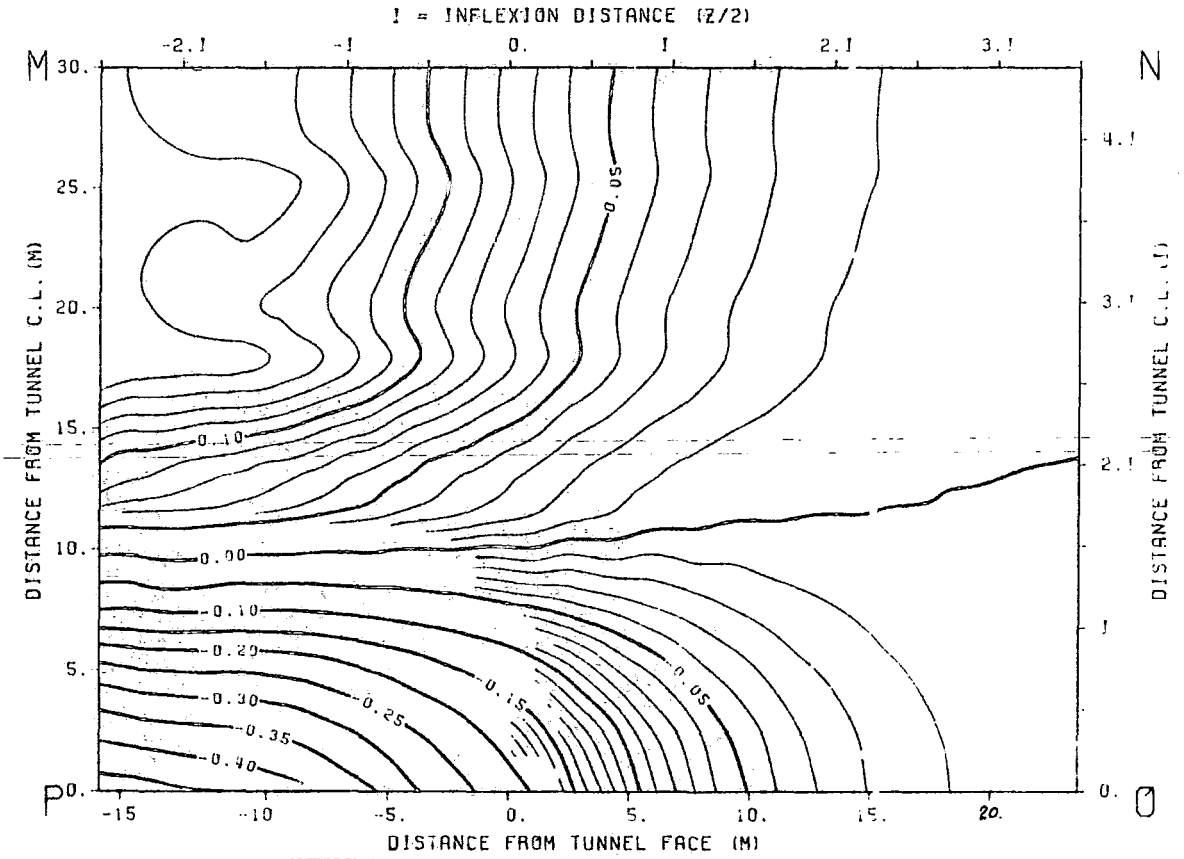

FIG. 7.5.17) Contours of equal lateral strain (10^{-3} %). Ground surface. Step 5.

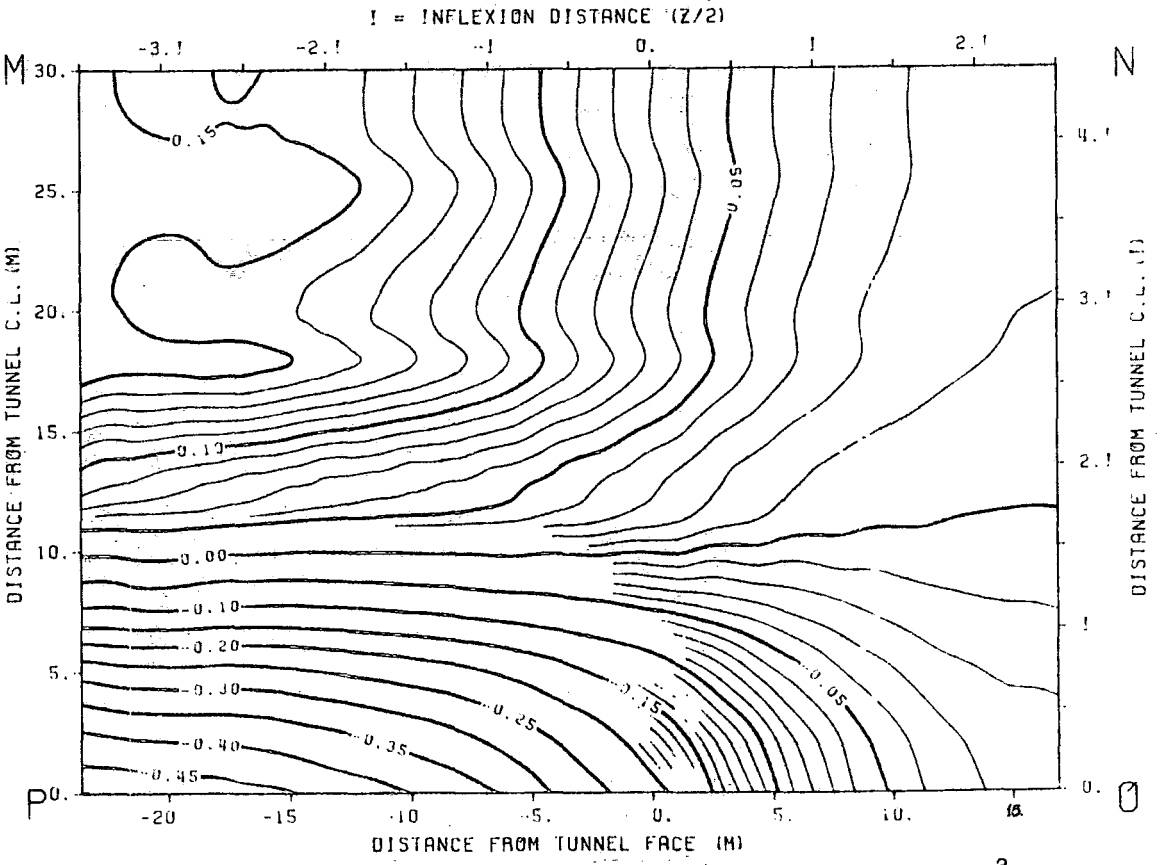

FIG. 7.5.18) Contours of equal lateral strains (10^{-3} %). Ground surface. Step 7.

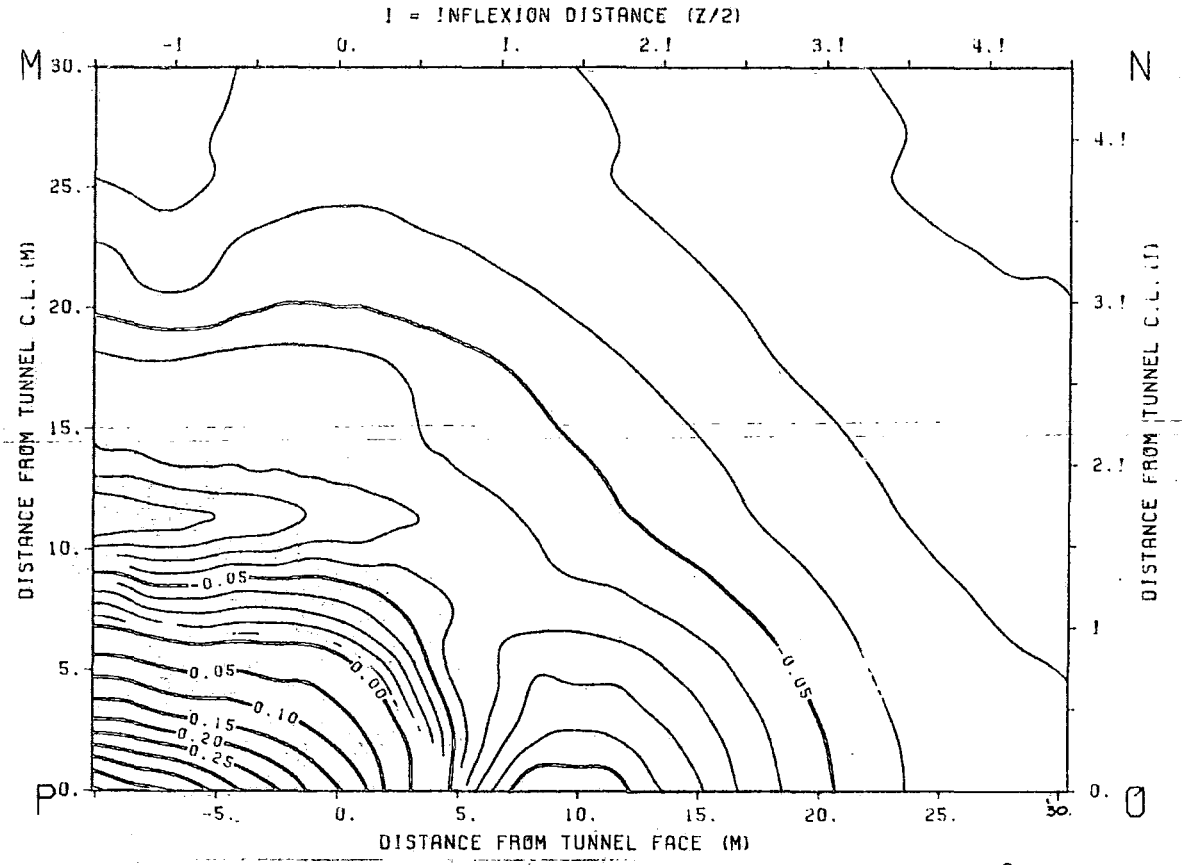

FIG. 7.5.19) Contours of equal vertical strains (10^{-3} %). Ground surface. Step 3.

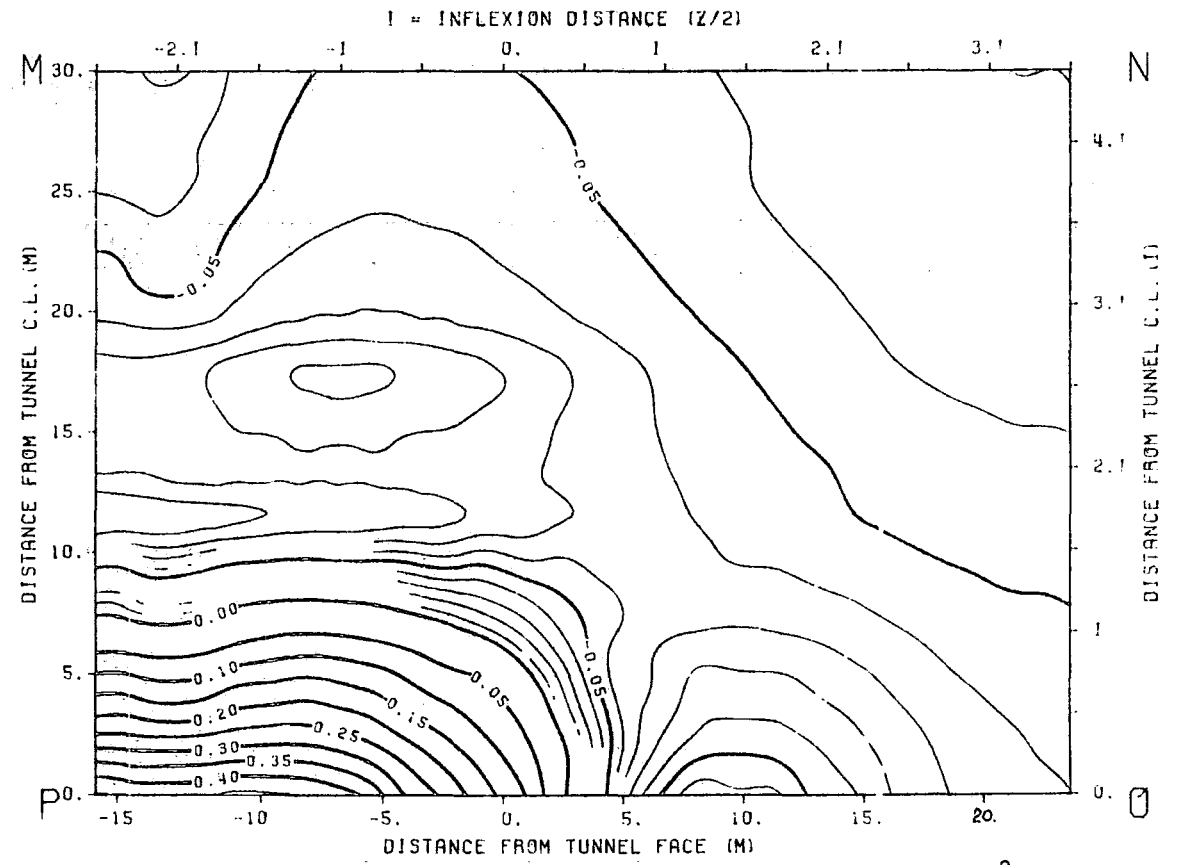

FIG. 7.5.20) Contours of equal vertical strains (10^{-3} %). Ground surface. Step 5.

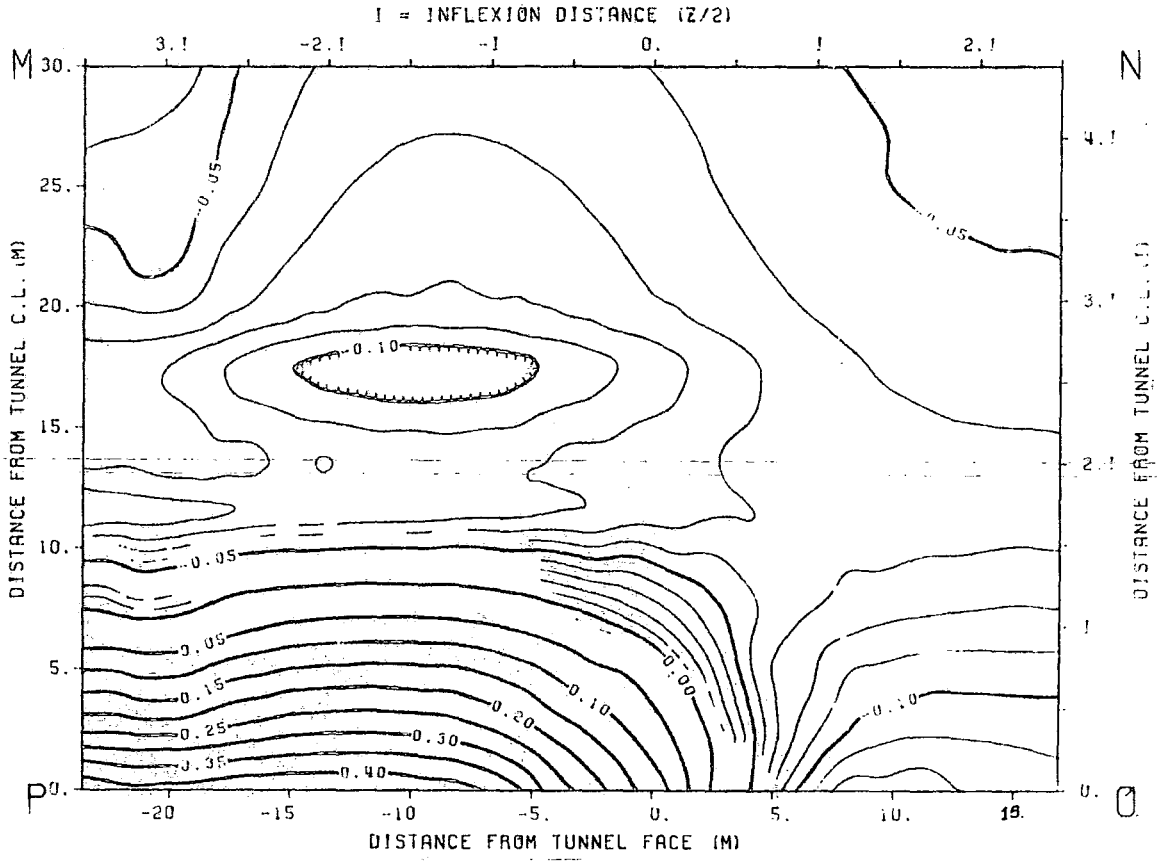

FIG. 7.5.21) Contours of equal vertical strains (10^{-3} %). Ground surface. Step 7.

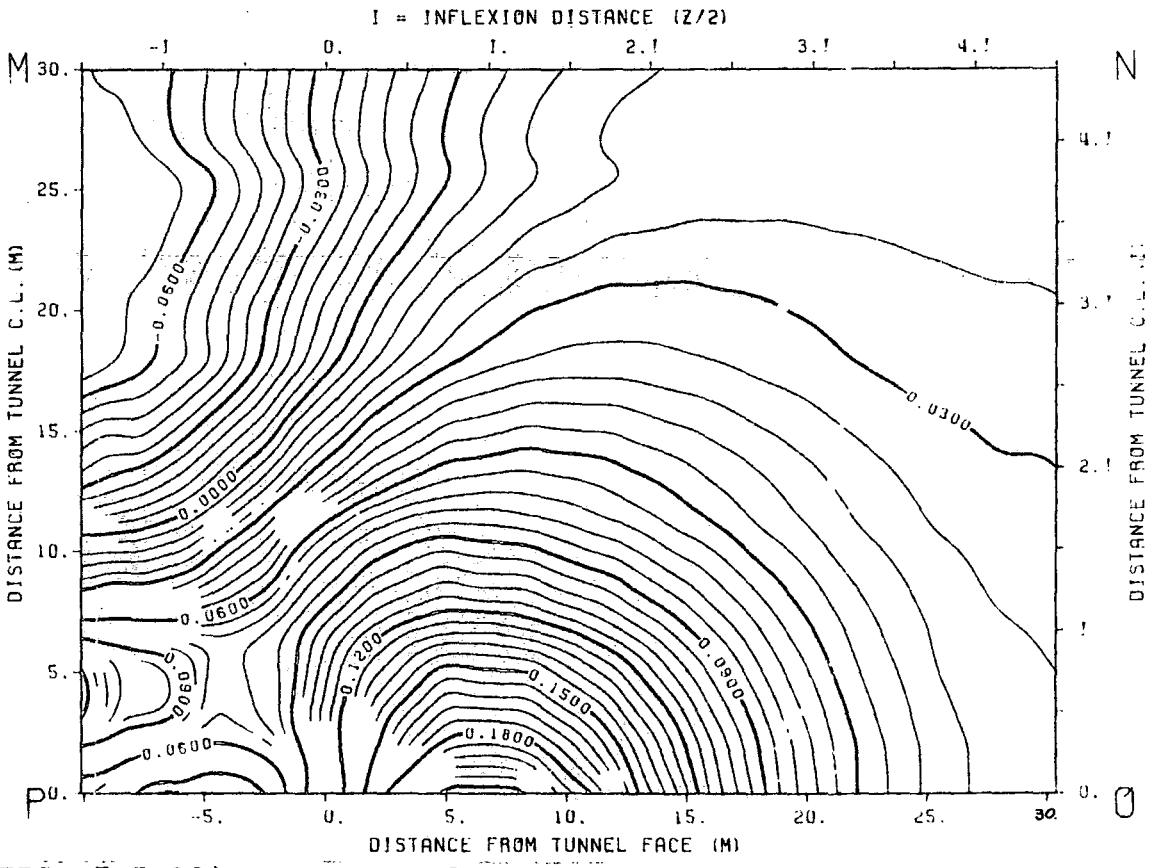

FIG. 7.5.22) Contours of equal longitudinal strains (10^{-3} %). Ground surface. Step 3.

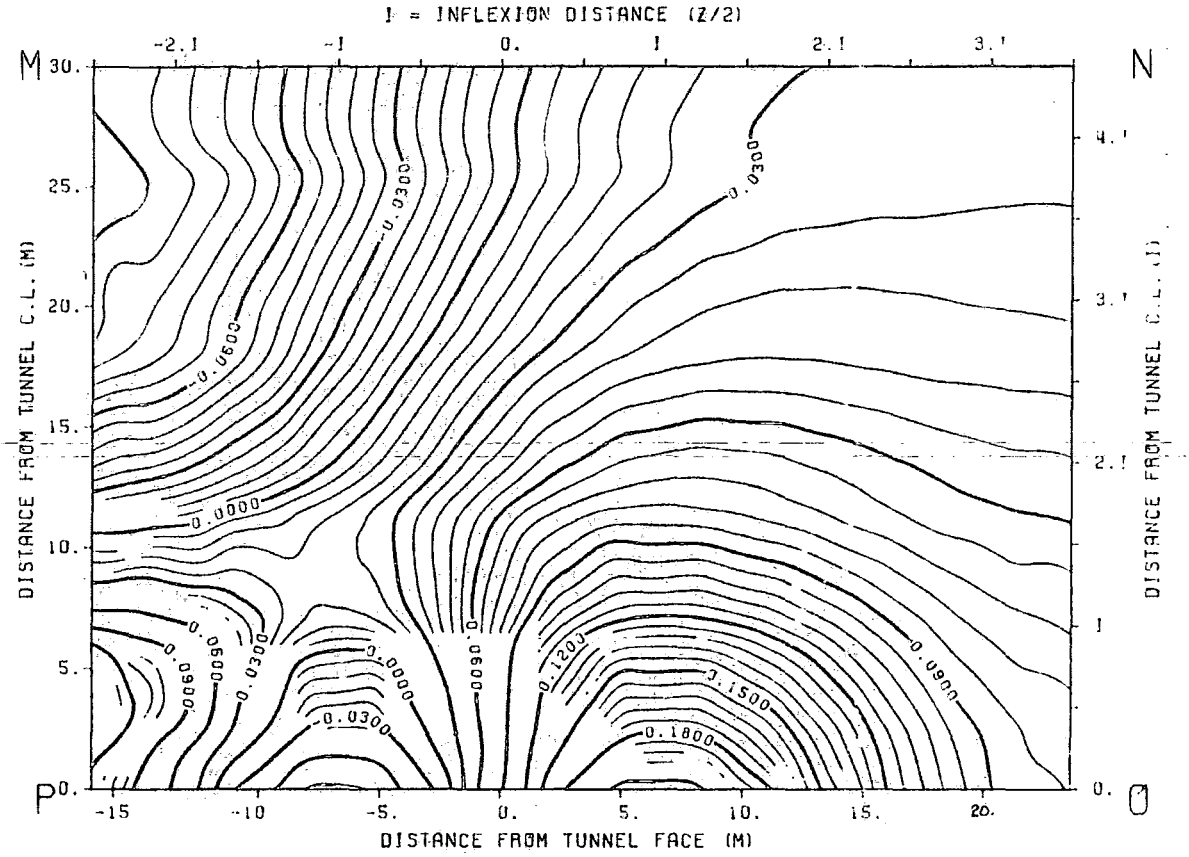

FIG. 7.5.23) Contours of equal longitudinal strains (10^{-3} %). Ground surface. Step 5.

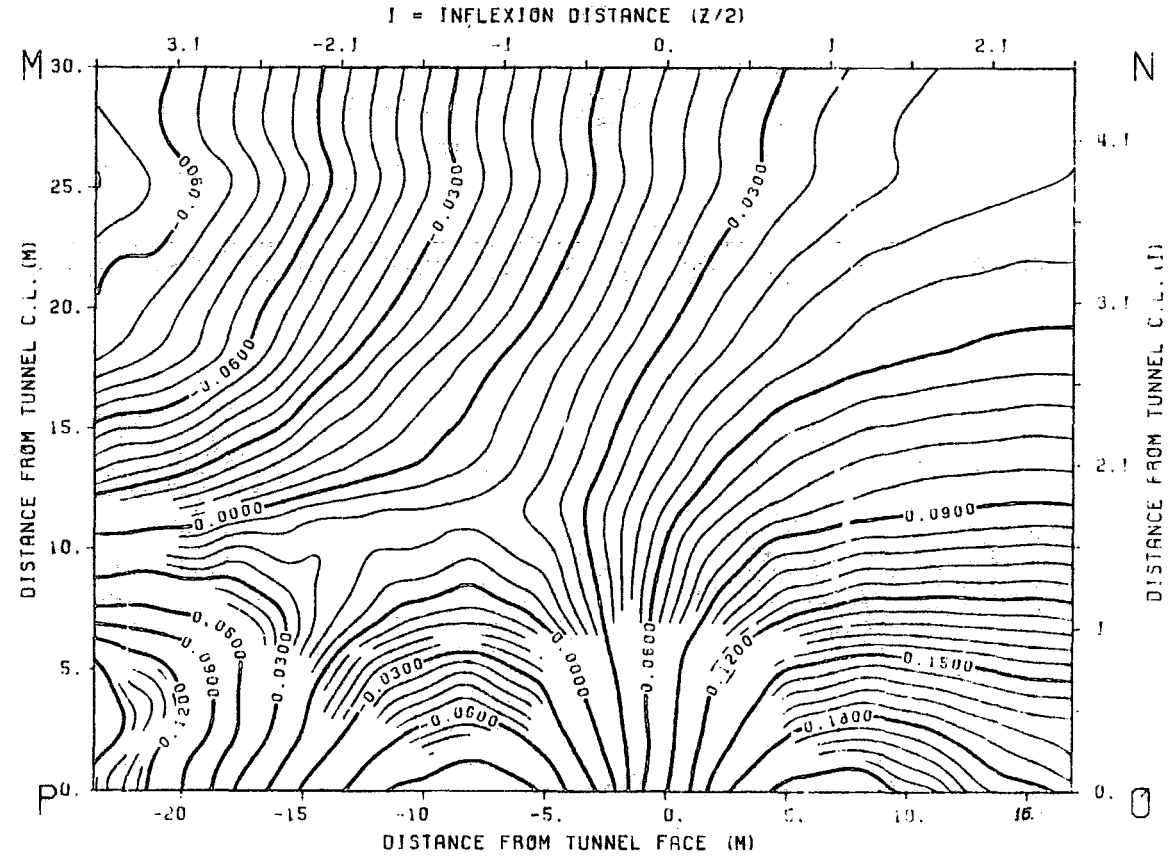

FIG. 7.5.24) Contours of equal longitudinal strains (10^{-3} %). Ground surface. Step 7.

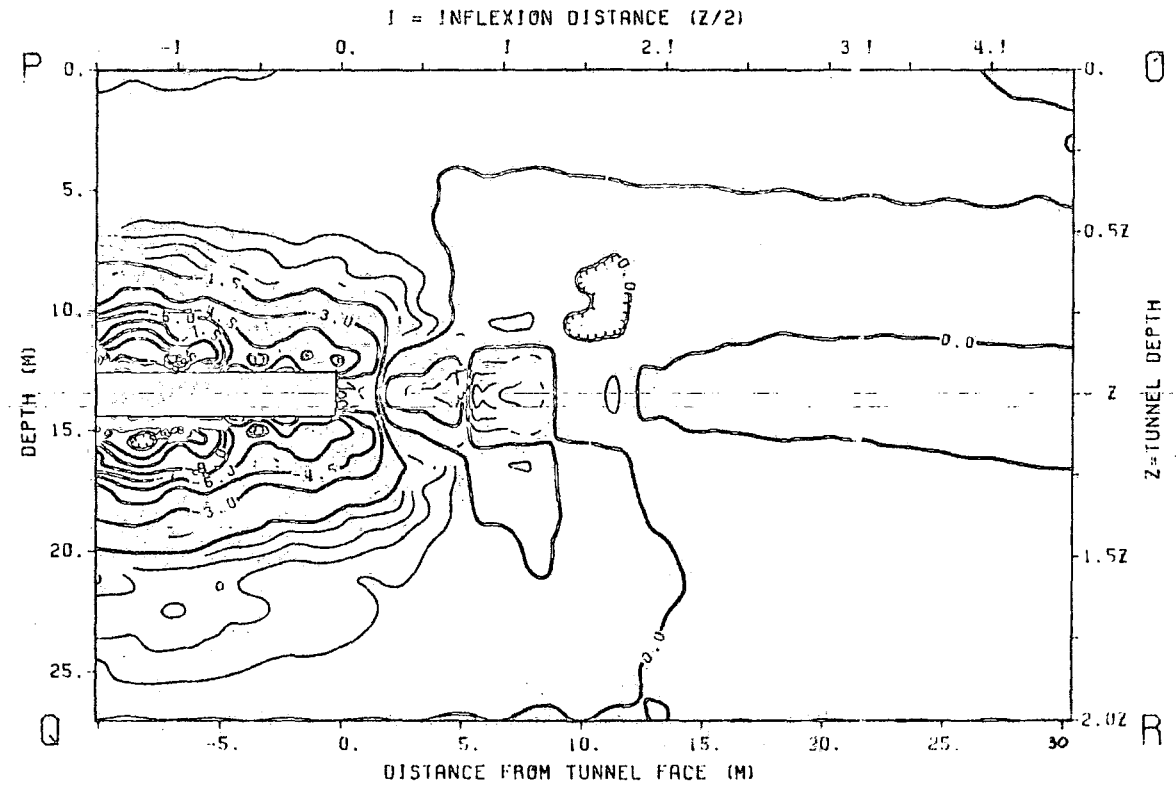

FIG. 7.5.25) Contours of equal lateral strains (10^{-3} %). Longitudinal section. Step 3.

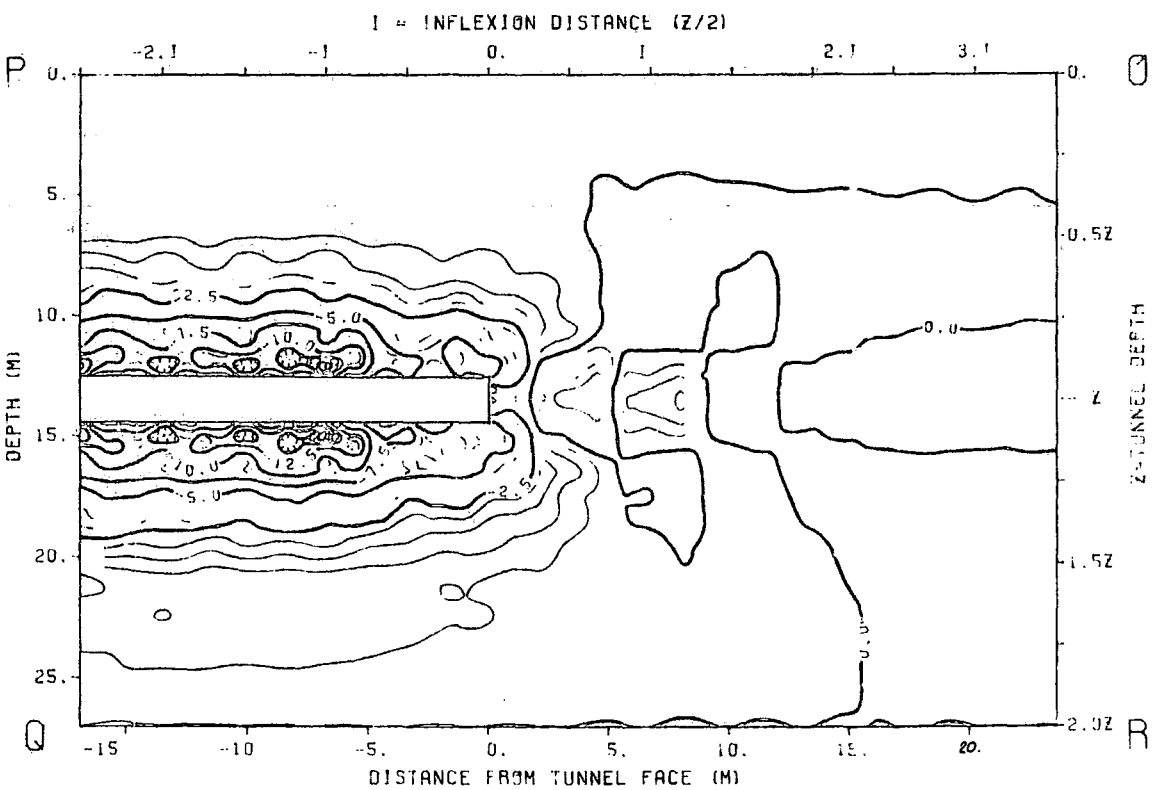

FIG. 7.5.26) Contours of equal lateral strains (10^{-3} %). Longitudinal sectin. Step 5.

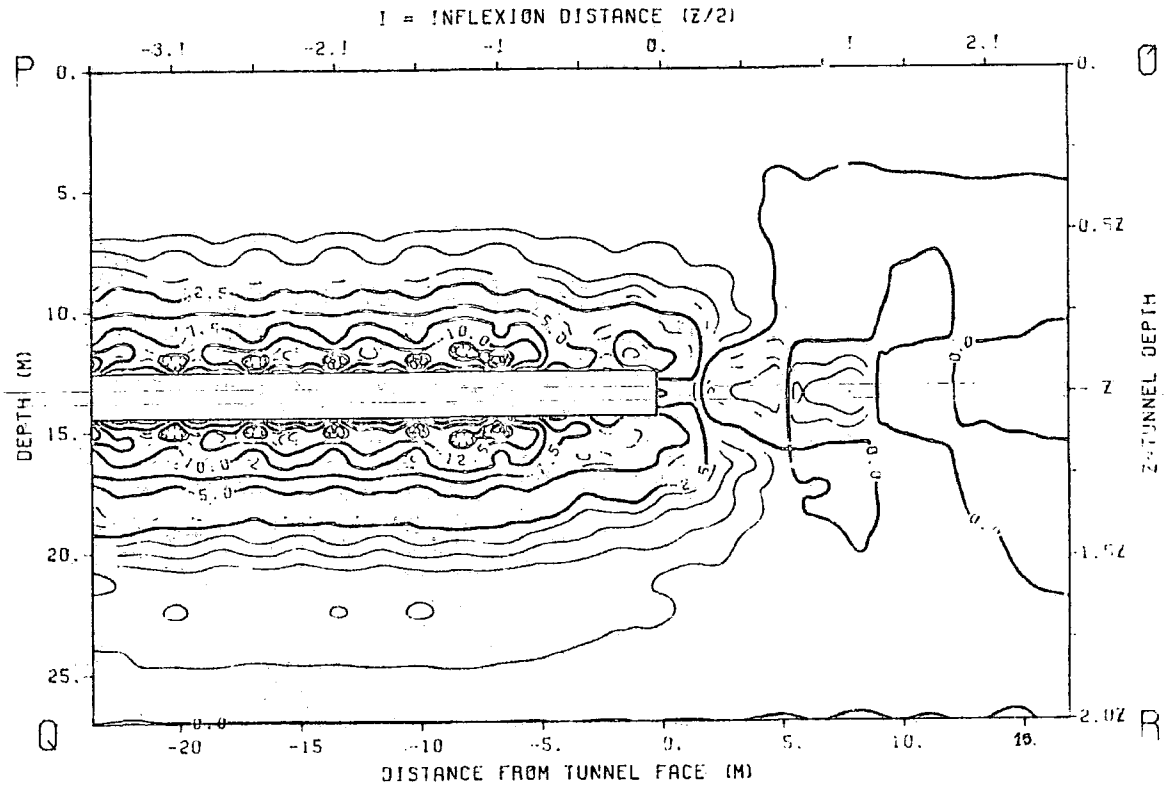

FIG. 7.5.27) Contours of equal lateral strains (10^{-3} %). Longitudinal section. Step 7.

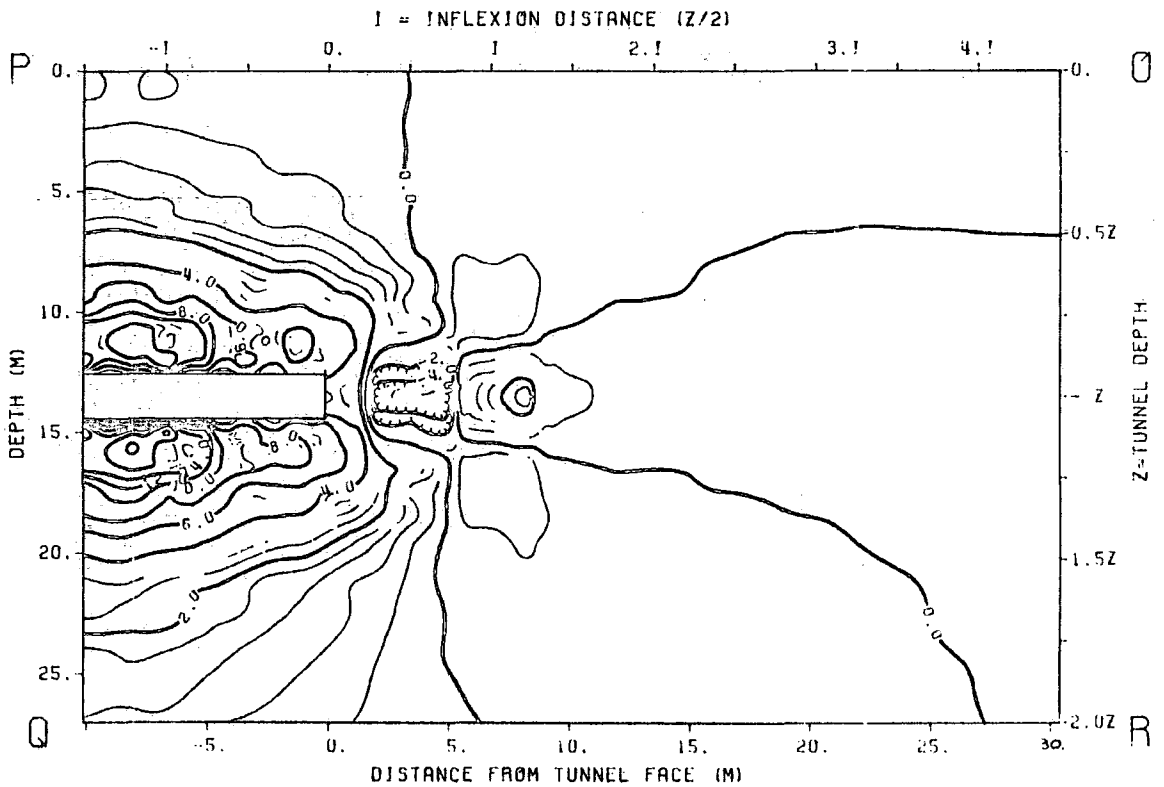

FIG. 7.5.28) Contours of equal vertical strains (10^{-3} %). Longitudinal section. Step 3.

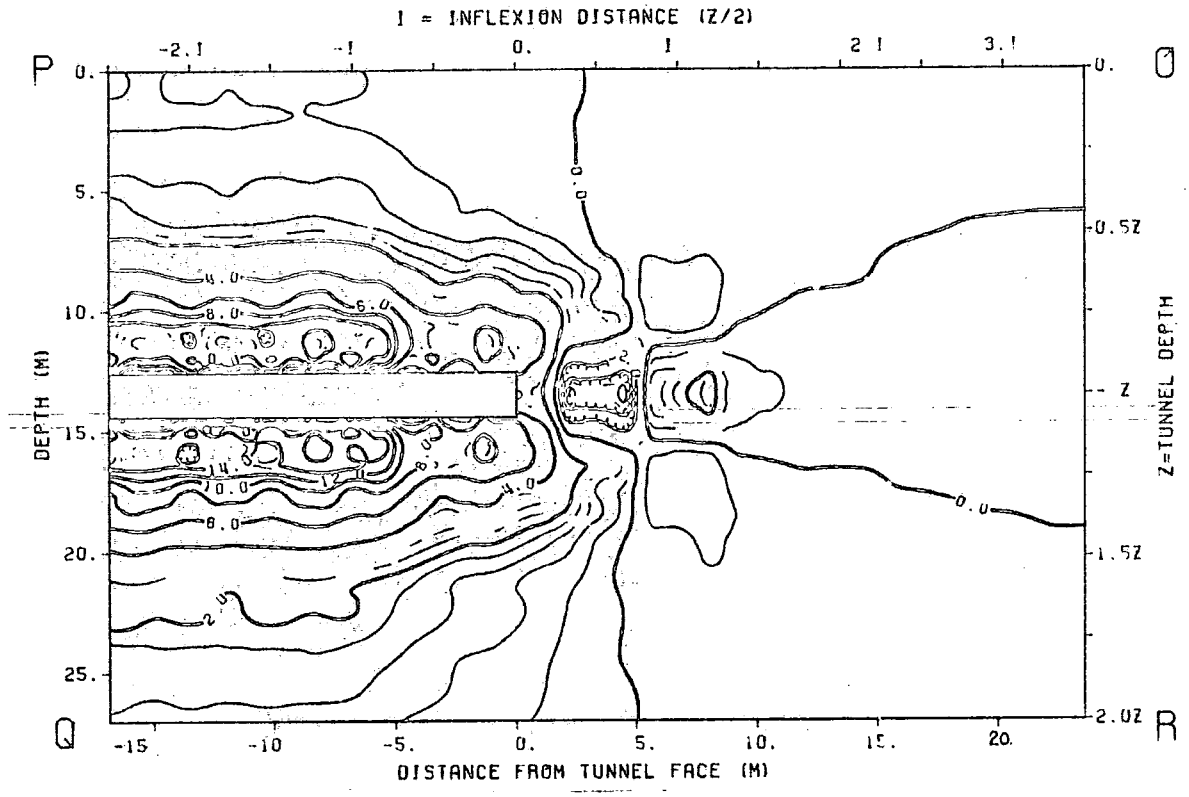

FIG. 7.5.29) Contours of equal vertical strains (10^{-3} %). Longitudinal section. Step 5.

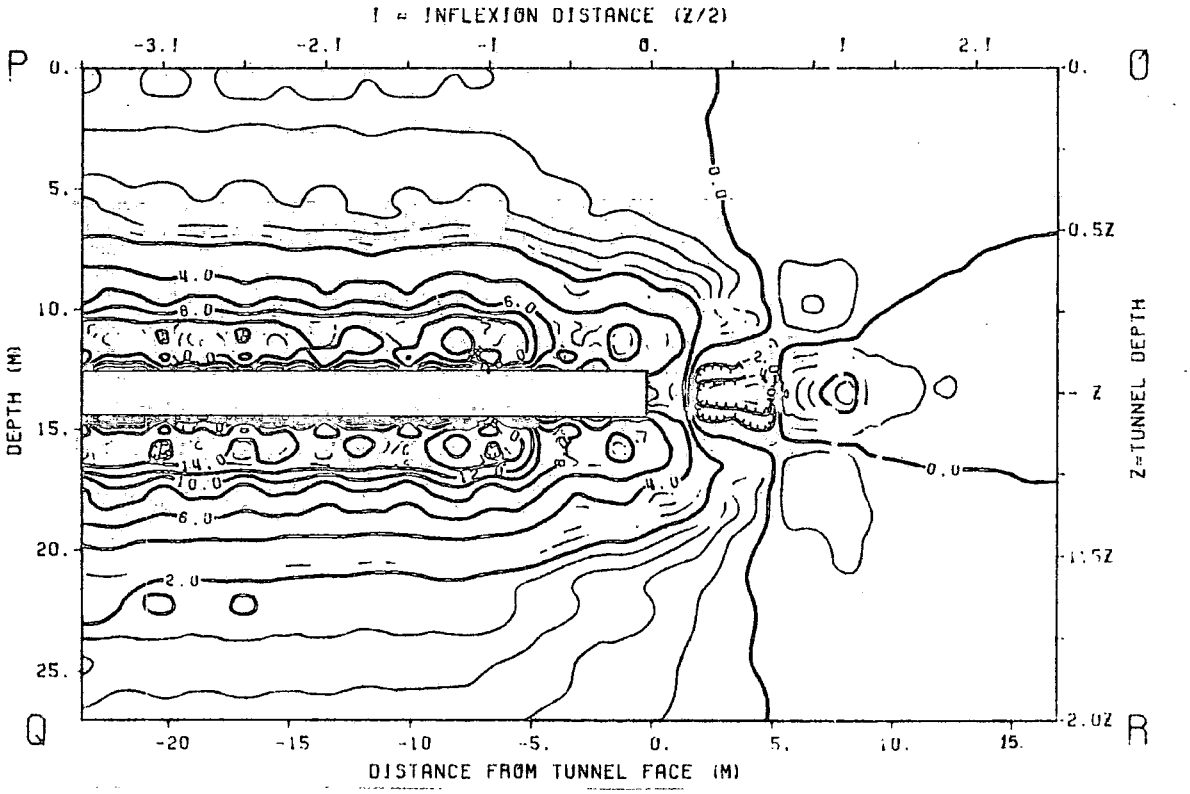

FIG. 7.5.30) Contours of equal vertical strains (10^{-3} %). Longitudinal section. Step 7.

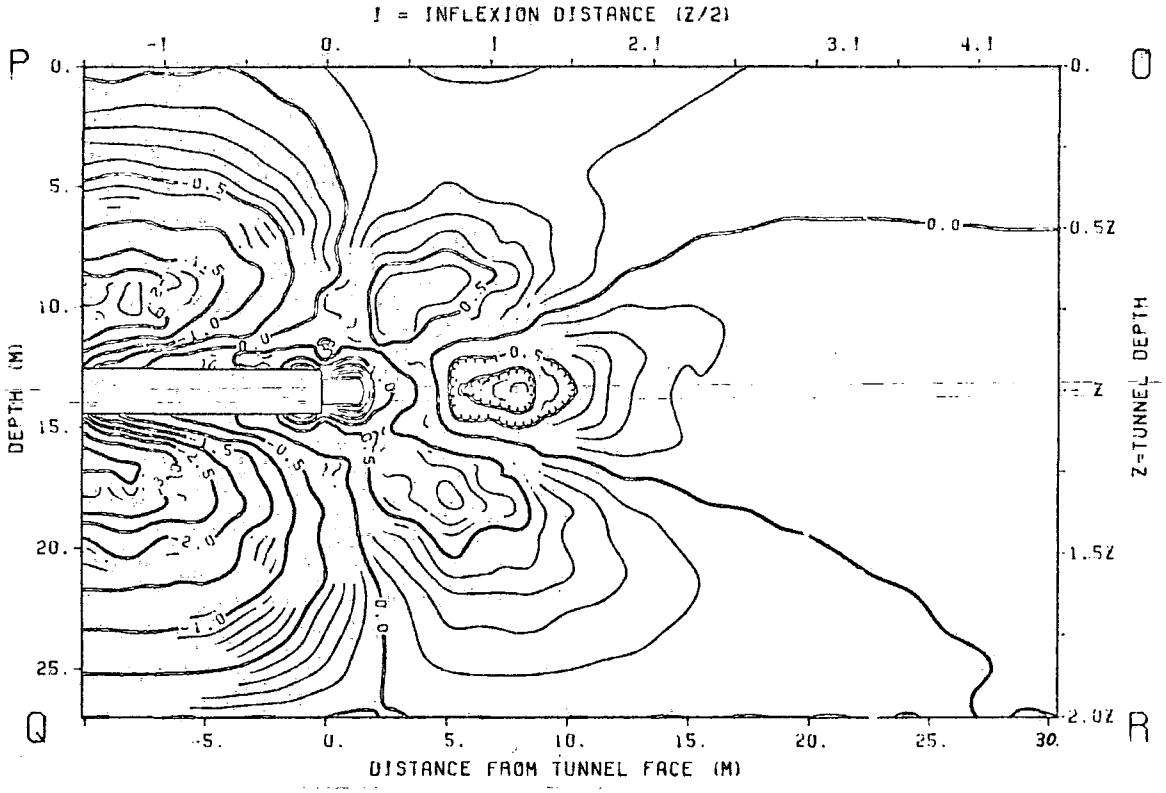

FIG. 7.5.31) Contours of equal longitudinal strains (10^{-3} %). Longitudinal section. Step 3.

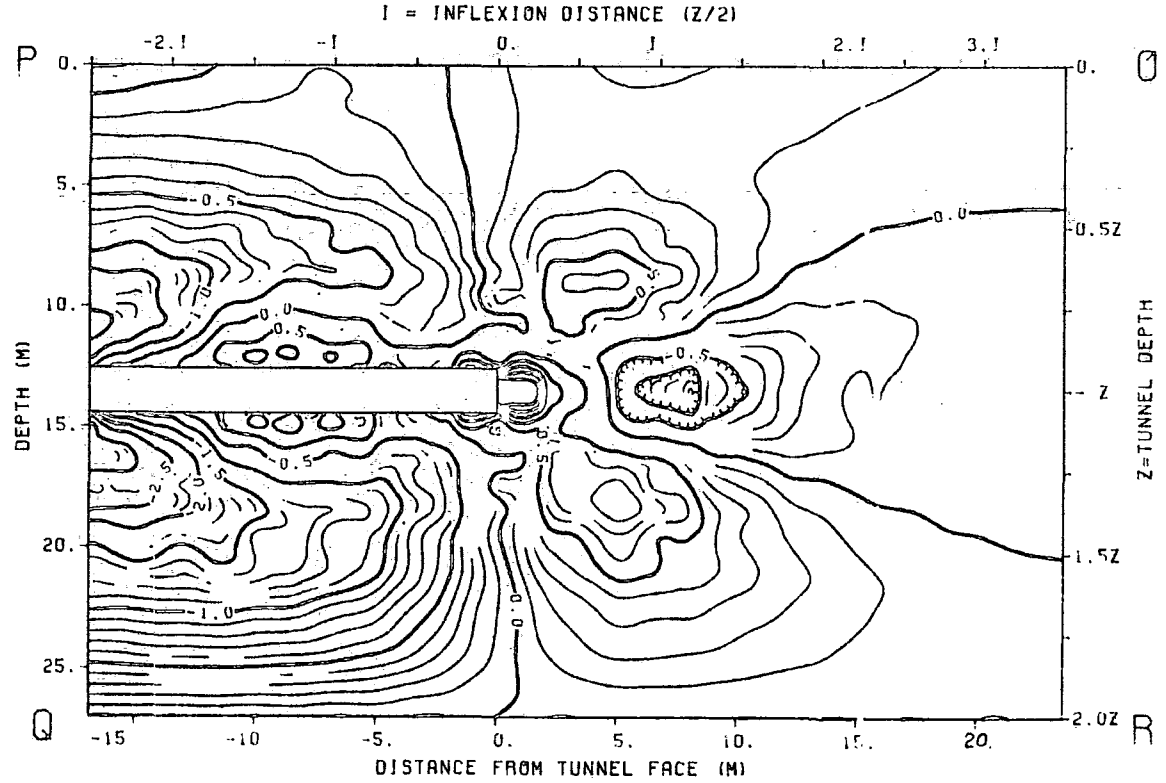

FIG. 7.5.32) Contours of equal longitudinal strains (10^{-3} %). Longitudinal section. Step 5.

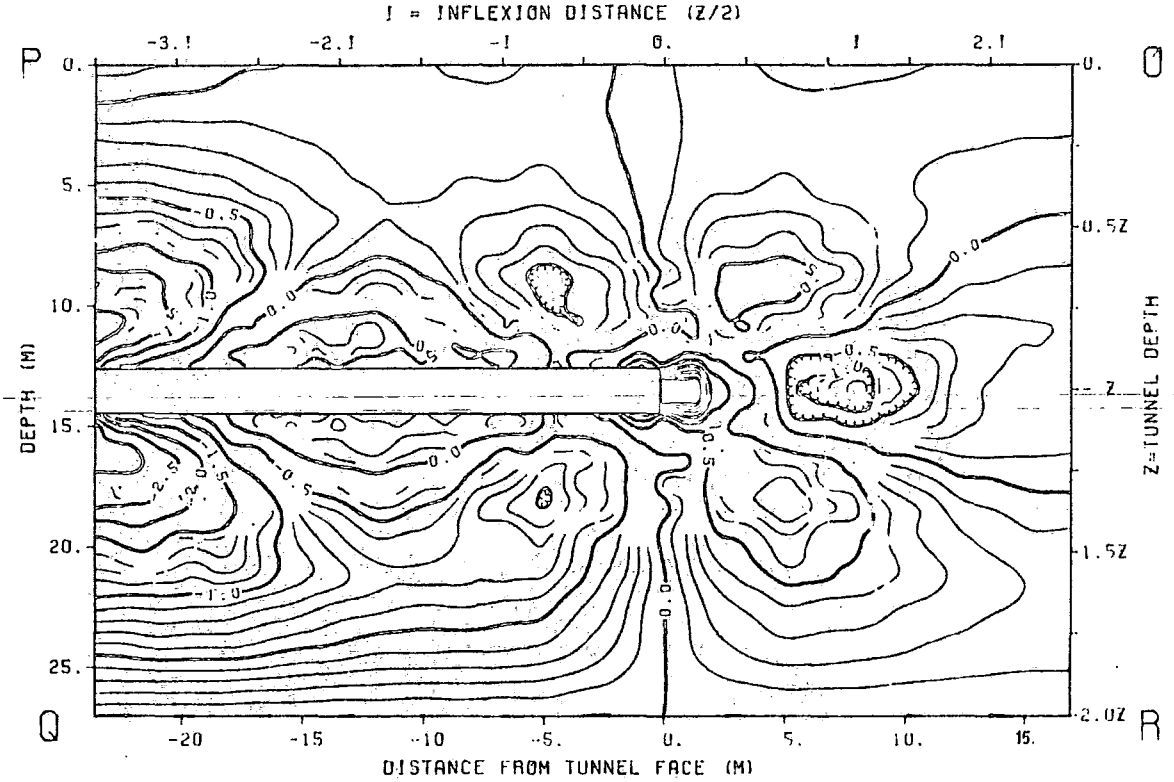

FIG. 7.5.33) Contours of equal longitudinal strains (10^{-3} %). Longitudinal section. Step 7.

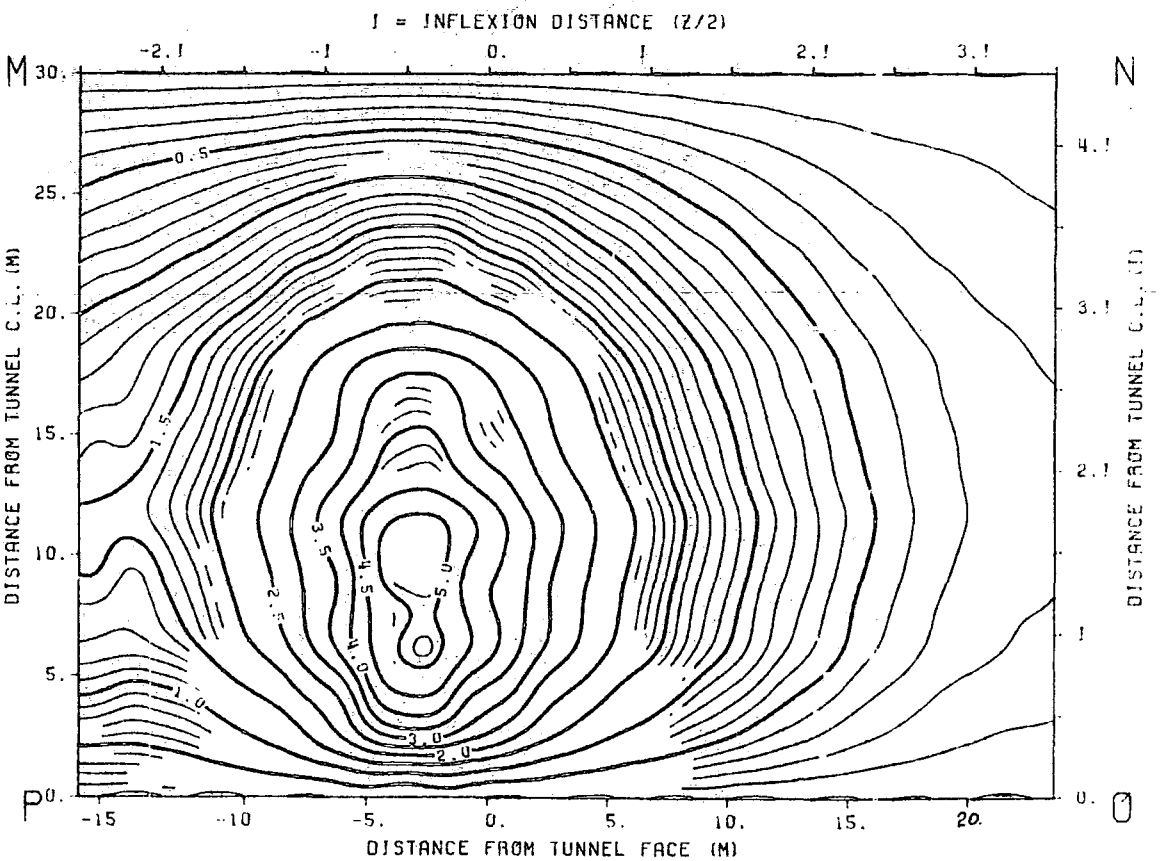

FIG. 7.5.34) Contours of equal variation of lateral displacements (10^{-3} mm) between steps 4 and 5. Ground surface.

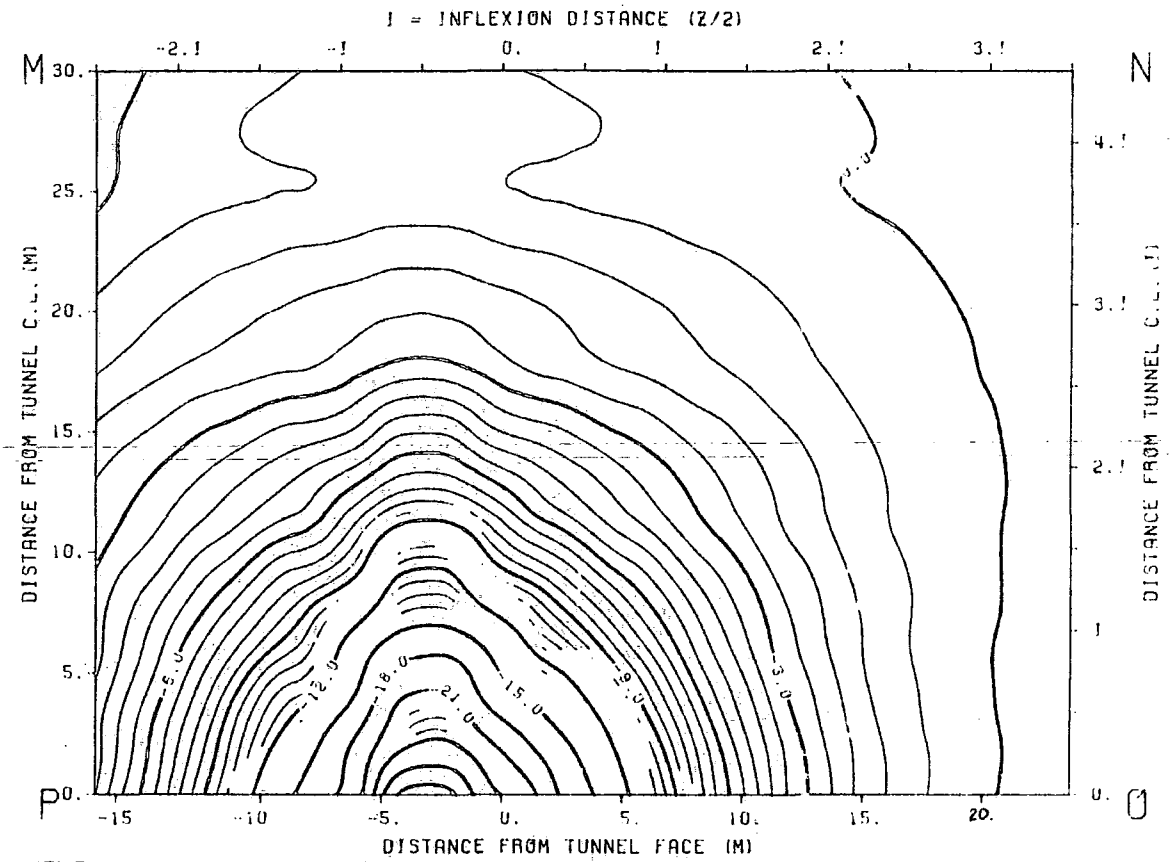

FIG. 7.5.35) Contours of equal variation of vertical displacements (10^{-3} mm) between steps 4 and 5. Ground surface.

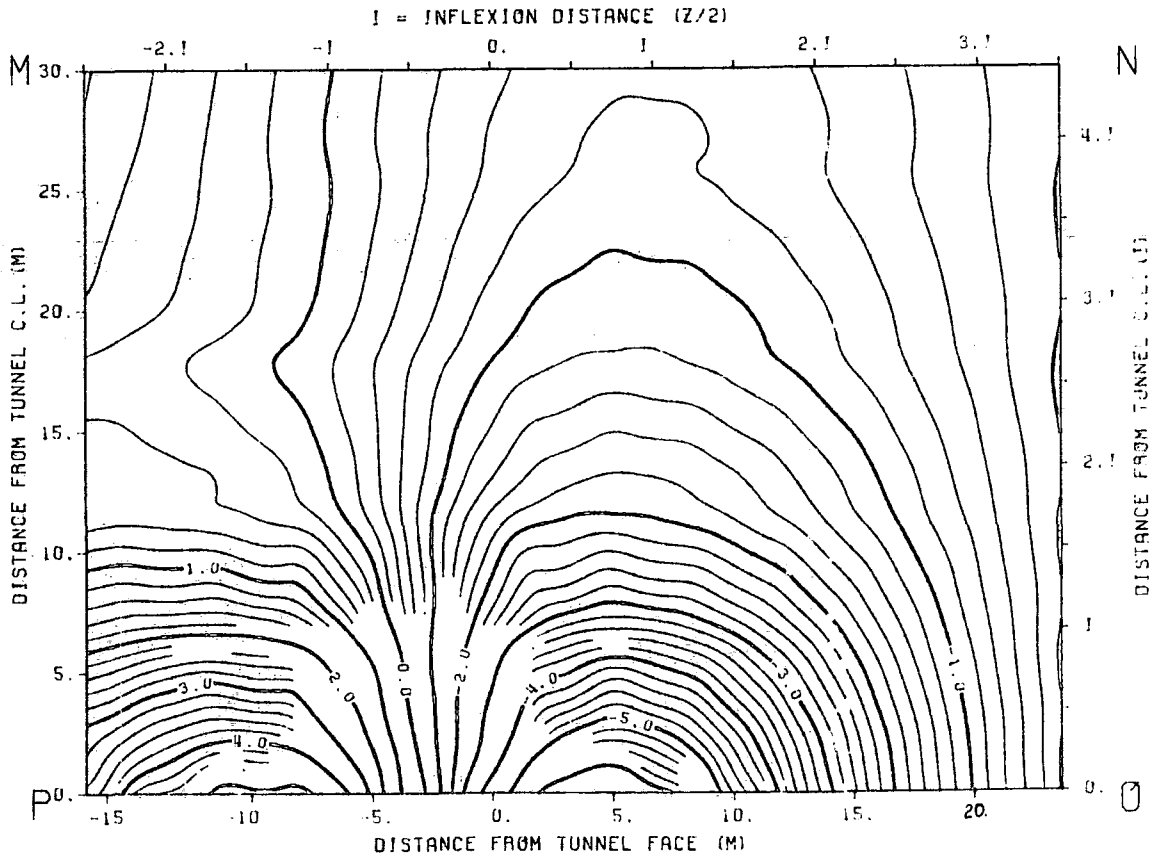

FIG. 7.5.36) Contours of equal variation of longitudinal displacements (10^{-3} mm) between steps 4 and 5. Ground surface.

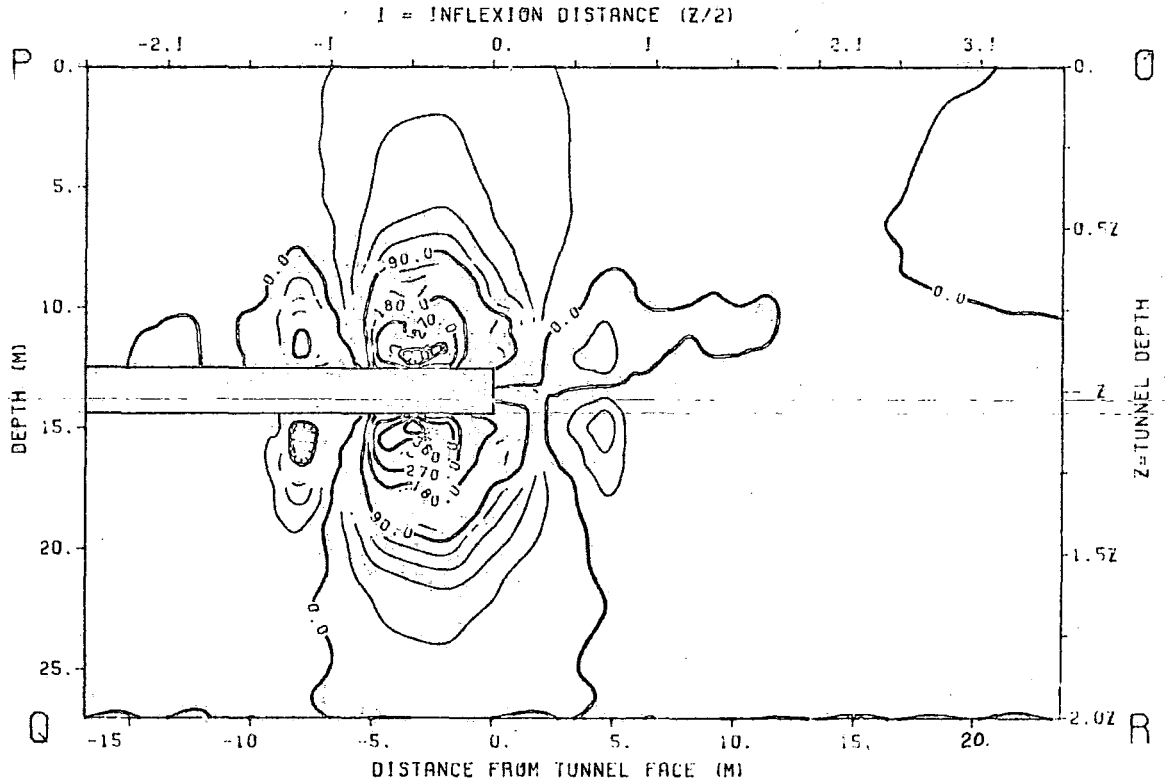

FIG. 7.5.37) Contours of equal variation of vertical displacements (10^{-3} mm) between steps 4 and 5. Longitudinal section.

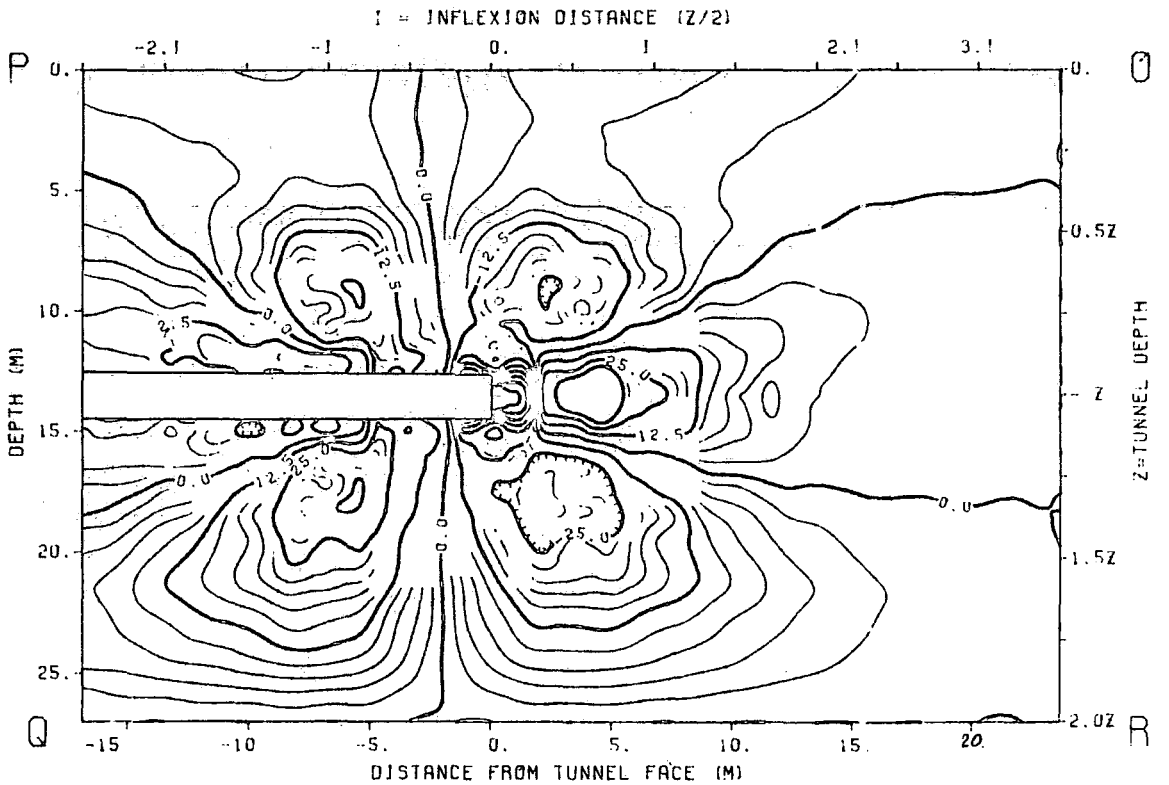

FIG. 7.5.38) Contours of equal variation of longitudinal displacements (10^{-3} mm) between steps 4 and 5. Longitudinal section.

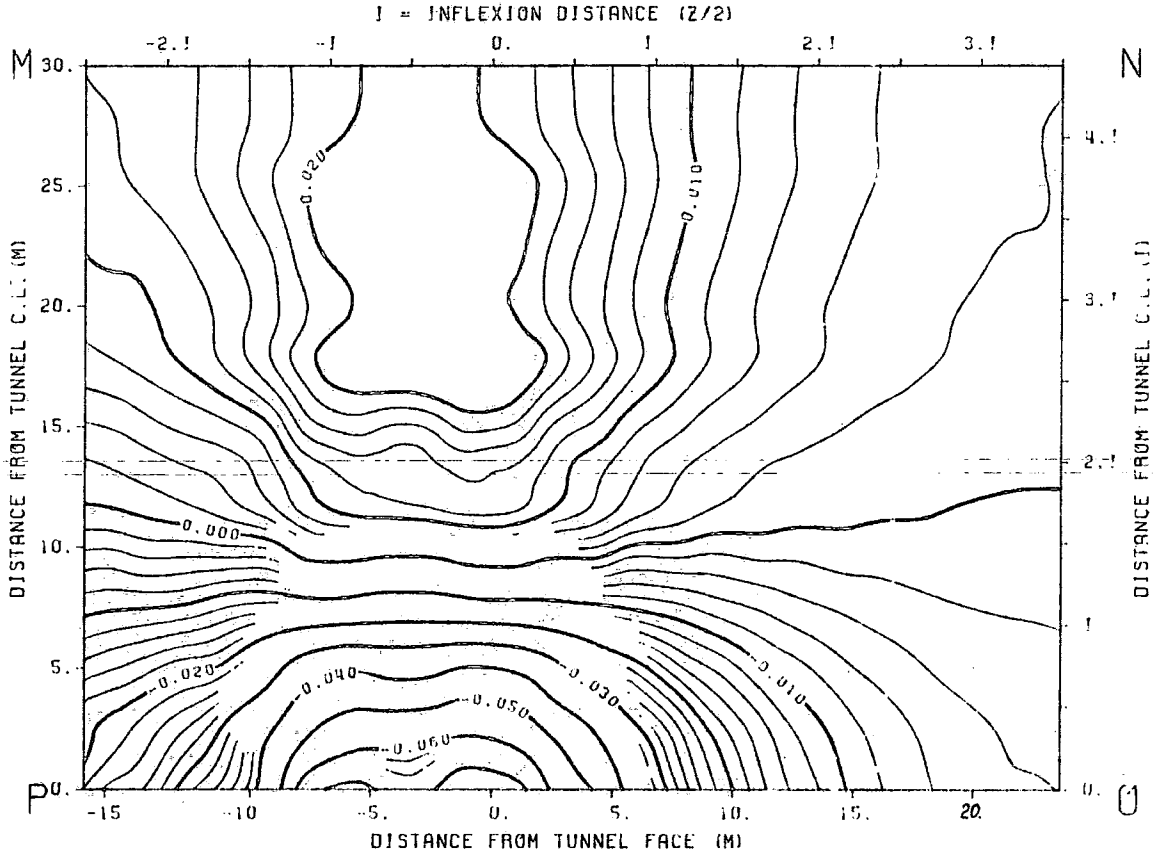

FIG. 7.5.39) Contours of equal variation of lateral strains (10^{-3} %) between steps 4 and 5. Ground surface.

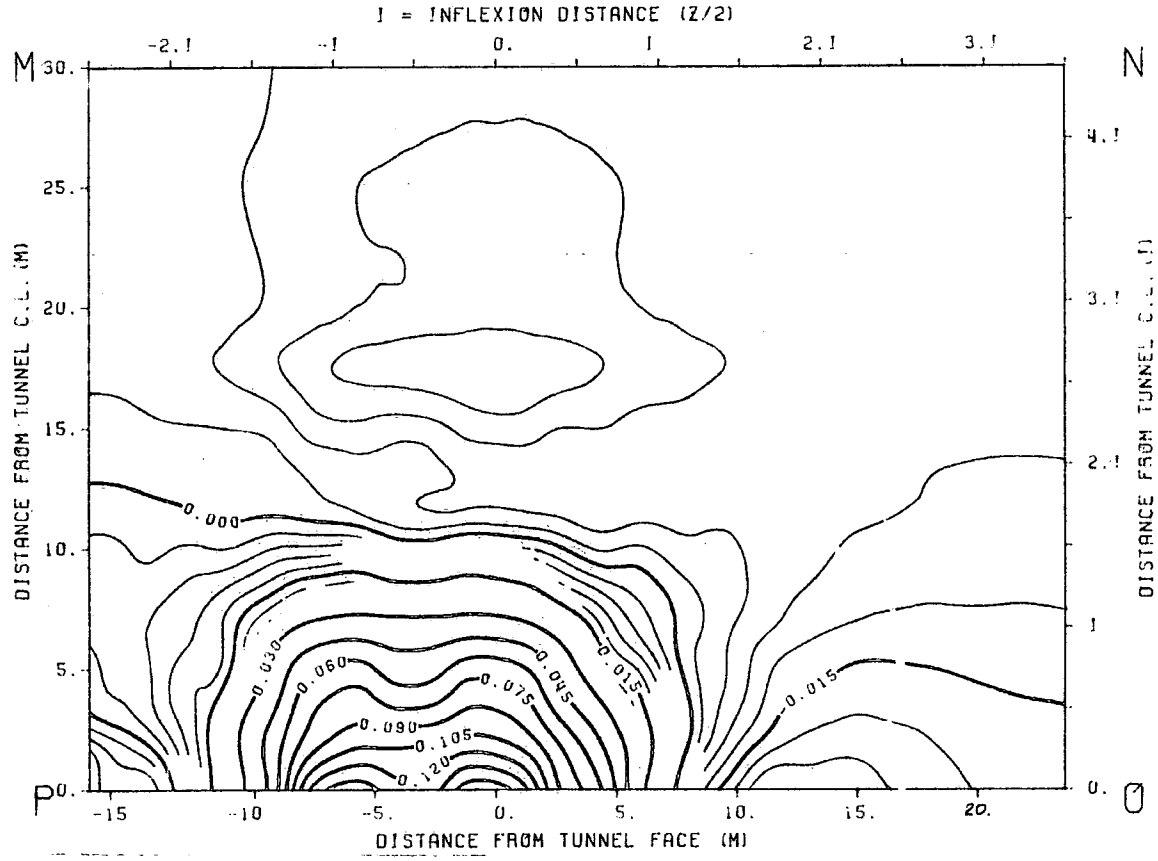

FIG. 7.5.40) Contours of equal variation of vertical strains (10^{-3} %) between steps 4 and 5. Ground surface.

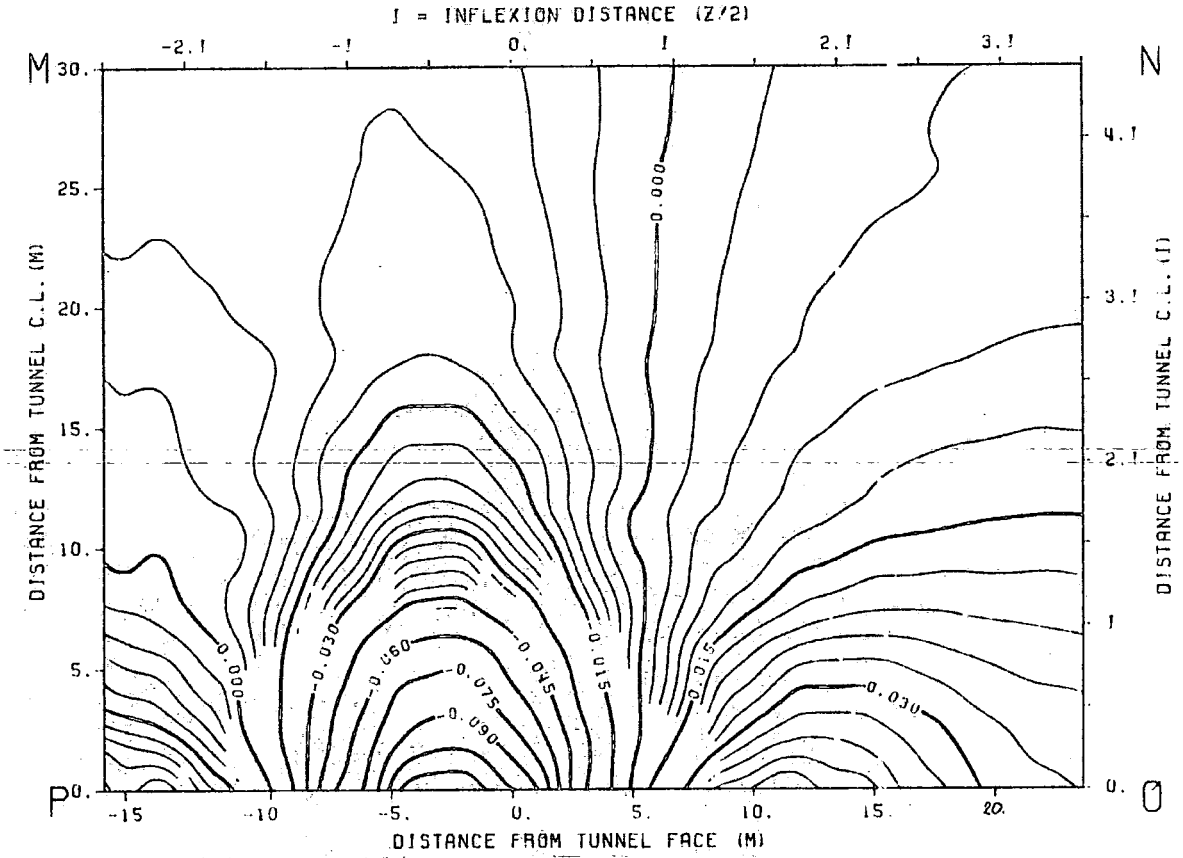

FIG. 7.5.41) Contours of equal variation of longitudinal strains (10^{-3} %) between steps 4 and 5. Ground surface.

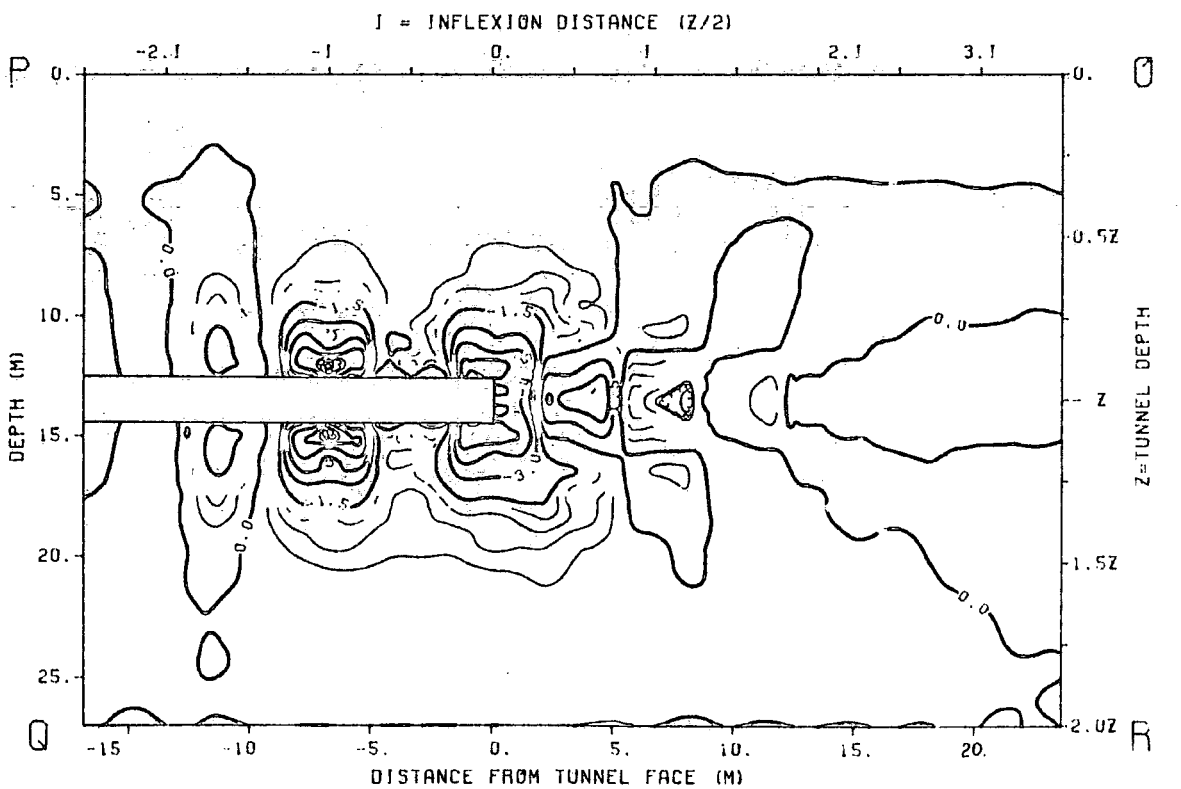

FIG. 7.5.42) Contours of equal variation of lateral strains (10^{-3} %) between steps 4 and 5. Longitudinal section.

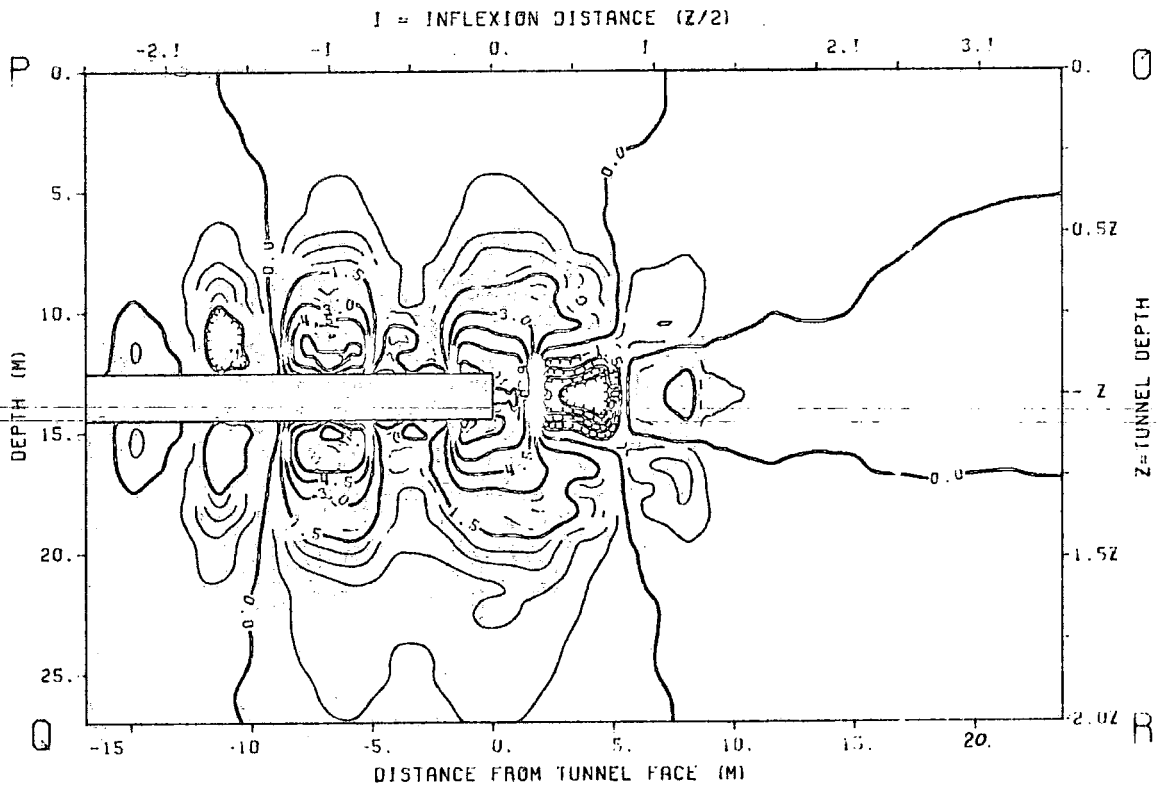

FIG. 7.5.43) Contours of equal variation of longitudinal strains (10^{-3} %) between steps 4 and 5. Ground surface.

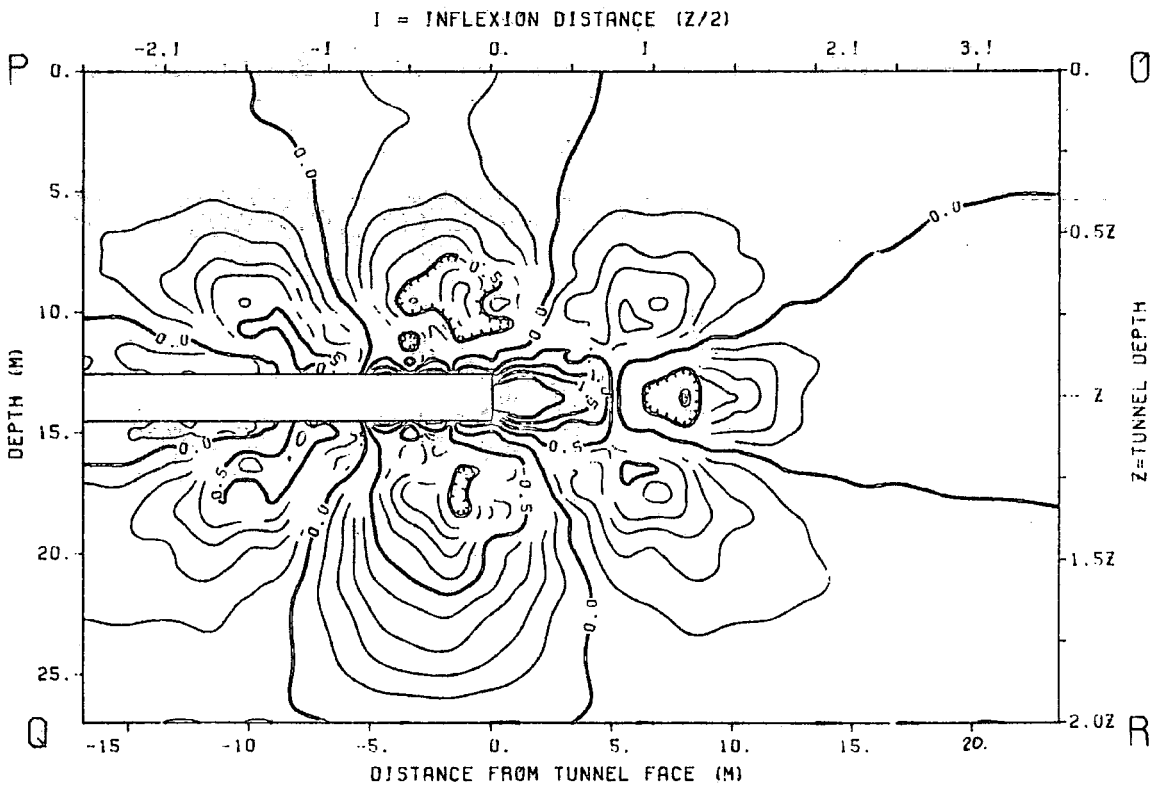

FIG. 7.5.44) Contours of equal variation of longitudinal strains (10^{-3} %) between steps 4 and 5. Longitudinal section.

CHAPTER 8

CONCLUSIONS.

A three-dimensional finite element method has been used for analysing ground movements caused by tunnelling with or without lining installation, and for investigating the response of superadjacent buried pipelines to those movements. The effect of these movements on above-ground structures has not been considered in this work. An alternative hybrid technique combining analytical/ empirical and finite element approaches to overcome some difficulties such as finite element idealization of the medium, and the computational precision necessary to analyse the soil/pipe system subjected to the ground movements, was examined. Sequences of construction, difficulties and limitations of the procedure adopted to analyse a tunnelling process with lining installation have also been discussed.

From the experience gained during the course of studying case history data of tunnelling in soft ground and performing three-dimensional finite element analyses of tunnelling in soil (with or without lining installation) and the response of buried pipelines, the following observations can be made :

1) Differential vertical movements always exist when a tunnel is excavated in soft ground. The magnitude of the settlements increases from near zero at the outer edges of a settlement trough to a maximum at some point behind and on the line of a moving disturbance source.

2) The finite element results have shown that in a settlement trough caused by tunnel excavation in soil, the points of maximum lateral displacement on the ground surface correspond to the points of zero lateral strain.

3) In a buried pipeline lying close to and parallel to the tunnel centre line, the section of the pipe located behind (or ahead of) the tunnel face may be subjected to direct longitudinal compressive (or tensile) stress higher than the bending tensile (or compressive) stress induced by differential vertical displacements.

4) The fixity conditions on the boundaries of the finite element mesh together with the positions of pipes and their directions relative to that of the moving source of ground disturbance dictate the pipe response to

the ground movements.

5) The quality of prediction of ground movement caused by tunnelling is dependent on the character, particularly the complexity, of the local surficial (soil) geology. It is necessary to adopt empirical geotechnical parameters representative of the local ground conditions.

6) The development of mathematical models in applied geomechanics must be conditioned by the following points :

a) The nature of the four interacting inputs : prescription of the ground material, the pre-existing state of stress, the imposed loading/unloading conditions and the geometrical profile of the tunnel in-situ (its size and depth).

b) The dependence of the soil properties on their stress and deformation history (although in most instances these factors can only be conjectured).

7) Despite great progress in recent years on numerical computational methods, a clear and precise definition of the safety factor for tunnel construction does not exist even today because of difficulties in modelling the soil behaviour and soil-support interaction mathematically.

8) The presence of rigid structures in soft ground reduces significantly the computed strains in some areas of the medium because the rigidity of the included

structures provides resistance to potential deformation of the medium. Therefore, it may be over-conservative to design such a structure based on the strains developed in the free field and assuming that these strains are accepted by the structure concordantly.

9) Improved knowledge and understanding of soil-structure interaction effects is required if safe and economical designs are to be produced in areas to be disturbed by tunnelling.

10) The combination of analytical/empirical and finite element methods of analysis would seen, from the experience in this work, to offer some advantages over each method used singly. It has been particularly useful in the present work for resolving displacements, stresses and strains in a structure that is small on the scale of the disturbing field.

11) Any computational method, sophisticated as it may be, can never represent real tunnel construction and its effects on nearby buried pipelines in all their complexities without much more detailed information on ground geology and in-situ deformation measurements for checks on computational veracity.

12) The selection of a suitable method for predicting ground movements at a particular site to be tunnelled is not an easy task for the designer engineer. It depends on the importance of the project, availability

of a large computer facility, the time in-hand before construction, the funds available and so on. However, it is hoped that, in the course of time, more actual observations and measurements on tunnel excavations and the behaviour of buried pipelines, together with closer matching to theoretical/analytical/ numerical calculated data will result in improvements on presently-available methods of analysis and/or development of new techniques that will enable an engineer to predict more accurately the ground movements caused by tunnelling and their effects on structures.

REFERENCES

Atkinson,J.H. and Bransby,P.L. - The Mechanics of Soils - An Introduction to Critical State Soil Mechanics, McGraw-Hill Book Co., London, 1978.

Atkinson,J.H. and Potts,D.M. - Subsidence above shallow circular tunnels in soft ground, Department of Civil Engineering, Univ. of Cambridge, Report CUED/C - Soils/T.R.27, 1976.

Attewell,P.B. - Ground movements caused by tunnelling in soil, Conference on Large Ground Movements and Structures, UWIST, Dept. of Civil Eng. and Build. Technology, Cardiff, 1977, Ed. J. D. Geddes, Publ. Pentech Press, London, 1978, pp. 812-948.

Attewell,P.B. and Boden,J.B. - Development of stability ratio for tunnels driven in clay , Tunnels and Tunnelling, Vol. 3, No. 3, May 1971, pp. 195-198.

Attewell,P.B., Farmer,I.W. and Glossop,N.H. - Ground deformation caused by tunnelling in a silty alluvial clay, Ground Engineering, November 1978, pp. 32-41.

Attewell,P.B. and Woodman,J.P. - Predicting the dynamics of ground settlement and its derivatives caused by tunnelling in soil, Ground Engineering, Vol.15, No. 8, pp. 13-22+36.

Attewell,P.B. and Yeates,J. - Tunnelling in Soil. In-Ground Movements in Engineering, Eds.Attewell,P.B. and Taylor,R.K. , Blackie and Sons Ltd., Glasgow, 1984. In press.

Brand,E.W. and Brenner,R.P. - Soft Clay Engineering, Elsevier Scientific Publishing Co., Amsterdam, The Netherlands, 1981.

Broms,B.B. and Bennermark,H. - Stability of clay at vertical openings, Journal of the Soil Mech. and Found. Div., ASCE, Vol. 93, No. SM1, Proc. Paper 5063, January 1967, pp. 71-94.

Burland,J.B., Simpson,B. and John,H.D.S. - Movements around excavations in London Clay, Symposium on Tunnelling and Deep Excavations in Soils, 27-29 April 1981 , São Paulo , Brazil , Associação Brasileira de Mecânica dos Solos, pp. 19-61.

Burland,J.B. and Wroth,C.P. - Settlement of Buildings and associated damage, Proc. Conf. of Settlements of Structures, London, pp. 611-654.

Cairncross,A.M. - Deformations around model tunnels in stiff clay, Ph.D. thesis , Cambridge University, October 1973.

Carter,J.P. - CAMFE a computer program for the analysis of a cylindrical cavity expansion in soil, CUED / C-Soils/T.R.52, 1978.

Chandrasekaran,V.S. and King,G.J.W. - Simulation of excavations using finite elements, Journal of the Geotech. Eng. Div., ASCE, Technical Notes,Vol.100, No. GT8, Proc. Paper 10744, August 1974, pp. 1086-1089.

Cheung,Y.K. and Yeo,M.F. - A Practical Introduction to Finite Element Analysis, Pitman Publishing Co. Limited, 1979.

Cording,E.J. and O'Rourke,T.D. - Excavation , ground movements and their influence on buildings, Preprint prepared for Section 40 . Protection of structures adjacent to braced excavations, October 1977, ASCE, San Francisco.

Corotis,R.B., Farzin,M.H. and Krizek,R.J. - Nonlinear stress-strain formulation for soils, Journal of the Geotech. Eng. Div., ASCE, Vol. 100, No. GT9, Proc. Paper 10811, September 1974, pp. 993-1008.

Desai,C.S. and Abel,J.F. - Introduction to the Finite Element Method - A Numerical Method for Engineering Analysis, Van Nostrand Reinhold Co., New York, 1972.

Dumbleton,M.J. and West,G. - A guide to site investigation procedures for tunnels, Transport and Road Research Laboratory, Dept. of the Environment, TRRL Laboratory Report 740, 1976, p. 23.

Duns,C.S. and Butterfield,R. - Flexible buried cylinders, Part I - Static response, Int. Journal Rock Mech. Min. Science, Vol. 8, 1970, pp. 577-600.

Ghaboussi,J.,Ranken,R.E. and Karshenas,M. - Analysis of subsidence over soft-ground tunnels, Proc. of the International Conf. Evaluation and Prediction of Subsidence, ASCE, Florida, 1978, pp. 182-196.

Ghaboussi,J. and Gioda,G. - On the time-dependent effects in advancing tunnels, Int. Journal for Numerical and Analytical Methods in Geomechanics , Vol. 1, 1977, pp. 249-269.

Glossop,N.H. and Farmer,I.W. - Settlement associated with removal of compressed air pressure during tunnelling in alluvial clay, Geotechnique,Vol. 29, No. 1, 1979, pp. 67-72.

Glossop,N.H. and O'Reilly,M.P. - Settlement caused by tunnelling through soft marine silty clay, Tunnels and Tunnelling , Vol. 14 , No. 9 , October 1982, pp. 13-16.

Gordon,R.I.G. - Ground movements associated with soft ground tunnelling and its effects on buried services, Dissertation : MSc Advanced Course in Engineering Geology, University of Durham, 1981.

Gudehus,G. - Finite Elements in Geomechanics, John Wiley & Sons, New York, 1977.

Hanafy,E.A. Emery,J.J. - Advancing face simulation of tunnel excavations and lining placement, Second Conf. on Large Ground Mov. and Struct., UWIST, Dept. of Civil Eng. and Build Technology, Cardiff , 1980 , Ed. J. D. Geddes, Publ. Pentech Press, London, pp. 1-17.

Hinton,E. and Owen,D.R . - Finite Element Programming, Academic Press, London, 1977.

Howland,A.F. - The prediction of the settlement above soft ground tunnels by considering the groundwater response with the aid of flow net constructions, Second Conf. on Large Ground Mov. and Struct., UWIST, Dept. of Civil Eng. and Build. Technology, Cardiff, April 1980, Ed. J.D. Jones, Publ. Pentech Press, London, pp. 1-13.

Huang,Y.H. - Consolidation-time relationship for layered clays, Journal of the Soil Mech. and Found. Div., ASCE, Vol. 96, No. SM1, Proc. Paper 7022, 1967, pp. 371-375.

Huang,R.N. and Lysmer,J. - Response of buried structures to travelling waves, Journal of the Geotech. Eng. Div., ASCE, Vol. 107, No. GT2, Proc. Paper 16052, February 1981, pp. 183-200.

Hurrell, M.R. - Monitoring of ground and structural response to shield tunnelling is soft ground beneath Collingwood Street in Newcastle upon Tyne, Project Supervisor P.B. Attewell, Report presented to Northumbrian Water Authority and Water Research Centre, Swindon, Engineering Geology Laboratories, University of Durham, June 1983, p. 40.

Ishihara,K. - Relations between process of cutting and uniqueness of solution, Soils and Foundations, Vol. 10, No. 3, September 1970, pp. 27-35.

Kawamoto,T. and Okuzono,K. - Analysis of ground surface settlement due to shallow shield tunnels, Intern. Journal for Numerical and Analytical Methods in Geomechanics, Vol. 1, 1977, pp. 271-281.

Lee,K.L. and Shen,C.K. - Horizontal movements related to subsidence, Journal of the Soil Mech. and Found. Div., ASCE, Vol. 95, No. SM1 , Proc. Paper 6336, January 1969, pp. 139-166.

Lee,I.K., White,W. and Ingles,O.G. - Geotechnical Engineering , Pitman Publishing Limited , Massachussets, 1983.

Mair,R.J., Gunn,M.J. and O'Reilly,M.P. - Ground movements around shallow tunnels in soft clay, Tunnels and Tunnelling, Vol. 14, No. 5, June 1982, pp. 45-48.

Matsushita,H. - Earth pressure balanced shield method, Tunnels and Tunnelling, Vol. 12. No. 1, January / February 1980, pp. 47-49.

Meek,J.L. - Excavation in rock. An appreciation of the finite element method of analysis, Proc. of the 1973 Tokyo Seminar on Finite Element Analysis, Univ. of Tokyo Press, pp. 195-213.

Myrianthis,M.L. - Quelques relations phenomenologiques sur le tassement d'un terrain de faible resistance surmontant un tunnel, Ann. Inst. Techn. Bat. Trav. Publ, Suppl., No. 317, 1974, pp.118-128.

Nath,P. - Finite elements analysis of a large diameter buried steel pipeline, Transport and Road Research Laboratory, Dept. of Environment and Dept. of Transport , TRRL Laboratory Report 778, 1977.

Nayak,G.C., Prakash, S. and Gupta,R. - Finite element analysis of ditch conduits, Int. Symp. on Soil-structure Interaction , Univ. of Roorkee, Roorkee, India, 1977, pp. 1-8.

Negro,A. and Eisenstein,Z. - Ground control techniques compared in three Brazilian water tunnels, Part I, Tunnels and Tunnelling , Vol. 13 , No. 9, October 1981, pp. 11-14.

Negro,A. and Eisenstein,Z. - Ground control techniques compared in three Brazilian water tunnels, Part II , Tunnels and Tunnelling , Vol. 13 , No. 10 , November 1981, pp. 52-54.

Negro,A. and Eisenstein,Z. - Ground control techniques compared in three Brazilian water tunnels , Part III, Tunnels and Tunnelling , Vol. 15 , No. 11 , December 1981, pp. 48-50.

New,B.M., Wild,P.T. and Bishop,C.J. - Bentonite tunnelling beneath major services in loose ground , Tunnels and Tunnelling , Vol. 12 , No. 15 , June 1980 , pp. 14-16.

Norrie,D.R.J. and Vries,G. - An Introduction to Finite Element Analysis , Academic Press , London , 1978.

O'Reilly,M.P. and New,B.M. - Settlements above tunnels in the United Kindom - Their magnitude and prediction, Tunnelling'82, Proc. of the Symposium, London , Ed. M.J. Jones, Published Inst. of Mining and Metallurgy, pp. 173-181.

O'Reilly,M.P., Ryley,M.D., Barratt,D.A. and Johnson,P.E. - Comparison of settlements resulting from three methods of tunnelling in loose cohesioless soil , Second Conf. on Large Ground Mov. and Struct., UWIST, Dept. of Civil Eng. and Build. Technology, Cardiff, April 1980, Ed. J.D. Jones, Publ. Pentech Press, London, pp. 1-18.

Rowe,R.K., Lo,K.Y. and Kack, G.J. - A method of estimating surface settlement above tunnels constructed in soft ground, Canadian Geotech. Journal , Vol. 20, No. 1, February 1983, pp. 11-22.

Sagaseta,C., Moya,J.F. and Oteo,C.S. - Estimation of ground subsidence over urban tunnels, Second Conf. on Large Ground Mov. and Struc. , UWIST , Dept. of Civil Enf. and Build. Technology , Cardiff , April 1980, Ed.J.D. Geddes, Publ. Pentech Press, London, pp. 1-15.

Sandhu,R.S. and Wilson,E.L. - Finite element analysis of land subsidence , Proc. Int. Symposium on Land Subsidence , Int. Assoc. Hydr. Research , Tokyo, 1969, pp. 393-400.

Sakurai,S. - Approximate time-dependent analysis of tunnel support structure considering progress of tunnel face, Int. Journal for Numerical and Analytical Method in Geomechanics, Vol. 2, 1978, pp. 159-175.

Schwartz,C.W., Azzouz,A.S. and Einstein,H.H. - Example cost fo 3-D FEM for underground openings , Journal of the Geotech. Eng. Div., ASCE, Vol.108, No. GT9, September 1982, pp. 1186-1191.

Seneviratne,H.N. - Deformations and pore pressure dissipation around shallow tunnels in soft clay, Ph.D. thesis, Univ. of Cambridge, 1979.

Shen,C.K., Bang,S. and Hermann,L.R. - Ground movement analysis of earth support system , Journal of the Geotech. Eng. Div. , ASCE , Vol. 107 , No. GT12 , Proc. Paper 16732 , December 1981 , pp. 1609-1624.

Skempton,A.W. and MacDonald,D.H. - Allowable settlement in buildings , Proc. Inst. Civil Eng. , Vol. 5 , Part III, 1956, pp. 727-768.

Schmidt,B. - Settlements and ground movements associated with tunnelling in soil , Ph.D. thesis , Univ. of Illinois, 1969.

Sozio,L.E. - Settlements in a Sao Paulo shield tunnel , Tunnels and Tunnelling, Vol. 10 , No. 7, September 1978, pp. 53-55.

Sweet,A.L. and Bogdanoff,J.L. - Stochastic model for predicting subsidence , Journal of the Eng. Mech. Div., Proc. of the ASCE , Vol. 91 , No. EM2 , April 1965, pp. 21-45.

Thomson,S. and El-Nahhas,F. - Field measurements in two tunnels in Edmonton , Alberta , Canadian Geotech. Journal, Vol. 17, No. 1, February 1980, pp. 20-23.

Toombs,A.F. and West,G. - Ground movements as a result of thrust boring through a railway embankment,Tunnels and Tunnelling , Vol. 12 , No. 8 , September 1980, pp. 11-16.

Tsutsumi,M. - Simulação de escavação escorada por meio de elementos isoparamétricos , MSc. thesis , COOPE - Universidade Federal do Rio de Janeiro, 1975.

Valliapan,S. Matsuzaki,K. and Raja Sekar,H.L. - Nonlinear stress analysis of buried pipes, Int. Symposium on Soil-Structure Interaction , Univ. of Roorkee , Roorkee, India, 1977, pp. 1-8.

Voight,B. and Pariseau,W. - State of predictive art in subsidence in engineering , Journal of the Soil Mech. and Found. Div. , ASCE , Vol. 96 , No. SM2 , Proc. Paper 7187, March 1970, pp. 721-750.

Wahls,H.E. - Tolerable settlement of buildings, Journal of the Geotech. Eng. Div., ASCE , Vol. 107, No. GT11, Proc. Paper 16628 , November 1981 , pp. 1489-1504.

Wilson,N.E. - Stress re-distribution around tunnels and shafts resulting in small ground movements, Second Conf. on Large Ground Mov. and Struct. , UWIST , Dept. of Civil Eng. and Build. Technology , Cardiff, April 1980, Ed.J.D. Geddes, Publ. Pentech Press, London, pp. 1-15.

Wood,L.A. and Larnach,W.J. - The interactive behaviour of a soil - structure system and its effect on settlements , Symp. on Recent Development in the Analysis of Soil Behaviour and Their Application to Geotech. Struct., July 1975, Univ. of New South Wales, Australia, pp. 75-87.

Ziekiewicz,O.C. - The Finite Element Method in Engineering Science, McGraw-Hill, London, 1971.

APPENDIX A

SUBROUTINE DESCRIPTIONS AND DETAILS

ACTIVE - Calculates the element stiffness matrix and stores it in file number 9. This routine is called when elements are activated at a designated step.

MESH - Read input data. Coordinates, stresses, boundary conditions and element node numbers are given in a similar way to that in two - dimensional analysis. The routine will generate the mesh automatically in the direction of the tunnel centre line.

LINEAR - Reads material properties.

EXCTN - Defines the surface of tunnel to be excavated.

DEFIN - Defines the geometry of the opening in the first transverse section.

JACOB - Calculates the inverse Jacobian matrix and the strain/stress matrix.

AMATRX - Prepares the abscissa and weight coefficients for the Gaussian quadrature integration. Three integration points for each direction were used.

FORCE1 - Calculates the equivalent nodal forces on the boundary of the opening from the initial stresses.

MSHOUT - Prints out the problem data.

RIGID - Stores stiffness matrix of elements located between first and second transverse sections of the mesh in file 11.

ZIB8 - Calculates the element stiffness matrix.

DDFIN - Defines the boundary of loading forces.

DISPLAC - Reads input prescribed displacements.

FORCE3 - Calculates the equivalent forces to input prescribed displacements.

LODTYP - Reads and defines loading conditions.

STEPS - Defines applied forces for each step.

LODCON - Reads concentrated forces.

LLOAD - Defines applied forces for each node.

STIFF - Assembles the global stiffness matrix and sets up load vectors. Requires file number 3.

MODIFY - Sets up mesh boundary conditions into the global stiffness matrix.

FORCE2 - Calculates forces equivalent to the displacement on nodes located on the excavated surface. This routine is called if the excavation is simulated in incremental process.

BANSOL - Solves system of linear equations by the Gauss elimination method to obtain increments of nodal displacements. Requires file numbers 1 and 3.

COMPUT - Calculates stresses and strains for each node.

OUTPUT - Prints out calculated results.

FILE12 - Stores nodal coordinates, displacements, stresses and strain in file number 12.

APPENDIX B

LISTING OF THE PROGRAM FEP3DES.

A listing of the program is included at the end of this thesis, and its general description is presented in Chapter 5.

Detailed action of each subroutine included in FEP3DES is described in Appendix A.

APPENDIX C

LISTING OF THE PROGRAM GRAF.

A listing of the program GRAPH is included at the end of this thesis. This program selects appropriate variables (displacements, stresses or strains) calculated by the program FEP3DES and prepares them to be contoured by using GPCP public package program.

A P P E N D I X B

```
C*********************************************************************
C   FEP3DES : FINITE ELEMENT PROGRAM FOR 3-D ELASTIC SOLUTION USING
C             3-NODE   HEXAHEDRAL   RECTANGULAR   ELEMENTS   (ZIB8).
C             REQUIRES 3 TEMPORARY FILES : 1,3 AND 11 (OR 4 TEMPORARY
C             FILES (1,3,9 & 11) IF LINING PLACEMENT IS SIMULATED) AND
C             ONE PERMANENT FILE (12).
C                                                LAST REVISION : 14/JUN/83.
C*********************************************************************
      COMMON /BLCK01/ TITLE(20), NUMEL, NUMNP, NUMPLN, NPPLN, NELINT
      COMMON /BLCK02/ DESLOC(3,1122), DEFOR(1122,6), SIGMA(1122,6), NODE
      COMMON /BLCK03/ CENTRO(2), RADIUS, DEPTH, FACTOR, LINER, NSTEPS,
     1       LOAD(3)
      COMMON /BLCK04/ DISPL(6732), NPO(3)
      COMMON /BLCK09/ COORD(3,1122), FXYZ(3,1122), ZDIST, NCODE(1122)
      PRINT 60
      PRINT 40
      PRINT 60
      JVEZ = 0
C   READ AND GENERATE MISSING INPUT DATA.
      CALL MESH
C   READ MATERIAL PROPERTIES.
      CALL LINEAR
C   OUTPUT MESH DATA.
      CALL MSHOUT
      DO 10 I = 1, NUMNP
        DO 10 J = 1, 3
          DEFOR(I,J) = 0.0
          DEFOR(I,J + 3) = 0.0
          FXYZ(J,I) = 0.0
          DESLOC(J,I) = 0.0
   10 DISPL(3*I + J - 3) = 0.0
C   INPUT CONTRUCTION OR LOADING TYPE.
      CALL LODTYP
C   COMPUTE APPLIED FORCES FOR EACH STEP.
      CALL STEPS
C   COMPUTE AND STORE STIFFNESS MATRIX OF ELEMENTS TO BE ACTIVATED.
      CALL RIGID
      PRINT 50
   20 JVEZ = JVEZ + 1
      IF (JVEZ .EQ. 3) STOP
      CALL LLOAD(JVEZ)
      CALL STIFF(JVEZ)
      CALL BANSOL
      CALL COMPUT(JVEZ)
      CALL OUTPUT(JVEZ)
      CALL FIL812(JVEZ)
      IF (JVEZ .EQ. NSTEPS) STOP
      GO TO 20
   30 FORMAT (20A4)
   40 FORMAT (//, ' FEP3DES : FINITE ELEMENT PROGRAM FOR 3-D ELASTIC SOL
     1UTION USING 8-NODE HEXAHEDRAL RECTANGULAR ELEMENTS (ZIB8)', /, 1X,
     2       7('*'), 3X, 99('='), /, 11X,
     3       'WRITTEN AT UNIVERSITY OF DURHAM BY M.TSUTSUMI (1983)', /,
     4       11X, 52('='), /, 11X, 'LAST REVISION : 14/JUN/1983.', /,
```

```
     5       11X, 27('=='))
    50 FORMAT (//, 30X, 34('*'), /, 28X, '  *** DATA PREPARATION COMPLETE
      1D ***', /, 30X, 34('*'))
    60 FORMAT (//, 1X, 120('*'))
       END



C*********************************************************************
       SUBROUTINE MESH
C*********************************************************************
       DIMENSION DSIG(6)
       COMMON /BLCK01/ TITLE(20), NUMEL, NUMNP, NUMPLN, NPPLN, NELINT
       COMMON /BLCK02/ DESLOC(3,1122), DEFCR(1122,6), SIGMA(1122,6), NODE
       COMMON /BLCK03/ CENTRO(2), RADIUS, DEPTH, FACTOR, LINER, NSTEPS,
      1        LOAD(8)
       COMMON /BLCK06/ IX(840,9), KL
       COMMON /BLCK09/ COORD(3,1122), EXYZ(3,1122), ZDIST, NCODE(1122)
       COMMON /BLCK12/ GLOBL(702,351), MBAND, NUMBLK, NEQBLK
C    NPPLN  = NUMBER OF NODES PER SECTION.
C    NELINT = NUMBER OF ELEMENTS BETWEEN TWO CONCROSS SECUTIVE SECTIONS.
C    NUMPLN = NUMBER OF CROSS SECTIONS.
C    ZDIST  = DISTANCE BETWEEN TWO CONCROSS SECUTIVE CROSS SECTIONS.
       READ 270, (TITLE(I),I=1,20)
       READ 300, NPPLN, NELINT, NUMPLN, NODE, ZDIST, FACTOR, RADIUS
C    CENTRO = CO-ORDINATE OF TUNNEL CENTRE(X-DIR=1;Y DIREC=2)
C    LINER=1 --> IF LINING IS PLACED.
       LINER = 0
       IF (RADIUS .NE. 0.0) READ 310, LINER, (CENTRO(I),I=1,2), DEPTH
       NUMBLK = 0
       NEQBLK = 0
       NUMNP = NUMPLN * NPPLN
       NUMEL = NELINT * (NUMPLN - 1)
       IF (NUMNP .LE. 1122 .AND. NUMEL .LE. 840) GO TO 10
       PRINT 320, NUMNP, NUMEL
       STOP
C
C    INPUT DATA FOR NODES LOCATED IN THE FIRST SECTION ONLY.
C
C     DIRECTION X = HORIZONTAL (POSITIVE LEFT TO RIGHT)
C     DIRECTION Y = VERTICAL (POSITIVE UPWARD)
C     DIRECTION Z = PERPENDICULAR TO XY PLANE (POSITIVE FORWARD)
C
C    NCODE=1 - RESTRAINED TO MOVE LATERALLY (X-DIRECTION).
C    NCODE=2 - RESTRAINED TO MOVE VERTICALLY (Y-DIRECTION).
C     NCODE=3 - RESTRAINED TO MOVE PARALLEL TO THE TUNNEL CENTRE LINE
C  (Z-DIRECTION).
C    NCODE=4 - ALLOWED TO MOVE IN Z-DIRECTION ONLY.
C    NCODE=5 - ALLOWED TO MOVE IN X-DIRECTION ONLY.
C    NCODE=6 - ALLOWED TO MOVE IN Y-DIRECTION ONLY.
C    NCODE=7 - NODE RESTRAINED TO MOVE IN ALL DIRECTIONS.
    10 L = 0
C    I     = NODE NUMBER
C    NCODE = NODAL CODE ACCORDING TO ABOVE LISTING.
    20 READ 290, I, NCODE(I), COORD(1,I), COORD(2,I), SIGMA(I,1),
      1SIGMA(I,2)
       COORD(3,I) = 0.0
       SIGMA(I,3) = SIGMA(I,1)
       DO 30 J = 4, 6
         DSIG(J - 3) = 0.0
```

```
      DSIG(J) = 0.0
   30 SIGMA(I,J) = 0.0
      IF (I .EQ. (L + 1)) GO TO 50
      IL = I - L
      DX = (COORD(1,I) - COORD(1,L)) / FLOAT(IL)
      DY = (COORD(2,I) - COORD(2,L)) / FLOAT(IL)
      DO 40 JL = 1, 3
   40 DSIG(JL) = (SIGMA(I,JL) - SIGMA(L,JL)) / FLOAT(IL)
   50 L = L + 1
      IF (I - L) 90, 80, 60
   60 NCODE(L) = NCODE(L - 1)
      IF (NCODE(L) .NE. 7) NCODE(L) = 0
      COORD(1,L) = COORD(1,L - 1) + DX
      COORD(2,L) = COORD(2,L - 1) + DY
      COORD(3,L) = 0.0
      DO 70 MM = 1, 6
   70 SIGMA(L,MM) = SIGMA(L - 1,MM) + DSIG(MM)
      GO TO 50
   80 IF (NPPLN - I) 90, 100, 20
   90 PRINT 330, I
      STOP
  100 CONTINUE
      LL = NPPLN + 1
      DO 110 J = LL, NUMNP
        NCODE(J) = NCODE(J - NPPLN)
        COORD(1,J) = COORD(1,J - NPPLN)
        COORD(2,J) = COORD(2,J - NPPLN)
        COORD(3,J) = COORD(3,J - NPPLN) + ZDIST
        DO 110 MM = 1, 6
  110 SIGMA(J,MM) = SIGMA(J - NPPLN,MM)
      NPP = NUMNP - NPPLN + 1
      DO 120 NP = NPP, NUMNP
        NCODE(NP) = 3
        IF (NCODE(NP - NPPLN) .EQ. 1) NCODE(NP) = 6
        IF (NCODE(NP - NPPLN) .EQ. 2) NCODE(NP) = 5
        IF (NCODE(NP - NPPLN) .GE. 4) NCODE(NP) = NCODE(NP - NPPLN)
  120 CONTINUE
      N = 0
C
C    INPUT DATA FOR ELEMENTS LOCATED IN THE FIRST 'SLICE' ONLY'.
C    (INPUT FIRST FOUR NODE NUMBERS ONLY FOR EACH ELEMENT).
C    IX(ELEMENT,9) = MATERIAL NUMBER
  130 READ 230, M, (IX(M,I),I=1,4), IX(M,9)
  140 N = N + 1
      IF (M - N) 170, 170, 150
  150 DO 160 I = 1, 4
  160 IX(N,I) = IX(N - 1,I) + 1
      IX(N,9) = IX(N - 1,9)
  170 IF (M - N) 180, 180, 140
  180 IF (NELINT - N) 190, 190, 130
  190 CONTINUE
      DO 200 M = 1, NELINT
        DO 200 I = 5, 8
  200 IX(M,I) = IX(M,I - 4) + NPPLN
      LL = NELINT + 1
      DO 220 I = LL, NUMEL
        DO 210 J = 1, 8
  210   IX(I,J) = IX(I - NELINT,J) + NPPLN
  220 IX(I,9) = IX(I - NELINT,9)
      J = 0
```

```
C
C    BAND WIDTH COMPUTATION.
      DO 250 N = 1, NELINT
        DO 250 I = 1, 4
          DO 240 L = I, 4
            KK = IX(N,I) - IX(N,L)
            IF (KK .LT. 0) KK = -KK
            IF (KK - J) 240, 240, 230
  230       J = KK
            JEL = N
  240     CONTINUE
  250 CONTINUE
      MBAND = 3 * (J + NPPLN) + 3
      IF (MBAND .GT. 351) GO TO 260
      RETURN
  260 PRINT 340
      STOP
  270 FORMAT (20A4)
  280 FORMAT (16I5)
  290 FORMAT (2I5, 5F10.0)
  300 FORMAT (4I5, 3F10.0)
  310 FORMAT (I5, 7F10.0)
  320 FORMAT ('0EXCESSIVE SIZE OF MESH, NUMNP =', I5, '   NUMEL =', I5)
  330 FORMAT (/, '  ERROR IN INPUT DATA : NODE NUMBER =', I5, //,
     1        '  PROGRAM STOPPED DUE TO ABOVE ERROR', /, 2X, 33('*'))
  340 FORMAT (/, ' PROGRAM STOPPED DUE TO EXCESSIVE BAND WIDTH', /, 43(
     1        '*'))
      END



C*********************************************************************
      SUBROUTINE LINEAR
C*********************************************************************
      COMMON /BLCK07/ YOUNG(10), POISS(10), NMAT
      READ 30, NMAT
      IF (NMAT .LE. 10) GO TO 10
      PRINT 50, NMAT
      STOP
   10 DO 20 I = 1, NMAT
   20 READ 40, MAT, YOUNG(MAT), POISS(MAT)
   30 FORMAT (I5)
   40 FORMAT (I5, 2F10.0)
   50 FORMAT ('0TOO MANY MATERIALS - NMAT =', I5, /, 1X, 32('*'))
      RETURN
      END



C*********************************************************************
      SUBROUTINE EXCVTN(KKK)
C*********************************************************************
      COMMON /BLCK01/ TITLE(20), NUMEL, NUMNP, NUMPLN, NPPLN, NELINT
      COMMON /BLCK03/ CENTRO(2), RADIUS, DEPTH, FACTOR, LINER, NSTEPS,
     1        LOAD(9)
      COMMON /BLCK05/ NELESC(100,8), NDEACT(3), NPERON(550,8),
     1        NNERON(9), NELERO(550,8), NELE(9), NPDEAC(550,8),
     2        NNDEAC(9), NSLICE(8), NELACT(100,9), NACT(3)
      COMMON /BLCK06/ IX(840,9), KL
      COMMON /BLCK13/ TELESC(100), IDEACT, IPERON(100), INERON,
```

```
     1       IELFRO(100), IELF, IPDEAC(100), INDEAC
      JACT = 0
      JDEACT = 0
      JNFRON = 0
      JELF = 0
      JNDEAC = 0
      NSLIC = 0
      DO 10 I = 1, KKK
   10 NSLIC = NSLIC + NSLICE(I)
      DO 20 I = 1, NSLIC
        DO 20 J = 1, IDEACT
          JDEACT = JDEACT + 1
   20 NELESC(JDEACT,KKK) = IELESC(J) + (I - 1) * NELINT
      KSLIC = NSLIC + 1
      DO 30 I = 1, KSLIC
        DO 30 J = 1, INFRON
          JNFRON = JNFRON + 1
   30 NPFRON(JNFRON,KKK) = IPFRON(J) + (I - 1) * NPPLN
      DO 40 I = 1, NSLIC
        DO 40 J = 1, IELF
          JELF = JELF + 1
   40 NELFRO(JELF,KKK) = IELFRO(J) + (I - 1) * NELINT
      DO 50 J = 1, NSLIC
        DO 50 I = 1, INDEAC
          JNDEAC = JNDEAC + 1
   50 NPDEAC(JNDEAC,KKK) = IPDEAC(I) + (J - 1) * NPPLN
      IF (NSLIC .GE. (NUMPLN - 1)) GO TO 90
      DO 60 I = 1, INDEAC
        JNFRON = JNFRON + 1
   60 NPFRON(JNFRON,KKK) = IPDEAC(I) + NSLIC * NPPLN
      DO 70 I = 1, IELF
        JELF = JELF + 1
   70 NELFRO(JELF,KKK) = IELFRO(I) + NSLIC * NELINT
      DO 80 I = 1, IDEACT
        JELF = JELF + 1
   80 NELFRO(JELF,KKK) = IELESC(I) + NSLIC * NELINT
   90 IF (NSLIC = (NUMPLN - 1)) 120, 100, 120
  100 DO 110 I = 1, INDEAC
        JNDEAC = JNDEAC + 1
  110 NPDEAC(JNDEAC,KKK) = IPDEAC(I) + NSLIC * NPPLN
  120 IF (LINER .EQ. 0) GO TO 140
      NSLIC = NSLIC - 1
      IF (NSLIC .EQ. 0) GO TO 140
      DO 130 I = 1, NSLIC
        DO 130 J = 1, IDEACT
          JACT = JACT + 1
  130 NELACT(JACT,KKK) = IELESC(J) + (I - 1) * NELINT
  140 NDEACT(KKK) = JDEACT
      NNFRON(KKK) = JNFRON
      NNDEAC(KKK) = JNDEAC
      NELF(KKK) = JELF
      NACT(KKK) = JACT
      PRINT 160, KKK, NDEACT(KKK), NNFRON(KKK), NNDEAC(KKK), NELF(KKK),
     1NACT(KKK)
      PRINT 170
      PRINT 150, (NELESC(I,KKK),I=1,JDEACT)
      PRINT 180
      PRINT 150, (NPFRON(L,KKK),L=1,JNFRON)
      PRINT 190
      PRINT 150, (NPDEAC(I,KKK),I=1,JNDEAC)
```

```
      PRINT 200
      PRINT 150, (NELFRO(I,KKK),I=1,JELF)
      IF (JACT .EQ. 0) RETURN
      PRINT 210
      PRINT 150, (NELACT(I,KKK),I=1,JACT)
  150 FORMAT (16I5)
  160 FORMAT (/, ' STEP NO.', I2, ' - EXCAVATION DATA', /, 1X, 29('='),
     1        /, ' 1.1 NUMBER OF ELEMENTS DEACTIVATED.....................='
     2        , I4/
     3        ' 1.2 NUMBER OF NODES EXPOSED BY EXCAVATION.............=',
     4        I4/' 1.3 NUMBER OF NODES DEACTIVATED.....................='
     5        , I4/
     6        ' 1.4 NUMBER OF ELEMENTS EXPOSED BY EXCAVATION.........=',
     7        I4/' 1.5 NUMBER OF ELEMENTS ACTIVATED.....................='
     8        , I4, /)
  170 FORMAT (/, ' 2.DEACTIVATED ELEMENTS.')
  180 FORMAT (/, ' 3.NODES EXPOSED BY EXCAVATION.')
  190 FORMAT (/, ' 4.DEACTIVATED NODES.')
  200 FORMAT (/, ' 5.ELEMENTS EXPOSED BY EXCAVATION.')
  210 FORMAT (/, ' 6.ACTIVATED ELEMENTS.')
      RETURN
      END



C*********************************************************************
      SUBROUTINE DEFIN
C*********************************************************************
      DIMENSION ICUBO(30), MP(100), NELCOC(100)
      COMMON /BLCK01/ TITLE(20), NUMEL, NUMNP, NUMPLN, NPPLN, NELINT
      COMMON /BLCK03/ CENTRO(2), RADIUS, DEPTH, FACTOR, LINER, NSTEPS,
     1        LOAD(8)
      COMMON /BLCK06/ IX(840,9), KL
      COMMON /BLCK09/ COORD(3,1122), EXYZ(3,1122), IDIST, NCODE(1122)
      COMMON /BLCK13/ IELESC(100), IDEACT, IPFRON(100), INFRON,
     1        IELFRO(100), IELF, IPDEAC(100), INDEAC
      INFRON = 0
      IELF = 0
      NEL = 0
      IDEACT = 0
      INDEAC = 0
      X1 = CENTRO(1) + RADIUS
      X2 = CENTRO(1) - RADIUS
      Y1 = CENTRO(2) + RADIUS
      Y2 = CENTRO(2) - RADIUS
      DO 20 KL = 1, NELINT
        NELCOD(KL) = 1
        DO 10 I = 1, 4
          NO = IX(KL,I)
          IF (COORD(2,NO) .GT. Y1 .OR. COORD(2,NO) .LT. Y2)
     1        GO TO 20
          IF (COORD(1,NO) .GT. X1 .OR. COORD(1,NO) .LT. X2)
     1        GO TO 20
   10   CONTINUE
        NEL = NEL + 1
        ICUBO(NEL) = KL
   20 CONTINUE
      ML = 0
      DO 30 I = 1, NEL
        L = 0
```

```
      KL = ICUBO(I)
      DO 60 J = 1, 4
        NO = IX(KL,J)
        XNP = COORD(1,NO)
        YNP = COORD(2,NO)
        COMP = SQRT((XNP - CENTRO(1))**2 + (YNP - CENTRO(2))**2)
        IF (COMP .EQ. 0.0) GO TO 50
        ANG1 = ABS(XNP - CENTRO(1)) / COMP
        ANG2 = ABS(YNP - CENTRO(2)) / COMP
        IF (ANG2 .EQ. 1.0) GO TO 30
        XCSUP = CENTRO(1) + 0.95 * ANG1 * RADIUS
        XCMAX = CENTRO(1) + 1.05 * ANG1 * RADIUS
        XCINF = CENTRO(1) - 0.95 * ANG1 * RADIUS
        XCMIN = CENTRO(1) - 1.05 * ANG1 * RADIUS
        IF (XNP .GT. XCMAX .OR. XNP .LT. XCMIN) GO TO 80
        IF (XNP .GT. XCINF .AND. XNP .LT. XCSUP) GO TO 50
        GO TO 40
 30     YCMAX = CENTRO(2) + 1.05 * ANG2 * RADIUS
        YCSUP = CENTRO(2) + 0.95 * ANG2 * RADIUS
        YCINF = CENTRO(2) - 0.95 * ANG2 * RADIUS
        YCMIN = CENTRO(2) - 1.05 * ANG2 * RADIUS
        IF (YNP .GT. YCMAX .OR. YNP .LT. YCMIN) GO TO 80
        IF (YNP .LT. YCSUP .AND. YNP .GT. YCINF) GO TO 50
 40     ML = ML + 1
        MP(ML) = NO
 50     L = L + 1
 60   CONTINUE
      IF (L - 4) 30, 70, 80
 70   IDEACT = IDEACT + 1
      IELESC(IDEACT) = KL
      NELCOD(KL) = 0
 80 CONTINUE
    NL = ML - 1
    DO 90 I = 1, NL
      N1 = MP(I)
      K = I + 1
      DO 90 J = K, ML
        N2 = MP(J)
        IF (N1 .EQ. N2) MP(J) = 0
 90 CONTINUE
    DO 100 I = 1, ML
      IF (MP(I) .EQ. 0) GO TO 100
      INFRON = INFRON + 1
      IPFRON(INFRON) = MP(I)
100 CONTINUE
    DO 130 I = 1, IDEACT
      KL = IELESC(I)
      DO 130 J = 1, 4
        NO = IX(KL,J)
        DO 110 K = 1, INFRON
          NF = IPFRON(K)
          IF (NO .EQ. NF) GO TO 130
110     CONTINUE
        INDEAC = INDEAC + 1
        IPDEAC(INDEAC) = NO
        IF (INDEAC .EQ. 1) GO TO 130
        I1 = INDEAC - 1
        LL = INDEAC
        DO 120 I2 = 1, I1
          N1 = IPDEAC(I2)
```

```
          I3 = I2 + 1
          DO 120 I4 = I3, LL
            N2 = IPDEAC(I4)
            IF (N1 .NE. N2) GO TO 120
            INDEAC = INDEAC - 1
            GO TO 130
  120     CONTINUE
  130 CONTINUE
      DO 160 KL = 1, NELINT
        IF (NELCOD(KL) .EQ. 0) GO TO 160
        DO 140 I = 1, 4
          NO = IX(KL,I)
          DO 140 J = 1, INFRON
            NPF = IPFRON(J)
            IF (NO - NPF) 140, 150, 140
  140   CONTINUE
        GO TO 160
  150   IELF = IELF + 1
        IELFRO(IELF) = KL
  160 CONTINUE
      RETURN
      END


C*************************************************************
      SUBROUTINE JACOB(K)
C*************************************************************
      DIMENSION FIN(3,8), RJACB(3,3), RIJACB(3,3)
      COMMON /BLCK10/ B(3,8), A(3,27), DET, XE(8,3), W(27)
      FIN(1,1) = (1. - A(2,K)) * (1. - A(3,K)) / 8.
      FIN(1,2) = (1. + A(2,K)) * (1. - A(3,K)) / 8.
      FIN(1,3) = -(1. + A(2,K)) * (1. - A(3,K)) / 8.
      FIN(1,4) = -(1. - A(2,K)) * (1. - A(3,K)) / 8.
      FIN(1,5) = (1. - A(2,K)) * (1. + A(3,K)) / 8.
      FIN(1,6) = (1. + A(2,K)) * (1. + A(3,K)) / 8.
      FIN(1,7) = -(1. + A(2,K)) * (1. + A(3,K)) / 8.
      FIN(1,8) = -(1. - A(2,K)) * (1. + A(3,K)) / 8.
      FIN(2,1) = -(1. + A(1,K)) * (1. - A(3,K)) / 8.
      FIN(2,2) = (1. + A(1,K)) * (1. - A(3,K)) / 8.
      FIN(2,3) = (1. - A(1,K)) * (1. - A(3,K)) / 8.
      FIN(2,4) = -(1. - A(1,K)) * (1. - A(3,K)) / 8.
      FIN(2,5) = -(1. + A(1,K)) * (1. + A(3,K)) / 8.
      FIN(2,6) = (1. + A(1,K)) * (1. + A(3,K)) / 8.
      FIN(2,7) = (1. - A(1,K)) * (1. + A(3,K)) / 8.
      FIN(2,8) = -(1. - A(1,K)) * (1. + A(3,K)) / 8.
      FIN(3,1) = -(1. + A(1,K)) * (1. - A(2,K)) / 8.
      FIN(3,2) = -(1. + A(1,K)) * (1. + A(2,K)) / 8.
      FIN(3,3) = -(1. - A(1,K)) * (1. + A(2,K)) / 8.
      FIN(3,4) = -(1. - A(1,K)) * (1. - A(2,K)) / 8.
      FIN(3,5) = (1. + A(1,K)) * (1. - A(2,K)) / 8.
      FIN(3,6) = (1. + A(1,K)) * (1. + A(2,K)) / 8.
      FIN(3,7) = (1. - A(1,K)) * (1. + A(2,K)) / 8.
      FIN(3,8) = (1. - A(1,K)) * (1. - A(2,K)) / 8.
      DO 10 I = 1, 3
        DO 10 J = 1, 3
          RJACB(I,J) = 0.0
          DO 10 M = 1, 8
   10 RJACB(I,J) = RJACB(I,J) + FIN(I,M) * XE(M,J)
      DET = RJACB(1,1) * (RJACB(2,2)*RJACB(3,3) - RJACB(3,2)*RJACB(2,3))
```

```
     1 - RJACB(1,2) * (RJACB(2,1)*RJACB(3,3) - RJACB(3,1)*RJACB(2,3)) +
     2RJACB(1,3) * (RJACB(2,1)*RJACB(3,2) - RJACB(3,1)*RJACB(2,2))
      RIJACB(1,1) = (RJACB(2,2)*RJACB(3,3) - RJACB(3,2)*RJACB(2,3)) /
     1DET
      RIJACB(1,2) = -(RJACB(1,2)*RJACB(3,3) - RJACB(3,2)*RJACB(1,3)) /
     1DET
      RIJACB(1,3) = (RJACB(1,2)*RJACB(2,3) - RJACB(2,2)*RJACB(1,3)) /
     1DET
      RIJACB(2,1) = -(RJACB(2,1)*RJACB(3,3) - RJACB(3,1)*RJACB(2,3)) /
     1DET
      RIJACB(2,2) = (RJACB(1,1)*RJACB(3,3) - RJACB(3,1)*RJACB(1,3)) /
     1DET
      RIJACB(2,3) = -(RJACB(1,1)*RJACB(2,3) - RJACB(2,1)*RJACB(1,3)) /
     1DET
      RIJACB(3,1) = (RJACB(2,1)*RJACB(3,2) - RJACB(3,1)*RJACB(2,2)) /
     1DET
      RIJACB(3,2) = -(RJACB(1,1)*RJACB(3,2) - RJACB(3,1)*RJACB(1,2)) /
     1DET
      RIJACB(3,3) = (RJACB(1,1)*RJACB(2,2) - RJACB(2,1)*RJACB(1,2)) /
     1DET
      DO 20 J = 1, 8
        DO 20 I = 1, 3
          B(I,J) = 0.0
          DO 20 M = 1, 3
   20 B(I,J) = B(I,J) + RIJACB(I,M) * FIN(M,J)
      DET = DET * W(K)
      RETURN
      END


C*****************************************************************
      SUBROUTINE AMATRX
C*****************************************************************
      COMMON /BLCK10/ B(3,8), A(3,27), DET, XE(8,3), W(27)
      Q1 = 0.77459666924
      Q2 = 0.0
      D1 = 0.55555555556
      D2 = 0.88888888889
      DO 10 I = 1, 9
        A(1,3*I - 2) = -Q1
        A(1,3*I - 1) = Q2
        A(1,3*I) = Q1
        A(3,I) = -Q1
        A(3,I + 9) = Q2
   10 A(3,I + 18) = Q1
      DO 20 I = 1, 3
        K = 9 * (I - 1)
        DO 20 J = 1, 3
          A(2,J + K) = -Q1
          A(2,J + K + 3) = Q2
   20 A(2,J + K + 6) = Q1
      W(1) = D1 * D1 * D1
      W(3) = W(1)
      W(7) = W(1)
      W(9) = W(1)
      W(19) = W(1)
      W(21) = W(1)
      W(25) = W(1)
      W(27) = W(1)
```

```
      W(2) = D1 * D1 * D2
      DO 30 I = 2, 13
   30 W(2*I) = W(2)
      W(5) = D1 * D2 * D2
      W(11) = W(5)
      W(13) = W(5)
      W(15) = W(5)
      W(17) = W(5)
      W(23) = W(5)
      W(14) = D2 * D2 * D2
      RETURN
      END



C*********************************************************************
      SUBROUTINE FORCE1(KKK)
C*********************************************************************
      DIMENSION FOR(3,8), SIG(3)
      COMMON /BLCK01/ TITLE(20), NUMEL, NUMNP, NUMPLN, NPPLN, NELINT
      COMMON /BLCK02/ DESLOC(3,1122), DEFOR(1122,6), SIGMA(1122,6), NODE
      COMMON /BLCK03/ CENTRO(2), RADIUS, DEPTH, FACTOR, LINER, NSTEPS,
     1        LOAD(8)
      COMMON /BLCK05/ NELESC(100,8), NDEACT(8), NPERON(550,8),
     1        NNPERON(8), NELPRO(550,8), NELP(8), NPDEAC(550,8),
     2        NNDEAC(8), NSLICE(8), NELACT(100,8), NACT(8)
      COMMON /BLCK06/ IX(840,9), KL
      COMMON /BLCK09/ COORD(3,1122), EXYZ(3,1122), ZDIST, NCODE(1122)
      COMMON /BLCK10/ B(3,9), A(3,27), DET, XE(8,3), W(27)
      COMMON /BLCK11/ FORCEX(1122,8), FORCEY(1122,8), FORCEZ(1122,8)
      JNPERON = NNPERON(KKK)
      DO 10 I = 1, JNPERON
        FORCEX(I,KKK) = 0.0
        FORCEY(I,KKK) = 0.0
   10 FORCEZ(I,KKK) = 0.0
      JELP = NELP(KKK)
      DO 60 MM = 1, JELP
        KL = NELPRO(MM,KKK)
        DO 20 I = 1, 8
          JL = IX(KL,I)
          DO 20 K = 1, 3
            FOR(K,I) = 0.0
   20   XE(I,K) = COORD(K,JL)
        DO 30 K = 1, 27
          CALL JACOB(K)
          DO 30 I = 1, 8
            NO = IX(KL,I)
            DO 30 LL = 1, 3
   30   FOR(LL,I) = FOR(LL,I) + B(LL,I) * SIGMA(NO,LL) * DET
        DO 50 I = 1, 8
          NO = IX(KL,I)
          DO 40 J = 1, JNPERON
            NP = NPERON(J,KKK)
            IF (NO .NE. NP) GO TO 40
            FORCEX(J,KKK) = FORCEX(J,KKK) + FOR(1,I)
            FORCEY(J,KKK) = FORCEY(J,KKK) + FOR(2,I)
            FORCEZ(J,KKK) = FORCEZ(J,KKK) + FOR(3,I)
            GO TO 50
   40     CONTINUE
   50   CONTINUE
```

```
   60 CONTINUE
      DO 70 I = 1, JNFRON
        NP = NPFRON(I,KKK)
        FORCEX(I,KKK) = -FORCEX(I,KKK)
        FORCEY(I,KKK) = -FORCEY(I,KKK)
        FORCEZ(I,KKK) = -FORCEZ(I,KKK)
        IF (NP .GT. NPPLN .AND. NP .LT. (NUMNP - NPPLN)) GO TO 70
        FORCEZ(I,KKK) = 0.0
   70 CONTINUE
      DO 80 I = 1, JNFRON
        NP = NPFRON(I,KKK)
        FORCEX(I,KKK) = FORCEX(I,KKK) / FACTOR
   80 FORCEZ(I,KKK) = FORCEZ(I,KKK) / FACTOR
      RETURN
      END



C*********************************************************************
      SUBROUTINE MSHOUT
C*********************************************************************
      COMMON /BLCK01/ TITLE(20), NUMEL, NUMNP, NUMPLN, NPPLN, NELINT
      COMMON /BLCK02/ DESLOC(3,1122), DEFOR(1122,6), SIGMA(1122,6), NODE
      COMMON /BLCK03/ CENTRO(2), RADIUS, DEPTH, FACTOR, LINER, NSTEPS,
     1       LOAD(8)
      COMMON /BLCK06/ IX(340,9), KL
      COMMON /BLCK07/ YOUNG(10), POISS(10), NMAT
      COMMON /BLCK09/ COORD(3,1122), FXYZ(3,1122), ZDIST, NCODE(1122)
      PRINT 40, (TITLE(I),I=1,20)
      PRINT 50, NUMEL, NUMNP, NMAT, NUMPLN, NPPLN, NELINT, ZDIST
      IF (RADIUS .NE. 0.0) PRINT 110, RADIUS, DEPTH, (CENTRO(I),I=1,2),
     1FACTOR
      IF (LINER - 1) 20, 10, 10
   10 IF (RADIUS .NE. 0.0) PRINT 120
      GO TO 30
   20 IF (RADIUS .NE. 0.0) PRINT 130
   30 PRINT 100, (MAT,YOUNG(MAT),POISS(MAT),MAT=1,NMAT)
      PRINT 90, (I,NCODE(I),(COORD(J,I),J=1,3),I=1,NPPLN)
      PRINT 60
      PRINT 70, (M,(IX(M,L),L=1,9),M=1,NELINT)
      PRINT 80, (I,(SIGMA(I,J),J=1,3),I=1,NPPLN)
   40 FORMAT (//, 20A4, //)
   50 FORMAT ('01.GEOMETRIC DATA OF THE MESH'/, 1X, 28('='), /
     1       ' NUMBER OF ELEMENTS.....=',
     2       , I4/
     3       ' NUMBER OF NODAL POINTS.....=',
     4       , I4/
     5       ' NUMBER OF MATERIALS.....=',
     6       , I4/
     7       ' NUMBER OF CROSS SECTIONS.....=',
     8       , I4/
     9       ' NUMBER OF NODES PER SECTION.....=',
     *       , I4/
     1       ' NUMBER OF ELEMENTS BETWEEN TWO CONSECUTIVE SECTIONS....=',
     2       , I4/
     3       ' DISTANCE BETWEEN TWO CONSECUTIVE SECTIONS (M).....=',
     4       , E12.4)
   60 FORMAT (/, '04.ELEMENT DATA (BETWEEN SECTIONS 1 & 2 ONLY)', /, 1X,
     1       44('='), /, 2(' EL I J K L M N O P MATL'
     2       ,6X))
```

```
   70 FORMAT (2X, 10I4, 9X, 10I4)
   80 FORMAT (//, '05.INITIAL STRESSES (TAU-XY=TAU-YZ=TAU-ZX=0.0) (KN/M2)
     1 - (FIRST SECTION ONLY) ', /, 1X, 76('='), /, 2(
     2        ' NODE    SIG-XX        SIG-YY        SIG-ZZ',9X), /,
     3        (1X,I3,3E13.4,8X,I3,3E13.4))
   90 FORMAT (//, ' 3.NODAL CO-ORDINATES (M) - (FIRST SECTION ONLY)'/,
     1        1X, 47('='), /, 3(' I  CODE     X          Y          Z   ',
     2        2X), /, (2I4,3F9.4,3X,2I4,3F9.4,3X,2I4,3F9.4))
  100 FORMAT ('02.MATERIAL PROPERTIES'/, 1X, 21('='), /
     1        '   MATL YOUNG(KN/M2)     POISS        ', /, (1X,I4,2(2X,
     2        E12.4)))
  110 FORMAT (' RADIUS OF THE TUNNEL (M).....................................=
     1', E12.4/
     2        ' DEPTH OF THE TUNNEL CENTRE LINE (M).....................='
     3        , E12.4/
     4        ' X-COORDINATE OF THE TUNNEL CENTRE LINE (M)..............='
     5        , E12.4/
     6        ' Y-COORDINATE OF THE TUNNEL CENTRE LINE (M)..............='
     7        , E12.4/
     8        ' VERTICAL FORCE/HORIZONTAL FORCE.........................='
     9        , E12.4)
  120 FORMAT (' LINING PLACEMENT.............................................=
     1  YES')
  130 FORMAT (' LINING PLACEMENT.............................................=
     1  NO ')
      RETURN
      END



C*************************************************************
      SUBROUTINE RIGID
C*************************************************************
      COMMON /BLCK01/ TITLE(20), NUMEL, NUMNP, NUMPLN, NPPLN, NELINT
      COMMON /BLCK07/ YOUNG(10), POISS(10), NMAT
      COMMON /BLCK06/ IX(840,9), KL
      COMMON /BLCK08/ S(24,24)
      REWIND 11
      DO 10 KL = 1, NELINT
        CALL ZIBB
        DO 10 I = 1, 24
   10 WRITE (11) (S(I,J),J=1,24)
      RETURN
      END



C*************************************************************************
      SUBROUTINE ZIBB
C*************************************************************************
      COMMON /BLCK06/ IX(840,9), KL
      COMMON /BLCK07/ YOUNG(10), POISS(10), NMAT
      COMMON /BLCK08/ S(24,24)
      COMMON /BLCK09/ COORD(3,1122), EXYZ(3,1122), ZDIST, NCODE(1122)
      COMMON /BLCK10/ B(3,8), A(3,27), DET, XE(8,3), W(27)
      DO 10 I = 1, 24
        DO 10 J = 1, 24
   10 S(I,J) = 0.0
      MTYPE = IX(KL,9)
      DO 20 I = 1, 8
```

```
      J = IX(KL,I)
      DO 20 K = 1, 3
   20 XE(I,K) = COORD(K,J)
      CC = YOUNG(MTYPE) / ((1. + POISS(MTYPE))*(1. - 2.*POISS(MTYPE)))
      C1 = CC * (1. - POISS(MTYPE))
      C2 = CC * POISS(MTYPE)
      C3 = CC * (1. - 2.*POISS(MTYPE)) / 2.
      DO 40 K = 1, 27
        CALL JACOB(K)
        DO 30 I = 1, 8
          DO 30 J = 1, 8
            S(3*I - 2,3*J - 2) = S(3*I - 2,3*J - 2) + C1 * B(1,I) * B(1,
     1      J) * DET + C3 * B(2,I) * B(2,J) * DET + C3 * B(3,I) * B(3,J)
     2       * DET
            S(3*I - 2,3*J - 1) = S(3*I - 2,3*J - 1) + C2 * B(1,I) * B(2,
     1      J) * DET + C3 * B(2,I) * B(1,J) * DET
            S(3*I - 2,3*J) = S(3*I - 2,3*J) + C2 * B(1,I) * B(3,J) *
     1      DET + C3 * B(3,I) * B(1,J) * DET
            S(3*I - 1,3*J - 2) = S(3*I - 1,3*J - 2) + C2 * B(2,I) * B(1,
     1      J) * DET + C3 * B(1,I) * B(2,J) * DET
            S(3*I - 1,3*J - 1) = S(3*I - 1,3*J - 1) + C1 * B(2,I) * B(2,
     1      J) * DET + C3 * B(1,I) * B(1,J) * DET + C3 * B(3,I) * B(3,J)
     2       * DET
            S(3*I - 1,3*J) = S(3*I - 1,3*J) + C3 * B(3,I) * B(2,J) *
     1      DET + C2 * B(2,I) * B(3,J) * DET
            S(3*I,3*J - 2) = S(3*I,3*J - 2) + C2 * B(3,I) * B(1,J) *
     1      DET + C3 * B(1,I) * B(3,J) * DET
            S(3*I,3*J - 1) = S(3*I,3*J - 1) + C2 * B(3,I) * B(2,J) *
     1      DET + C3 * B(2,I) * B(3,J) * DET
   30   S(3*I,3*J) = S(3*I,3*J) + C1 * B(3,I) * B(3,J) * DET + C3 * B(2,
     1  I) * B(2,J) * DET + C3 * B(1,I) * B(1,J) * DET
   40 CONTINUE
      RETURN
      END



C*********************************************************************
      SUBROUTINE DOFIN(II)
C*********************************************************************
      COMMON /BLCK01/ TITLE(20), NUMEL, NUMNP, NUMPLN, NPPLN, NELINT
      COMMON /BLCK05/ NELESC(100,8), NDEACT(8), NPFRON(550,8),
     1        NNFRON(8), NELFRO(550,8), NELF(8), NPDEAC(550,8),
     2        NNDEAC(8), NSLICE(8), NELACT(100,8), NACT(8)
      COMMON /BLCK06/ IX(840,9), KL
      IELF = 0
      JNFRON = NNFRON(II)
      DO 20 KL = 1, NUMEL
        DO 10 I = 1, 8
          DO 10 J = 1, JNFRON
            IF (IX(KL,I) .NE. NPFRON(J,II)) GO TO 10
            IELF = IELF + 1
            NELFRO(IELF,II) = KL
            GO TO 20
   10   CONTINUE
   20 CONTINUE
      NELF(II) = IELF
      RETURN
      END
```

```
C*****************************************************************
      SUBROUTINE DISPLC(I)
C*****************************************************************
      DIMENSION PD(3)
      COMMON /BLCK01/ TITLE(20), NUMEL, NUMNP, NUMPLN, NPPLN, NELINT
      COMMON /BLCK04/ DISPL(6732), NPO(3)
      COMMON /BLCK05/ NELESC(100,8), NDEACT(8), NPFRON(550,8),
     1        NNFRON(8), NELFRO(550,8), NELF(8), NPDEAC(550,8),
     2        NNDEAC(8), NSLICE(8), NELACT(100,8), NACT(8)
      READ 20, NPLN
      NN = 0
      DO 10 J = 1, NPLN
        READ 20, JPLAN, NNOD
        DO 10 K = 1, NNOD
          NN = NN + 1
          READ 30, NP, (PD(L),L=1,3)
          NP = (JPLAN - 1) * NPPLN + NP
          NPFRON(NN,I) = NP
          DO 10 M = 1, 3
   10 DISPL(3*NP + M - 3) = PD(M)
      NNFRON(I) = NN
   20 FORMAT (16I5)
   30 FORMAT (I5, 3F10.0)
      RETURN
      END



C*****************************************************************
      SUBROUTINE FORCE3(III)
C*****************************************************************
      DIMENSION RMIN(3), V(24), DF(24)
      COMMON /BLCK01/ TITLE(20), NUMEL, NUMNP, NUMPLN, NPPLN, NELINT
      COMMON /BLCK02/ DESLOC(3,1122), DEFOR(1122,6), SIGMA(1122,6), NODE
      COMMON /BLCK04/ DISPL(6732), NPO(3)
      COMMON /BLCK05/ NELESC(100,3), NDEACT(8), NPFRON(550,8),
     1        NNFRON(8), NELFRO(550,8), NELF(8), NPDEAC(550,8),
     2        NNDEAC(8), NSLICE(8), NELACT(100,8), NACT(8)
      COMMON /BLCK06/ IX(940,9), KL
      COMMON /BLCK07/ YOUNG(10), POISS(10), NMAT
      COMMON /BLCK08/ S(24,24)
      COMMON /BLCK09/ COORD(3,1122), FXYZ(3,1122), ZDIST, NCODE(1122)
      COMMON /BLCK11/ FORCEX(1122,8), FORCEY(1122,8), FORCEZ(1122,8)
      JELF = NELF(III)
      JNFRON = NNFRON(III)
      DO 10 KK = 1, JNFRON
        FORCEX(KK,III) = 0.0
        FORCEY(KK,III) = 0.0
   10 FORCEZ(KK,III) = 0.0
      KNFRON = NNFRON(III) / 2
      LNFRON = KNFRON
      IF ((KNFRON*2) .NE. NNFRON(III)) LNFRON = KNFRON + 1
      DO 20 I = 1, KNFRON
        NP1 = NPFRON(I,III)
        NP2 = NPFRON(I + LNFRON,III)
   20 PRINT 130, NP1, DISPL(3*NP1 - 2), DISPL(3*NP1 - 1), DISPL(3*NP1),
     1NP2, DISPL(3*NP2 - 2), DISPL(3*NP2 - 1), DISPL(3*NP2)
      IF ((KNFRON*2) .EQ. NNFRON(III)) GO TO 30
```

```
      NP3 = NPFRON(LNFRON,II)
      PRINT 130, NP3, DISPL(3*NP3 - 2), DISPL(3*NP3 - 1), DISPL(3*NP3)
   30 CONTINUE
      DO 40 I = 1, 3
   40 RMIN(I) = 10000.
      DO 50 I = 1, NPPLN
        NP = (NUMPLN - 1) * NPPLN + I
        DO 50 J = 1, 3
   50 IF (ABS(DISPL(3*NP + J - 3)) .LT. ABS(RMIN(J))) RMIN(J) = DISPL(3*
     1NP + J - 3)
      DO 60 I = 1, NUMNP
        DO 60 J = 1, 3
   60 DISPL(3*I + J - 3) = DISPL(3*I + J - 3) - RMIN(J)
C  15 CONTINUE
      DO 110 II = 1, JELF
        KL = NELFRO(II,III)
        CALL ZI88
        DO 70 J = 1, 8
          LL = IX(KL,J)
          DO 70 L = 1, 3
   70   V(3*J + L - 3) = DISPL(3*LL + L - 3)
        DO 80 K = 1, 24
          DF(K) = 0.0
          DO 80 J = 1, 24
   80   DF(K) = DF(K) + S(J,K) * V(J)
        DO 100 LL = 1, 8
          NO = IX(KL,LL)
          DO 90 J = 1, JNFRON
            IF (NO .NE. NPFRON(J,III)) GO TO 90
            FORCEX(J,III) = FORCEX(J,III) + DF(3*LL - 2)
            FORCEY(J,III) = FORCEY(J,III) + DF(3*LL - 1)
            FORCEZ(J,III) = FORCEZ(J,III) + DF(3*LL)
            GO TO 100
   90       CONTINUE
  100     CONTINUE
  110 CONTINUE
      POISS(1) = PPS
  120 CONTINUE
      PRINT 140
  130 FORMAT (2(I6,3E12.4,5X))
  140 FORMAT (/, 1X, 'EQUIVALENT FORCES', /, 1X, 17('='), /,
     1        2('  NODE',6X,'FX',10X,'FY',10X,'FZ',10X))
      RETURN
      END



C*********************************************************************
      SUBROUTINE LODTYP
C*********************************************************************
      DIMENSION TYPE(15)
      COMMON /BLCK01/ TITLE(20), NUMEL, NUMNP, NUMPLN, NPPLN, NELINT
      COMMON /BLCK03/ CENTRO(2), RADIUS, DEPTH, FACTOR, LINER, NSTEPS,
     1        LOAD(8)
      COMMON /BLCK04/ DISPL(6732), NPO(3)
      COMMON /BLCK05/ NELESC(100,2), NDEACT(8), NPFRON(550,8),
     1        NNFRON(8), NELFRO(550,8), NELF(8), NPDEAC(550,8),
     2        NNDEAC(8), NSLICE(8), NELACT(100,8), NACT(8)
      DATA EXCV /'X'/, DISP /'P'/, CONC /'C'/, BLANK /' '/, END /'N'/
      NSTEPS = 0
```

```
   10 READ 60, (TYPE(I),I=1,15)
      DO 50 I = 1, 15
        IF (TYPE(I) .EQ. BLANK) GO TO 50
        IF (TYPE(I + 1) .EQ. END) RETURN
        NSTEPS = NSTEPS + 1
        NDEACT(NSTEPS) = 0
        NNFRON(NSTEPS) = 0
        NELF(NSTEPS) = 0
        NNDEAC(NSTEPS) = 0
        NSLICE(NSTEPS) = 0
        NACT(NSTEPS) = 0
        IF (TYPE(I + 1) .EQ. EXCV) GO TO 20
        IF (TYPE(I) .EQ. CONC) GO TO 40
        IF (TYPE(I) .EQ. DISP) GO TO 30
C    DISTRIBUTED LOAD NOT INCLUDED.
        GO TO 10
   20   LOAD(NSTEPS) = 0
        READ 70, NSLICE(NSTEPS)
        GO TO 10
   30   LOAD(NSTEPS) = 1
        CALL DISPLC(NSTEPS)
        GO TO 10
   40   LOAD(NSTEPS) = 3
        CALL LODCON(NSTEPS)
        GO TO 10
   50 CONTINUE
   60 FORMAT (15A1)
   70 FORMAT (16I5)
      RETURN
      END



C*********************************************************************
      SUBROUTINE STEPS
C*********************************************************************
      COMMON /BLCK01/ TITLE(20), NUMEL, NUMNP, NUMPLN, NPPLN, NELINT
      COMMON /BLCK03/ CENTRO(2), RADIUS, DEPTH, FACTOR, LINER, NSTEPS,
     1        LOAD(3)
      COMMON /BLCK04/ DISPL(6732), NPO(3)
      COMMON /BLCK05/ NELESC(100,3), NDEACT(3), NPFRON(550,8),
     1        NNFRON(8), NELFRC(550,3), NELF(8), NPDEAC(550,8),
     2        NNDEAC(8), NSLICE(8), NELACT(100,3), NACT(3)
      COMMON /BLCK09/ COORD(3,1122), FXYZ(3,1122), ZDIST, NCODE(1122)
      COMMON /BLCK11/ FORCEX(1122,8), FORCEY(1122,8), FORCEZ(1122,8)
      PRINT 130
      JK = 0
      CALL AMATRX
      DO 110 I = 1, NSTEPS
        IF (LOAD(I) .NE. 0) GO TO 10
        IF (JK .EQ. 0) CALL DEFIN
        CALL EXCVTN(I)
        JK = 1
        PRINT 140
        CALL FORCE1(I)
        GO TO 40
   10   IF (LOAD(I) - 2) 20, 110, 30
   20   PRINT 150
        CALL DEFIN(I)
        CALL FORCE3(I)
```

```
      GO TO 40
   30 PRINT 160
   40 JNFRON = NNFRON(I)
      DO 80 II = 1, JNFRON
        NP = NPFRON(II,I)
        NC = NCODE(NP)
        IF (NC .EQ. 0) GO TO 80
        IF (NC .EQ. 1 .OR. NC .EQ. 4) GO TO 50
        IF (NC .EQ. 2 .OR. NC .EQ. 5) GO TO 60
        IF (NC .EQ. 3 .OR. NC .EQ. 6) GO TO 70
        FORCEX(II,I) = DISPL(3*NP - 2)
        FORCEY(II,I) = DISPL(3*NP - 1)
        FORCEZ(II,I) = DISPL(3*NP)
        GO TO 80
   50   FORCEX(II,I) = DISPL(3*NP - 2)
        IF (NC .EQ. 4) FORCEY(II,I) = DISPL(3*NP - 1)
        GO TO 80
   60   FORCEY(II,I) = DISPL(3*NP - 1)
        IF (NC .EQ. 5) FORCEZ(II,I) = DISPL(3*NP)
        GO TO 80
   70   FORCEZ(II,I) = DISPL(3*NP)
        IF (NC .EQ. 6) FORCEX(II,I) = DISPL(3*NP - 2)
   80 CONTINUE
      DO 90 J = 1, NUMNP
        DO 90 K = 1, 3
   90 DISPL(3*J + K - 3) = 0.0
      NF = NNFRON(I) / 2
      LF = NF
      IF ((NF*2) .NE. NNFRON(I)) LF = LF + 1
      DO 100 J = 1, NF
        NP = NPFRON(J,I)
        NP1 = NPFRON(J + LF,I)
  100 PRINT 120, NP, FORCEX(J,I), FORCEY(J,I), FORCEZ(J,I), NP1,
     1 FORCEX(J + NF,I), FORCEY(J + NF,I), FORCEZ(J + NF,I)
      IF ((2*NF) .EQ. NNFRON(I)) GO TO 110
      NP3 = NPFRON(NF + 1,I)
      PRINT 120, NP3, FORCEX(NF + 1,I), FORCEY(NF + 1,I), FORCEZ(NF +
     1 1,I)
  110 CONTINUE
  120 FORMAT (2(I6,3E12.4,5X))
  130 FORMAT (/, ' CONSTRUCTION OR LOADING TYPE.', /, 1X, 23('*'))
  140 FORMAT (/, 1X, 'APPLIED FORCES', /, 1X, 14('='), /,
     1        2('  NODE',6X,'FX',10X,'FY',10X,'FZ',9X))
  150 FORMAT (/, 1X, 'PRESCRIBED DISPLACEMENTS', /, 1X, 24('='), /, 2(
     1        '  NODE',6X,'DX',10X,'DY',10X,'DZ',9X))
  160 FORMAT (/, 1X, 'CONCENTRATED LOADS', /, 1X, 18('='), /,
     1        2('  NODE',6X,'FX',10X,'FY',10X,'FZ',9X))
      RETURN
      END



C*******************************************************************************
      SUBROUTINE LODCON(ISTP)
C*******************************************************************************
      COMMON /BLCK35/ NELESC(100,8), NDEACT(8), NPFRON(550,8),
     1        NNFRON(8), NELFRO(550,8), NELF(8), NPDEAC(550,8),
     2        NNDEAC(8), NSLICE(8), NELACT(100,8), NACT(8)
      COMMON /BLCK11/ FORCEX(1122,8), FORCEY(1122,8), FORCEZ(1122,8)
      READ 20, NNFRON(ISTP)
```

```
      NFORCE = NNFRON(ISTP)
      DO 10 I = 1, NFORCE
        READ 30, NP, FORCEX(I,ISTP), FORCEY(I,ISTP), FORCEZ(I,ISTP)
   10 NPFRON(I,ISTP) = NP
   20 FORMAT (16I5)
   30 FORMAT (I5, 3F10.0)
      RETURN
      END



C*************************************************************
      SUBROUTINE LLOAD(JVEZ)
C*************************************************************
      COMMON /BLCK03/ CENTRO(2), RADIUS, DEPTH, FACTOR, LINER, NSTEPS,
     1        LOAD(8)
      COMMON /BLCK05/ NELESC(100,8), NDEACT(8), NPFRON(550,8),
     1        NNFRON(8), NELFRO(550,8), NELF(8), NPDEAC(550,8),
     2        NNDEAC(8), NSLICE(8), NELACT(100,8), NACT(8)
      COMMON /BLCK06/ IX(340,9), KL
      COMMON /BLCK07/ YOUNG(10), POISS(10), NMAT
      COMMON /BLCK09/ COORD(3,1122), FXYZ(3,1122), ZDIST, NCODE(1122)
      COMMON /BLCK11/ FORCEX(1122,8), FORCEY(1122,8), FORCEZ(1122,8)
      PRINT 140, JVEZ
      JNFRON = NNFRON(JVEZ)
      JDEACT = NDEACT(JVEZ)
      JACT = NACT(JVEZ)
      IF (LOAD(JVEZ) .NE. 0) GO TO 30
      DO 10 I = 1, JDEACT
        KL = NELESC(I,JVEZ)
   10 IX(KL,9) = 0
      IF (JACT .EQ. 0) GO TO 30
      DO 20 I = 1, JACT
        KL = NELACT(I,JVEZ)
   20 IX(KL,9) = 0
   30 DO 40 I = 1, JNFRON
        NP = NPFRON(I,JVEZ)
        FXYZ(1,NP) = FXYZ(1,NP) + FORCEX(I,JVEZ)
        FXYZ(2,NP) = FXYZ(2,NP) + FORCEY(I,JVEZ)
   40 FXYZ(3,NP) = FXYZ(3,NP) + FORCEZ(I,JVEZ)
      IF (LOAD(JVEZ) .NE. 0) GO TO 50
      PRINT 100
      GO TO 90
   50 IF (LOAD(JVEZ) - 2) 60, 70, 80
   60 PRINT 110
      GO TO 90
   70 PRINT 120
      GO TO 90
   80 PRINT 130
   90 CONTINUE
      RETURN
  100 FORMAT (/, ' APPLIED FORCES (DUE TO EXCAVATION)', /, 1X, 34('='))
  110 FORMAT (/, 'APPLIED FORCES (EQUIVALENT TO PRESCRIBED DISPLACEMENTS
     1)', /, 1X, 55('='))
  120 FORMAT (/, ' APPLIED FORCES (EQUIVALENT TO DISTRIBUTED LOADS)', /,
     1        1X, 43('='))
  130 FORMAT (/, ' APPLIED FORCES (CONCENTRATED LOADS)', /, 1X, 35('='))
  140 FORMAT (/, 5X, 21('*'), /, 5X, '*** STEP NUMBER', I2, ' ***', /,
     1        5X, 21('*'))
      END
```

```
C*****************************************************************
      SUBROUTINE STIFF(JVEZ)
C*****************************************************************
      DIMENSION LM(8)
      COMMON /BLCK01/ TITLE(20), NUMEL, NUMNP, NUMPLN, NPPLN, NELINT
      COMMON /BLCK03/ CENTRO(2), RADIUS, DEPTH, FACTOR, LINER, NSTEPS,
     1        LOAD(8)
      COMMON /BLCK04/ DISPL(6732), NPO(3)
      COMMON /BLCK05/ NELESC(100,8), NDEACT(8), NPFRON(550,8),
     1        NNFRON(8), NELFRO(550,8), NELF(8), NPDEAC(550,8),
     2        NNDEAC(8), NSLICE(8), NELACT(100,8), NACT(8)
      COMMON /BLCK06/ IX(840,9), KL
      COMMON /BLCK07/ YOUNG(10), POISS(10), NMAT
      COMMON /BLCK08/ S(24,24)
      COMMON /BLCK09/ COORD(3,1122), FXYZ(3,1122), ZDIST, NCODE(1122)
      COMMON /BLCK12/ GLOBL(702,351), MBAND, NUMBLK, NEQBLK
      JACT = NACT(JVEZ)
      IF (NSLICE(JVEZ) .NE. 0) IDEACT = JACT / NSLICE(JVEZ)
      REWIND 3
      NB = 117
      NEQBLK = 3 * NB
      ND2 = 2 * NEQBLK
      NUMBLK = 0
      INTERV = NUMPLN - 1
      DO 10 N = 1, ND2
        DISPL(N) = 0.0
        DO 10 M = 1, MBAND
   10 GLOBL(N,M) = 0.0
C    ASSEMBLE GLOBAL MATRIX.
   20 NUMBLK = NUMBLK + 1
      NH = NB * (NUMBLK + 1)
      NM = NH - NB
      NL = NM - NB + 1
      KSHIFT = 3 * NL - 3
      DO 110 KKL = 1, INTERV
        REWIND 11
        DO 110 KLL = 1, NELINT
          KL = KLL + (KKL - 1) * NELINT
          MTYPE = IX(KL,9)
          DO 30 I = 1, 24
   30     READ (11) (S(I,J),J=1,24)
          IF (MTYPE) 110, 110, 40
   40     DO 60 I = 1, 8
            IF (IX(KL,I) - NL) 60, 50, 50
   50       IF (IX(KL,I) - NM) 70, 70, 60
   60     CONTINUE
          GO TO 110
   70     CONTINUE
          IX(KL,9) = -IX(KL,9)
          DO 80 I = 1, 8
   80     LM(I) = 3 * IX(KL,I) - 3
          DO 100 I = 1, 8
            DO 100 K = 1, 3
              II = LM(I) + K - KSHIFT
              KK = 3 * I - 3 + K
              DO 100 J = 1, 8
                DO 100 L = 1, 3
```

```
                JJ = LM(J) + L - II + 1 - KSHIFT
                IF (JJ) 100, 100, 90
   90           LL = 3 * J - 3 + L
                GLOBL(II,JJ) = GLOBL(II,JJ) + S(KK,LL)
  100       CONTINUE
  110 CONTINUE
      IF (NM .GT. NUMNP) NM = NUMNP
      DO 120 N = NL, NM
        K = 3 * N - KSHIFT
        DO 120 M = 1, 3
  120 DISPL(K + M - 3) = DISPL(K + M - 3) + FXYZ(M,N)
C   SET UP BOUNDARY CONDITIONS.
      DO 180 M = NL, NH
        IF (M - NUMNP) 130, 130, 190
  130   IF (NCODE(M) .EQ. 0) GO TO 180
        N = 3 * M - 2 - KSHIFT
        IF (NCODE(M) .EQ. 1 .OR. NCODE(M) .EQ. 4) GO TO 140
        IF (NCODE(M) .EQ. 2 .OR. NCODE(M) .EQ. 5) GO TO 150
        IF (NCODE(M) .EQ. 3 .OR. NCODE(M) .EQ. 6) GO TO 160
        GO TO 170
  140   U = FXYZ(1,M)
        CALL MODIFY(ND2, N, U)
        IF (NCODE(M) .EQ. 1) GO TO 180
        U = FXYZ(2,M)
        N = N + 1
        CALL MODIFY(ND2, N, U)
        GO TO 180
  150   U = FXYZ(2,M)
        N = N + 1
        CALL MODIFY(ND2, N, U)
        IF (NCODE(M) .EQ. 2) GO TO 180
        U = FXYZ(3,M)
        N = N + 1
        CALL MODIFY(ND2, N, U)
        GO TO 180
  160   U = FXYZ(3,M)
        N = N + 2
        CALL MODIFY(ND2, N, U)
        IF (NCODE(M) .EQ. 3) GO TO 180
        U = FXYZ(1,M)
        N = N - 2
        CALL MODIFY(ND2, N, U)
        GO TO 180
  170   U = FXYZ(1,M)
        CALL MODIFY(ND2, N, U)
        U = FXYZ(2,M)
        N = N + 1
        CALL MODIFY(ND2, N, U)
        U = FXYZ(3,M)
        N = N + 1
        CALL MODIFY(ND2, N, U)
  180 CONTINUE
  190 CONTINUE
C   STORE EQUATIONS INTO FILE 3.
      DO 200 N = 1, NEQBLK
  200 WRITE (3) DISPL(N), (GLOBL(N,M),M=1,MBAND)
      DO 210 N = 1, NEQBLK
        K = N + NEQBLK
        DISPL(N) = DISPL(K)
        DISPL(K) = 0.0
```

```
        DO 210 M = 1, MBAND
          GLOBL(N,M) = GLOBL(K,M)
  210 GLOBL(K,M) = 0.0
      IF (NM - NUMNP) 20, 220, 220
  220 CONTINUE
      RETURN
      END



C*********************************************************************
      SUBROUTINE MODIFY(NEQ, N, U)
C*********************************************************************
      COMMON /BLCK04/ DISPL(6732), NPO(3)
      COMMON /BLCK12/ GLOBL(702,351), MBAND, NUMBLK, NEQBLK
      DO 40 M = 2, MBAND
        K = N - M + 1
        IF (K) 20, 20, 10
   10   DISPL(K) = DISPL(K) - GLOBL(K,M) * U
        GLOBL(K,M) = 0.0
   20   K = N + M - 1
        IF (NEQ - K) 40, 30, 30
   30   DISPL(K) = DISPL(K) - GLOBL(N,M) * U
        GLOBL(N,M) = 0.0
   40 CONTINUE
      GLOBL(N,1) = 1.0
      DISPL(N) = U
      RETURN
      END



C*********************************************************************
      SUBROUTINE BANSOL
C*********************************************************************
C    SOLVE SYSTEM OF EQUATIONS BY GAUSS ELIMINATION METHOD.
      DOUBLE PRECISION C, DIS, GBL
      COMMON /BLCK04/ DISPL(6732), NPO(3)
      COMMON /BLCK12/ GLOBL(702,351), MBAND, NUMBLK, NEQBLK
      NL = NEQBLK + 1
      NH = NEQBLK + NEQBLK
      REWIND 1
      REWIND 3
      NB = 0
      GO TO 30
   10 NB = NB + 1
      DO 20 N = 1, NEQBLK
        NM = NEQBLK + N
        DISPL(N) = DISPL(NM)
        DISPL(NM) = 0.0
        DO 20 M = 1, MBAND
          GLOBL(N,M) = GLOBL(NM,M)
   20 GLOBL(NM,M) = 0.0
      IF (NUMBLK - NB) 30, 50, 30
   30 DO 40 N = NL, NH
   40 READ (3) DISPL(N), (GLOBL(N,M),M=1,MBAND)
      IF (NB) 50, 10, 30
C    GAUSS REDUCTION.
   50 DO 100 N = 1, NEQBLK
        IF (GLOBL(N,1)) 60, 100, 60
```

```
   60   DIS = DBLE(DISPL(N)) / DBLE(GLOBL(N,1))
        DISPL(N) = SNGL(DIS)
        DO 90 L = 2, MBAND
          IF (GLOBL(N,L)) 70, 90, 70
   70     C = DBLE(GLOBL(N,L)) / DBLE(GLOBL(N,1))
          I = N + L - 1
          J = 0
          DO 80 K = L, MBAND
            J = J + 1
            GBL = DBLE(GLOBL(I,J)) - C * DBLE(GLOBL(N,K))
   80     GLOBL(I,J) = SNGL(GBL)
          DIS = DBLE(DISPL(I)) - DBLE(GLOBL(N,L)) * DBLE(DISPL(N))
          DISPL(I) = SNGL(DIS)
          GLOBL(N,L) = SNGL(C)
   90   CONTINUE
  100 CONTINUE
      IF (NUMBLK - NB) 110, 130, 110
  110 DO 120 N = 1, NEQBLK
  120 WRITE (1) DISPL(N), (GLOBL(N,M),M=2,MBAND)
      GO TO 10
C   BACK-SUBSTITUTION.
  130 DO 150 M = 1, NEQBLK
        N = NEQBLK + 1 - M
        DIS = DBLE(DISPL(N))
        DO 140 K = 2, MBAND
          L = N + K - 1
  140   DIS = DIS - DBLE(GLOBL(N,K)) * DBLE(DISPL(L))
        DISPL(N) = SNGL(DIS)
        NM = N + NEQBLK
        DISPL(NM) = DISPL(N)
  150 GLOBL(NM,NB) = DISPL(N)
      NB = NB - 1
      IF (NB) 160, 200, 160
  160 DO 170 N = 1, NEQBLK
  170 BACKSPACE 1
      DO 180 N = 1, NEQBLK
  180 READ (1) DISPL(N), (GLOBL(N,M),M=2,MBAND)
      DO 190 N = 1, NEQBLK
  190 BACKSPACE 1
      GO TO 130
  200 K = 0
      DO 210 NB = 1, NUMBLK
        DO 210 N = 1, NEQBLK
          NM = N + NEQBLK
          K = K + 1
  210 DISPL(K) = GLOBL(NM,NB)
      RETURN
      END



C*******************************************************************************
      SUBROUTINE COMPUT(JVEZ)
C*******************************************************************************
      DIMENSION ZG(6,1122), IU(1122), DISP(3,3), Z1(6,3)
      DIMENSION DEF(8,6), STRAIN(1122,6)
      COMMON /BLCK01/ TITLE(20), NUMEL, NUMNP, NUMPLN, NPPLN, NELINT
      COMMON /BLCK02/ DESLOC(3,1122), DEFOR(1122,6), SIGMA(1122,6), NODE
      COMMON /BLCK03/ CENTRO(2), RADIUS, DEPTH, FACTOR, LINER, NSTEPS,
     1       LOAD(3)
```

```
      COMMON /BLCK04/ DISPL(6732), NPO(3)
      COMMON /BLCK05/ NELESC(100,3), NDEACT(8), NPFRON(550,8),
     1        NNFRON(8), NELFRO(550,8), NELF(8), NPDEAC(550,8),
     2        NNDEAC(8), NSLICE(8), NELACT(100,8), NACT(8)
      COMMON /BLCK06/ IX(840,9), KL
      COMMON /BLCK07/ YOUNG(10), POISS(10), NMAT
      COMMON /BLCK09/ COORD(3,1122), FXYZ(3,1122), ZDIST, NCODE(1122)
      COMMON /BLCK10/ B(3,8), A(3,27), DET, XE(8,3), W(27)
      COMMON /BLCK12/ GLOBL(702,351), MBAND, NUMBLK, NEQBLK
      COMMON /BLCK14/ PDES(1122,3)
      A(1,1) = 1.
      A(1,2) = 1.
      A(1,3) = -1.
      A(1,4) = -1.
      A(1,5) = 1.
      A(1,6) = 1.
      A(1,7) = -1.
      A(1,8) = -1.
      A(2,1) = -1.
      A(2,2) = 1.
      A(2,3) = 1.
      A(2,4) = -1.
      A(2,5) = -1.
      A(2,6) = 1.
      A(2,7) = 1.
      A(2,8) = -1.
      A(3,1) = 1.
      A(3,2) = 1.
      A(3,3) = 1.
      A(3,4) = 1.
      A(3,5) = -1.
      A(3,6) = -1.
      A(3,7) = -1.
      A(3,8) = -1.
      DO 10 N = 1, NUMNP
        DO 10 M = 1, 3
          PDES(N,M) = 0.0
10    DESLOC(M,N) = DESLOC(M,N) + DISPL(3*N + M - 3) * 1000.
      DO 20 I = 1, 3
20    NPO(I) = 1
      DO 30 N = 2, NUMNP
        DO 30 J = 1, 3
          IF (ABS(DESLOC(J,N)) .GT. ABS(DESLOC(J,NPO(J))))
     1    NPO(J) = N
30    CONTINUE
      DO 40 I = 1, NUMNP
        DO 40 J = 1, 3
          IF (DESLOC(J,NPO(J)) .EQ. 0.0) GO TO 40
          PDES(I,J) = (DESLOC(J,I)/DESLOC(J,NPO(J))) * 100.
40    CONTINUE
      DO 50 M = 1, NUMNP
        IU(M) = 0
        DO 50 JK = 1, 6
          STRAIN(M,JK) = 0.0
50    ZG(JK,M) = 0.
      DO 110 KL = 1, NUMEL
        IX(KL,9) = IABS(IX(KL,9))
        MTYPE = IX(KL,9)
        IF (MTYPE .EQ. 0) GO TO 110
        CC = YOUNG(MTYPE) / ((1. + POISS(MTYPE))*(1. - 2.*POISS(MTYPE)))
```

```
      C1 = CC * (1. - POISS(MTYPE))
      C2 = CC * POISS(MTYPE)
      C3 = CC * (1. - 2.*POISS(MTYPE)) / 2.
      DO 60 I = 1, 8
        J = IX(KL,I)
        DO 60 K = 1, 3
          XE(I,K) = COORD(K,J)
   60 DISP(K,I) = DISPL(3*J + K - 3)
      DO 70 I = 1, 8
        DO 70 J = 1, 6
          DEF(I,J) = 0.0
   70 Z1(J,I) = 0.0
      DO 90 K = 1, 8
        W(K) = 1.0
        CALL JACOB3(K)
        DO 80 I = 1, 8
          DEF(K,1) = DEF(K,1) + B(1,I) * DISP(1,I)
          DEF(K,2) = DEF(K,2) + B(2,I) * DISP(2,I)
          DEF(K,3) = DEF(K,3) + B(3,I) * DISP(3,I)
          DEF(K,4) = DEF(K,4) + B(2,I) * DISP(1,I) + B(1,I) * DISP(2,
     1    I)
          DEF(K,5) = DEF(K,5) + B(3,I) * DISP(2,I) + B(2,I) * DISP(3,
     1    I)
   80     DEF(K,6) = DEF(K,6) + B(3,I) * DISP(1,I) + B(1,I) * DISP(3,I)
        Z1(1,K) = C1 * DEF(K,1) + C2 * DEF(K,2) + C2 * DEF(K,3)
        Z1(2,K) = C2 * DEF(K,1) + C1 * DEF(K,2) + C2 * DEF(K,3)
        Z1(3,K) = C2 * DEF(K,1) + C2 * DEF(K,2) + C1 * DEF(K,3)
        Z1(4,K) = C3 * DEF(K,4)
        Z1(5,K) = C3 * DEF(K,5)
        Z1(6,K) = C3 * DEF(K,6)
   90 CONTINUE
      DO 100 J = 1, 8
        I = IX(KL,J)
        IU(I) = IU(I) + 1
        DO 100 L = 1, 6
          STRAIN(I,L) = STRAIN(I,L) + DEF(J,L) * 100.
  100   ZG(L,I) = ZG(L,I) + Z1(L,J)
  110 CONTINUE
      DO 120 I = 1, NUMNP
        IF (IU(I) .EQ. 0) IU(I) = 1
        DO 120 J = 1, 6
          ZZ = ZG(J,I) / IU(I)
          IF (ABS(ZZ) .LT. 0.000001) ZZ = 0.0
  120 SIGMA(I,J) = SIGMA(I,J) + ZZ
      DO 130 I = 1, NUMNP
        DO 130 J = 1, 6
          DD = STRAIN(I,J) / IU(I)
          IF (ABS(DD) .LT. 0.0000000001) DD = 0.0
  130 DEFOR(I,J) = DEFOR(I,J) + DD
      IF (LOAD(JVEZ) .NE. 0) GO TO 150
      JNERON = NNERON(JVEZ)
      DO 140 I = 1, JNERON
        K = NPERON(I,JVEZ)
        DO 140 J = 1, 6
  140 SIGMA(K,J) = 0.0
  150 IF (NNDEAC(JVEZ) .EQ. 0) RETURN
      JNDEAC = NNDEAC(JVEZ)
      DO 160 I = 1, JNDEAC
        II = NPDEAC(I,JVEZ)
        DO 160 J = 1, 3
```

```
          DESLOC(J,II) = 0.0
          DEFOR(II,J) = 0.0
          DEFOR(II,J + 3) = 0.0
          SIGMA(II,J) = 0.0
  160     SIGMA(II,J + 3) = 0.0
          RETURN
          END



C*****************************************************************
          SUBROUTINE OUTPUT(JVEZ)
C*****************************************************************
          COMMON /BLCK01/ TITLE(20), NUMEL, NUMNP, NUMPLN, NPPLN, NELINT
          COMMON /BLCK02/ DESLOC(3,1122), DEFOR(1122,6), SIGMA(1122,6), NODE
          COMMON /BLCK03/ CENTRO(2), RADIUS, DEPTH, FACTOR, LINER, NSTEPS,
         1        LOAD(8)
          COMMON /BLCK04/ DISPL(6732), NPO(3)
          COMMON /BLCK14/ PDES(1122,3)
          IF (DESLOC(2,NODE) .NE. 0.0) GO TO 10
          HOR = 0.0
          VERT = 0.0
          AXL = 0.0
          GO TO 20
   10     HOR = DESLOC(1,NPO(1)) / DESLOC(2,NODE)
          VERT = DESLOC(2,NPO(2)) / DESLOC(2,NODE)
          AXL = DESLOC(3,NPO(3)) / DESLOC(2,NODE)
   20     PRINT 110, NODE, DESLOC(2,NODE), NPO(1), DESLOC(1,NPO(1)), NPO(2),
         1DESLOC(2,NPO(2)), NPO(3), DESLOC(3,NPO(3)), HOR, VERT, AXL
          DO 30 II = 1, NUMPLN
            PRINT 100, II
            DO 30 K = 1, NPPLN
              NP = (II - 1) * NPPLN + K
   30     PRINT 60, NP, K, (DESLOC(J,NP),PDES(NP,J),J=1,3)
          PRINT 120
          DO 40 II = 1, NUMPLN
            PRINT 150, II
            DO 40 K = 1, NPPLN
              KP = (II - 1) * NPPLN + K
   40     PRINT 70, KP, K, (SIGMA(KP,I),I=1,6)
          PRINT 130
          DO 50 II = 1, NUMPLN
            PRINT 160, II
            DO 50 L = 1, NPPLN
              LP = (II - 1) * NPPLN + L
   50     PRINT 70, LP, L, (DEFOR(LP,I),I=1,6)
          IF (JVEZ .EQ. NSTEPS) PRINT 140
   60     FORMAT (I5, '(', I2, ')', 3(E12.4,'(',F6.1,')'))
   70     FORMAT (I5, '(', I2, ')', 6E12.4)
   80     FORMAT (I5, '(', I2, ')', 6F12.0)
   90     FORMAT (//, 5X, 21('*'), /, 5X, '*** STEP NUMBER', I2, ' ***', /,
         1        5X, 21('*'), /)
  100     FORMAT (/, '     <<< SECTION NO.', I2, ' >>>     ', /,
         1
         2'     NODE      X(LAT.) (% MAX.)    Y(VERT.) (% MAX.)    Z(LONG.) (% M
         3AX.) ')
  110     FORMAT (//, '    A) DISPLACEMENTS ', /, 3X, 16('='), //,
         1        ' A.1)::: PARAMETERS :::'//
         2        '      NODE WITH MAXIMUM SETTLEMENT.....................=', I4/
         3        '      MAXIMUM SETTLEMENT (MM)..........................=', E12.4/
```

```
     4         '      NODE WITH MAXIMUM LATERAL DISPLACEMENT.....=', I4/
     5         '      MAXIMUM LATERAL DISPLACEMENT (MM)..........=', E12.4/
     6         '      NODE WITH MAXIMUM VERTICAL DISPLACEMENT....=', I4/
     7         '      MAXIMUM VERTICAL DISPLACEMENT (MM).........=', E12.4/
     8         '      NODE WITH MAXIMUM LONGIT. DISPLACEMENT.....=', I4/
     9         '      MAXIMUM LONGIT. DISPLACEMENT (MM)..........=', E12.4/
     *         '      MAX.HORIZ.DISPLACEMENT/MAX.SETTLEMENT......=', E12.4/
     1         '      MAX.VERT.DISPLACEMENT/MAX.SETTLEMENT.......=', E12.4/
     2         '      MAX.LONG.DISPLACEMENT/MAX.SETTLEMENT.......=', E12.4/
     3        /' A.2)*** AMPLITUDE (MM) ***')
  120 FORMAT (//, '   B) STRESSES (KN/M2) ', /, 3X, 16('='))
  130 FORMAT (//, '   C) STRAINS (%) ', /, 3X, 14('='))
  140 FORMAT (//, 2(/,25X,24('*')), /, 24X, ' *** END OF EXECUTION ***',
     1       2(/,25X,24('*')), //)
  150 FORMAT (/, '     <<< SECTION NO.', I2, ' >>>', /,
     1
     2'     NODE      SIG-XX       SIG-YY       SIG-ZZ       TAU-XY       TAU-
     3YZ       TAU-ZX ')
  160 FORMAT (/, '     <<< SECTION NO.', I2, ' >>>', /,
     1
     2'    NODE          EXX          EYY          EZZ          EXY          EYZ
     3          EXZ       ')
  170 FORMAT (/, '     <<<SECTION NO.', I2, ' >>>', /,
     1         '      NODE      X(LAT.)     Y(VERT.)     Z(LONG.)         ')
  180 FORMAT (/, '     <<< SECTION NO.', I2, ' >>>', /,
     1         '      NODE      SIG-XX       SIG-YY       SIG-ZZ')
      RETURN
      END



C*************************************************************************
      SUBROUTINE FILE12(JVEZ)
C*************************************************************************
      COMMON /BLCK01/ TITLE(20), NUMEL, NUMNP, NUMPLN, NPPLN, NELINT
      COMMON /BLCK02/ DESLOC(3,1122), DEFOR(1122,6), SIGMA(1122,6), NODE
      COMMON /BLCK04/ DOSPL(6732), NPO(3)
      IF (JVEZ .EQ. 1) GO TO 10
      REWIND 12
      WRITE (12) NUMNP, NUMPLN, NPPLN
      WRITE (12) ((COORD(I,K),I=1,3),K=1,NUMNP)
   10 WRITE (12) JVEZ
      WRITE (12) ((DESLOC(J,K),J=1,3),(SIGMA(K,J),J=1,6),(DEFOR(K,J),J=
     1       1,6),K=1,NUMNP)
      RETURN
      END
```

A P P E N D I X C

```
C
C*********************************************************************
C     PROGRAM GRAPH
C*********************************************************************
      DIMENSION COORD(3,1122), XGR(300), YGR(300), FGR(300), DIREC(80),
     1          VAR(80), FUNC(8,6,1122), NPL(13), JNODE(300)
      DATA BLANK /' '/, HOR /'H'/, RLONG /'L'/, END /'E'/
      DATA DISPL /'P'/, STRAIN /'A'/
      PRINT 150
      REWIND 4
      REWIND 12
      READ (12) NUMNP, NUMPLN, NPPLN
      READ (12) ((COORD(I,K),I=1,3),K=1,NUMNP)
C
      READ 140, (VAR(I),I=1,80)
      DO 10 II = 1, 80
        IF (VAR(II) .EQ. BLANK) GO TO 10
        IF (VAR(II) .EQ. END) STOP
        IF (VAR(II + 3) .EQ. DISPL) NNN = 1
        IF (VAR(II + 3) .EQ. END) NNN = 2
        IF (VAR(II + 3) .EQ. STRAIN) NNN = 3
        GO TO 20
   10 CONTINUE
   20 READ 140, (DIREC(I),I=1,80)
      READ 120, IDIR, IVEZ
      DO 40 II = 1, 80
        IF (DIREC(II) .EQ. BLANK) GO TO 40
        IF (DIREC(II) .EQ. END) STOP
        IF (DIREC(II) .EQ. HOR) GO TO 60
        IF (DIREC(II) .EQ. RLONG) GO TO 50
        READ 120, LSECT
        NPP = NPPLN
        LL1 = 1
        LL2 = 2
        DO 30 I = 1, NPP
          NP = (LSECT - 1) * NPPLN + I
   30   JNODE(I) = NP
        GO TO 90
   40 CONTINUE
   50 LL1 = 3
      LL2 = 2
      GO TO 70
   60 LL1 = 1
      LL2 = 3
   70 READ 120, NN
      READ 120, (JNODE(I),I=1,NN)
      NPP = 0
      DO 80 I = 1, NUMPLN
        DO 80 J = 1, NN
          NPP = NPP + 1
   80 JNODE(NPP) = JNODE(J) + (I - 1) * NPPLN
      LSECT = 1
   90 CONTINUE
  100 READ (12) JVEZ
```

```
      READ (12) ((FUNC(1,J,K),J=1,3),(FUNC(2,J,K),J=1,6),(FUNC(3,J,K),J=
     1     1,6),K=1,NUMNP)
      IF (JVEZ .NE. IVEZ) GO TO 100
      NN = JNODE(1)
      FMIN = FUNC(NNN,IDIR,NN)
      FMAX = FMIN
      XMIN = COORD(LL1,1)
      XMAX = XMIN
      YMAX = COORD(LL2,1)
      YMAX = YMIN
      DO 110 J = 1, NPP
        NP = JNODE(J)
        XGR(J) = COORD(LL1,NP)
        YGR(J) = COORD(LL2,NP)
        FGR(J) = FUNC(NNN,IDIR,NP)
        IF (FGR(J) .LT. FMIN) FMIN = FGR(J)
        IF (FGR(J) .GT. FMAX) FMAX = FGR(J)
        IF (XGR(J) .LT. XMIN) XMIN = XGR(J)
        IF (XGR(J) .GT. XMAX) XMAX = XGR(J)
        IF (YGR(J) .LT. YMIN) YMIN = YGR(J)
        IF (YGR(J) .GT. YMAX) YMAX = YGR(J)
        IF (XGR(J) .EQ. 0.0 .AND. YGR(J) .EQ. 0.0) XGR(J) = 0.0001
        WRITE (4,130) XGR(J), YGR(J), FGR(J)
  110 CONTINUE
      XGR(NPP + 1) = 0.0
      YGR(NPP + 1) = 0.0
      FGR(NPP + 1) = 0.0
      WRITE (4,130) XGR(NPP + 1), YGR(NPP + 1), FGR(NPP + 1)
      BLEV = ABS(FMAX) + ABS(FMIN)
      DIV = BLEV / 60
      PRINT 160, (VAR(I),I=1,15), (DIREC(I),I=1,15), IDIR, IVEZ, LSECT,
     1NPP, FMIN, FMAX, DIV, XMIN, XMAX, YMIN, YMAX
      PRINT 150
  120 FORMAT (16I5)
  130 FORMAT (3F15.4)
  140 FORMAT (80A1)
  150 FORMAT (/, 1X, 60('*'))
  160 FORMAT (//, ' FUNCTION TO BE DRAWN.....= ', 15A1/
     1        ' POSITION OF THE SECTION.....= ', 15A1/
     2        ' DIRECTION OF THE FUNCTION.....=', I4/
     3        ' INCREMENT NUMBER.....=', I4/
     4        ' NUMBER OF THE SECTION.....=', I4/
     5        ' NUMBER OF NODAL POINTS.....=', I4/
     6        ' MINIMUM VALUE OF THE FUNCTION.....=', E12.4/
     7        ' MAXIMUM VALUE OF THE FUNCTION.....=', E12.4/
     8        ' SUGGESTED VALUE FOR BLEV.....=', E12.4/
     9        ' XMIN.....=', E12.4/
     *        ' XMAX.....=', E12.4/)
      STOP
      END
```